# The Study of Natural and Unnatural Peptides: Changing Medicinal & Structural Properties

*A thesis presented in partial fulfilment of the requirements for the degree of*

Master of Science

in Chemistry

Suraj Patel

MASSEY UNIVERSITY
TE KUNENGA KI PŪREHUROA
UNIVERSITY OF NEW ZEALAND

Supervisor: Gareth J. Rowlands

Co-Supervisor: Preet Singh

2021

***"When we hit our lowest point, we are open to the greatest change."***

***Avatar Aang***

# Abstract

Nature creates the foundations of life by linking together small, yet versatile, building blocks. Using this principle it can build information storage-molecules like DNA or functional catalyst like peptides and proteins. With the aid of non-covalent interactions these molecules form elegant 3D structures that allow them to have a range of functions and to complete a variety of tasks. However, the natural synthesis of the molecules are often limited by the biological resources available. As chemists, we have limitless choice in building blocks at our disposal, allowing us to make tweaks until we get the most efficient outcome.

The purpose of this study is to see how chemists are able to improve on nature through the use of synthetic chemistry. This was attempted through two strands of research. The first strand tried to improve the efficiency of a naturally occurring peptide, opiorphin, by altering the chemical structure without inhibiting its analgesic potency. While the second project investigated a class of synthetic peptide, known as a foldamer, by using a unnatural amino acid building block.

A viable design of a prodrug for opiorphin was proposed, which requires further research but has begun to show some promise. While the synthesis of a peptide was not achieved in the second project, issues seen during the synthesis of a dimer have been highlighted and alternative routes have been proposed. In addition, a novel substitution pattern for a cyclophane product has been reported.

## Acknowledgements

Firstly, I would like to thank my supervisor, Assoc. Prof. Gareth J. Rowlands. From the first lecture in 123.101, your enthusiasm for synthetic chemistry has been contagious and has motivated me to become a better chemist. The dedication you show your students hugely surpasses what is expected, and I feel incredibly fortunate to have had you as a mentor. Your insightful comments, suggestions, and knowledge have been greatly appreciated. In particular, your anal retentiveness for ChemDraw structures has been a blessing and curse, which I am grateful has been passed onto me.

I must also thank my unofficial supervisor, Leonie Etheridge. You have taught me nearly everything I know about wet chemistry, lab maintenance and health and safety procedures. Your constant support, quiet words of wisdom and walks to the car park have been much appreciated over the years (and sorely missed in this last year).

This work would not have been possible without some key staff members at Massey that have helped me through the years. Thank you to Graham Freeman for his constant sass and synthetic expertise. Dr Pat Edwards for his NMR guidance. David Lun for running high-res mass spectroscopy samples. Tyson Dais for collecting X-ray crystal structures and interpreting the data. Natisha Magan for turning me into a wine connoisseur and teaching me every wine is “a bit oaky at the back of the palate”.

To the ‘Smart People + Suju’ gang, thank you for declining my invites to the pub every time I asked, this thesis would have never been completed without your heart-breaking rejections. Thank you to the Rowlands, Plieger and Filichev groups for their advice. I would particularly like to thank Tyson and Siddle (kinda Sam too, I guess) for their vast knowledge and proofreading skills. Oh, and Marryllyn for providing me with some form of a social life over the last two years.

Lastly, I would like to thank my friends outside of university that have supported me through the last two years. To begin, Ditchell, for no longer living in Palmerston North and not wanting to see me, as again, I would not have been able to complete this research with you around. Secondly; Callum, Leila, Zara, Alex, Amy, and Dakota for supporting me through what have been a difficult set of years. The friendship and distractions you have provided me over the years has been thoroughly enjoyed, and I would not be here without your company.

# *Contents*

# List of Abbreviations

| | | | |
|---|---|---|---|
| **22pc** | [2.2]Paracyclophane | **HOMO** | Highest occupied molecular orbital |
| **2D** | Two-dimensional | **HPLC** | High-performance liquid chromatography |
| **AAP** | Alanine aminopeptidase | **HRMS** | High Resolution Mass Spectrometry |
| **Ac** | Acetyl | **Hz** | Hertz |
| **Arg** | Arginine | **IR** | Infrared |
| **aq** | Aqueous | ***J*** | Coupling constant |
| **BBB** | Blood-brain barrier | **LUMO** | Lowest unoccupied molecular orbital |
| **BINAP** | 2,2'-bis(Diphenylphosphino)-1,1'-binaphthyl | **Me** | Methyl |
| **Boc** | *tert*-Butoxycarbonyl | **Mp** | Melting point |
| **bs** | Broad singlet | ***m/z*** | Mass to charge ratio |
| **CIP** | Cahn-Ingold-Prelog | **NDI** | 1,4,5,8-naphthalenetetracarboxylic acid diimide |
| **COSY** | Correlation Spectroscopy | **NEP** | Neprilysin |
| **d** | doublet | **NHS** | *N*-Hydroxysuccinimide |
| **DAN** | 1,5-dialkoxynaphthalene | **NMR** | Nuclear Magnetic resonance |
| **DCC** | *N*,*N*'-dicyclohexylcarbodiimide | **NOESY** | Nuclear Overhasuser Effect Spectroscopy |
| **DCE** | 1,2-Dichloroethane | **Phe** | Phenylalanine |
| **DEPT** | Distortionless Enhancement by Polarisation Transfer | **ppm** | Parts per million |
| **dd** | Doublet of doublets | **q** | Quartet |
| **ddd** | Doublet of doublets of doublets | **quint** | Quintet |
| **L-DOPA** | L-3,4-dihydroxyphenylalanine | **s** | Singlet |
| **DMF** | *N*,*N*-Dimethylformamide | **Ser** | Serine |
| **DMS** | Dimethyl sulfide | **Sxt** | Sextet |
| **DPP3** | Dipeptidyl peptidase 3 | $R_f$ | Retention factor |
| **dt** | Doublet of triplets | **RT** | Room temperature |
| ***ee*** | Enantiomeric excess | **t** | Triplet |
| **eq** | Equivalents | **td** | Triplet of doublets |
| **ESI-MS** | Electrospray Ionization Mass Spectrometry | **Tf** | trifluoromethanesulfonate |
| **Et** | Ethyl | **THF** | Tetrahydrofuran |
| **Gln** | Glutamine | **TLC** | Thin Layer chromatography |
| **HMBC** | Heteronuclear Multiple Bond Correlation | **Ts** | *p*-toluenesulfonyl |
| **HMQC** | Heteronuclear Multiple Quantum Coherence | **UV** | Ultraviolet |

Chapter 1

# Introduction

## 1.1 Natural vs Unnatural Amino Acids

The term amino acid describes a diverse range of molecules with many functions. Most people know that amino acids are abundant in nature, but they are also found in synthetic molecules including chiral ligands,[1] organocatalysts,[2] and synthetic polymers.[3] By definition, an amino acid is any molecule that contains an amine and carboxylic acid. The term amino acid is most commonly limited to the 20 proteinogenic α-amino acids; those amino acids coded by our genes used in the synthesis of proteins.[4] However, nature has synthesised more than 300 amino acids, all of which play critical roles in biology. An example of this is the natural amino acid, folate vitamin $B_9$ **1**, a glutamic acid derivative (Figure 1).

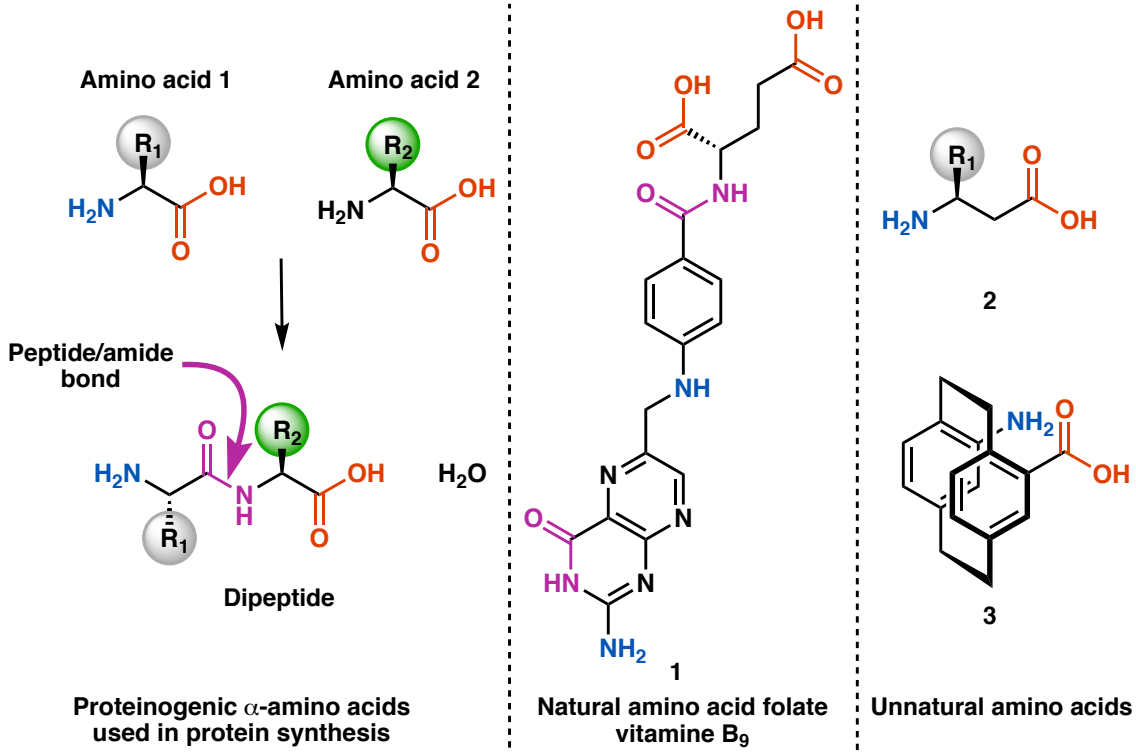


*Figure 1 – Formation of dipeptide through the formation of a peptide/amide bond (left); the natural amino acid glutamic acid derivative folate vitamin $B_9$ (centre); two examples of unnatural amino acids.*

Unnatural amino acids are synthetic derivatives containing both amine and carboxylic functionalities, which aren't seen in nature. Proteins, formed from natural amino acids, invariably form secondary structures comprising of α-helices or β-sheets. Chemists,

using natural amino acids, should have access to different structures and can incorporate an unlimited range of functionality. However, with unnatural amino acids, there is a limitless choice of building blocks allowing chemists to improve on nature and create new structures with alternative functions. Numerous studies on unnatural amino acid have been completed, including β-amino acids **2**, and have been incorporated into interesting scaffolds like **3**. A diverse assortment of natural and unnatural amino acids have been seen in applications including synthetic polymers,[5] C—H bond activation,[6] organometallics,[7] and the synthesis of foldamers.[8] This thesis investigates two key areas, natural and unnatural amino acids. However, both areas look to answer one question: are we able to improve on nature?

## 1.2 Natural Peptide - Opiorphin

Opiorphin **4** is a naturally occurring peptide, consisting of the five amino acid sequence; Gln-Arg-Phe-Ser-Arg (Figure 2).[9] It can be isolated from saliva, and has been reported to have an analgesic effect five times stronger than morphine.[10] Opiorphin extends the duration of enkephalin activity, another peptide responsible for regulating pain, which is released in response to painful stimuli. Opiorphin induces a pain-killing effect by inhibiting three proteases, neprilysin (NEP), alanine aminopeptidase (AAP), and dipeptidyl peptidase (DPP3), which are responsible for the breakdown of enkephalin.[10–12] Inhibiting these three proteases results in an increased duration of enkephalin activity, allowing it to bind to the opioid receptors, thus regulating the sensory nervous system reaction to pain. Most administered narcotics result in adverse effects, while **4** has only been shown to have an anti-depressive effect, which makes it promising candidate for future pain relief.[11]

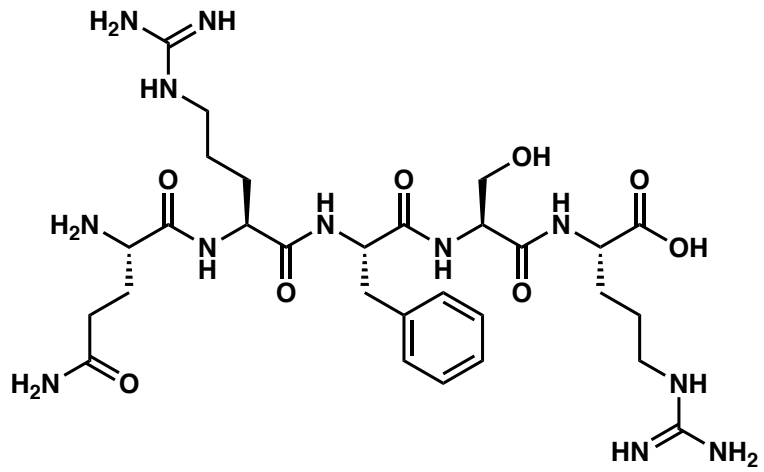

**4**

*Figure 2 – Molecular Structure of Opiorphin 4 (shown in it's non-zwitterionic form).*

A study by Dr. Preet Singh from Massey University in 2019 showed **4** is less effective *in vivo* than morphine.[13] This study looked at the changes in electroencephalogram (EEG) and results of a hot-plate and tail-flick test from female Sprague-Dawley rats when exposed to noxious stimuli.[13] The study compared the analgesic effect of morphine (1 mg/kg), opiorphin (2 mg/kg), and saline (0.5 mL) after five minutes from receiving an intravenous injection. The results show opiorphin can pass through the cerebral spinal fluid to affect the spinal cord but is unable to target the brain effectively. Currently, the low efficacy could be due to two reasons; firstly, opiorphin is unable to pass through the blood-brain barrier (BBB) effectively; secondly, due to the short half-life (15 minutes) it is unable to effectively inhibit the proteases.[12] Both of these issues can be resolved by altering the structures of opiorphin. Although altering the half-life and permeability of opiorphin may be possible at the same time, this thesis focused on modifying the permeability through the BBB.

### 1.2.1 Blood-Brain Barrier

The BBB prevents damage to the brain and is a vital physiological barrier comprised of a complex network of micro-vessels, which protect the organ from external factors while providing it with the required nutrients.[14] However, this also makes it an obstacle for chemists when designing drugs that target the central nervous system. In comparison to peripheral capillaries where there is relatively free exchange between tissue and blood,

the capillaries found in the brain are the least permeable in the body.[14] This is due to the addition of tight junctions; these are protein complexes that stitch adjacent cells together preventing the leakage of substances between cells (Figure 3).[14] Due to the physiological architecture of the BBB, it is typically considered the rate-limiting factor for bioavailability, as it prevents the movement of 98% of small molecular drugs through and around the cells.[15]

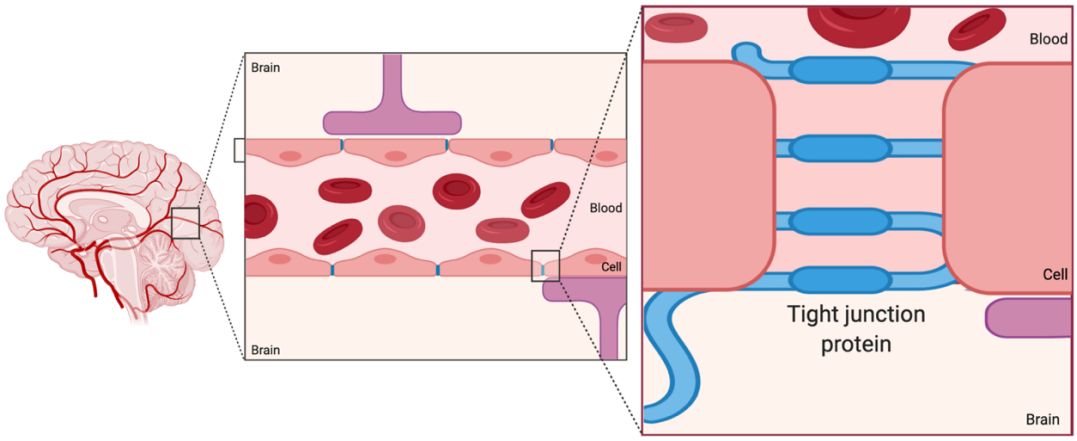


*Figure 3 – Cartoon representation of the blood-brain barrier.*

Potential drugs need to be absorbed from the blood to the endothelial cells. A pre-requisite for this movement is lipid solubility, a property which can be quantified by log P measurements. The partition coefficient, P, is the ratio of solute concentration between two solvents. When one phase is $H_2O$, and the other is a non-polar solvent like *n*-octanol, log P is a measurement of lipophilicity. Opiorphin has a log P value (partition coefficient) of -3.42 and studies show a permeability of ~3% through the BBB, which is considered very low for an analgesic drug.[10,16] The optimal log P for passive permeability through the cell membrane has been thoroughly investigated and is between -0.2 and 1.3.[17] Opiorphin's glutamine residue can be converted to pyroglutamate in physiological conditions, and this transformation preserves the analgesic effect while increasing the stability and lipophilicity as observed as an increase in log P from -3.42 to -2.49.[10] Previous studies have shown the pyroglutamate-opiorphin derivative has increased bioavailability when administered to mice.[10] An established study showed permeability to the BBB is based on surface activity, which takes into account hydrophobic and charged residues, and the molecular weight of the molecule.[18] The study showed molecules that are highly charged or comprised of larger molecule weight have lower

permeability, whereas amphipathic molecules show optimal permeability. This highlights the primary reason for the low permeability of opiorphin; under acidic conditions a positive charge on both arginine residues is stabilised by the delocalised electron lone pair of the adjacent nitrogen groups, resulting in a highly positively charged molecule, obstructing its permeability through the BBB.

The chemical modification of **4** has not been thoroughly investigated, with only one group reporting any variation of **4**.[19] A structure-activity relationship (SAR) study of **4** conducted by Rosa *et al*. demonstrated the importance of the aromatic ring on opiorphin's bioactivity with the protease NEP.[20] Further studies have shown the glutamine residues interact with DPP3, limiting the functional groups of **4** which can be modified exclusively to the arginine and serine residue.[21,22] However, as mentioned the arginine groups play the largest role in the low permeability of **4**, masking them with a physiologically labile group is advantageous and will be the greatest tool for this stream of research.

### 1.2.1 Prodrugs

With only 10% of all newly approved drugs being prodrugs, chemist have only recently started to realise their potential.[23] A prodrug consists of an active parent drug attached to a non-toxic moiety masking or altering its physiological properties (Figure 5). The moiety allows the drug to be dormant during its administration, and typically requires minimal chemical or enzymic transformation to reveal the active component.[24] Ideally, a prodrug delivers the active drug with high recovery. The first and most notable example of a viable prodrug that is still currently administered is L-3,4-dihydroxyphenylalanine (L-DOPA) **5**.[25] Initially used in 1961 to relieve symptoms of Parkinson's disease, L-DOPA is a metabolic precursor to dopamine **6** and can efficiently pass through the BBB. While dopamine has no permeability, L-DOPA is broken down by DOPA carboxylase into dopamine and $CO_2$ **7**.[26]

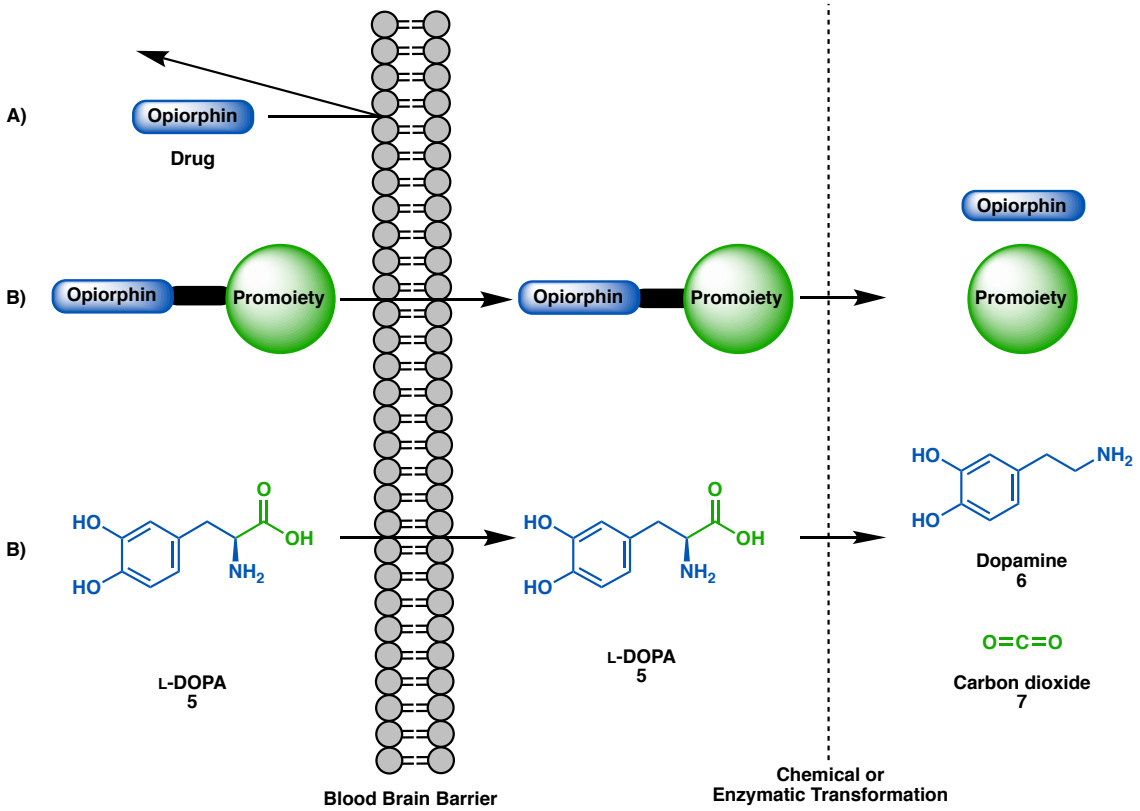


*Figure 4 – Comparison of the BBB permeability mechanism for A) unmodified drug vs B) prodrugs.*

As mentioned earlier, SAR studies have shown both arginine residues of opiorphin have no direct effect on the analgesic properties of the compound. They are also problematic for the BBB, therefore altering these groups would be the most beneficial as it could solve bioavailability without comprising activity. As the arginine residues are the core reason for the molecule's poor permeability through the BBB focusing on altering these groups would be the most beneficial route to increase permeability. Although the literature has shown the arginine side chain can be protected through the use of common protecting groups like the tosyl group, it is likely these methods would result in a permanent change. Such a derivative would not be a prodrug. Due to this, we searched for a protecting group that has been shown to detach form the arginine side chain under mild conditions. Numerous 1-(4-hydroxyphenyl)ethan-1-one derivates have been shown to mask the guanidino groups of arginine and other molecules in a reversible fashion.[27–36] Currently, the reaction between hydrate derivatives with the arginine side chain has been examined in various biological-based studies. These include selective labelling of arginine residues engaged in sulfated glycosaminoglycans binding, experiments to improve mass spectroscopy analysis of protein structures by binding cross-linkers to arginine, or various

other peptide based applications.[27,30,31] Most reports in the literature have used methylglyoxal to cap the guanidine moiety to form advanced glycation end-products (AGEs).[37] This has been highly investigated as AGEs are bio-markers that are believed to play a role in ageing and many degenerative diseases like diabetes, chronic kidney disease and Alzheimer's disease.[37,38] This indicates that a hydrate and arginine side chain reaction is possible and has been thoroughly investigated through a biological perspective. However, information that is critical to a chemist has been ignored throughout a lot of these studies. As these investigations are completed in a physiological setting, they require micro concentrations and are analysed through highly sensitive techniques. Due to this, isolation of the product has not been completed and thus yields cannot be stated. In the rare examples where yields have been stated they have come with other chemical inconsistency, which leads us to question the chemical methodology of the investigation.[31] Nevertheless, the research provides a foundation of our work to begin. The reaction conditions have been reported, and by working on a macro scale we should be able to optimise the reaction between a hydrate and the arginine side chain to produce a viable prodrug.

## 1.3 Unnatural Amino Acids – Foldamers

A foldamer is a synthetic oligomer, a molecule comprising of a monomeric units that self-organise and fold into periodic secondary structure in solution.[39] As such, foldamers mimic biopolymers, like proteins and polysaccharides. The goal of foldamer research is not to recreate natural biopolymers, nature has already perfected these structures, but to be inspired by the same principles and form new structures with properties not observed in nature. The remarkable diversity of both large and compact structures reported in the literature demonstrates that foldamers have the ability to form architectures outside of the typical α-helices and β-sheets found in nature.[39] As the selection of viable building blocks significantly increases, so too does the diversity of structures; allowing them to possess unique properties and increasing the applicability of the sequences. This has allowed foldamers to be utilised in various fields including cell penetration,[40] interactions with biomolecules,[41] catalysis,[42] medicine,[43] and more. The structures produced are direct result of the non-covalent interactions, which govern the formation of the various architectures depicted in Figure 5.[39] The intramolecular interactions driving foldamer formation are largely predesigned within the backbone sequence of the molecule in the form of aliphatic or aromatic building blocks.[39] Aliphatic foldamers have been a key focus in the majority of the literature, while aromatic foldamers are relatively unexplored and will be the key area investigated in this thesis.

This section will first outline the interactions that control secondary structure formation before looking at some of the recent examples. Although these examples highlight what the field is capable of doing now, it is only natural this is followed by looking at the roots of the field and look at the decade's worth of research required to catch up with nature.

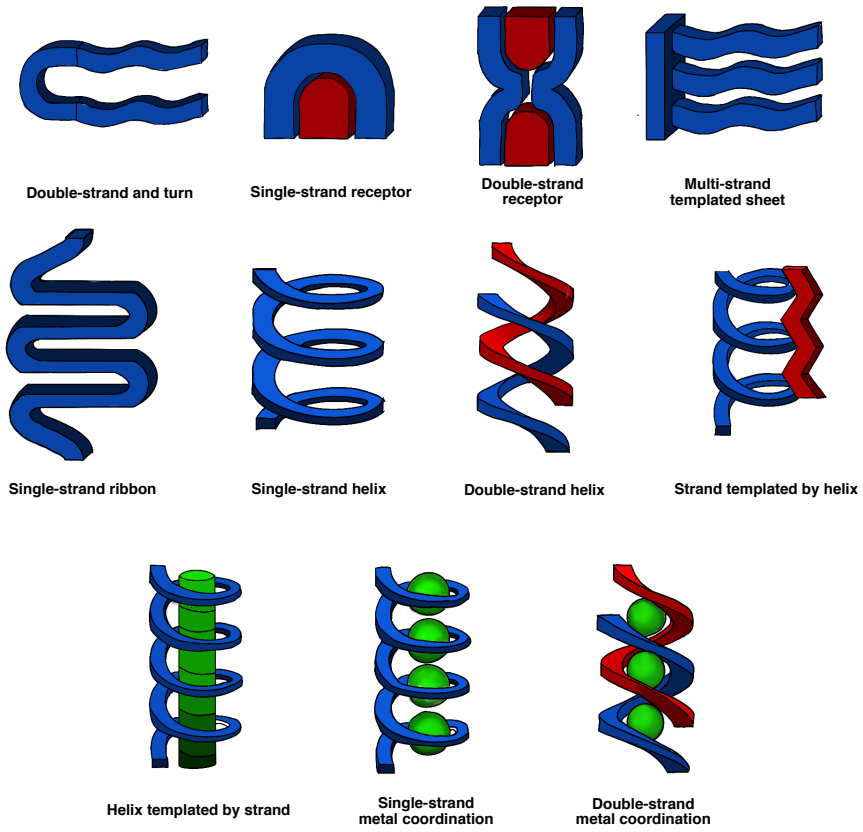


*Figure 5 – Various foldamer structures reported in literature. Adapted from reference.*[39]

## 1.3.1 Non-Covalent Interactions

### 1.3.1.1 Hydrogen Bonding

As with the secondary structure of proteins produced by natural amino acids, hydrogen bonding between repeating units is key to the formation of artificial architectures.[44] In supramolecular chemistry, hydrogen bonding is one of the most commonly exploited driving forces in the formation of highly ordered structures.[44] A variety of foldamers have been reported in the literature, highlighting the flexibility of hydrogen bonding in the primary structure of foldamers.[44,45]

### 1.3.1.2 π-π Interactions

In aromatic foldamers, the electrostatic π-π interactions between two aromatic rings play a large role in the formation and stabilisation of secondary structures.[46] The π-cloud of an aromatic ring results in a region of high electron density sitting above and below the plane of the benzene ring, while the C—H bonds are polarised towards the carbon atom, as shown in Figure 6.[47] These electronic properties play a crucial role in determining the conformation two aromatic rings will adopt.[46,47] Three main possible motifs can be used in constructing aromatic foldamers these are face-to-face, offset face-to-face, or edge-to-face (Figure 6).[47] The face-to-face orientation results in a high energy arrangement due to the repulsive electrostatic forces caused by the π electron clouds being in close proximity to one another. The offset face-to-face orientation is favoured as this allows attractive interactions.[47] The edge-to-face conformation is the most favourable conformation of two aromatic rings due to the dipole-dipole interaction of a hydrogen atom interacting with the electron cloud of the other aromatic ring, creating a C–H···π interaction.[46,47] However, to the best of our knowledge, the edge-to-face orientation has not been utilised for the construction of foldamer architectures.

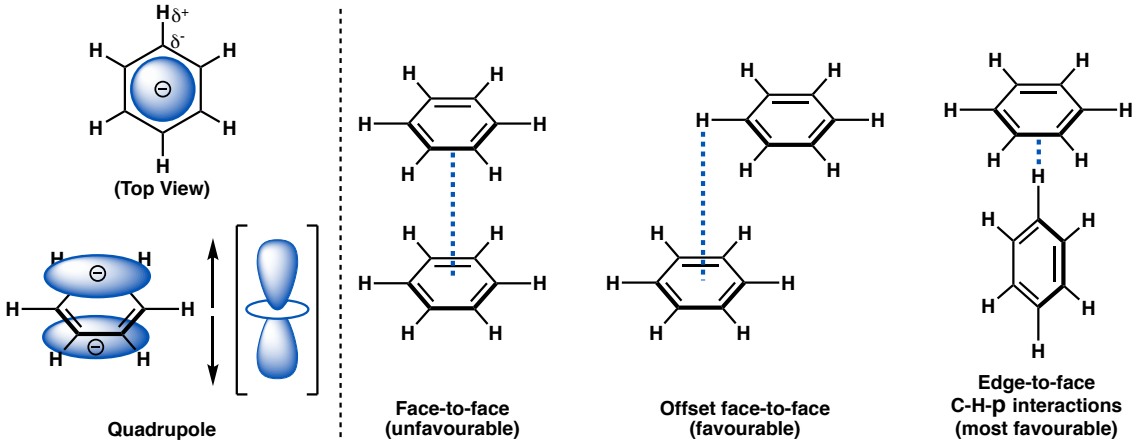


*Figure 6 – Electron distribution of a benzene ring (left) and the various interactions between two benzene rings.*

### 1.3.1.3 Solvophobic Effects

Solvophobic effects are responsible for the association of poorly solvated molecules or sections of molecules.[48] However, unlike hydrogen bonding and other specific interactions, solvophobic effects rely on the collective interactions between solvent,

solutes, and non-specific functional groups.[48] Solvent effects can be either direct or indirect.[49] Direct solvent effects compete for the supramolecular reactive sites and impede the folding, in other words they disrupt hydrogen bonding.[49] This is why hydrogen bonded supramolecular structures breakdown in $H_2O$ or DMSO.[49] Indirect solvent effects are typified by hydrophobic effects, where the forces driving association of non-polar groups in aqueous solution is from the unique properties of $H_2O$ (size and hydrogen bonding), and not the dispersive interactions among solute molecules.[48–50]

### 1.3.2 Recent Examples of Foldamers

Research into foldamers commenced over 60 years ago, and covers a range of topics.[39] There are a number of good reviews [39,51–55] so in the following section only recent, interesting examples will be discussed below.

#### 1.3.2.1 Macrocyclisation-Induced by Catalytic Foldamer

One goal of foldamer chemistry is to synthesise structures that have a function not observed in natural systems. A means of achieving this is by combining two or more types of unnatural amino acids; one gives the molecule structure while the other adds functionality.[56] This extends the scope of available transformations in comparison to those seen in nature. Gellman *et al*. have produced a heptapeptide foldamer that catalyses the macrocyclisation of various aldehydes and has led to the synthesis of two natural products; robustol **9** and nostocyclyne A **10** (Figure 7).[57] The formation of macrocycles is an entropically disfavoured process and is considered a challenge for chemists.[57]

A sequence of α- and β- amino acids was used to create a specific secondary structure, a helix.[56] This created a stable three-dimensional framework, from which reactive functionality could be suspended; positioning it so that selective intramolecular aldol condensation reactions to occur. Gellman *et al*. analysed multiple derivatives, altering the position of the two reactive functional groups, which influenced the efficiency of cyclisation.[57] The optimal sequence, **8,** is shown in Figure 7. This sequence was then compared to small-molecular catalysts which served as analogues of the active site of the foldamer but without the positioning effect. These failed to furnish the desired macrocycle under the same conditions.[57] This demonstrates how the three-dimensional structure formed by the foldamer plays a crucial role in macrocyclisation. The foldamer was

capable of synthesising macrocycles as large as 22 atoms, proving foldamers can control the selectivity and reactivity that previously were characteristics exclusive to enzymes and proteins.[57] This recent example shows how the development of a new foldamer catalyst opens up the possibility of alternative transformations beyond the aldol reaction, enriching the general synthetic repertoire currently available to chemists.

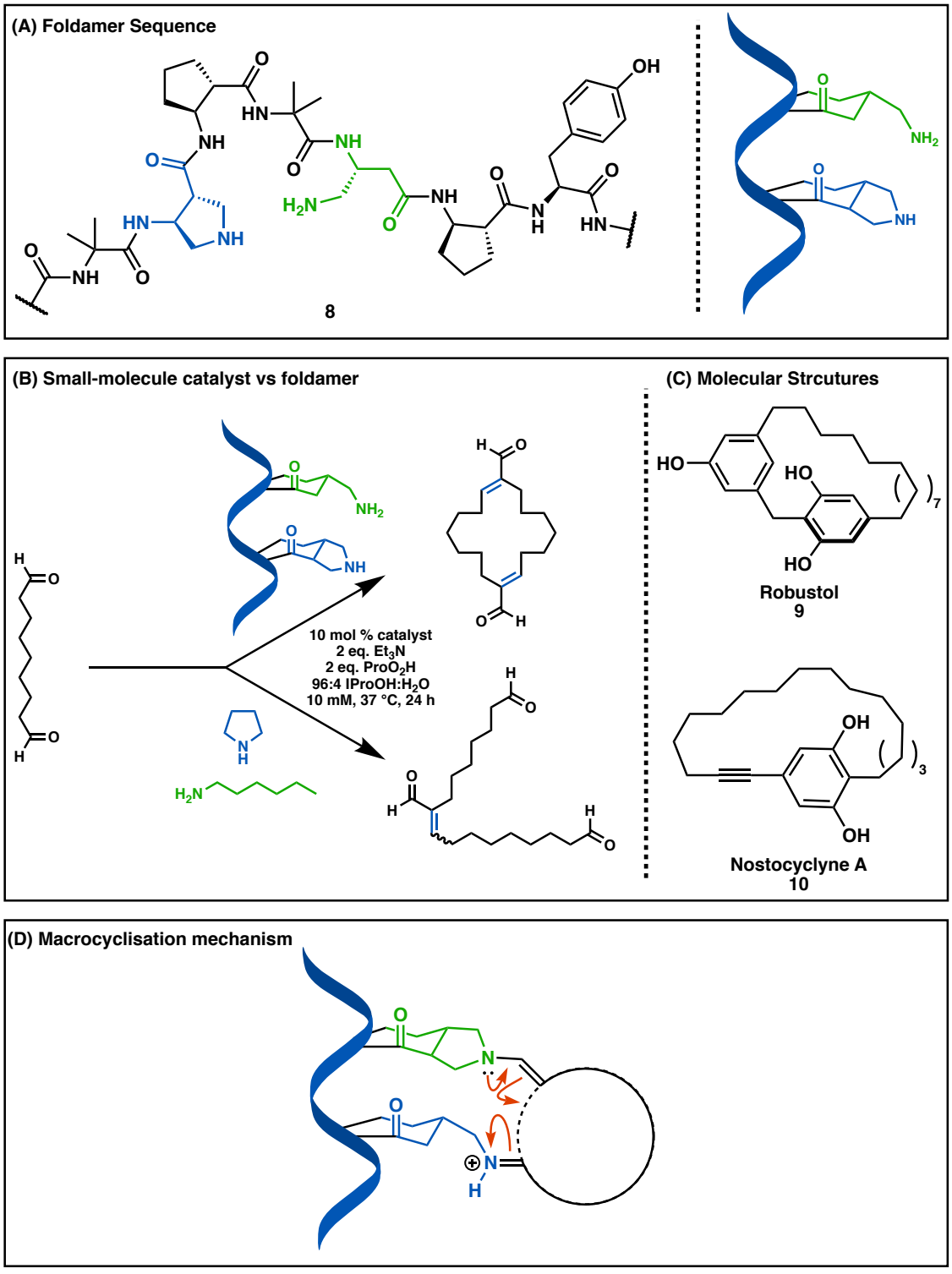


*Figure 7 – (A) Molecular structure of the most effective foldamer sequence synthesised for*

*macrocyclisation.[57] (B) Reaction conditions for macrocyclisation comparing a small-molecular catalyst to a synthesised foldamer. (C) Molecular structure of the two natural products synthesised using foldamer sequence. (D) Macrocyclisation mechanism utilising the foldamer developed by Gellman et al.[57]*

### 1.3.2.2 Foldamers for Biological Cures

Huc *et al*. have developed aromatic foldamers containing phosphonate and carbonyl groups that mimic B-DNA in both the charged surface and solid-state structure, as determined by X-ray crystallography (Figure 8).[58] This type of foldamer has been reported to be a competitive inhibitor of DNA topoisomerase 1 (Top1) and human immunodeficiency virus integrase (HIV-1 IN).[59] The group synthesised a foldamer using $Q^{Pho}$, $^{m}Q^{Pho}$, and $Q^{5Pho}$ (**11**-**13**, respectively) building blocks. A alternating sequence of $^{m}Q^{Pho}$ and $Q^{Pho}$ or $Q^{5Pho}$ was shown to develop a helical structure with a ~35° minor groove twist. The helical structure is a result of electrostatic repulsion and offsets face-to-face orientation of the aromatic building blocks stabilised by hydrogen bonding similar to the helical structure adopted by DNA, as shown in Figure 8B. Although they were initially designed to resemble DNA, the most remarkable properties are due to their differences. These alterations result in the formation of a more versatile sequence, while maintaining stability. A homogenous sequence of $(Q^{Pho})_8$ showed remarkable stability of the secondary structure in protic solvents. The helical structure was maintained even at 120 °C in DMSO, whereas DNA begins to denature at 60 °C.[58] The foldamers were found to be able to bind and inhibit several DNA-binding enzymes at a higher affinity than DNA itself. The sequence of $(^{m}Q^{Pho}Q^{Pho})_8$ was shown to inhibit HIV-IN, while in comparison $(^{m}Q^{Pho}Q^{5Pho})_8$ was shown to have a lower binding affinity.[59] Camptothecin and raltegravir are considered the best inhibitors for Top1 and HIV-1 IN, respectively, and were shown to have a lower affinity than the designed foldamer, demonstrating the versatility of these compounds and efficiency over natural biomolecules.[59]

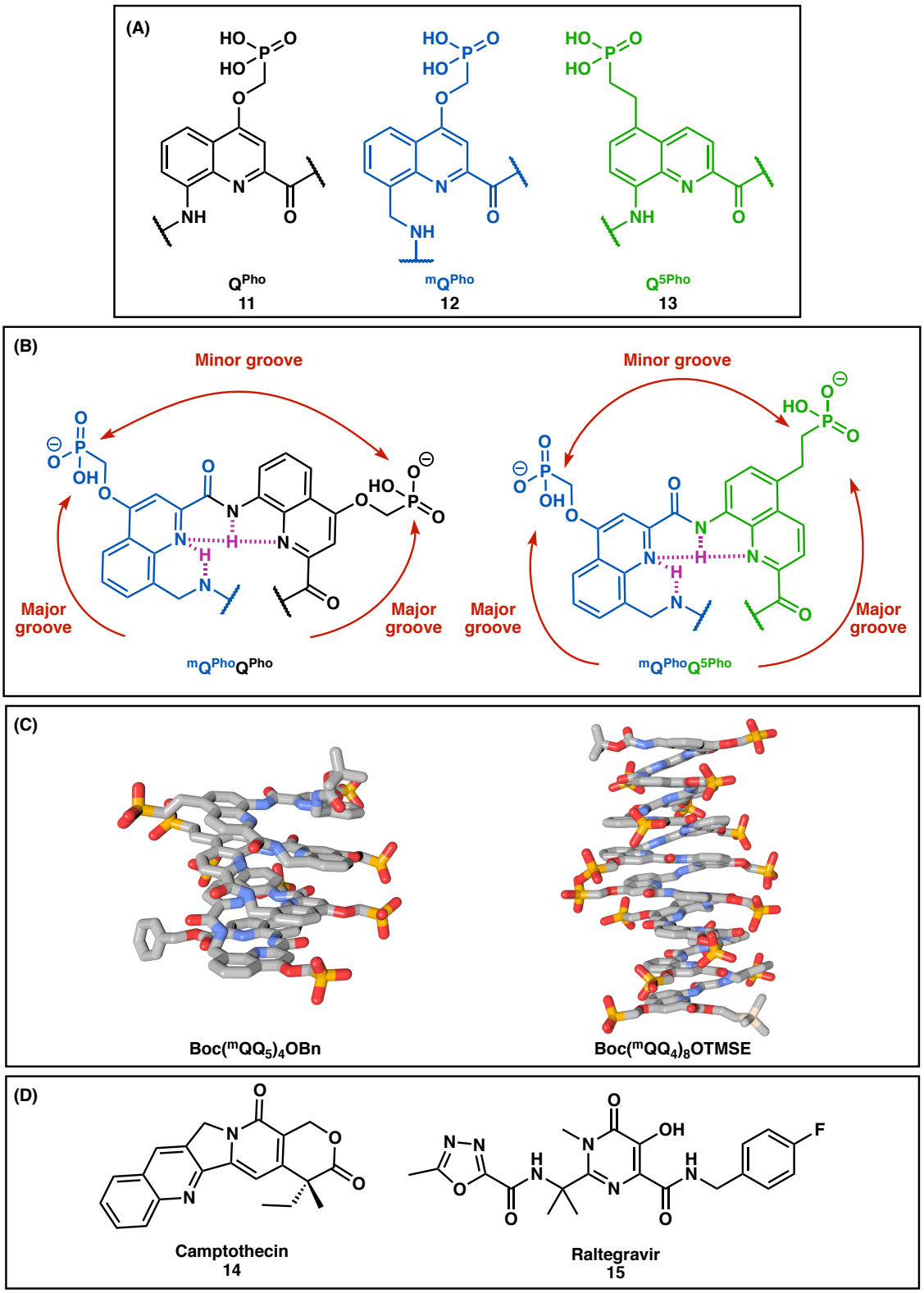


*Figure 8 – (A) building blocks used to mimic DNA synthesised by Huc et al. (B) Foldamer heterogenic sequence synthesised for HIV-IN and Top-1 inhibition. (C) X-ray structures of the two foldamer sequences synthesised. (D) Molecular structure of Camptothecin and Raltegravir.*

Although foldamers have only recently begun to be used in biological and chemical applications, the architectures being developed today are a result of decades of research

looking at various techniques and building blocks to induce folding. The following section will briefly look at the two classes of foldamers, aliphatic or aromatic, and highlight related examples and principals to this thesis.

### 1.3.3 Aliphatic Foldamers

The vast majority of foldamer research has focused on aliphatic foldamers, which are sequences comprised of saturated building blocks relying on hydrogen bonding and solvophobic effects to induce folding.[39,43,60,61] Peptidomimetic foldamers are a sub-class that have been the initial driving force of foldamer research. Peptidomimetic foldamers mimic natural proteins but are comprised of unnatural amino acids. Most of these are β-, γ-, or δ- amino acids. These differ from standard α-amino acids by addition of extra methylene (-$CH_2$-) groups between the amine and carboxylic acid. These backbone sequences can be functionalised to produce a variety of foldamers and are summarised in Figure 9.[39] Although these foldamers were the foundation of the field, the research completed in this thesis revolves around the development of an aromatic foldamer. For this reason, the details of aliphatic foldamers will not be discussed further.

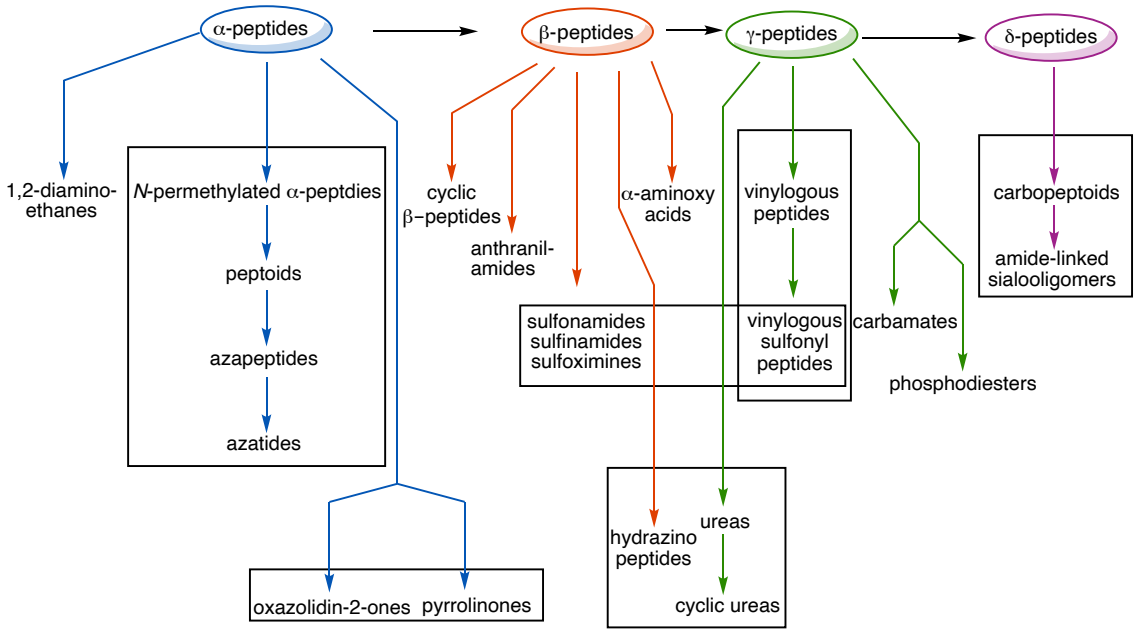


*Figure 9 – Various categories of aliphatic foldamers seen in the literature. Adapted from reference.*[39]

### 1.3.4 Aromatic Foldamers

Aromatic building blocks offer an alternative route to the synthesis of novel architectures. Amide linkages are used to promote hydrogen bonding, but other non-covalent interactions also play a critical role in developing higher order architectures. Since the 1990s, a range of aromatic foldamers with unique architectures have been constructed.[41,46] One may intuitively presume rigid aromatic rings hamper the formation of secondary structures like helices as they prevent conformational freedom. However, the rigid backbone allows for a predictable arrangement of monomers. This means isomeric structures can readily be synthesised by changing the substitution pattern of the aromatic ring, resulting in different secondary structures. Alternatively, different aromatic rings (benzene, naphthalene, anthracene, pyridine etc.) are capable of producing unique structures when utilised as building blocks.

#### 1.3.4.1 Examples of Aromatic Foldamers

While aromatic foldamers permit greater control and predictability of secondary structure this comes at a cost. The lipophilic nature of aromatic rings reduces water solubility and makes it more problematic to prepare biologically active assemblies. Chemists have risen to the challenge with a number of innovative solutions. Iverson *et al*. synthesised a water-soluble aromatic foldamer called an "aedamer".[63] This involved alternating 1,5-dialkoxynaphthalene (DAN) and 1,4,5,8-naphthalenetetracarboxylic acid diimide (NDI) linked by amino acids (Figure 10). The success of this system is due to the strong interactions between the electron rich DAN core and the electron deficient NDI core. The complementary groups allow for charge-transfer absorbance from the HOMO of the donor (DAN) to the LUMO of the acceptor (NDI), stabilising a face-centred geometry of the aromatic rings.[63] This system is now an archetypal foldamer due to its π-π interactions and electrostatic complementarity. Many new foldamers are based on this design principle as it promotes secondary structure formation. Two oligo sequences were designed with aromatic units that are linked by aspartic acid residues, providing water solubility. The use of aspartic acid residues is chosen to mimic DNA, where the negative charges result in non-specific oligomer aggregation, driving the DAN-NDI interaction,

and showed a 1:1 binding stoichiometry with the ability to discriminate between the two strands.[63]

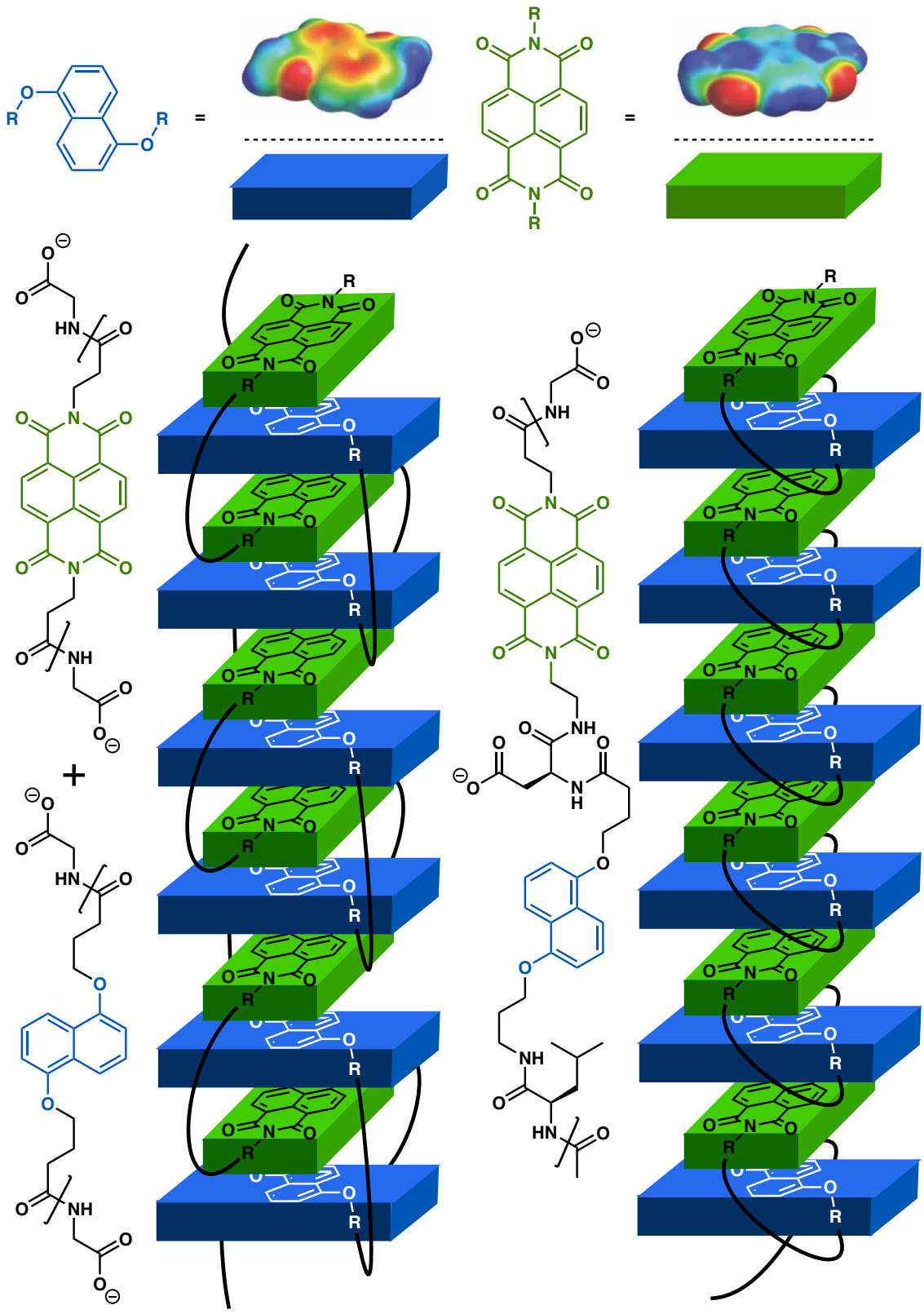

*Figure 10 – Molecular structure and folded conformation of two DAN-NDI foldamers.*

Moore *et al*. showed *m*-phenylene ethynylene will fold into a dynamic helical conformation when dissolved in polar solvents like MeCN.[64] Solvophobic interactions cause the structure to unravel into a random conformation in less polar solvents, such as $CHCl_3$.[64] The foldamer is photoresponsive and irradiation causes the helix to switch directions, a characteristic which is rarely reported. Modelling shows the diameter of a foldamer of 12-units has an interval cavity of 8.7 Å.[64] This cavity has been shown to host small solvent molecules that are readily displaced in a mixture of 40% water and MeCN. Hydrophobic molecules with binding energies in the range of 4-5 kcal/mol can bind within the cavity. Due to the larger size of an oligomer built from 22 monomers, it is able to constrain rod-like guest such as *cis*-(2*S*,5*S*)-2,5-dimethyl-*N,N'*-diphenylpiperazine, as shown in Figure 11.[39,64] The host guest interaction is solvophobically driven by the burial of poorly solvated surfaces. The tightest binding is found when there are complementary interactions between host and guest. This occurs when the host and guest molecules are matching in terms of shape and size.[64] The highest binding of *cis*-(2*S*,5*S*)-2,5-dimethyl-*N,N'*-diphenylpiperazine occurs when n = 20 and 22 as shown by circular dichroism measurements.[64] Despite these aromatic oligomers solely relying on non-covalent interactions, the restricted rotation and strong geometric constraints are essential to the formation of secondary structures of these foldamers.

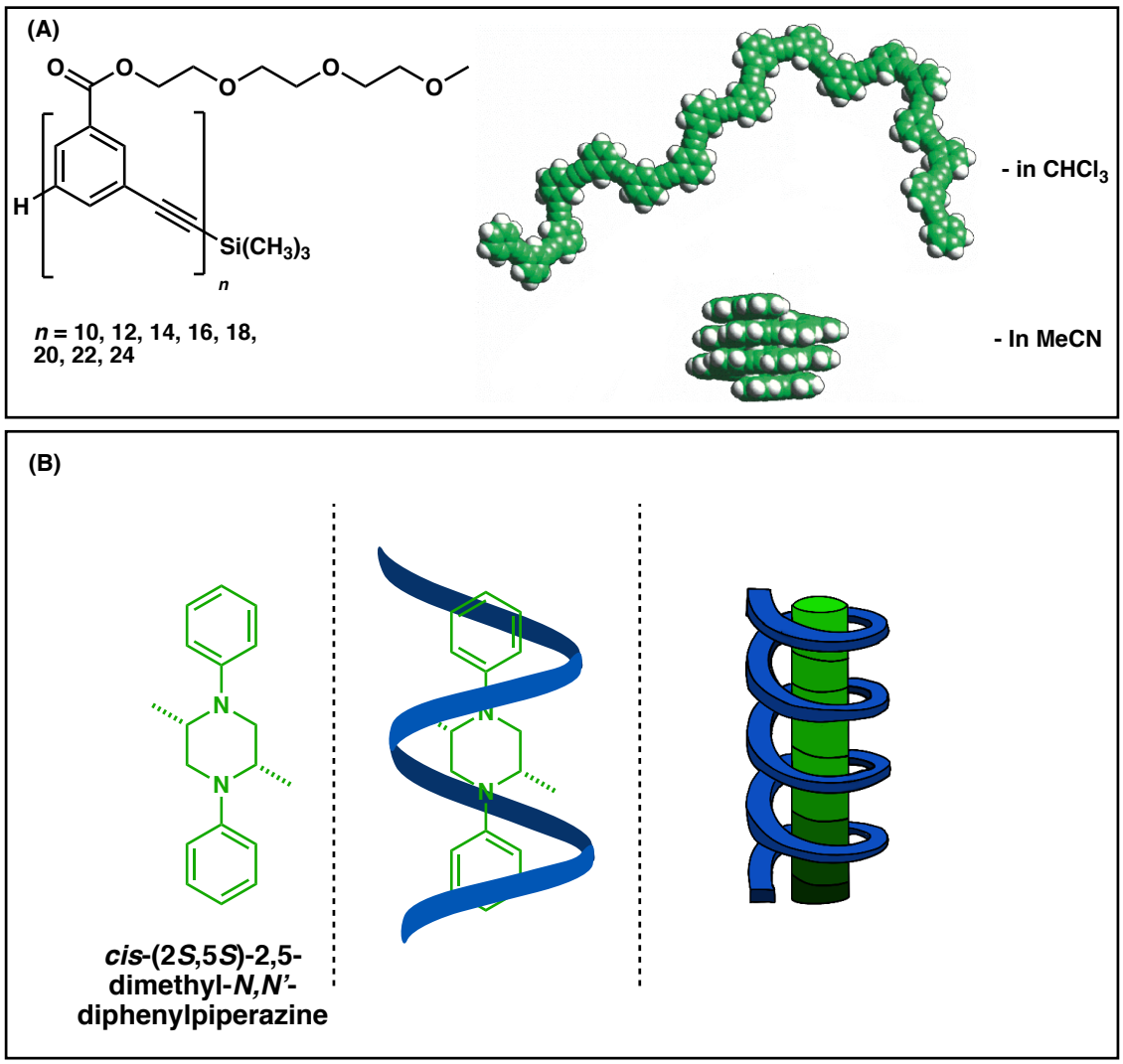


*Figure 11 – (A) Chemical structure of and oligo(m-phenylene ethynylene)-based foldamer with X-ray crystal structure (with PEG R group omitted for clarity). (B) Chemical structure of rod-like guest with a cartoon representation of the helix templated by strand foldamer structure.*

Large strides in the formation of novel architectures have been made in the past three decades. From the common α-helices, first produced using β-amino acids in the 1990s, to the formation of rod-helix templates, catalyst and functional foldamers that can out preform small molecular catalysts. The successful synthesis of future foldamers will need to take into consideration two key design principles; first, the balance of attractive and repulsive non-covalent interactions to stabilise the desired structure. Secondly, the flexibility and rigidity of the backbone of these structures need to be taken into account, as these structures need to be able to readily form. There is still a significant amount of work to be completed within this field, with many more avenues to be explored. It is clear that nature is not alone anymore, and synthetic chemists now have the tools to be able to improve on the foundation it has provided us.

## 1.4 [2.2]Paracyclophane

Cyclophanes are a class of molecule that consists of at least one aromatic ring joined by an aliphatic chain, between two non-adjacent positions. Cyclophanes constitute a diverse range of structures (Figure 12), from [2.2]paracyclophane **16** and [2.2]metaparacyclophane **17** to natural products such as cylindrocyclophane A **18** and (±)-haouamine A **19**.[65–68]

The most studied cyclophane is probably [2.2]paracyclophane. First discovered in 1949 by Brown and Farthing, it has fascinated chemists due to its unique chemical properties arising from the close proximity of the two aromatic rings.[65,69] [2.2]Paracyclophane consists of two benzene rings joined by two ethylene bridges *para* to one another in a face-to-face conformation. It is a versatile framework used in applications such as asymmetric catalysis,[70] stereoselective synthesis,[71] and its original application as a precursor to a polymeric surface coating.[72] [2.2]Paracyclophane will be used in this strand of research, as the scaffold for a foldamer.

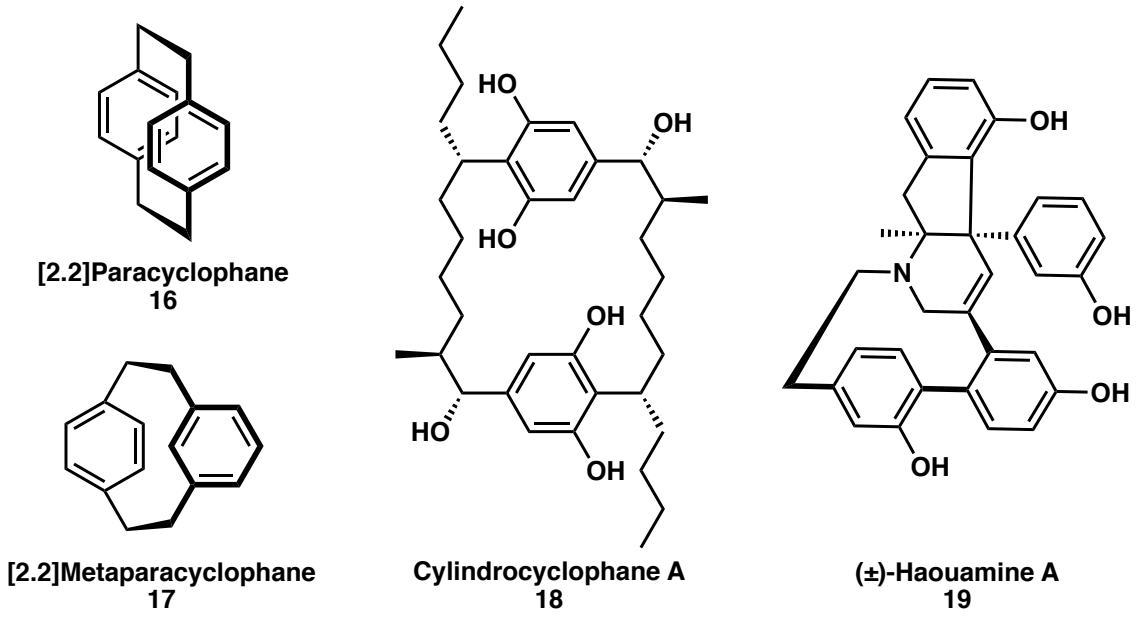


*Figure 12 – Examples of cyclophanes. [2.2]Paracyclophane **16**, the core building block for this strand of research. [2.2]Metaparacyclophane **17**, a rare cyclophane explored in later chapters. Cylindrocyclophane A **18**, a [7.7]paracyclophane natural product isolated from cyanobacteria and the first class of cyclophane compounds found in nature.[68] (±)-Haouamine A (±)-**19**, a cyclophane compound isolated from Aplidium haouarianum, a marine invertebrate.[67]*

Although [2.2]paracyclophane **16** is commonly depicted as two eclipsing rings, the rings are slightly distorted and rotated around 5°, with the ethylene bridges being extended by 0.09 Å more than the usual 1.54 Å for a C-C bond.[73,74] The unique bent and battered boat-like structure of [2.2]paracyclophane results in its distinctive properties as the π-electron clouds of each ring overlap.[73] This leads to the highest occupied molecular orbital (HOMO) of [2.2]paracyclophane being higher in energy than other alkylbenzenes derivatives such as *p*-xylene, causing it to have increased reactivity in many reactions.[75] The chemistry of [2.2]paracyclophane is full of idiosyncrasies, with many traditional reactions giving surprising products. These differences can be attributed to the steric and π-π interactions.

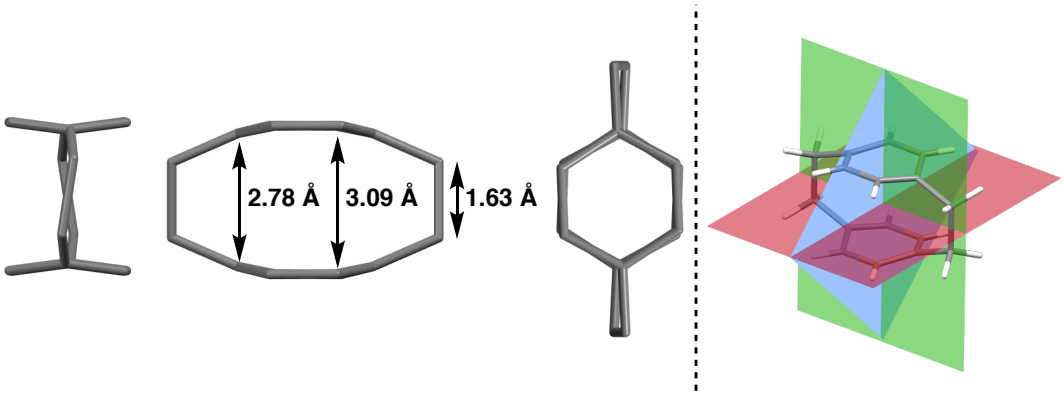


*Figure 13 – X-ray crystallography data of [2.2]paracyclophane **16** highlighting structural features and mirror planes.*[76]

An attractive feature of [2.2]paracyclophane as a scaffold is the ease of accessing planar chirality. As shown in Figure 13, [2.2]paracyclophane contains three mirror plans resulting in the parent compound being achiral. However, once a substituent is added to the scaffold the mirror planes no longer exist and the [2.2]paracyclophane derivative will exist as enantiomers. Numerous substituted [2.2]paracyclophane have been reported and a few of the common substitution patterns are highlighted in Figure 14.[77] It is important to note some substitutions patterns are inherently chiral, regardless of R groups, while others require unlike substituents ($R^1 \neq R^2$). Additionally, although Figure 14 only highlights mono- and di- substituted [2.2]paracyclophane , tri- and tetra- substitution patterns are also known.[78,79] Some substitution patterns are more easily prepared than others. This can be attributed to the unique directing effects of functional groups attached to [2.2]paracyclophane that allow them to direct reactions to the opposite ring. Positions on the second ring are defined by the suffix *pseudo*. An example of these directing effects

can be seen in Chapter 2 where a nitro group can influence the adjacent ring to produce *pseudo-geminal* derivatives. As a result, the *pseudo-geminal* position is considered one of the easiest substitution patterns to form. For this reason, this arrangement is used in this strand of research.

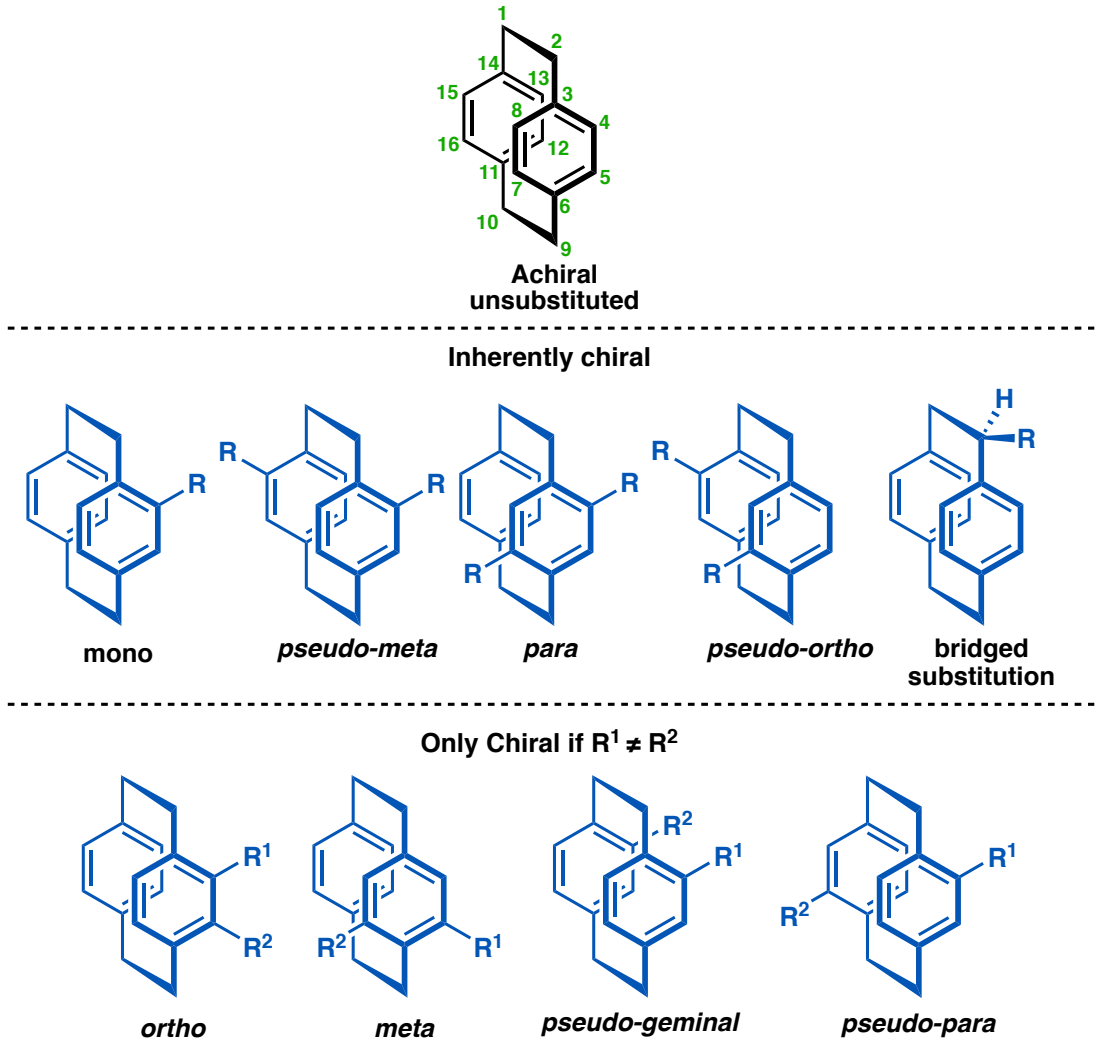


*Figure 14 – Common substitution patterns for [2.2]paracyclophane with chiral substituent patterns highlighted.*

## 1.4.1 [2.2]Paracyclophanes as Asymmetric Catalysts

The growing importance of [2.2]paracyclophane in asymmetric catalysis has been demonstrated by phosphines, such as PhanePhos **20** [80] or the imines developed by Stefan Bräse **21** [81] or Daniel Glatzhofer **22**.[82] Each of these catalysts has been thoroughly investigated in the literature and utilised in a variety of reactions including hydrogenation,[80] diorganozinc aryl and alkyl transfers,[81] metal complexation and cyclopropanation.[82] As catalysis is not a large focus of this research, only one example, PhanePhos **20**, will be discussed.

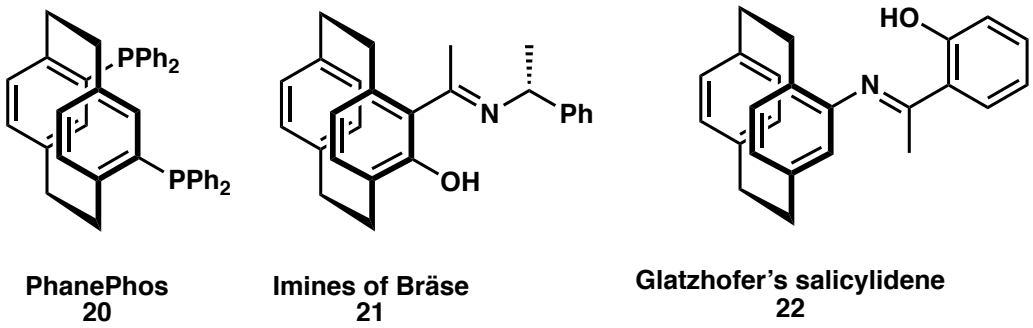


**PhanePhos 20** **Imines of Bräse 21** **Glatzhofer's salicylidene 22**

*Figure 15 – Molecular structures of a range of [2.2]paracyclophane asymmetric pre-catalysts.*

PhanePhos, developed by Roseen and Pye, has had the largest influence on the development of new [2.2]paracyclophane catalysts as it was possibly the first [2.2]paracyclophane catalyst and of the most used.[80,83] The catalyst has been reported to have high selectivity and increased efficiency than comparable rhodium and ruthenium-based catalysts.[83] As alluded to earlier, PhanePhos **20** is primarily used as a ligand for rhodium or ruthenium catalysed hydrogenations. The cationic rhodium catalyst **27** was found to give increased yields to the catalyst formed *in situ* and allow for hydrogenations to occur at low temperatures such as -45 °C (Scheme 1).[83] As seen in the hydrogenation of tetrahydropyrazine.[83] 2,2′-Bis(diphenylphosphino)-1,1′-binapthyl (BINAP) **23** had been utilised previously, resulting in only 56% *ee* and requiring harsher conditions (40 °C at 70 atm for 24 hours), while Et-DuPhos **24** gave 50% *ee.* PhanePhos gives 86% *ee* at -40 °C.

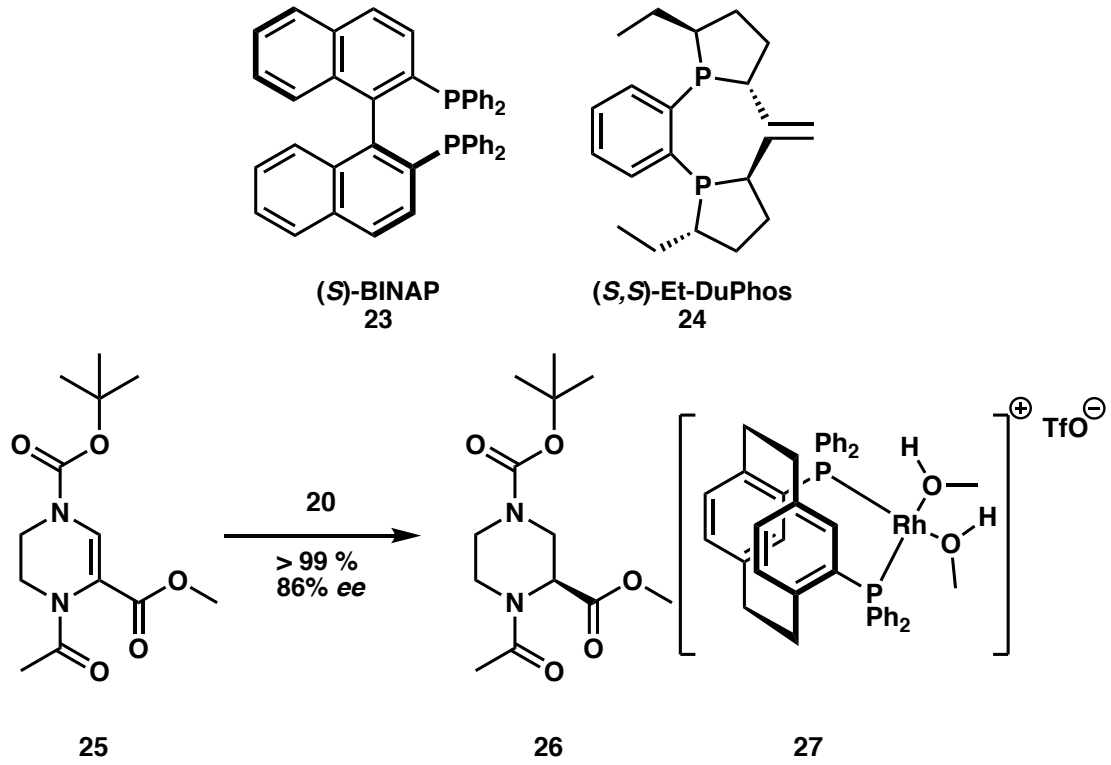


*Scheme **1** – Molecular structures of (S)-BINAP **23** and (S,S)-Et-DuPhos **24**, both poorly performing catalyst for the hydrogenation of tetrahydropyrazine. PhanePhos performs the reduction of **25** reliably under mild conditions (2% mol), $H_2$ (1.5 atm), -40 °C, 6 h, while yielding >99%, 86% ee.*[83]

## 1.4.2 [2.2]Paracyclophanes as a Scaffold for New Materials

Not only has [2.2]paracyclophane found applications in asymmetric catalysis but it is also a good scaffold due to its rigidity and ability to position substituents. Some examples are highlighted in Figure 16. Chujo *et al*. developed an optically active cyclic cage **28** (Figure 16 – A), containing a stacked π-electron system by utilising a *pseudo-ortho* isomer of [2.2]paracyclophane. While Filichev *et al*. incorporated enantiomerically pure [2.2]paracyclophane into DNA forming an architecture resembling a zipper (Figure 16 – B). The assembly **29** was shown to be stable at room temperature, which is a crucial component to for these chiral assemblies to be used in applications.[84] A tetra-substituted [2.2]paracyclophane **30** has been utilised to form unique hydrogen bonded extended structures (Figure 16 – C).[85] Castellano *et al*. has formed a tetraamide that self-assemblies by exploiting transannular and intramolecular hydrogen bonding interactions.[85] By balancing the enthalpically unfavourable face-to-face stacking and the enthalpically favourable formation of hydrogen bonds, the off-set stacking can reduce the enthalpic

cost producing a larger net binding energy assisting in self-assembly. This is very encouraging for our foldamer project.

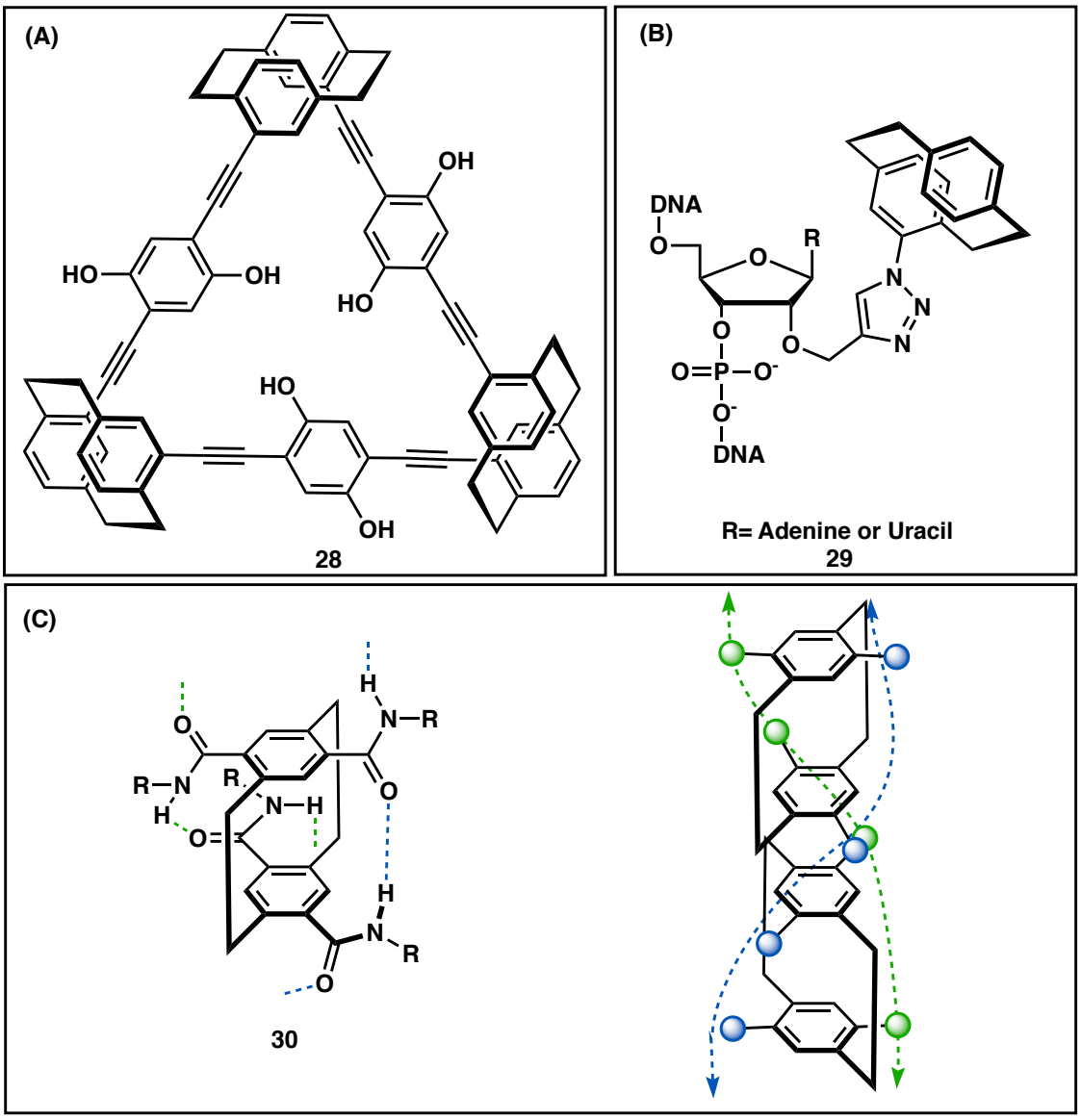


*Figure 16 – A variety of architectures that utilise [2.2]paracyclophane as a key building block. (A) [2.2]Paracyclophane used in the formation of a cage* ***28****.*[86] *(B) [2.2]Paracyclophane functionalised deoxyribonucleic acid* ***29*** *(C) A tubular [2.2]paracyclophane sequence* ***30****.* [85]

Another particular interesting oligomer, is the *pseudo-geminal* substituted [2.2]paracyclophane scaffold developed by Collard *et al* **33** (Scheme 2).[87] Collard's group was the first to develop a polymeric system that contained *pseudo-geminal* substituted [2.2]paracyclophane (**31, 34**), where the substitution pattern resulted in a U-turn structure, and is an example of an aromatic single-strand ribbon foldamer.[87] It shows how oligomers and conjugated polymers exhibit characteristics that allow them to be used as semiconductors in thin-film optoelectronic devices.[87] This behaviour is governed by the

delocalisation of charge carries and excitons along the conjugated backbone and by the interchain interactions the π-system of closely packed chains, properties drastically increased by the stacking nature of **33**.

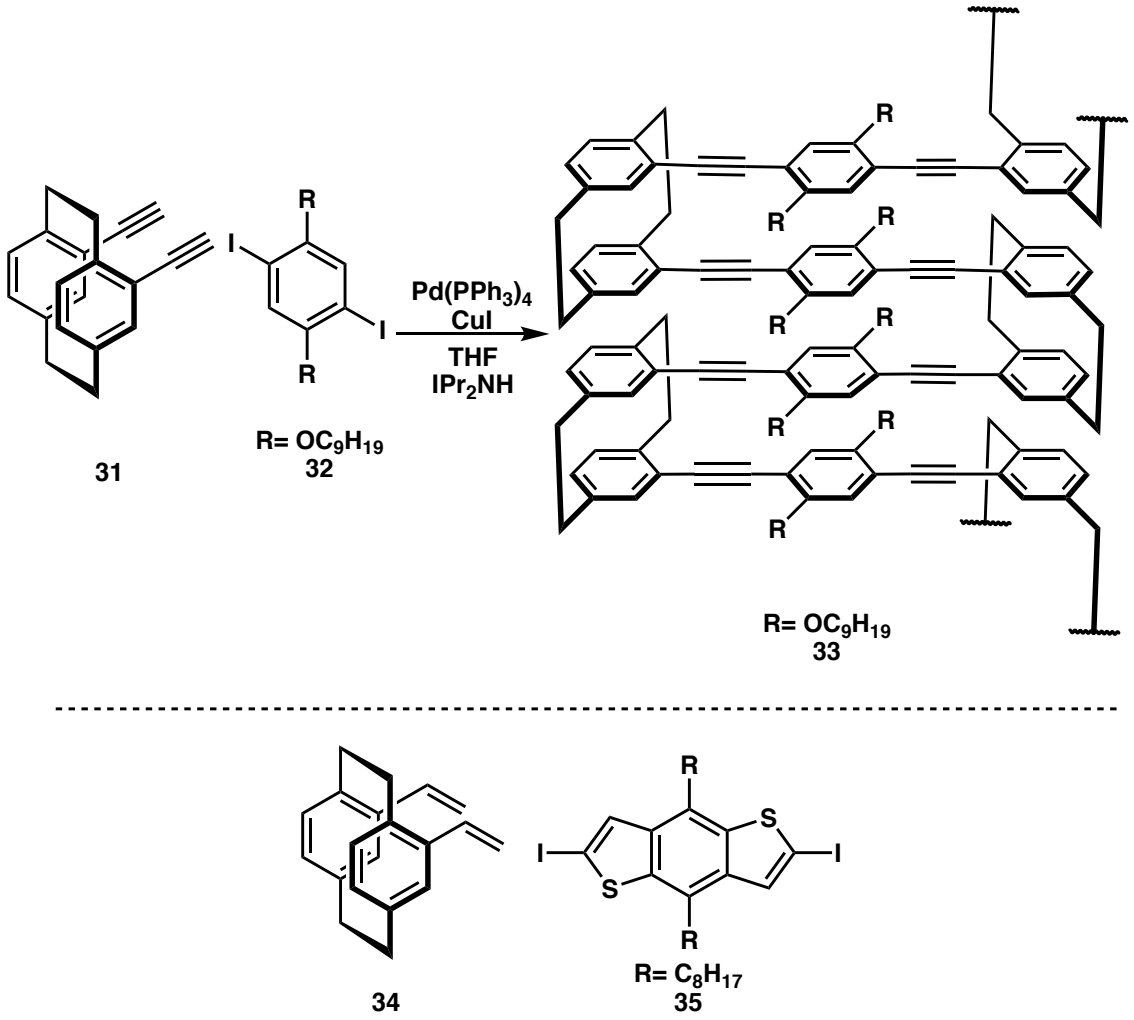


*Scheme 2 – Reaction between 4,13-diethynyl[2.2]paracyclophane **31** and **32** to produce stacked pseudo-geminal [2.2]paracyclophane scaffold **33**. Alternative building blocks **34**, and **35**, have also be used to produce scaffolds to from similar structure to **33**.*

The same group has synthesised various frameworks by linking *pseudo-geminal* [2.2]paracyclophane with aromatic units easily incorporated using Heck, Sonogashira cross-coupling polymerisation, and Stille coupling of **35** and **32**. These scaffolds have been analysed by UV-vis and fluorescence spectroscopies, as well as cyclic voltammetry and compared with their monomeric counterparts. Results showed the polymers had similar absorption maxima to their corresponding unstacked monomers. But the absorption edge of all scaffolds is red shifted by *ca*. 50 nm. This shows the stacked nature of the scaffolds synthesised has some influence on the electronic ground state. However,

the emission spectra between the stacked and non-stacked molecules show a significant difference. The unstacked controls show vibronic peaks that are sharp and distinctive, while the emission from the polymers is red shifted and broad. This can be attributed to the fluorescence quenching due to the stacking of the conjugated tiers, a commonly seen trait for thin films comprised of conjugated polymers. Additionally, all stacked polymers show a significantly larger Stokes shift of at least 60 nm, and up to 150 nm. The authors believe the two vinyl groups of [2.2]paracyclophane can be orientated away from the ethano bridge to minimise steric interaction. It is thought multiple orientations of cisoid and transoid conformations through the [2.2]paracyclophane scaffold can provide a break in stacking, limiting the extent of overlap of the π-system resulting in smaller Stokes shifts in comparison to **33** (Figure 17).

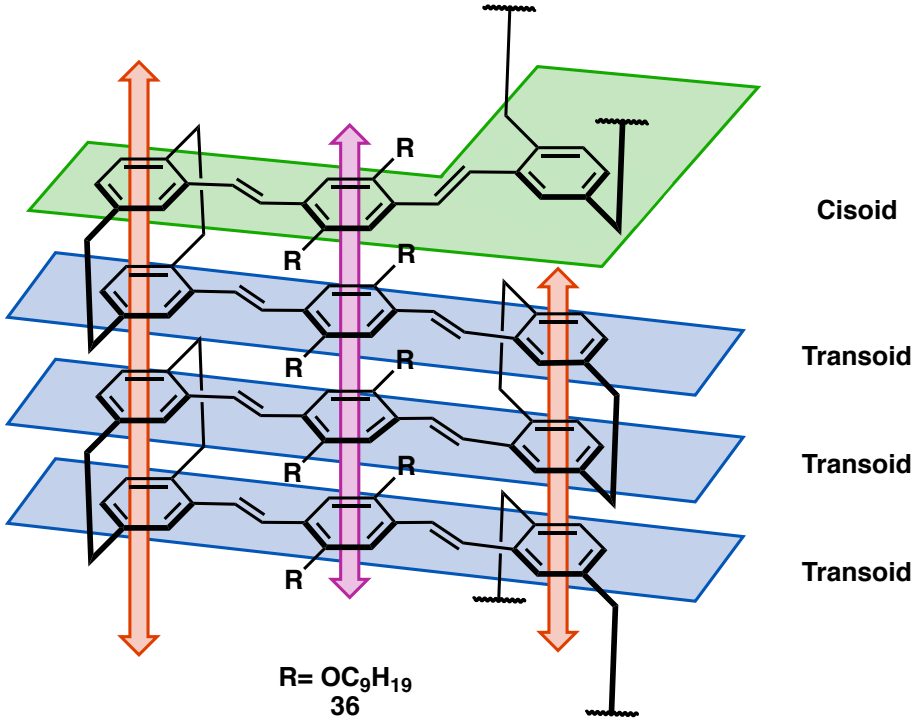


*Figure 17 – Chemical structure of pseudo-geminal phenylene vinylene [2.2]paracyclophane **36** polymer, highlighting the required overlap conformation for communication between planes.*

## 1.4.3 [2.2]Paracyclophane as Amino Acids

To form a planar chiral foldamer from [2.2]paracyclophane, an amino acid derivative of the scaffold will be joined together through a series of peptide bonds. Although there are seven possible motifs available (Figure 18), only two existing isomers have been reported in the literature. The most attractive is the *pseudo-ortho* isomer, but the synthesis is

challenging, lengthy, and low yielding. Therefore, the *pseudo-geminal* isomer was chosen as the first target. It also provides the shortest route to an amino-acid derivative; however, it possesses its own difficulties discussed in the next chapter. While the synthesis of both amino acid isomers has been reported, research utilising them has been uncommon. With the literature reporting the use of a proline-[2.2]paracyclophane derivative used in asymmetric catalysis, and the Rowlands group previously investigating *pseudo-geminal* organocatalyst.

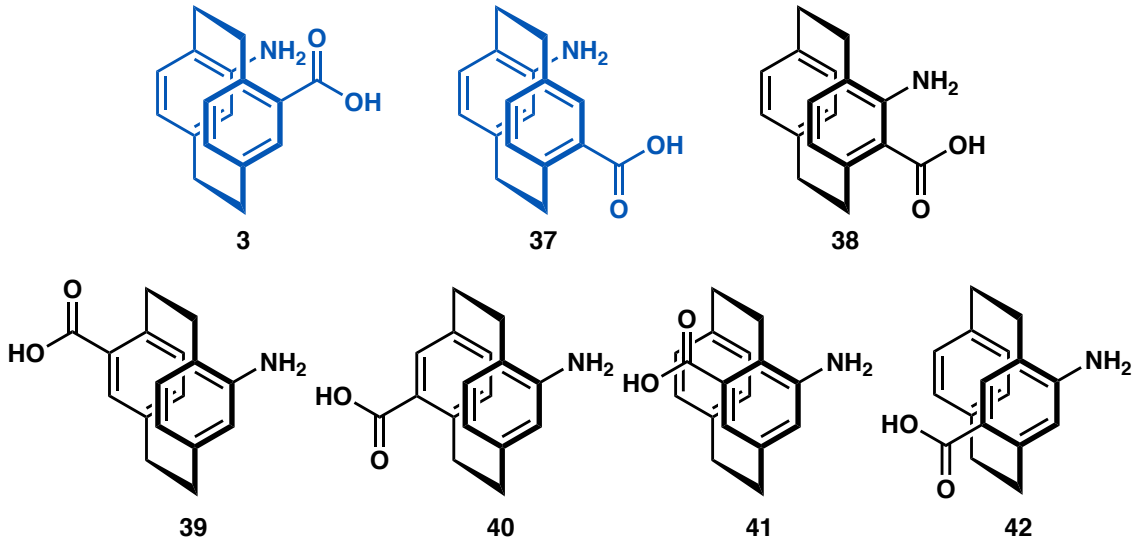


*Figure 18 – Molecule structures of possible amino acid scaffold, highlighting the isomers seen in literature.*

It is clear to see the synthesis of a foldamer utilising [2.2]paracyclophane as the core scaffold is an area that is ripe for study. Various architectures have already been produced using [2.2]paracyclophane and have been incorporated into numerous established structures like DNA. By utilising a unique framework that mimics the tools nature has provided, the potential of developing a new form of secondary structure not previously seen in the literature or nature increases.

## 1.5 Aims of this Research

As the literature review shows, the chemistry of amino acids, both natural and unnatural, is vast with numerous books written on both. Each topic still inspires chemist with research being completed daily. The goal for each strand of research narrows down to one straightforward question. Are we able to improve on nature?

### 1.5.1 Aim of Natural Amino Acid Research Strand

Opiorphin could be an effective painkiller, it is a stronger analgesic than most prescribed drugs, but it is limited by undesirable properties. Its low permeability and short duration of action must be addressed before it can be administered as a painkiller. For this strand of research, the aim is to increase opiorphin's permeability through the BBB by developing a reliable masking technique for the guanidine groups of both arginine residues and thus creating a potential prodrug.

Synthesis of a protected arginine **55** will initially be used as a template before attempting reactions on opiorphin as it is a simpler system and more abundant in a lab (Scheme 3). The literature has showed **44** derivatives as a viable masking agent for the guanidine group allowing us to incorporate varying R groups into the framework.[27–36]

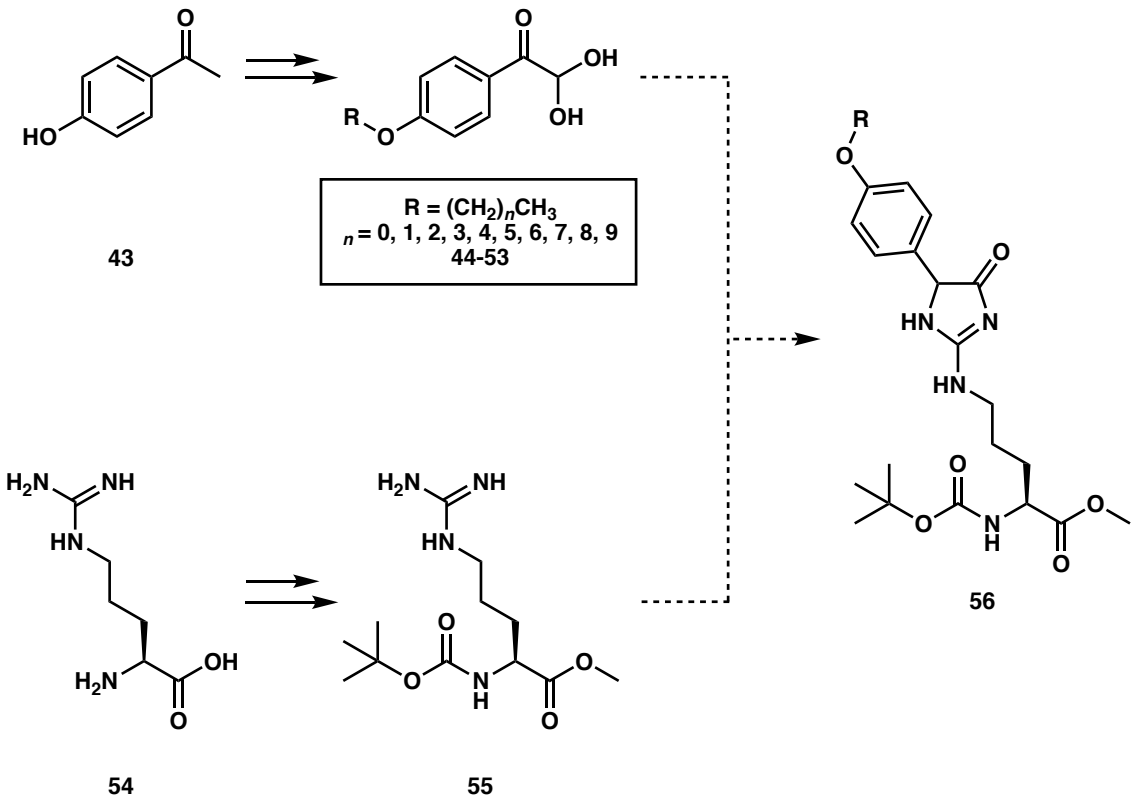


*Scheme 3 – The synthetic approach to produce the opiorphin prodrug utilising arginine as a prototype*.

Once the proof of concept has been established, synthesis of an opiorphin prodrug **57** (Scheme 4) will be completed allowing for the protected opiorphin's lipophilicity to be analysed. The synthesis of various derivatives will then be attempted to optimise the Log P between -0.2 to 1.3. The effectiveness and toxicity of the most optimal product will then be analysed by Dr Preet Singh (Massey University). From these results, the R substituent can be further explored to obtain desired results. From there, the prodrug can be finally tested as a painkiller for de-horning of animals.

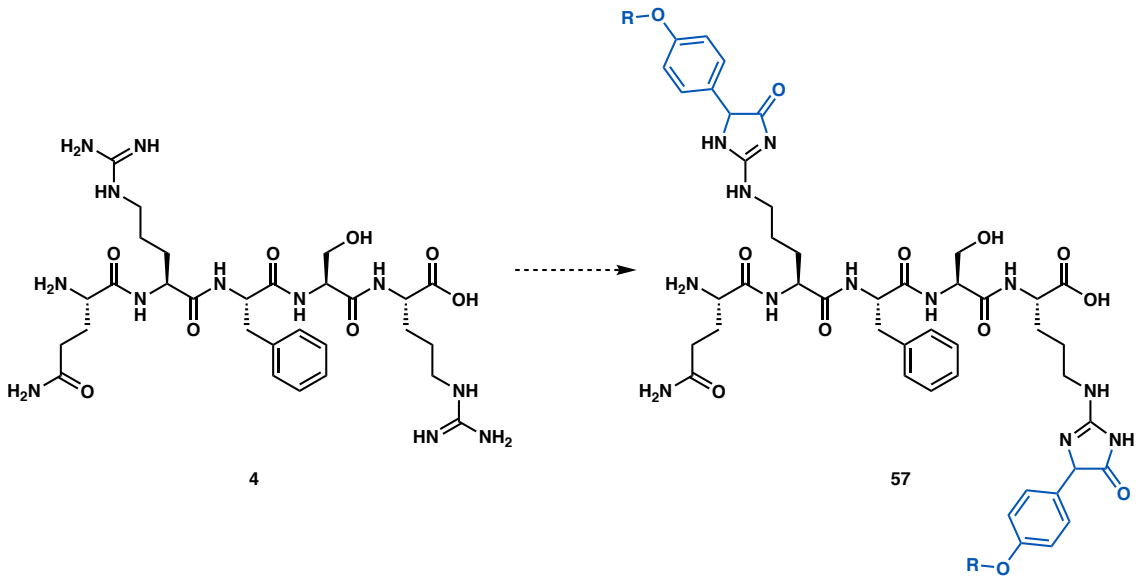


*Scheme 4 – The synthesis of an opiorphin prodrug, where R is altered to produce an optimal Log P between -0.2 to 1.3 and is non-toxic.*

## 1.5.2 Aim of Unnatural Amino Acid Research Strand

This strand of research focused on the development of the first planar chiral foldamer utilising a [2.2]paracyclophane backbone and structural studies to determine its conformation.

The foundation of the foldamer, the planar chiral amino acid precursor (±)-**58**, had to be synthesised first. Then these monomers were able to be joined by peptide bonds (Scheme 5). However, before linking multiple [2.2]paracyclophanes together, the initial monomer required a substituent to act as a cap, this prevented uncontrolled polymerisation. Once the capped derivative **59** was synthesised, we started coupling [2.2]paracyclophane amino acid derivatives to produce dipeptides **60**, **61**.

Once sufficient amounts of the dimer were obtained, the material could be split in half, allowing us to link dimer derivatives together to form a tetramer **62**. Once again, we planned to separate the acquired material in half, with each half undergoing reactions to couple them and ultimately produce an octamer, or react a tetramer with a dimer to form the hexamer **63**. This would allow us to examine the length required of our foldamer to first see folding.

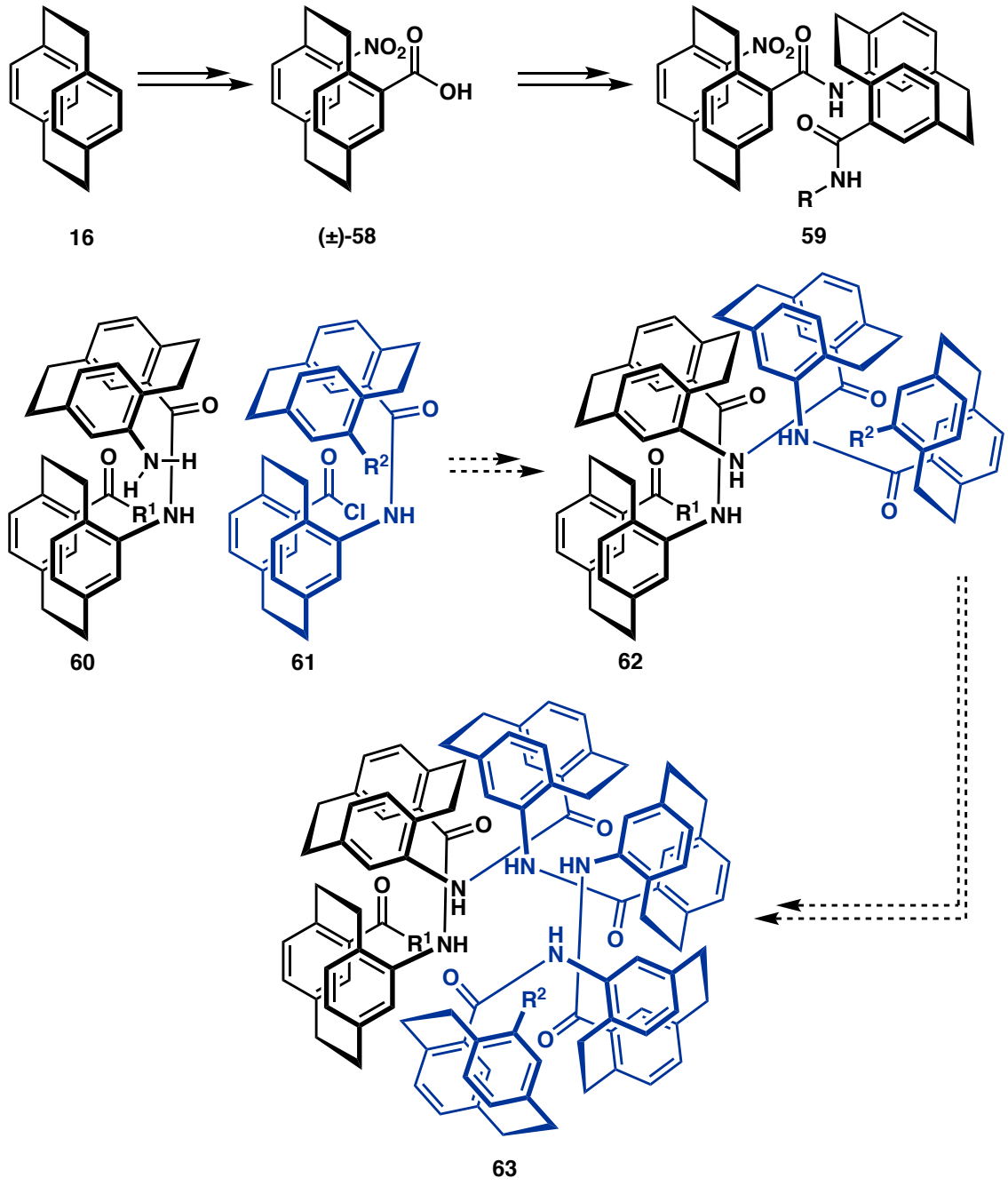


*Scheme 5 – The initial synthetic approach to synthesis a planar chiral foldamer.*

Chapter 2

# Results and Discussion

This thesis covers a broad range of topics. As such, the results & discussion will be broken up into four parts. Section 1 will discuss the results obtained from the attempted synthesis of a prodrug for opiorphin. Part two discusses our first attempts to couple [2.2]paracyclophane and the work required leading up to dimer formation. Section 3 continues the discussion of the foldamer synthesis building upon the knowledge gained in Section 3 and looks to resolve some of the issues accounted. Lastly, Section 4 investigates a reaction observed during the synthesis of (±)-4-nitro[2.2]paracyclophane.

## 2.1 Section 1 – Natural amino acids

### 2.1.1 Synthesis of Hydrate Derivatives

Our first goal was to form a greasy hydrate that would be used to protect and alter the properties of opiorphin. Synthesis of **50** was initially attempted by tosylation of the appropriate alcohol followed by substitution with a phenol (Scheme 6).[88] Activation of the alcohol was necessary as it is a poor leaving group. Tosylation was attempted by treatment of $Et_3N$ and DMAP; however, analysis of the reaction mixture by $^1H$ NMR spectroscopy revealed that no product formation had occurred. Repeating the reaction for an extended period was also unsuccessful.

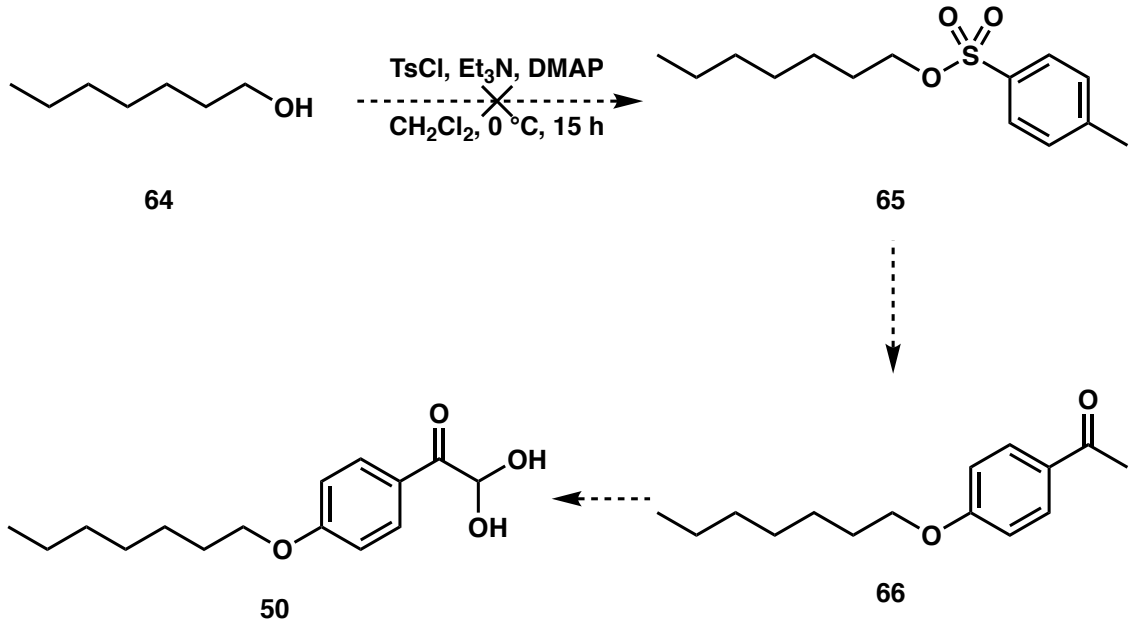


*Scheme 6 – First attempt to synthesise a hydrate derivative containing a long alkyl chain.*

For some reason the alcohol **64** was not reacting under standard conditions. This might be due to the influence of the hydrocarbon. A solvent-free, green approach, was attempted next. This required the reagents to be vigorously ground together for five minutes (Scheme 7).[89] Analysis of the $^1$H NMR of the crude reaction mixture showed that the tosylated product was the minor product with unreacted starting material making up the rest. Usually, the grinding of reagents for prolonged periods would be an automated process; we simply tried to vigorously stir the reaction overnight using ethanol and a magnetic flea as we did not have such equipment. Analysis of the $^1$H NMR showed no product formation demonstrating that the frictional force was a requirement for product formation in this reaction.

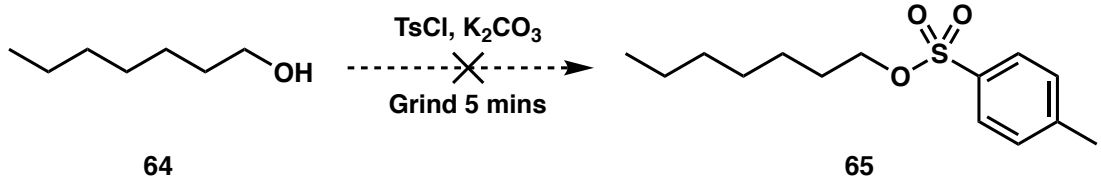


*Scheme 7 – Second attempt at synthesise of the tosylate **65**.*

As the reaction did not go to completion, an alternative and shorter route was explored. By using the alkyl halide **67**, we were able to add the aliphatic chain directly to **43** (Scheme 8). The synthesis of 1-(4-(decyloxy)phenyl)ethan-1-one **68** was achieved with yields ranging from 87-98%, with purification not required. The reaction of 1-bromodecane and 1-(4-hydroxyphenyl)ethan-1-one is a simple $S_N2$ substitution, with the

lone pair of electrons on the oxygen acting as the nucleophile, the carbon attached to the bromine leaving group, the electrophile.

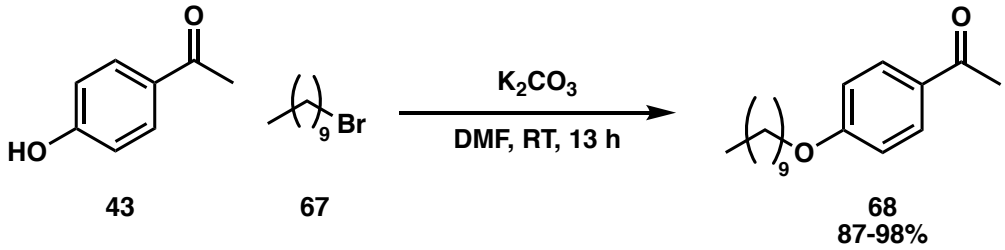


*Scheme 8 – Reaction conditions used to produce the hydrate precursor **68**.*

Synthesis of hydrate **53** was achieved in 77-83% yield through the use of $SeO_2$ (Scheme 9).[90,91] Aldehydes establish an equilibrium with $H_2O$ to produce a hydrate in the presence of an acid or base; this is known as the *gem*-diol equilibrium. Generally, the hydrate is unstable and cannot be isolated. However, due to the presence of the ketone, an electron-withdrawing group, the stability of the *gem*-diol increases, allowing β-keto-*gem*-diols to be isolated. Entropically, the equilibrium should favour the aldehyde **69** and water due to two molecules being preferred. However, both the hydrate and aldehyde are visible in the $^1$H NMR and the ratio of aldehyde to hydrate changes depending on the length of storage and storage conditions. A $^1$H NMR taken immediately after the reaction showed a larger proportion of aldehyde, while the proportion of hydrate increased, the longer the sample was left. There is a distinguishable colour change between the two, with the aldehyde being a whitish-green compound, and the hydrate appearing pink. Depending on the humidity, the colour of the compound would change daily between the two.

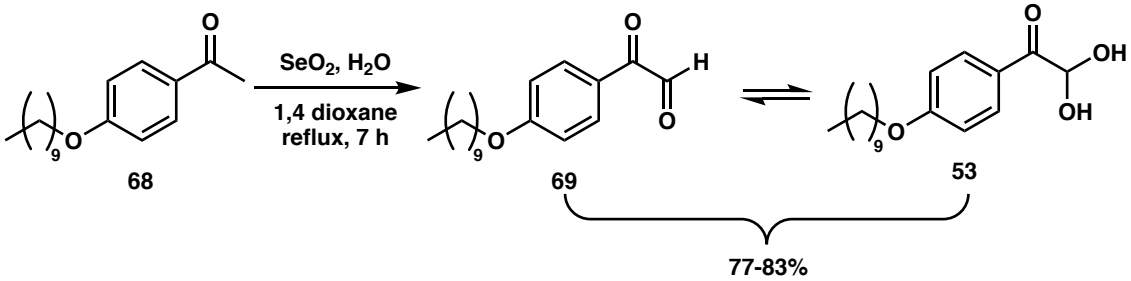


*Scheme 9 – Reaction conditions used to produce the desired hydrate **53**.*

The synthesis of **53** occurs by a selenium dioxide-mediated oxidation known as the Riley oxidation, which occurs by a series of sigmatropic rearrangements (Scheme 10). The reaction begins with enol tautomer of **68** attacking the electrophilic centre of the selenium dioxide. A Pummerer-like rearrangement occurs resulting in the loss of $H_2O$, which

attacks the alpha position causing the release of selenic acid and affording **53** in equilibrium with **69**.

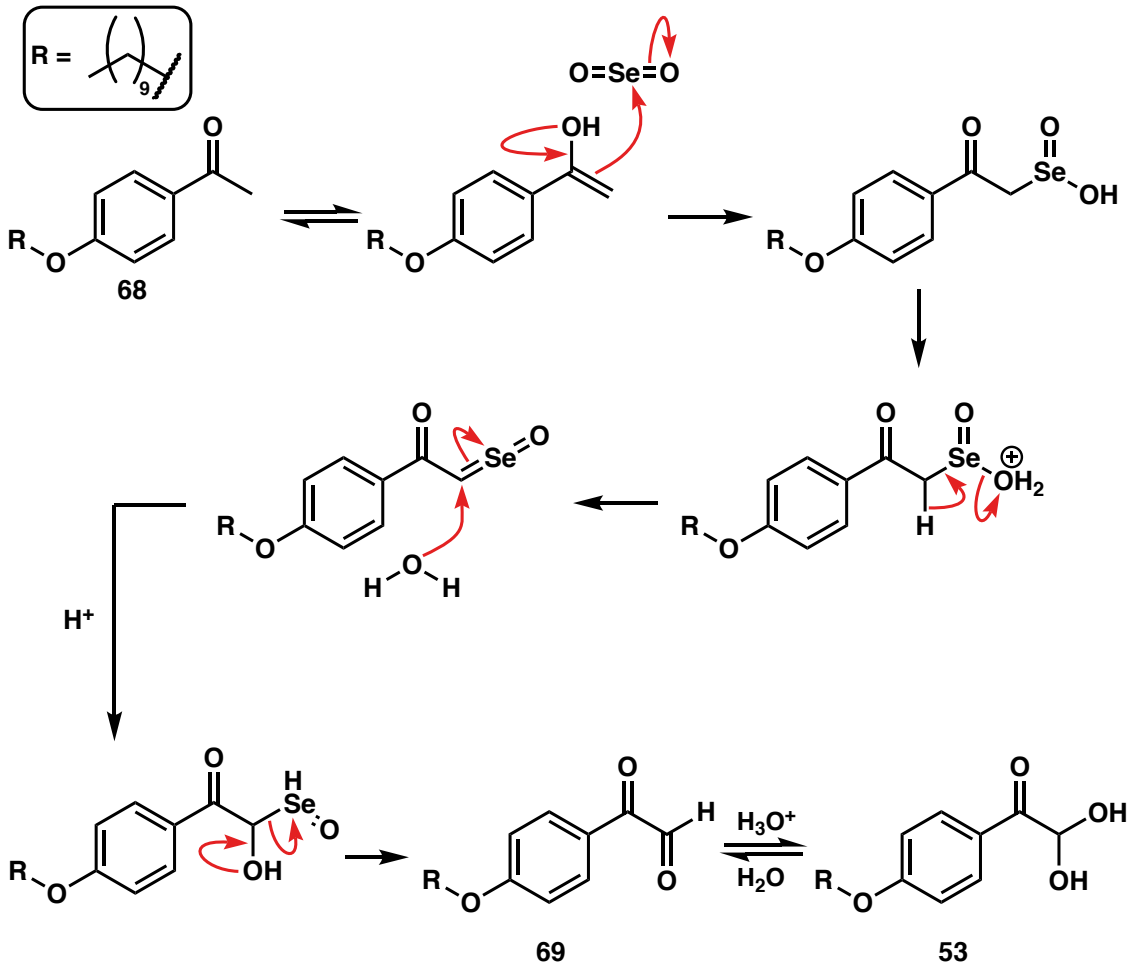


*Scheme 10 – Proposed mechanism for the Riley oxidation using $SeO_2$ to afford **53**.*

The equilibrium between the greasy *gem*-diol and the aldehyde made assignment of the $^1$H NMR spectrum challenging and caused us to question if the reaction had been successful. This, paired with mass spectroscopy not showing the desired molecular ion for either products, made us sceptical of the reaction outcome. To clarify the $^1$H NMR spectrum, the decane chain was substituted with a methyl chain to simplify the system. Both reactions (Scheme 11) appeared as successfully as the decane derivatives, with the isolation of **70** in 94-98% yield and the formation of **44** yielding 83-90%. For the synthesis of **70**, DMF was substituted for MeCN making the work-up require less brine washes. However, our efforts to simplify data analysis were in vain, as we continued to see the same issues as seen with the decane chain derivate. Efforts to push the equilibrium to the formation of **44** or **53** through the addition of $HCl_{(aq)}$ and water also proved inconclusive.

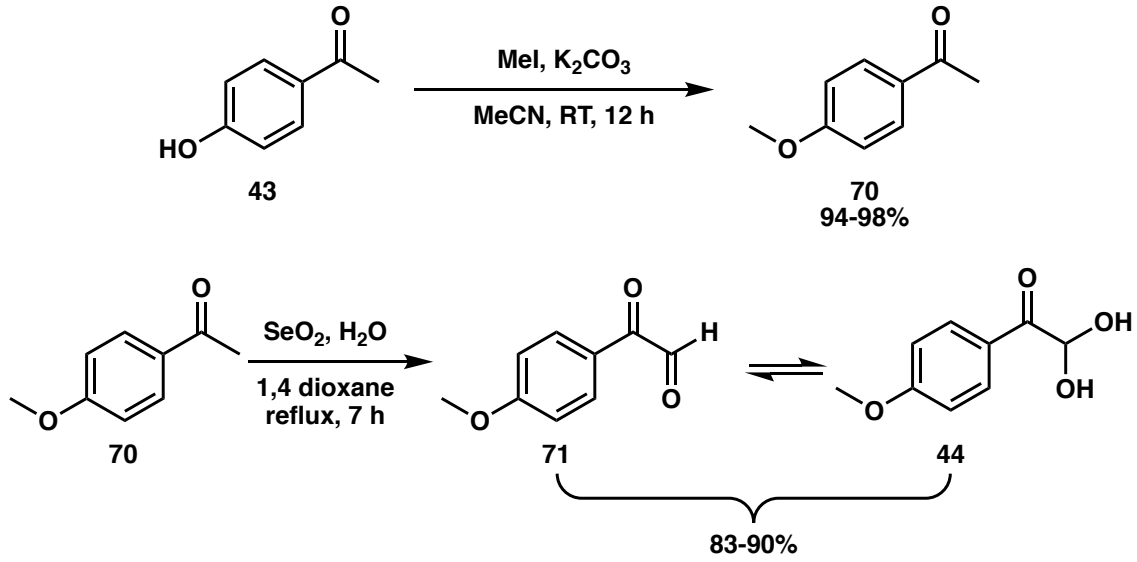


*Scheme 11 – Reaction conditions utilised to prepare **70** and the methyl hydrate derivative **44**.*

As the synthesis of both hydrates was uncertain, test reactions to produce **72** or **73** were attempted by reacting the hydrates with $NH_4OAc$ (Scheme 12).[92] If the hydrate synthesis was successful, either form of the hydrate should react with $NH_4OAc$ to produce an imidazole derivative that should be easily identifiable by $^1H$ NMR. However, the test reactions using either **44** or **53** were both unsuccessful.

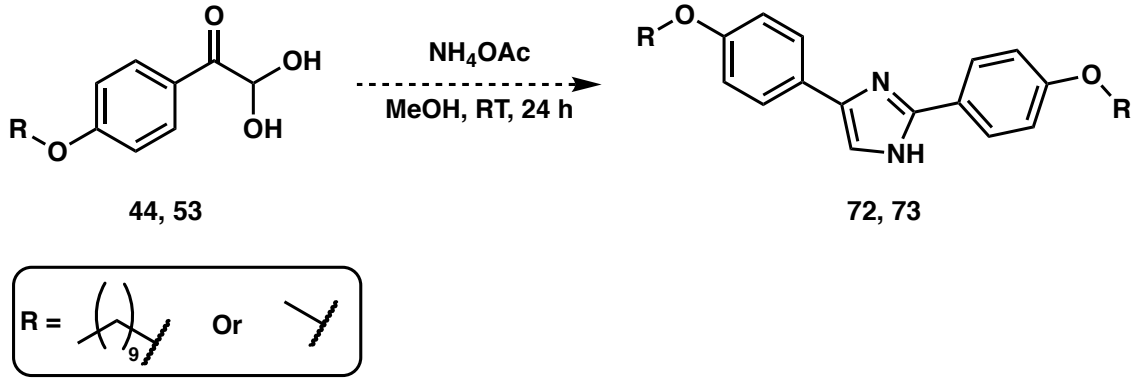


*Scheme 12 – Attempted imidazole formation, for the presence of **44** or **53**.*

It was noted, although both products are very soluble in most organic solvents, most $^1H$ NMR recorded in literature were specifically done using DMSO-$d_6$. When the $^1H$ NMR of **44** was recorded in DMSO-$d_6$, the sample showed full conversion to the hydrate form (Figure 18). We suspected this is a result of more significant hydrogen bonding between the hydrogen donor, the *gem*-diol hydrogen atoms, and hydrogen bond acceptor, the oxygen of the sulfoxide group, aiding the equilibrium to the hydrate. However, the $^1H$ NMR of **53** taken in DMSO-$d_6$ did not have this effect. Although, a larger percentage of

the hydrate was seen in the $^1$H NMR, we suspect the network of hydrogen-bonding is somehow diminished by the larger greasy chain.

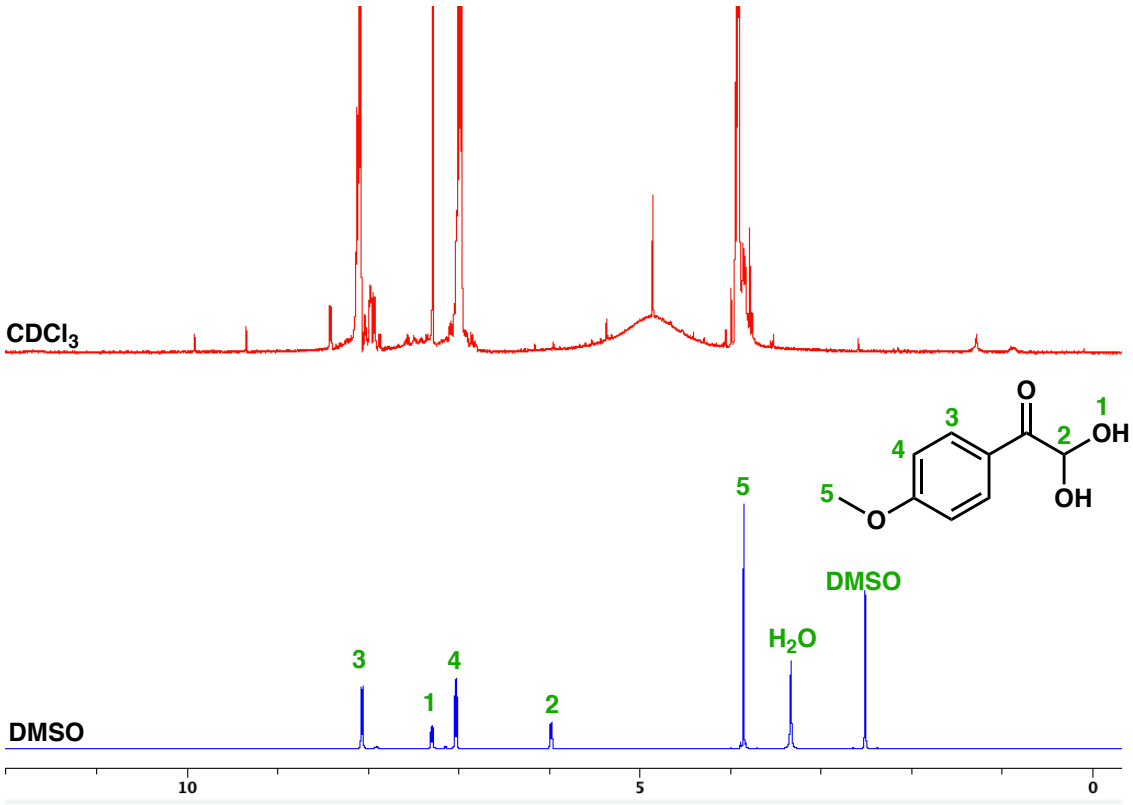


*Figure 18 – The difference in $^1$H NMR spectrum of **44** run in $CDCl_3$ (top, red) vs DMSO-$d_6$ (bottom, blue) using the same sample.*

## 2.1.2 Synthesis of Protected Arginine

The synthesis of **55** was completed in two steps, as shown in Scheme 13. The protection of the N and C termini of the arginine group will prevent any interactions between the hydrate and the arginine's functional groups, excluding the guanidine group. Using a protected arginine derivative first, we can simplify the chemistry and focus on optimising the guanidine's masking.

The synthesis of ***55*** was attempted using two routes, as shown in Scheme 13. The first route relies on Boc protection of the amine then conversion to a methyl ester, while the second route reverses the order of reactions.

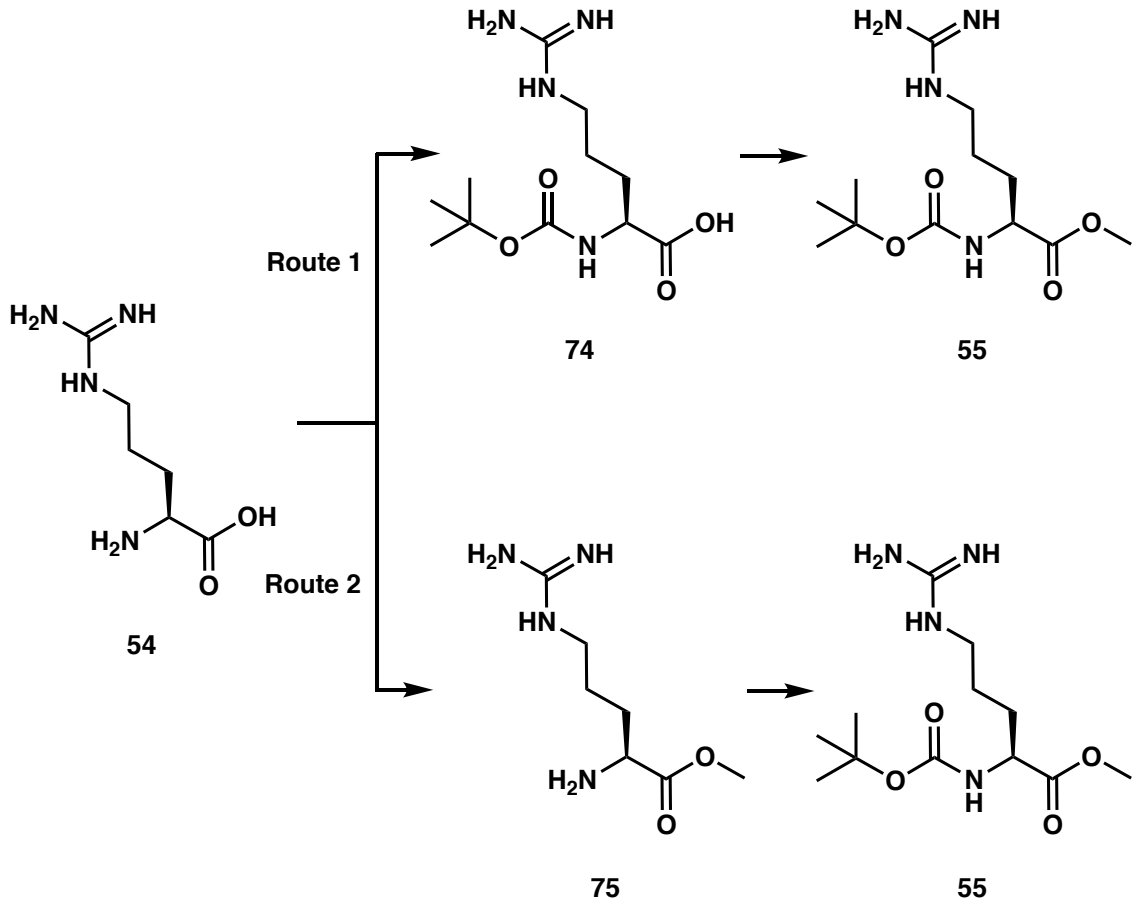


*Scheme 13 – The two proposed routes to afford the protected arginine **55** (shown in their non-zwitterionic form).*

Synthesis of the Boc-protected arginine **74** (Route 1) was attempted using two literature procedures (Scheme 14).[93,94] Nevertheless, neither showed any sign of product formation. These reactions were repeated, doubling the reaction time and were analysed by $^{1}$H NMR and TLC. However, again, showed no sign of product formation. As these reactions do not appear promising, we focused on the addition of the methyl ester first.

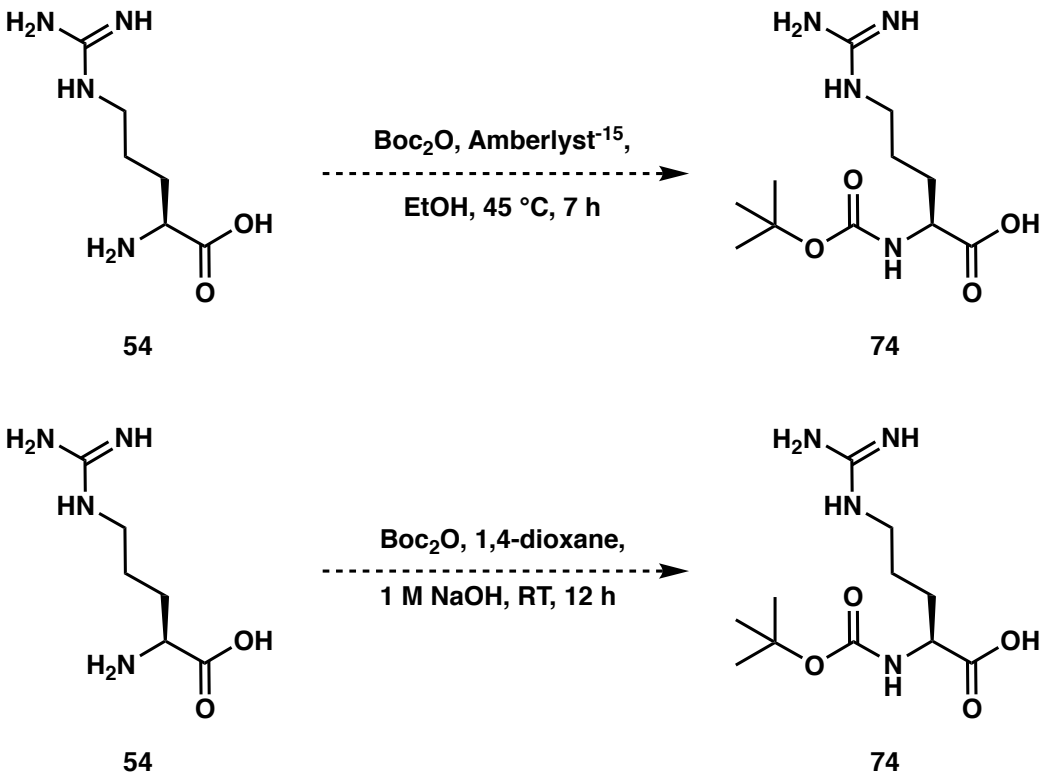


*Scheme 14 – Initial attempts to synthesise Boc-L-arginine.*

Synthesis of methyl L-arginine **75** was achieved as a dichloride salt **77**, with yields of 86%-90%. The starting material is sparingly soluble in MeOH, therefore the reaction was stirred for 90 minutes before the addition of $SOCl_2$. Mechanistically, the reaction proceeds in three key steps, as shown in Scheme 15. The lone pair of electrons on the hydroxy group drives nucleophilic attack on the sulfur displacing a chloride ion. Addition of the chloride ion to the carbonyl group is followed by collapse of the tetrahedral intermediate to give producing $SO_2$ and chloride anion. A Lewis basic species present deprotonates the oxonium ion affording the acyl chloride. This intermediate then undergoes nucleophilic attack by the lone pair of electrons of MeOH, followed by the collapse of the tetrahedral intermediate, affording **75**. Due to the formation of HCl gas during the conversion of the carboxylic acid to the methyl ester the compound was isolated as a hydrochloride salt.

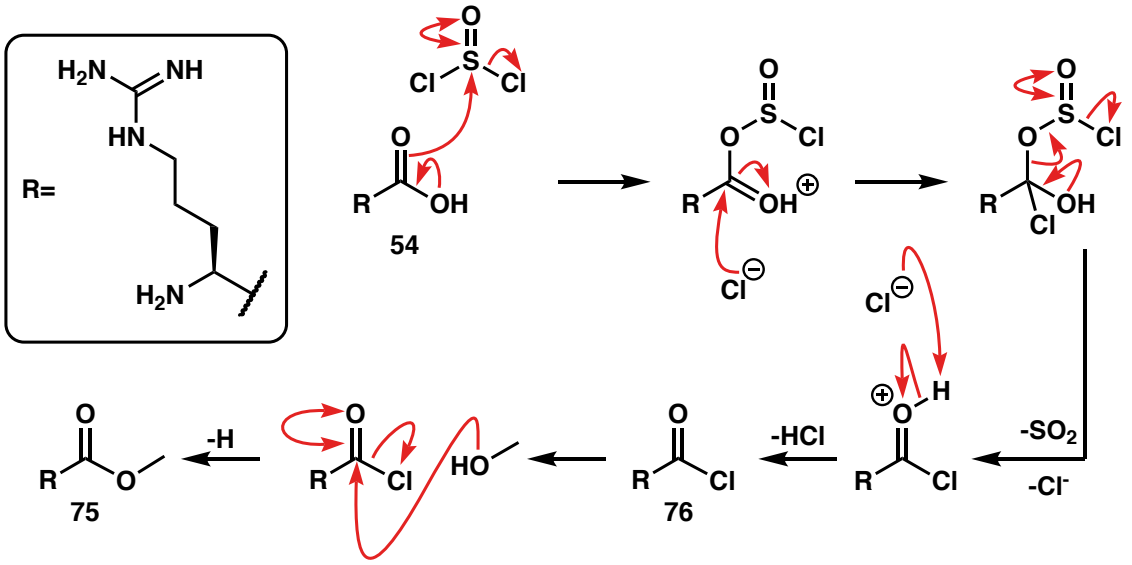


*Scheme 15 – A proposed mechanism to produce **75**.*

The Boc protection of methyl L-arginine was achieved in a yield of 40-66% (Scheme 16). Under mild conditions, Boc protection occurs specifically at the N-terminus due to the guanidine group and the amines having different reactivity. However, these conditions do not result in the complete consumption of starting material, even with the addition of excess $Boc_2O$. Purification of **55** was initially completed by silica-gel chromatography eluting 10% MeOH in $CH_2Cl_2$. It was later realised the purification of **55** could be simply accomplished by dissolving the crude solid in $CH_2Cl_2$ and passing through filter paper, separating the unprotected arginine derivative from **77**.

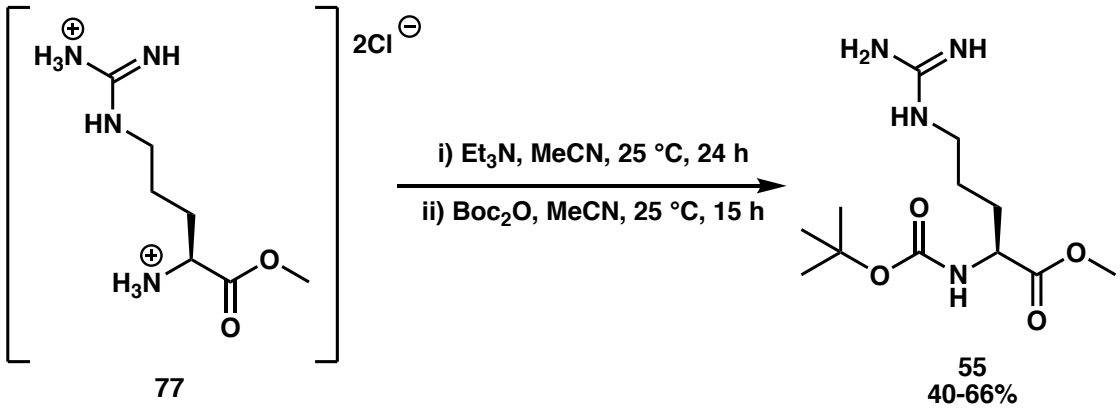


*Scheme 16 – Reaction conditions to afford Boc protected methyl arginine, **57**.*

Boc protection of **75** occurs in two steps; first, the lone pair of electrons of the terminal nitrogen attack one of the $Boc_2O$ carbonyls, resulting in *tert*-butyl carbonate acting as a leaving group, which will ultimately break down into $CO_2$ gas and *tert*-butoxide. In the

second step, a Lewis basic species abstracts the proton of the protonated amine. We managed to acquire *N*-*p*-tosyl-L-arginine methyl ester hydrochloride from a commercial source during the screening of test reactions, which was utilised in some of the test reactions.

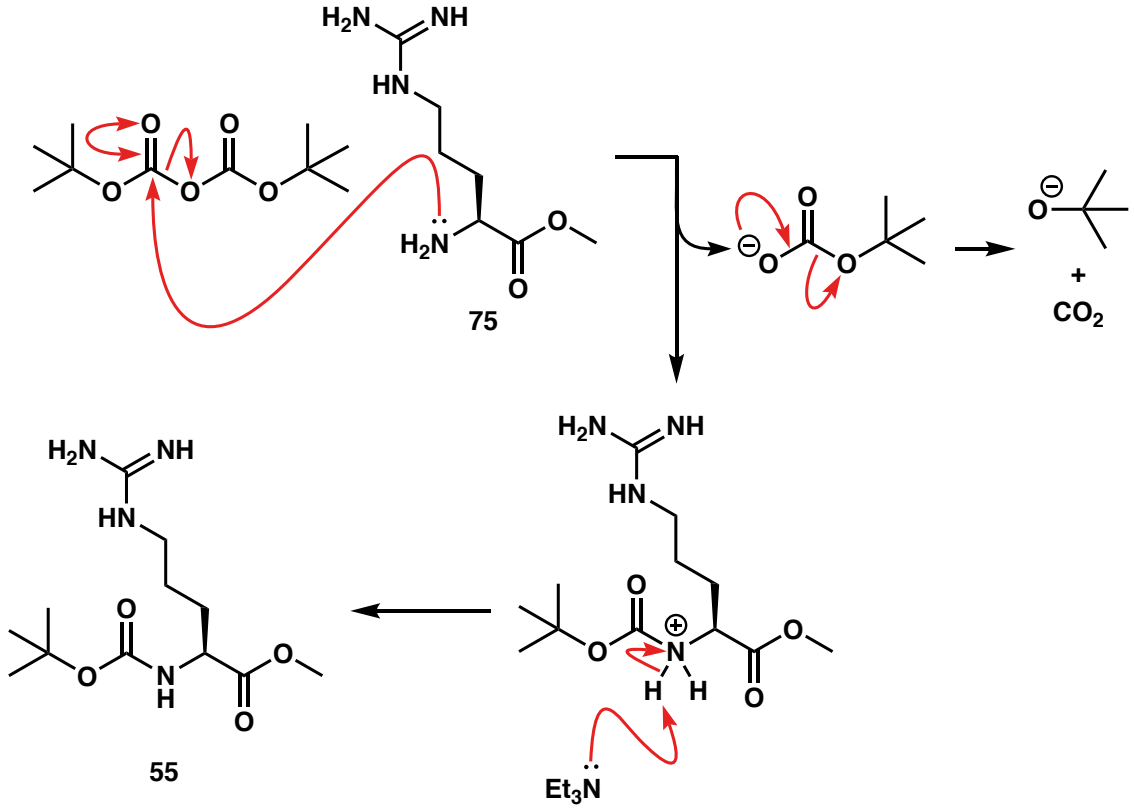


*Scheme 17 – A proposed mechanism for the Boc protection of **75**.*

## 2.1.3 Test Coupling Reactions

With a protected arginine and hydrate now in hand, we began our test reactions. As previously mentioned, the modification of arginine derivatives with **43** had been previously reported in the literature. Although the reported methods have questionable chemical analysis, they provided a foundation for our reactions. Various conditions were attempted and are reported in Table 1. In summary, the conditions reported in the literature proved to be unsuccessful. Similar to the literature, analysis of crude reaction material using highly sensitive techniques like mass spectroscopy showed the expected peaks for the desired material; however, $^{1}$H NMR showed the reaction had not proceeded, with only starting material present. This result was found throughout for all the conditions reported. During the screening of test reactions, we had come across reports of phenyl

glyoxal derivatives being sensitive to light, therefore some reactions were completed in the dark (indicated in the table entries). However, this had no effect in our results.

As these methods proved to be unsuccessful, we looked at exploring the grassroots of the reaction, condensation of the guanidino and hydrate or aldehyde. In principle, the desired product is formed by an imine formation between an amine and aldehyde, catalysed in the presence of acid. As such, we attempted more "conventional" organic reactions (Entry 29-33). The results of these reaction were much more promising than previous conditions, as mass spectrometry suggests the formation of two products, which could be **78**, **79**, or **80**, any of these products were desirable in our situation. More importantly, the $^{1}$H NMR spectrum of the crude reaction material indicated signs of the desired product forming in the aromatic and alkyl chain region of arginine. Attempts to optimise the formation of the product began with merely extending the duration of the reaction. This showed the formation of only one desired product, which we believe to be **79** due to the $^{1}$H NMR spectrum and analysis of the mass spectrometry results showing the presence of two hydroxy groups. Attempts to purify the crude mixture proved to be unsuccessful.

Table 1 – The reaction conditions utilised to join hydrate and arginine derivatives together with the expected product to be formed. * Entries were repeated in the dark.

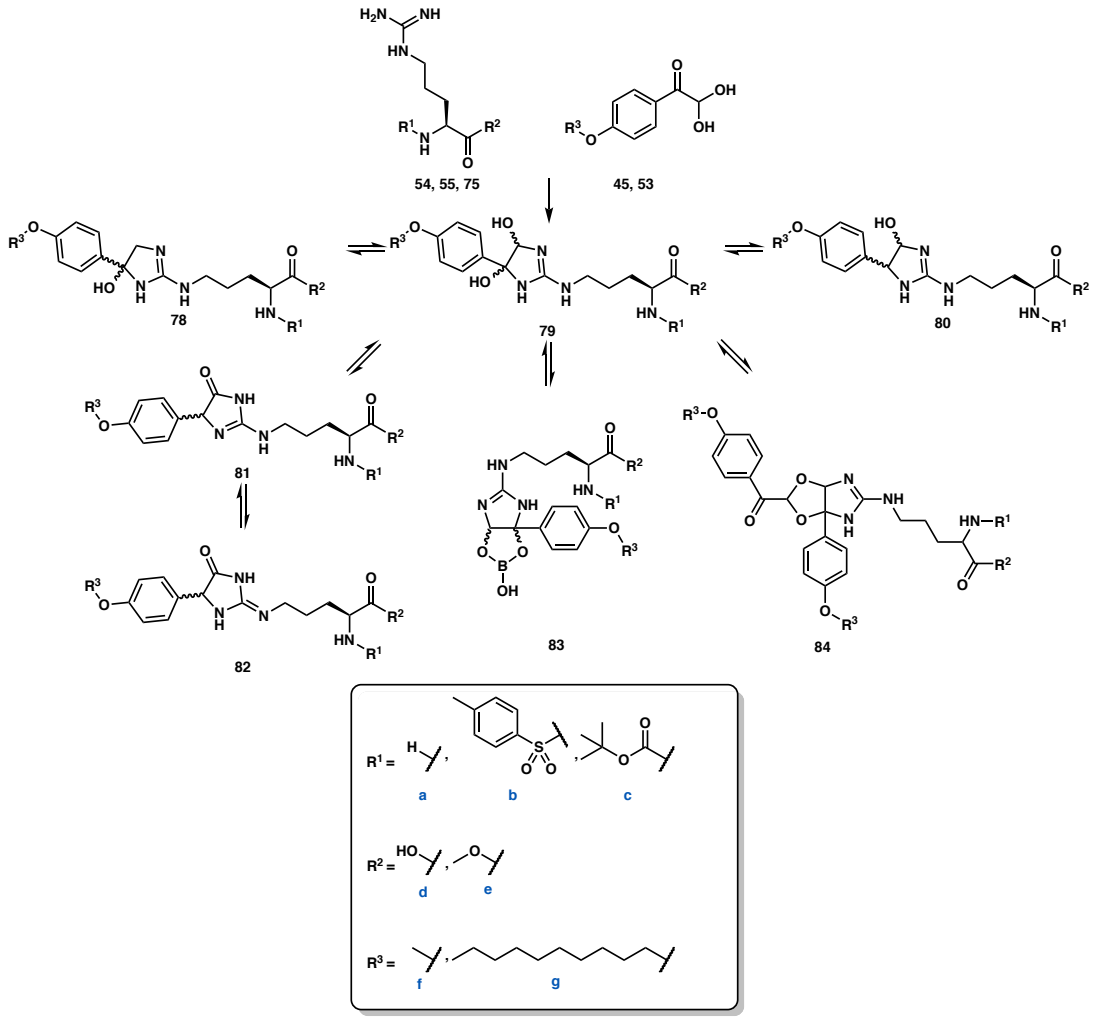


| **10 mM $NH_4OAc$ (pH 8), RT, 0.5 hours** | | | | |
|---|---|---|---|---|
| Entry | Arginine $R^1$ | Arginine $R^2$ | Hydrate $R^3$ | Expected product |
| 1* | -Ts | -OMe | -Me | **79bef** |
| 2 | -Ts | -OMe | $-C_{10}H_{21}$ | **79beg** |
| 3* | -Boc | -OMe | -Me | **79cef** |
| 4 | -Boc | -OMe | $-C_{10}H_{21}$ | **79ceg** |
| **100 mM Sodium borate buffer (pH 9), RT, 16 hours** | | | | |
| Entry | Arginine $R^1$ | Arginine $R^2$ | Hydrate $R^3$ | Expected product |
| 5* | -Ts | -OMe | -Me | **79bef** |
| 6 | -Ts | -OMe | $-C_{10}H_{21}$ | **79beg** |
| 7* | -Boc | -OMe | -Me | **79cef** |
| 8 | -Boc | -OMe | $-C_{10}H_{21}$ | **79ceg** |
| **DMF/AcOH (0.1%), RT, 8 hours** | | | | |
| Entry | Arginine $R^1$ | Arginine $R^2$ | Hydrate $R^3$ | Expected product |
| 9* | -Ts | -OMe | -Me | **81bef** |
| 10* | -Ts | -OMe | $-C_{10}H_{21}$ | **81beg** |
| 11* | -Boc | -OMe | -Me | **81cef** |

| | | | | |
|---|---|---|---|---|
| 12 | -Boc | -OMe | -$C_{10}H_{21}$ | **81ceg** |
| **100 mM Sodium borate buffer (pH 8), MeCN, 37 °C, 16 hours** | | | | |
| Entry | Arginine $R^1$ | Arginine $R^2$ | Hydrate $R^3$ | Expected product |
| 13* | -Ts | -OMe | -Me | **81bef** |
| 14 | -Ts | -OMe | -$C_{10}H_{21}$ | **81beg** |
| 15* | -Boc | -OMe | -Me | **81cef** |
| 16 | -Boc | -OMe | -$C_{10}H_{21}$ | **81ceg** |
| **$HCl_{(aq)}$, $H_2O$, 100 °C, 0.33 h; 60 °C, 24 h** | | | | |
| Entry | Arginine $R^1$ | Arginine $R^2$ | Hydrate $R^3$ | Expected product |
| 17* | -H | -OH | -Me | **81adf** |
| 18* | -H | -OH | -$C_{10}H_{21}$ | **81adg** |
| 19* | -H | -OMe | -Me | **81aef** |
| 20 | -H | -OMe | -$C_{10}H_{21}$ | **81aeg** |
| 21* | -Ts | -OMe | -Me | **81bef** |
| 22 | -Ts | -OMe | -$C_{10}H_{21}$ | **81beg** |
| 23* | -Boc | -OMe | -Me | **81cef** |
| 24 | -Boc | -OMe | -$C_{10}H_{21}$ | **81ceg** |
| **Phosphate buffer (pH 7.4), 40 °C, 4.5 hours** | | | | |
| Entry | Arginine $R^1$ | Arginine $R^2$ | Hydrate $R^3$ | Expected product |
| 25* | -Ts | -OMe | -Me | **79bef** |
| 26 | -Ts | -OMe | -$C_{10}H_{21}$ | **79beg** |
| 27* | -Boc | -OMe | -Me | **79cef** |
| 28 | -Boc | -OMe | -$C_{10}H_{21}$ | **79ceg** |
| **AcOH, $CH_2Cl_2$, RT, 24 hours** | | | | |
| Entry | Arginine $R^1$ | Arginine $R^2$ | Hydrate $R^3$ | Expected product |
| 29* | -Ts | -OMe | -Me | **81bef** |
| 30 | -Ts | -OMe | -$C_{10}H_{21}$ | **81beg** |
| 31 | -Boc | -OMe | -Me | **81cef** |
| 32 | -Boc | -OMe | -$C_{10}H_{21}$ | **81ceg** |
| **37% $HCl_{(aq)}$, 3 weeks** | | | | |
| Entry | Arginine $R^1$ | Arginine $R^2$ | Hydrate $R^3$ | Expected product |
| 33* | -H | -H | -Me | **81adf** |

It is unclear why reactions failed to proceed, although there are a few possible reasons. Firstly, as depicted in Table 1, the reaction is likely to be occurring in equilibrium, and like the issues encountered with the *gem-diol* hydrate equilibrium a similar issue could be occurring here. This makes analysis of the product through $^1H$ NMR difficult to interrupt. As mentioned earlier, reports in the literature have only characterised derivatised peptides by mass spectrometry or HPLC. In addition, they have rarely quoted yields. It is unclear how effective this reaction is. We could have been chasing an inherently flawed method.

Ultimately, this project was abandoned due to the lack of time, and successful results. Further steps required to explore this strand of research and form a prodrug with opiorphin have been expanded on in Chapter 4.

## 2.2 Section 2 – Unnatural Amino acid

Section 2 of results and discussion is split into two parts, in part 1, each step to produce the amino acid precursor (±)-**58** will be discussed in detail. While part two discusses coupling reactions involving the planar chiral amino acid reactions. This is done as the steps to produce the amino acid precursor (±)-**58**, plays a critical role and is the foundation of the results of Sections 3 and 4.

### 2.2.1 Part 1 – Synthesis of the Amino Acid Precursor

As noted in Chapter 1 the synthesis of (±)-4-nitro[2.2]paracyclophane-13-carboxylic acid has been reported in the literature. The previous method prepared (±)-**3** in five steps, the method used in this strand of research has been developed by members of the Rowlands group, and produces the desired precursor of (±)-**3** in three steps. Synthesis of (±)-**58** was achieved by nitration producing (±)-**85**, a directed formylation to give aldehyde (±)-**86** followed by oxidation to the desired amino acid precursor (Scheme 18).

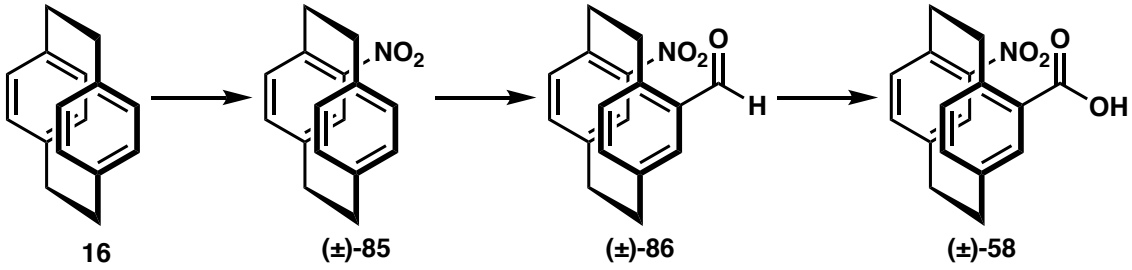


*Scheme 18 – Synthetic pathway for the synthesise of (±)-4-nitro[2.2]paracyclophane-13-carboxylic acid.*

**Nitration**

The first step of the synthesis of (±)-**58** was the electrophilic substitution of [2.2]paracyclophane to produce (±)-4-nitro[2.2]paracyclophane (±)-**85**. Nitration of [2.2]paracyclophane is a capricious reaction and, in our hands, led to an unexpected rearrangement that will be discussed in Section 4. Various methods have been reported in literature and they cover a bewildering spectrum of conditions. Some reactions cool the reaction -72 °C while others heat to 100 °C.[95,96] Time can vary from 10 minutes to 4 days.[97] The Rowlands group developed an alternative procedure utilising a 4:2 stoichiometry of $H_2SO_4$ to $HNO_3$ added separately in $CH_2Cl_2$ at 0 °C and stirred overnight. Lower temperature initially results in slower formation of side product, while the

increased equivalents of reagents ensures the reaction proceeds to completion. However, these conditions posed their own difficulties in the formation of a black-tar. This is likely a product of [2.2]paracyclophane polymerisation, and not further investigated. The tar was decanted before quenching the reaction, as the presence of this material results in the formation of an emulsion, making the work-up difficult and decreasing yield. Under these conditions the yield varied between 67-80%, but purification is simple using standard column chromatography.

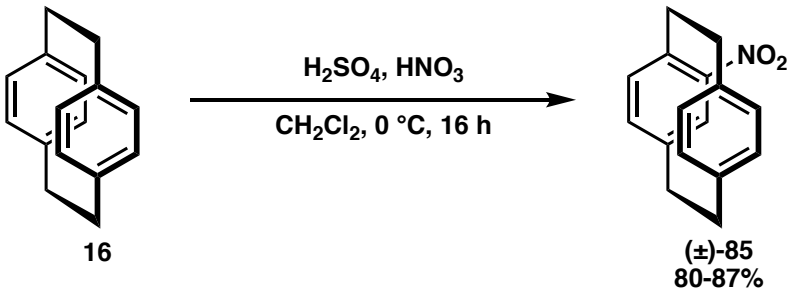


*Scheme 19 – Reaction conditions used to synthesise (±)-**85**.*

In an effort to reduce the formation of the black-tar substance the reaction was further optimised by developing a more controlled procedure. The $H_2SO_4$ was decreased to 2 equivalents and added to $HNO_3$ at 0 °C for 15 minutes before adding to the solution of [2.2]paracyclophane in $CH_2Cl_2$. Additionally, monitoring the reaction by TLC showed consumption of starting material after 8 hours even while keeping the reaction at 0 °C, rather than bringing it to RT overnight. The decreased ratio of reagents, reaction time and temperature prevented the formation of the black tar and other side products. These conditions afforded yields in the range of 80-87%.

Nitration of [2.2]paracyclophane occurs through electrophilic aromatic substitution as shown in Scheme 20. The nitronium ion is produced by dehydration of $HNO_3$ with $H_2SO_4$. Electrophilic aromatic substitution occurs *via* a carbocation intermediate known as an arenium ion intermediate, the aromaticity is then restored by the removal of the proton through the nucleophilic attack of any Lewis basic species present in solution. The mono-substitution of [2.2]paracyclophane leads to the symmetry being broken, resulting in formation of a mixture of enantiomers.

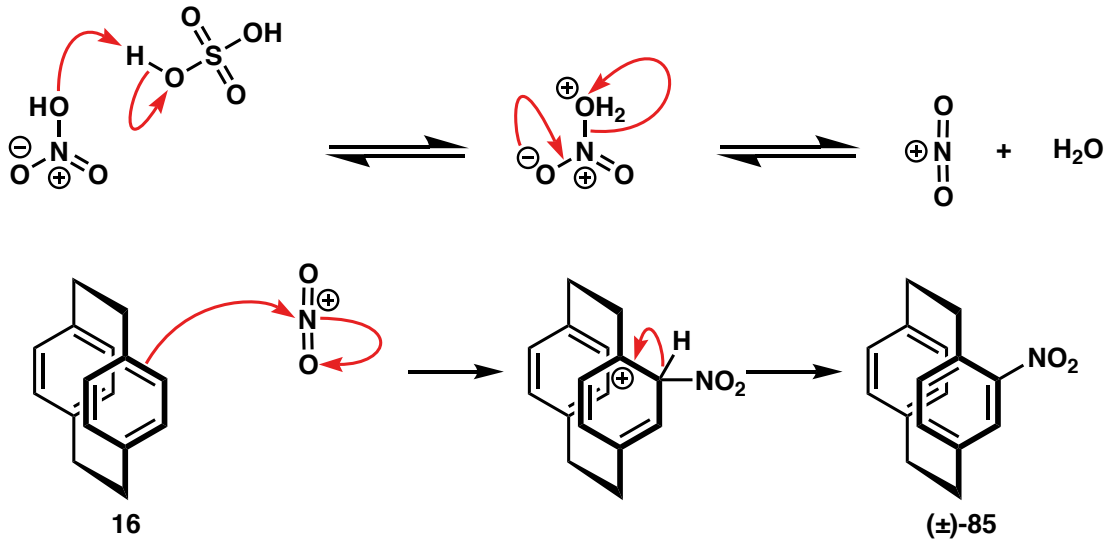


*Scheme 20 – Proposed mechanism for the nitration of [2.2]paracyclophane using $H_2SO_4$ and $HNO_3$.*

**Formylation**

Synthesis of (±)-4-nitro-13-formyl[2.2]paracyclophane (±)-**86** was achieved through Rieche formylation (Scheme 21). First reported by Alfred Rieche in 1960, the Rieche formylation utilises $MeOCHCl_2$ and $TiCl_4$ in a Friedel-Crafts-like aromatic substitution.[98] Formylation of (±)-**85** occurs successfully with yields ranging from 73-84% and can be purified by column chromatography. Slow evaporation of the eluent (40% EtOAc, 60% hexane) produces crystals suitable for X-ray crystallography analysis. Although this reaction works well, the use of $TiCl_4$ required careful handling and isn't user friendly due to it being sensitive to air. In an effort to find an alternative reagent, a range of Lewis acids, including $AlCl_3$, $FeCl_3$, or $ZrCl_4$ were screened. Although the reagents are significantly easier and safer to handle, all three reagents gave lower yields (17-34%), increased side products, and required longer reaction times.

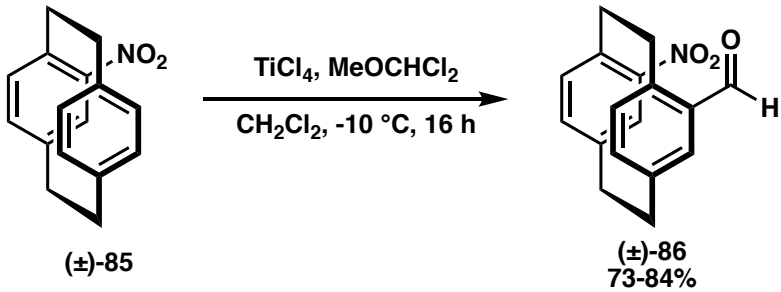


*Scheme 21 – Rieche formylation of (±)-**85** to afford (±)-**86**.*

Formylation of (±)-**85** begins with the Lewis acidic $TiCl_4$ activating $MeOCHCl_2$. Elimination of a chloride ion generates a powerful electrophilic oxonium species. The

regioselectivity can be explained by the transannular effect. This postulates that the initial addition is reversible and occurs anywhere on the rings, but the re-aromatisation of the Wheland intermediate is faster at C13 and this funnels the product down this route. Aromaticity is restored by an internal deprotonation by an oxygen atom on the nitro group. An additional chloride ion is lost, and $H_2O$ is added to the oxonium electrophile. Protonation of the hemiacetal results in the oxonium MeOH species, which acts as a good leaving group. Finally, deprotonation of the oxonium species affords the desired product (±)-**86**.

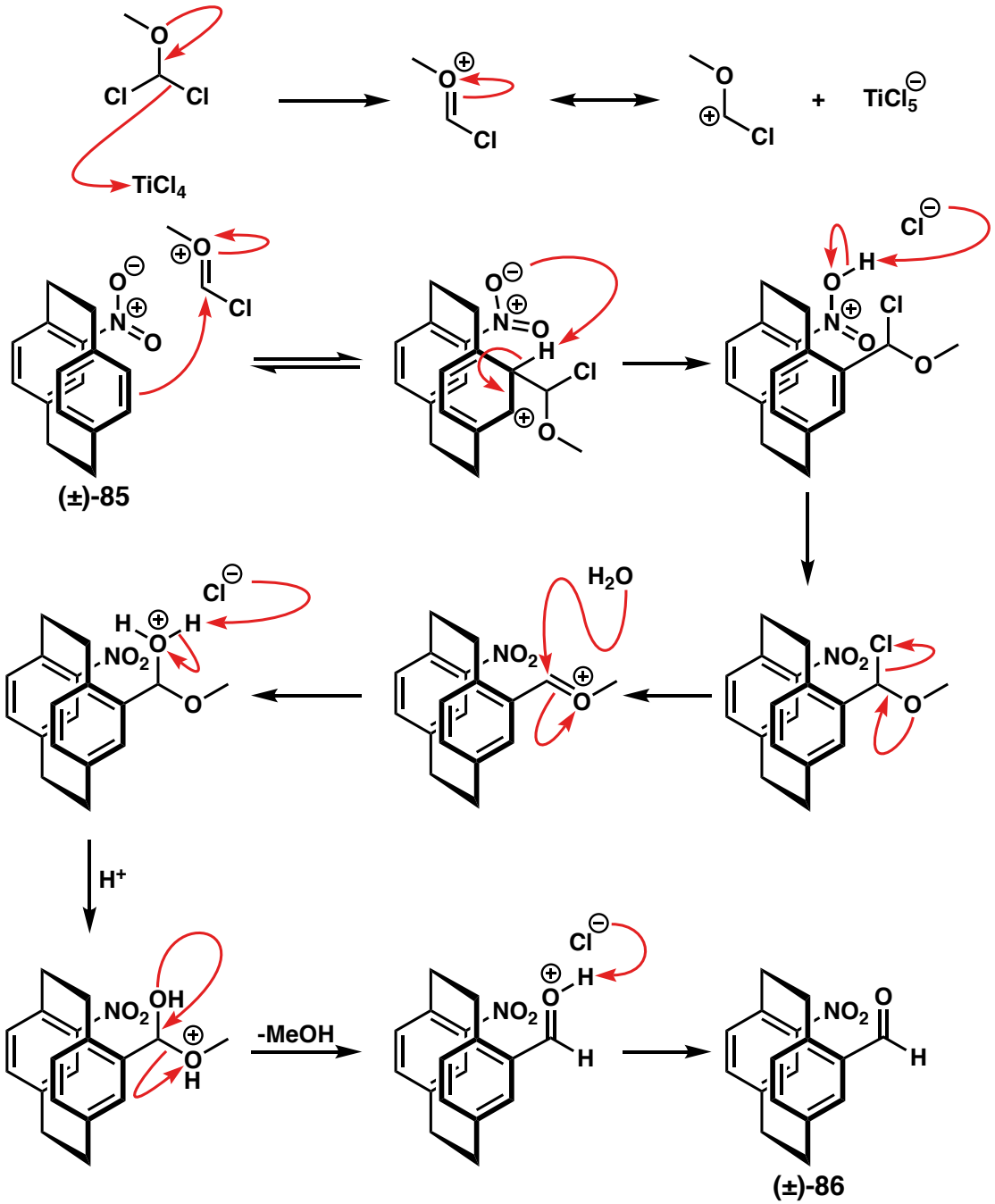


*Scheme 22 – Mechanism of Riche formylation of (±)-4-nitro[2.2]paracyclophane (±)-**86**.*

Formylation occurs specifically at the C13 position of (±)-**85** and with the regioselectivity explained by the transannular effect. The transannular effect isn't fully understood but a working model suggests it is a combination of the electronic properties of one aromatic ring influencing the other and an internal deprotonation. This can easily be seen by comparing two electron withdrawing groups, the nitro group and a nitrile. Normally, the rate determining step of aromatic substitution is the breaking of the aromaticity when the ring attacks a suitable electrophile. In [2.2]paracyclophane with an electron withdrawing substituent, this is probably not the case. Formation of the cationic intermediate is reversible and the ability to lose the hydrogen and regain aromaticity within the system appears to be key. A nitro group can aid internal deprotonation as there is a conformation in which the oxygen lone pair can act as a base. This accelerates irreversible re-aromatisation, causing substitution at the C13 position to be favoured. A nitrile group is also electron withdrawing but it does not direct to the *pseudo-geminal* position suggesting electronics are not that important. This can be attributed to the nitrile group being linear, forcing the lone pair to be orientated outwards so that it cannot participate in internal deprotonation. Other functional groups that can rotate can cause internal deprotonation and direct to *pseudo-geminal* position. This means the transannular effect is a result of selective internal deprotonation. It is further presumed the first step occurs in some form of equilibrium. This would allow the initial step to occur at alternative positions on the ring, but only productively proceed when internal deprotonation allowed. All other intermediates reform starting material. It is only at the C13 positions a rapid rearomatisation occurs, which drives the equilibrium to the product side.

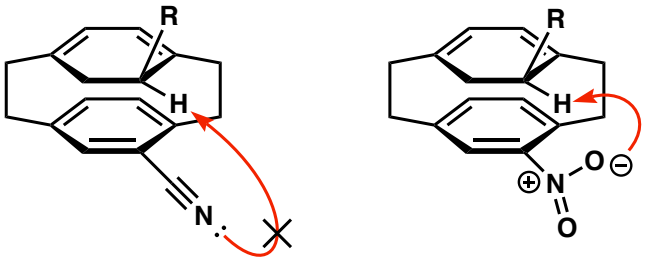


*Figure 19 – Visual representation showing how the lone pair orientation and rotation aids in internal deprotonation.*

**Oxidation**

The synthesis of (±)-4-nitro[2.2]paracyclophane-13-carboxylic acid (±)-**58** was achieved with yields ranging from 10-53%, while returning 28%-43% of starting material (±)-**86** (Scheme 23).

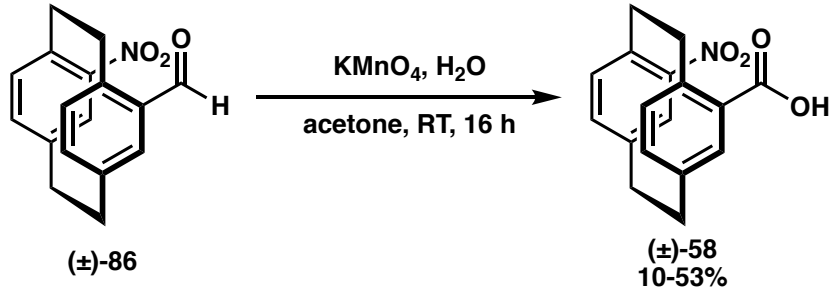


*Scheme 23 – Reaction conditions used to afford (±)-58*

Initially, it was believed that the reaction did not go to completion due to the oxidation of acetone to acetic acid. This was presumed due to a strong aroma of vinegar emitted during the work up and later confirmed by the presence of sodium acetate crystals. A lower concentration of acetone (0.4 M rather than 0.2 M) was used in following reactions with the intention of resolving this issue, increasing the average yield by 8%. However, this was not a significant increase in yield, so an alternative water-soluble solvent was attempted. However, no other solvent improved the yields. This suggests that oxidation of acetone was not the real issue. Currently, it is not known why oxidation is not occurring efficiently, but we believe optimisation of pH should be investigated. Purification by acid/base extraction gives a simple method to obtain clean product, as well recycling starting material (±)-**86**. An X-ray crystal structure of (±)-**58** was acquired by slow evaporation of $CD_3OD$. The connectivity of the compound has been confirmed, but the data quality was not sufficient for full structural characterisation.

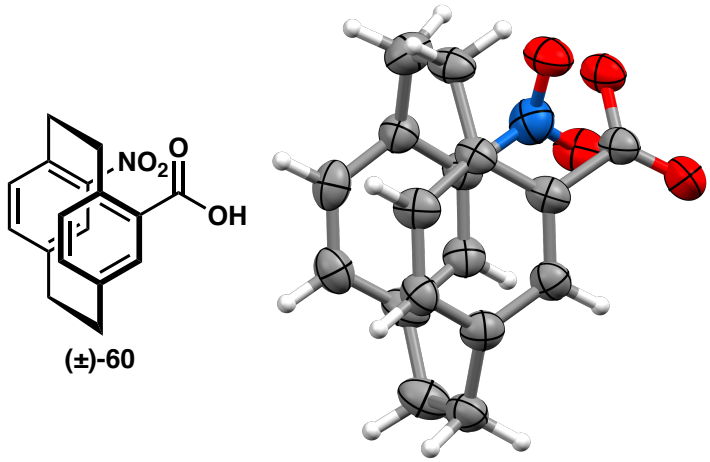


*Figure 20 – X-crystal structure of (±)-**58** acquired through slow evaporation of $CD_3OD$. Carboxylic acid hydrogen omitted. C=grey, H=white, N=blue, O=red. Thermal ellipsoid probability level 50%.*

Oxidation of (±)-**86** with $KMnO_4$ begins with the nucleophilic addition of $H_2O$ to the electrophilic carbonyl forming a hydrate (Scheme 24). Followed by the negatively charged oxygen to attack $KMnO_4$ allowing for proton transfer to oxidise the tetrahedral carbon producing the desired carboxylic acid (±)-**58**.

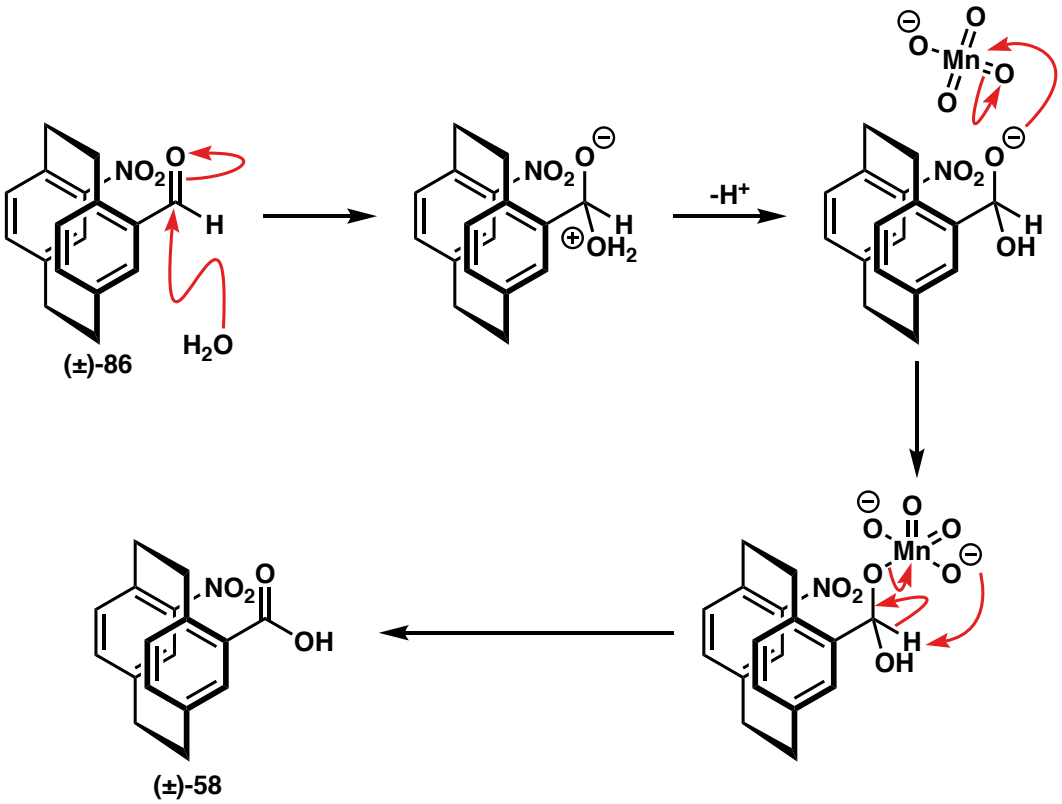


*Scheme 24 – Mechanism for the oxidation of (±)-4-nitro-13-formyl[2.2]paracyclophane to of (±)-4-nitro[2.2]paracyclophane-13-carboxylic acid (±)-**58**.*

This provided a short route of the preparation of amino acid surrogates. In this nitro form, the amine is effectively protected allowing selective reactions of the acid. Alternatively, reduction would allow access to the amine.

## 2.2.2 Part 2 – Synthesis of a Dimer

To couple the carboxylic acid, we needed to activate it. As a reaction between acid and base results in salt formation, conversion to an acyl chloride is a required step before reacting (±)-**58** with an amine. Conversion to an acyl chloride allows for the substitution of the halide when reacted with an amine, resulting in the formation of an amide. Additionally, the hydroxy group of a carboxylic acid is a poor leaving group, thus conversion to a more labile group is required. However, the lability of an acyl chloride can be a double-edge sword as (±)-**87** can be readily converted back to starting material in the presence of $H_2O$, which can be difficult to avoid due to moisture in the air. The synthesis of (±)-4-nitro[2.2]paracyclophane-13-carbanoyl chloride was completed using two procedures (Scheme 25). Initially, a mild procedure utilising $(COCl)_2$ with a sub-stoichiometric amount of DMF in $CH_2Cl_2$ was used. The $^1$H NMR spectrum obtained from the following transformation when using the $(COCl)_2$ and DMF pathway showed the presence of remaining starting material, demonstrating the reaction does not go to completion. As such, the procedure was changed to refluxing (±)-**58** in $SOCl_2$. Unsure of the stability of (±)-**87**, collection of $^1$H NMR was not attempted and the acyl chloride was used immediately for the following reactions. Although the yields for either procedur cannot be reported, yields for the following transformations were at least 15% higher when using $SOCl_2$.

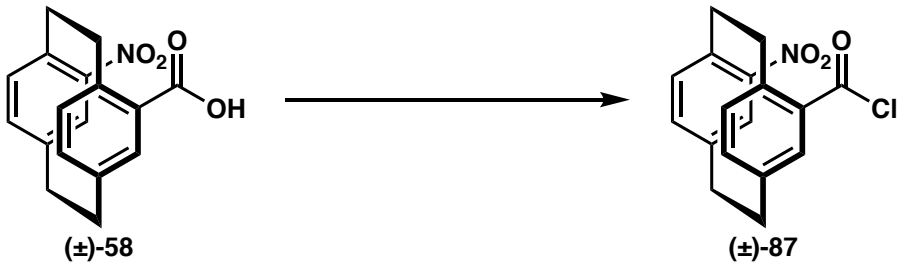


(±)-58 (±)-87

**Initial procedure - $(COCl)_2$, DMF in $CH_2Cl_2$, RT, 1 h**
**Final procedure - $SOCl_2$, reflux, 15 h**

*Scheme 25 – Reaction conditions used to synthesise (±)-**87**.*

The mechanism for the initial procedure begins with a reaction between DMF and $(COCl)_2$ to ultimately form the imidoyl chloride known as the Vilsmeier reagent. This imidoyl chloride derivative is the active chlorinating agent, which reacts with the lone pair of electrons on the carboxylic acid. Following the loss of hydrogen, the lone pair on the nitrogen forms a double bond causing a chloride to be eliminated. The chloride then

attacks the carbonyl group producing the desired product. The mechanism utilising $SOCl_2$ can be seen in Section 1 Scheme 15, however stops at the acyl chloride intermediate.

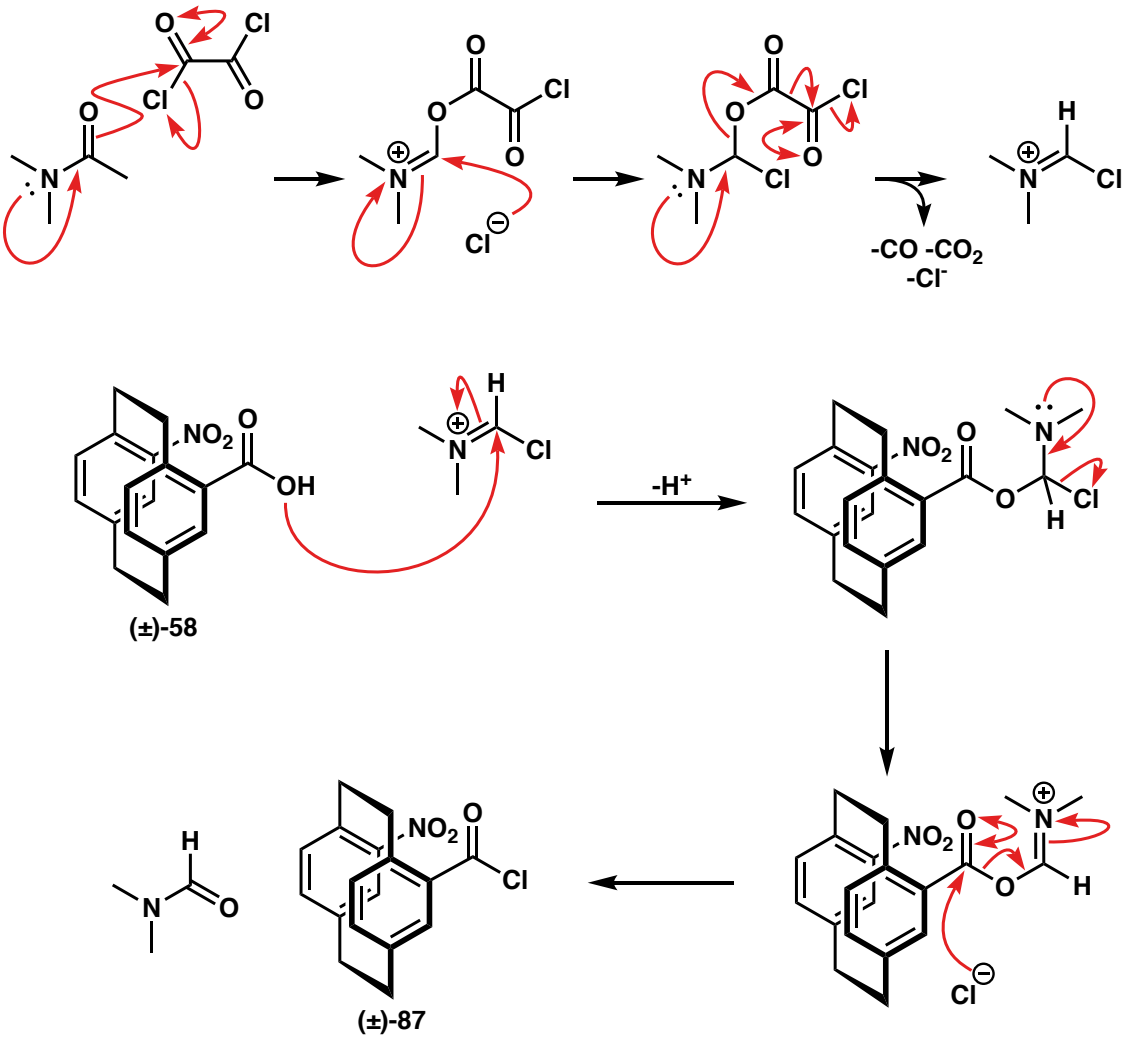


*Scheme 26 – The proposed mechanism to synthesise the Vilsmeier reagent and (±)-87.*

The synthesis of the first peptide bond is a crucial step in the synthesis of the foldamer as it produces the end terminus of the molecule, preventing uncontrolled polymerisation. Three carboxamides were synthesised (Scheme 27). Initially (*S*)-1-phenylethylamine was used; however, this was changed to (*R*)-1-phenylethylamine due to the limited quantity of the reagent present in the lab. The synthesis of **88a** was achieved in 56% yield while **88b** gave a range of 52-56%, both resulting in the formation of a 1:1 mixture of diastereoisomers. The use of a chiral amine was intended to give diastereoisomers in the hope that we could resolve the planar chirality of the [2.2]paracyclophane amino acid. We needed to resolve the planar chirality before we started linking [2.2]paracyclophane units in order to prevent the synthesis of mixtures of stereoisomers. Unfortunately, the $R_f$ values of the two were too close and resolution was impossible. It was noted during the

purification that a precipitate had formed in the collected fractions, and when analysed by $^1$H NMR, the precipitate showed a greater proportion of one diastereoisomer to the other. With further experimentation, recrystallisation of a single diastereoisomer may have been possible.

As the separation of the phenylethylamine diastereoisomers was not achieved, it was decided to simply form the amide as a racemic mixture. This would simplify the $^1$H NMR spectrum. Furthermore, in an attempt to increase yields $CH_2Cl_2$ was substituted for THF, which allowed the reaction to be heated at a higher temperature (Scheme 27). The isopropyl derivative (±)-**88c** was formed as a racemate in yields between 64-76% with no complications; this procedure showed an increase in yield by 17% compared to the diastereomeric mixture earlier.

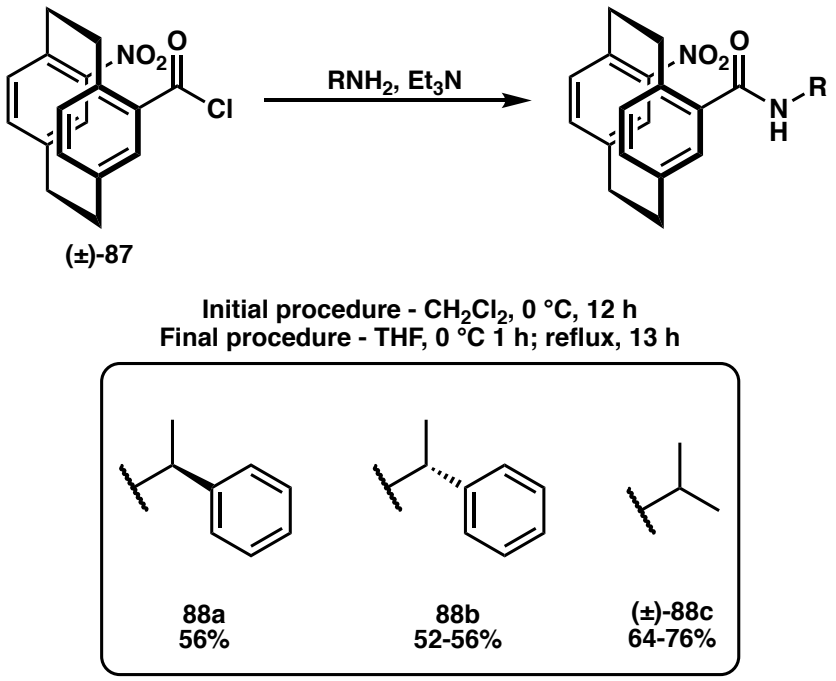


*Scheme 27 – Reaction conditions used to synthesise various (±)-4-nitro[2.2]paracyclophane carboxamide derivatives.*

Amide formation is a standard acyl substitution reaction involving an addition-elimination mechanism. The first step is the nucleophilic addition of the amine to the partially positive carbon of the carbonyl. The elimination proceeds by the collapse of the tetrahedral intermediate to reform the carbonyl group with the expulsion of the chloride ion, followed by the deprotonation of the nitrogen by any Lewis basic species present to afford the product.

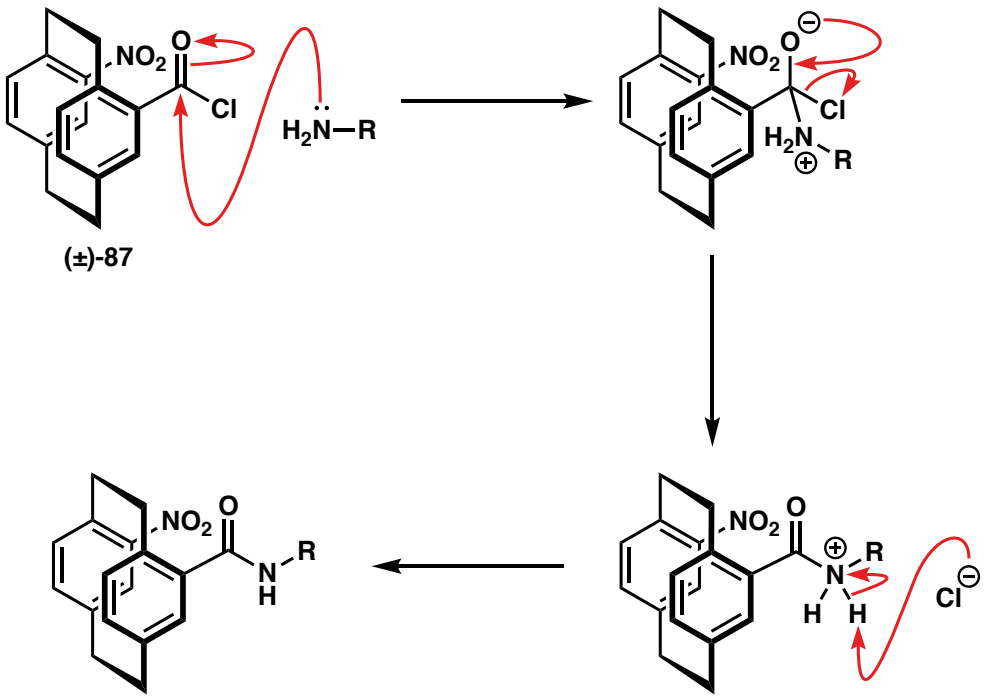


*Scheme 28 – A proposed mechanism to produce amide monomer building blocks.*

Reduction of the nitro amides to amino amides has been achieved for three compounds with yields ranging from 50-86%. The nitro group had effectively behaved as a protecting group up to this point, reduction to the amine unmasks the nucleophile required in subsequent couplings. The reduction of **88a** was acquired in 50% while **89b** was acquired with yields from 57%-64%. Reduction of (±)-**88c** resulted in a 86% yield, with no further purification required.

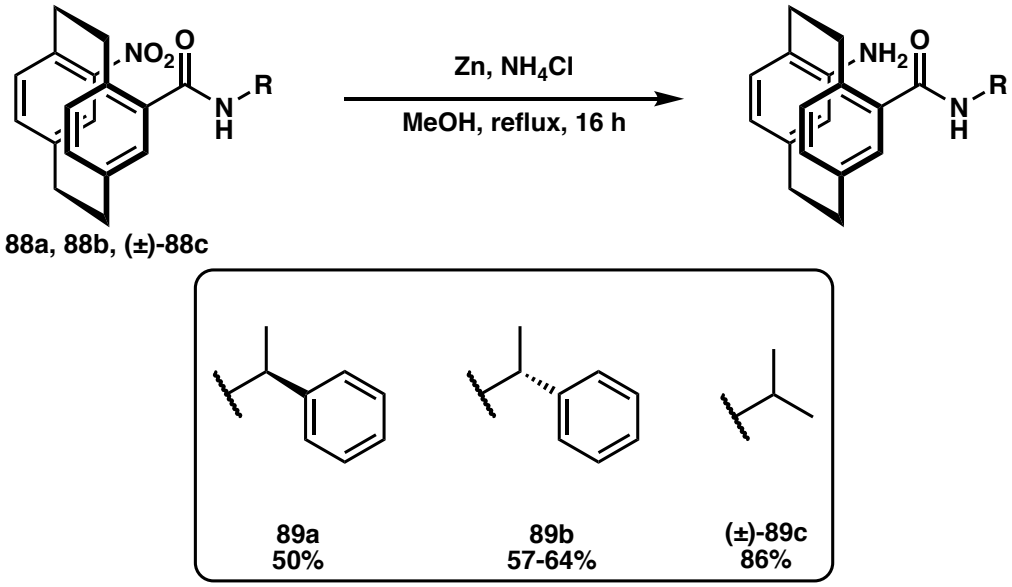


Scheme 29 – Reaction conditions used to synthesise 4-amino[2.2]paracyclophane carboxamide derivatives.

The mechanism of the reaction can be seen in Scheme 30. Conversion of the nitro to the amine begins with the protonation of the hydroxy group followed by a series of single-electron transfers (SET) and protonation to produce unstable oxonium species. Loss of $H_2O$ gives a nitroso group that is protonated and reduced by a second series of SETs. A strong acid is required to protonate the oxygen of the resulting hydroxylamine and not the nitrogen. Loss of $H_2O$ and reduction by yet another series of SETs creates a nitrenium ion, which is short-lived in an acid medium, being protonated to give the desired amine.

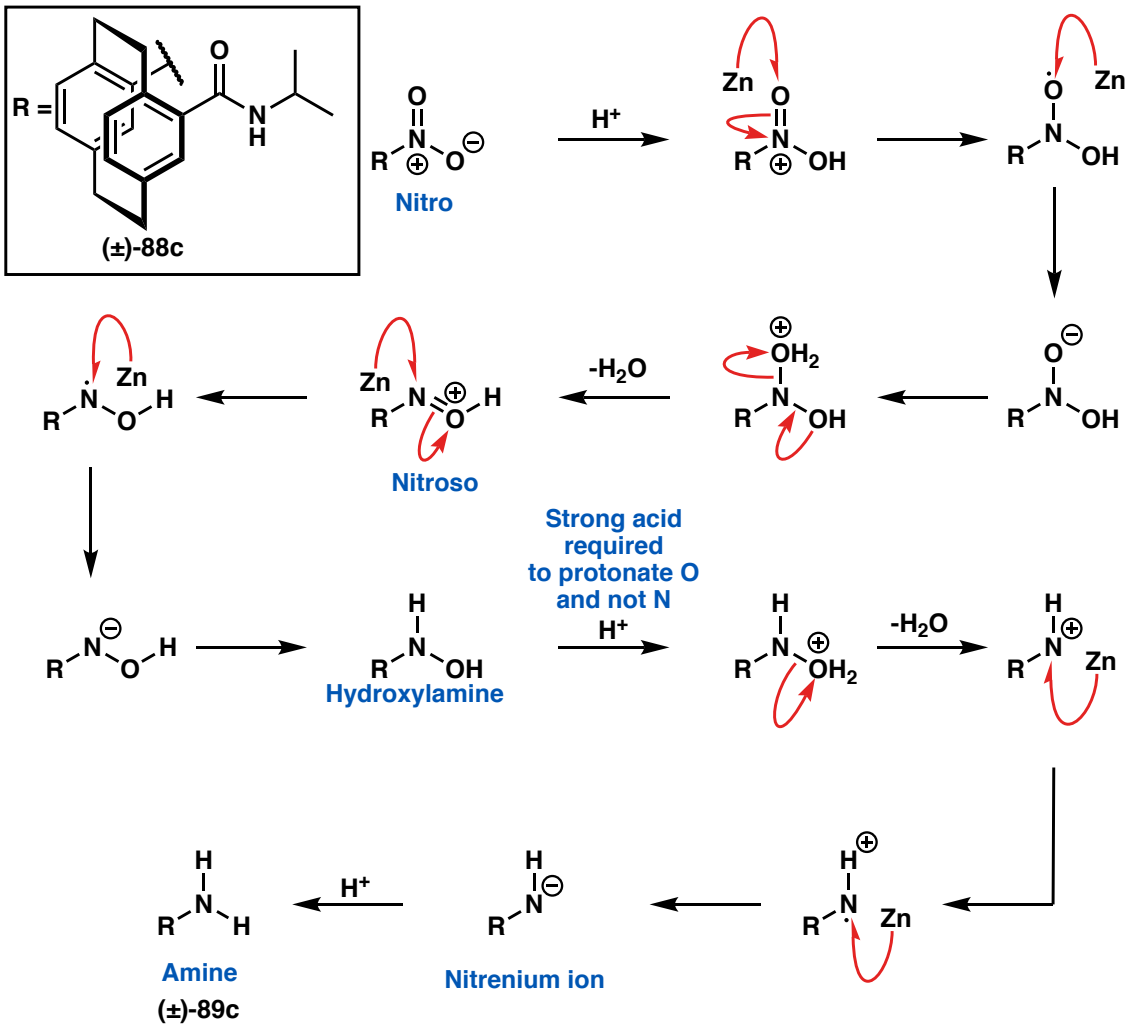


*Scheme 30 – Proposed mechanism to for the reduction of the nitro group to amino for (±)-**89c**.*

Amide formation between the capped amino amide derivatives and (±)-**87** is arguably the most fundamental reaction for this project as it allows for the coupling of monomers. The initial attempts at coupling [2.2]paracyclophane derivatives gave poor yields, with both phenylethyl derivatives resulting in a crude yield of 4%. As separation of diastereomers had not been achieved, the coupling results in up to eight stereoisomers. The $^1$H NMR

was inconclusive as it contained a mixture of potential products and impurities. The mass spectrometry analysis of the crude reaction mixture showed the desired mass and isotopic abundance splitting of a predicted $C_{42}H_{39}N_3O_4$ (Figure 21), however, purification was not attempted due to the limited amount of material. With both derivatives giving poor results, we knew we required better coupling conditions. Exploring alternative methods originated from these results and lead to the procedure discussed earlier using THF and refluxing.

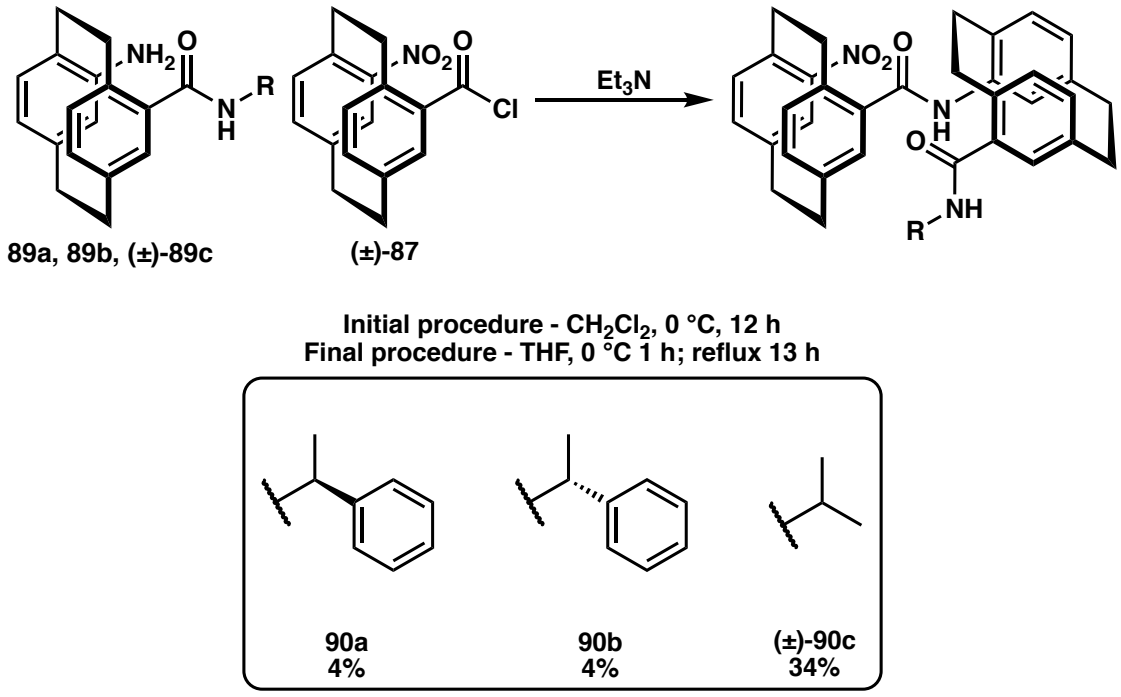


*Scheme 31 – Reaction conditions used to synthesise [2.2]paracyclophane dimer derivatives.*

The changes paid off and resulted in the isolation of (±)-**90c** obtaining a yield of 34% after purification, showing a significant increase in yield. Analysis of $^1$H NMR showed signs of hindered rotation of the isopropyl group, as the methyl groups are no longer equivalent to one another in the $^1$H NMR spectrum. However, further research is required to determine whether this restricted rotation is due to the adjacent [2.2]paracyclophane. This could explain the low yields acquired for **90a** and **90b**, as phenyl groups are much bulkier than isopropyl groups and thus hinder the reaction from occurring.

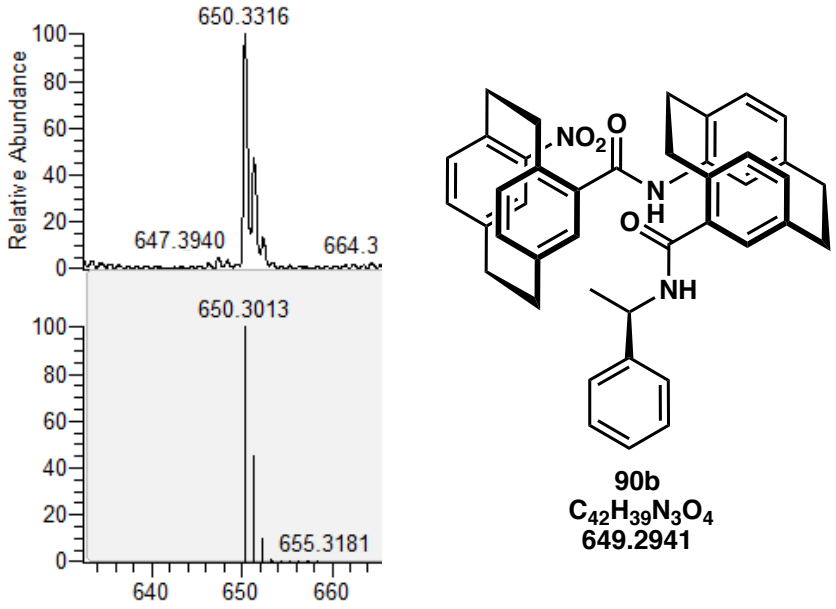


*Figure 21 – Mass spectrometry of **90b** highlighting the isotopic splitting and predicated splitting.*

The work-up for these reactions was complicated by the formation of gels. Adding extra organic solvent during separation failed to help the situation. These emulsions were observed in later coupling reactions (see compounds (±)-**103** and **110**). We wonder if these amides act as gelators analogous to the β-amino acids derivatives reported by Hirose *et al*.; or the phenylaniline derivatives synthesised by Díaz *et al*. The task of examining the gel is beyond the scope of this research.[99,100]

## 2.3 Section 3 – Learning from our First Attempts to Synthesise a Foldamer

Although, there were promising signs of progress up to this stage, we had not addressed a few critical problems. Firstly, the resolution of [2.2]paracyclophane derivatives had not been completed. As mentioned earlier, once [2.2]paracyclophane has been substituted the symmetry of the molecule is broken, producing a racemic mixture. Once we began coupling a racemic mixture of [2.2]paracyclophane, we exponentially increased the number of isomers present. If an octamer were to be synthesised using the initial method (Scheme 5), 256 stereoisomers would be present, which would be disastrous mixture of compounds. The resolution of [2.2]paracyclophane derivatives utilising oxazolines is an area of research the Rowland's group is actively investigating. Their results would produce the foundation to create enantiomerically pure [2.2]paracyclophane derivatives. Secondly, when coupling [2.2]paracyclophane together so far, the yields have been poor. In an attempt to increase yields and to stabilise secondary structure, aromatic linkers were

also explored. Literature has shown that aromatic units within the backbone sequence can be a valuable technique for forming secondary structure, evident by the examples shown in Chapter 1. Section 3 of results and discussions looks at resolution of [2.2]paracyclophane derivative using oxazolines (Scheme 32) and routes incorporating aromatic units within our [2.2]paracyclophane scaffold (Scheme 33).

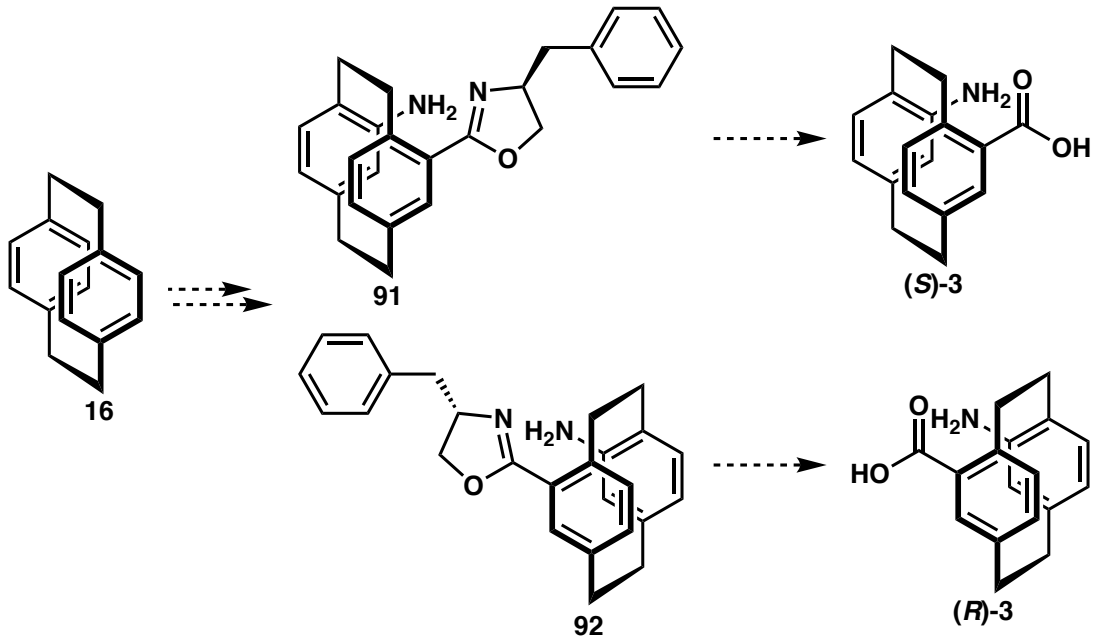


*Scheme 32 – Experimental approach to produce enantiomerically pure **3***

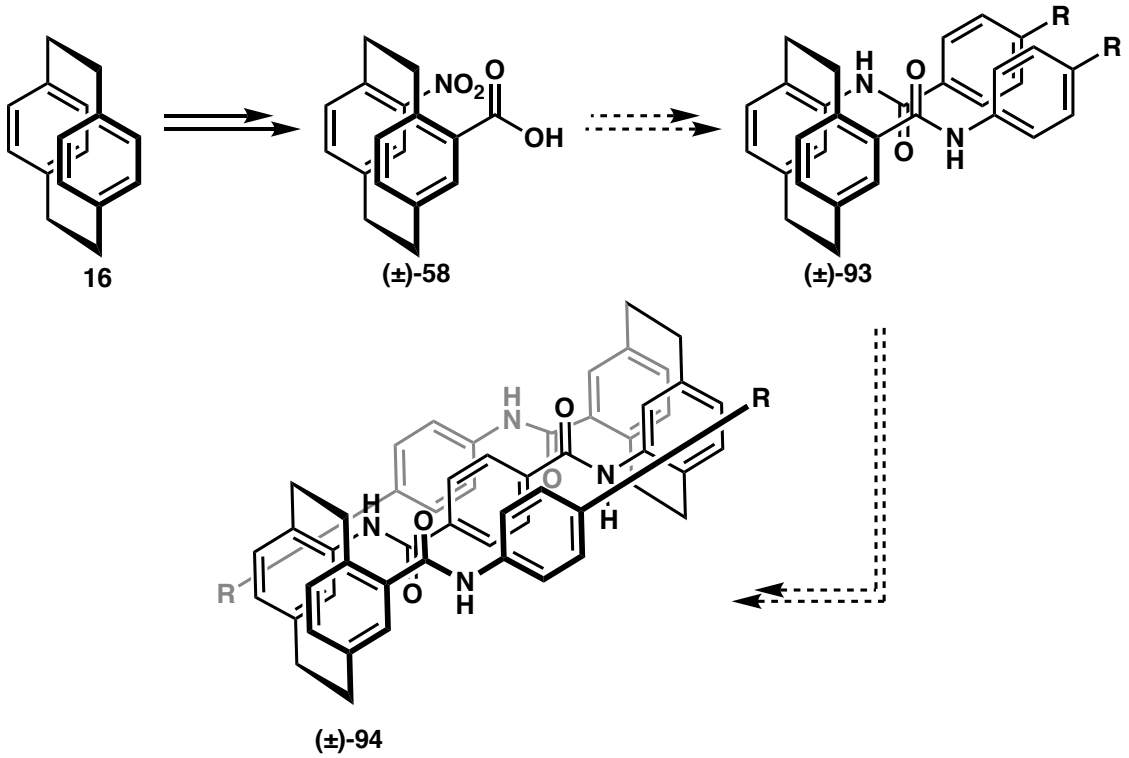


*Scheme 33 – One of the experimental approaches to incorporate aromatic linkers into the backbone sequence of a foldamer.*

### 2.3.1 Resolution

The Rowlands' group have shown that the resolution of [2.2]paracyclophane compounds can be achieved by incorporating an oxazoline derivative with fixed stereochemistry. By doing so, we obtain diastereoisomers that can be separated through silica-gel chromatography. With each diastereoisomer in hand, we can hydrolyse the oxazoline to afford enantiopure **3**. The overall steps to produce (*S*)-3 and (*R*)-**3** can be seen in Scheme 34.

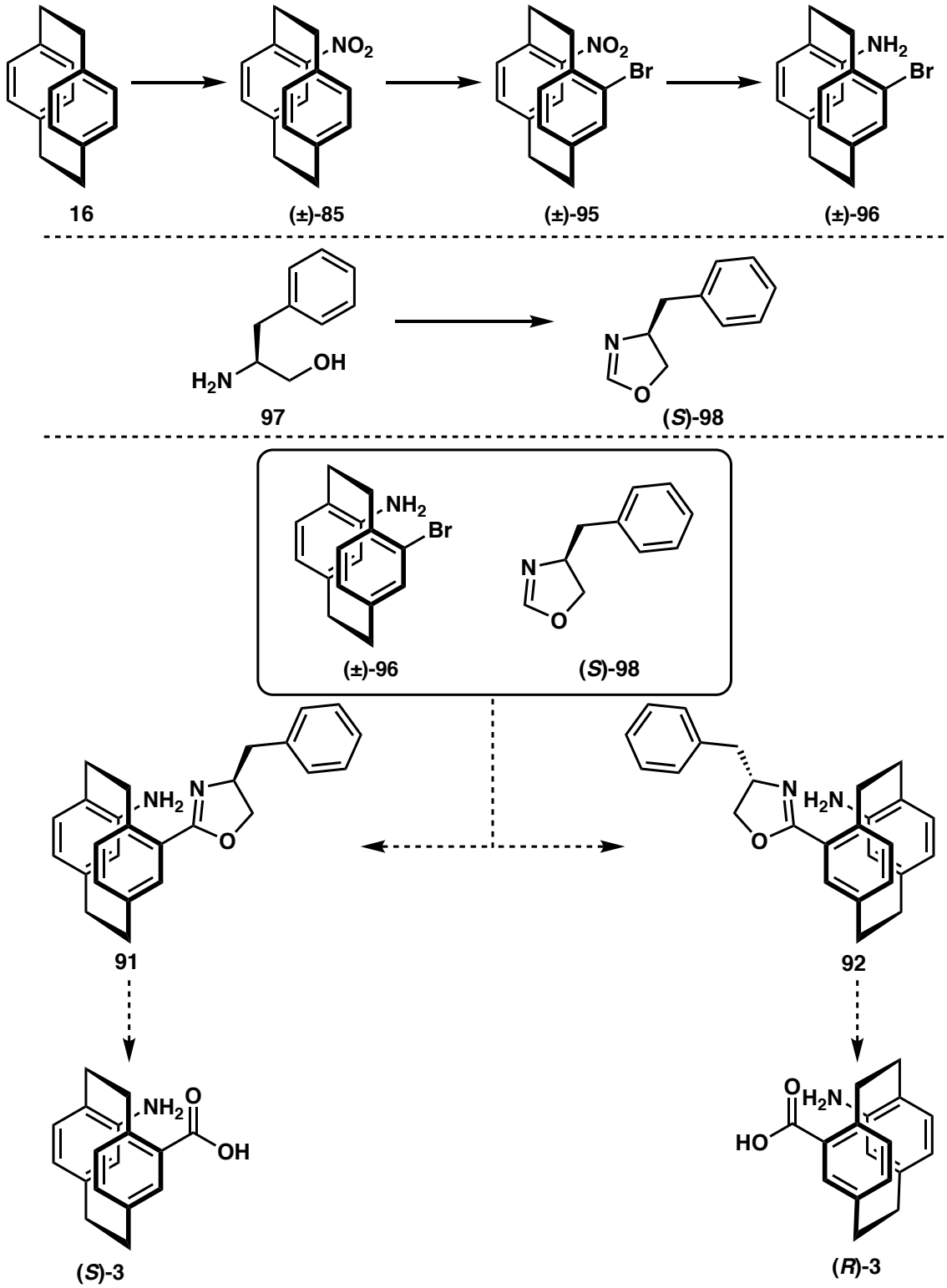


*Scheme 34 – Experimental approach to produce enantiomerically pure **3**.*

The synthesis of (±)-**96** occurs through three steps, as shown in Scheme 34, nitration, bromination, and lastly reduction. Nitration of [2.2]paracyclophane is discussed in Section 2 Part 1 and will be further discussed Section 4.

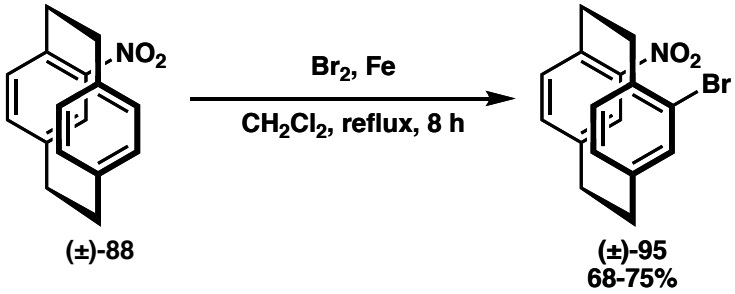


*Scheme 35 – Reaction conditions used to synthesise (±)-**95**.*

The synthesis of (±)-**95** is achieved in yields ranging from 68-75% with no complications. Bromination of the aromatic ring occurs by an electrophilic aromatic substitution reaction, as shown in Scheme 36. The regiochemistry of bromination is analogous to formylation seen in Section 2.

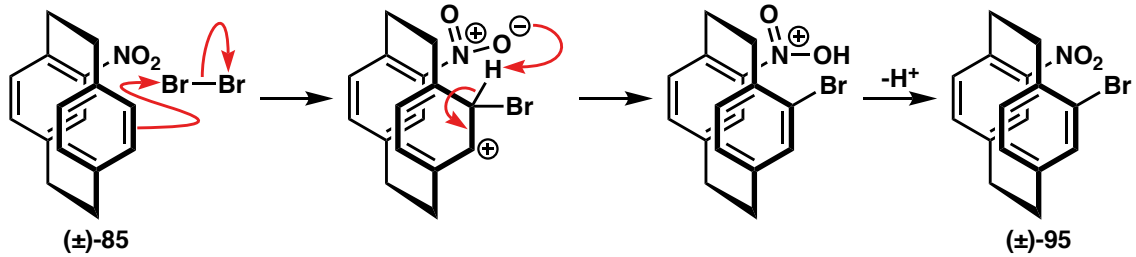


*Scheme 36 – A proposed mechanism for the bromination of (±)-**95**.*

The reduction of (±)-**95** was initially attempted using Zn and $NH_4Cl$, as seen in previous reactions. Surprisingly, these conditions were too harsh and resulted in reduction of both the nitro group and the bromo substituent to afford (±)-**99** in 87% yield (Scheme 37). As such, the reaction was attempted using an alternative method, the Béchamp reduction. This method provides milder conditions by utilising Fe as its reducing agent. The standard redox potential of Fe is -0.44 V, compared to -0.76 V of Zn, and so we believed it would be mild enough to afford the desired product. The alteration in procedure was successful, affording (±)-**96** in 66% yield and $Fe(OH)_2$ as a byproduct. The mechanism of this reaction follows the same pathway seen in Scheme 30.

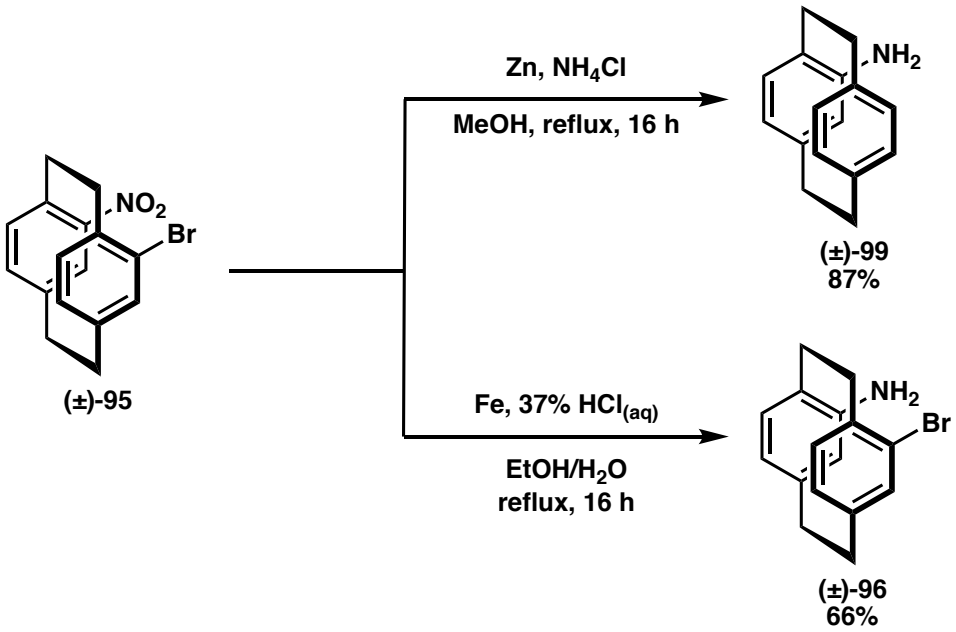


*Scheme 37 – Reactions conditions attempted to produce (±)-**96**.*

With (±)-**96** now in hand, synthesis of the oxazoline derivative commenced. The oxazoline synthesis could be completed in one step from commercially available **97** (Scheme 38). Formation of (*S*)-**98** was achieved with yields ranging between 50-61%, which was purified by Kugelrohr distillation at 55 °C (667 Pa).

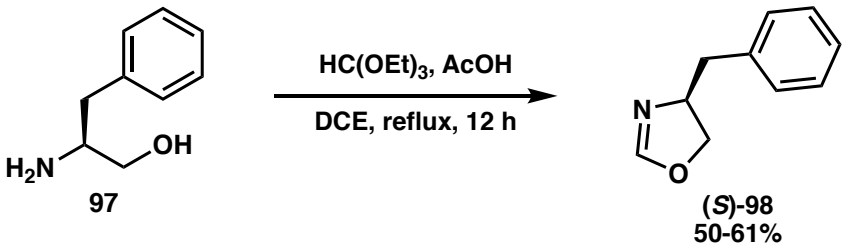


*Scheme 38 – Reaction conditions used to synthesise (S)-**98**.*

The mechanism for this reaction (Scheme 39) begins with the protonation of one of the alkoxy groups which allows the elimination of EtOH, to give a reactive oxonium species, which is attacked by the lone pair of electrons on the amine. A series of proton transfers permits a second elimination and formation of an iminium species. Cyclisation by nucleophilic attack of the alcohol's lone pair affords the final elimination of EtOH giving the desired oxazoline (*S*)-**98**. Unfortunately, due to time restrictions, resolution of [2.2]paracyclophane derivatives was not attempted.

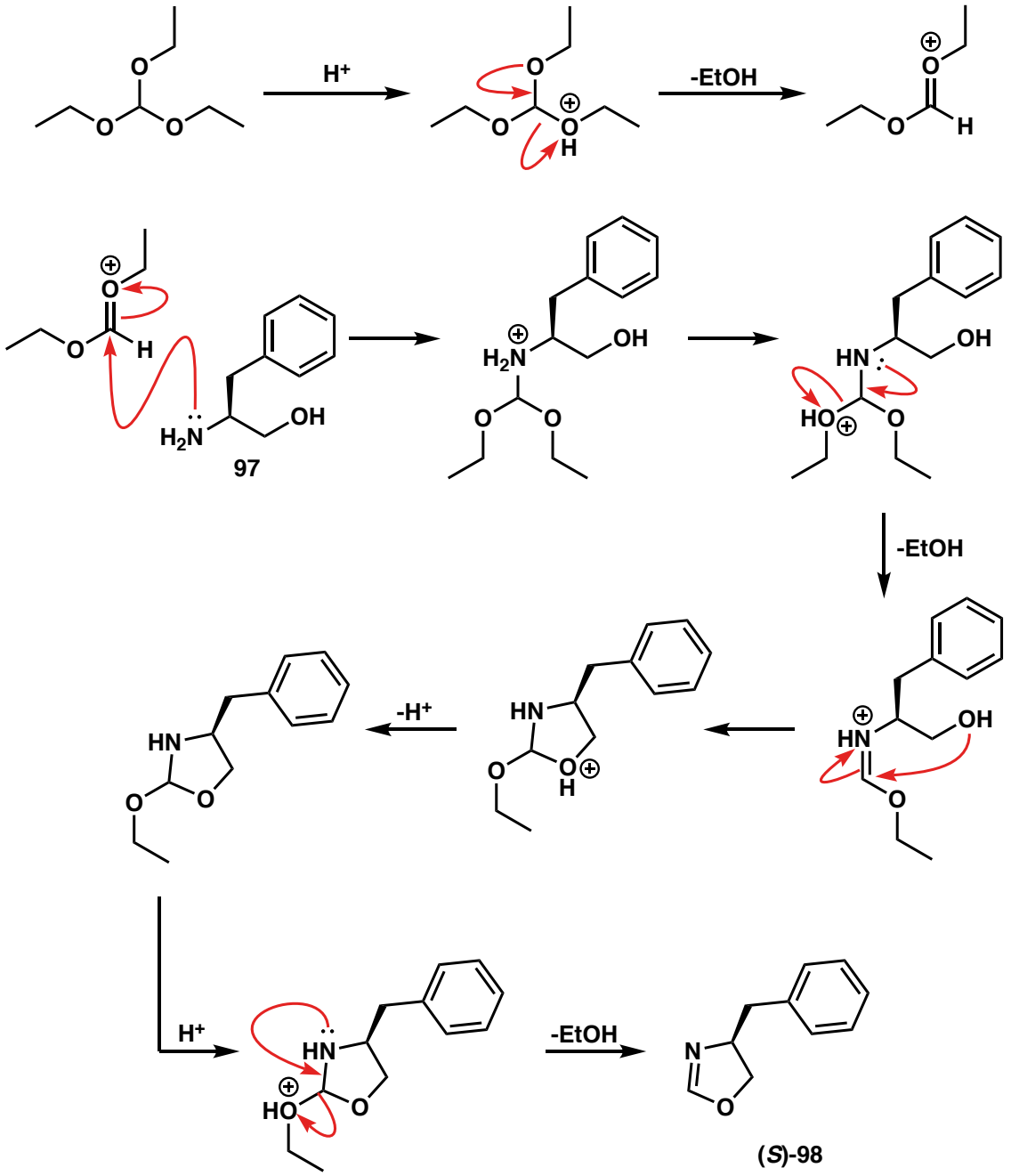


*Scheme 39 – Proposed mechanism for the cyclisation of **97** to give (S)-**98**.*

## 2.3.2 Aromatic Linker

As seen previously, the incorporation of aromatic linkers can be used to stabilise secondary structure in foldamers and [2.2]paracyclophane derivatives. For this reason, an experimental pathway to integrate additional aromatic units into the backbone sequence of our foldamer was pursued. Two routes were utilised and shown in Schemes 40. In the first route we simply expanded on the route previously utilised in Section 2 by using an

aniline derivative rather than a primary amine. The second route is an extension of the first route; however the sequence of reactions were reversed and the amine was coupled first.

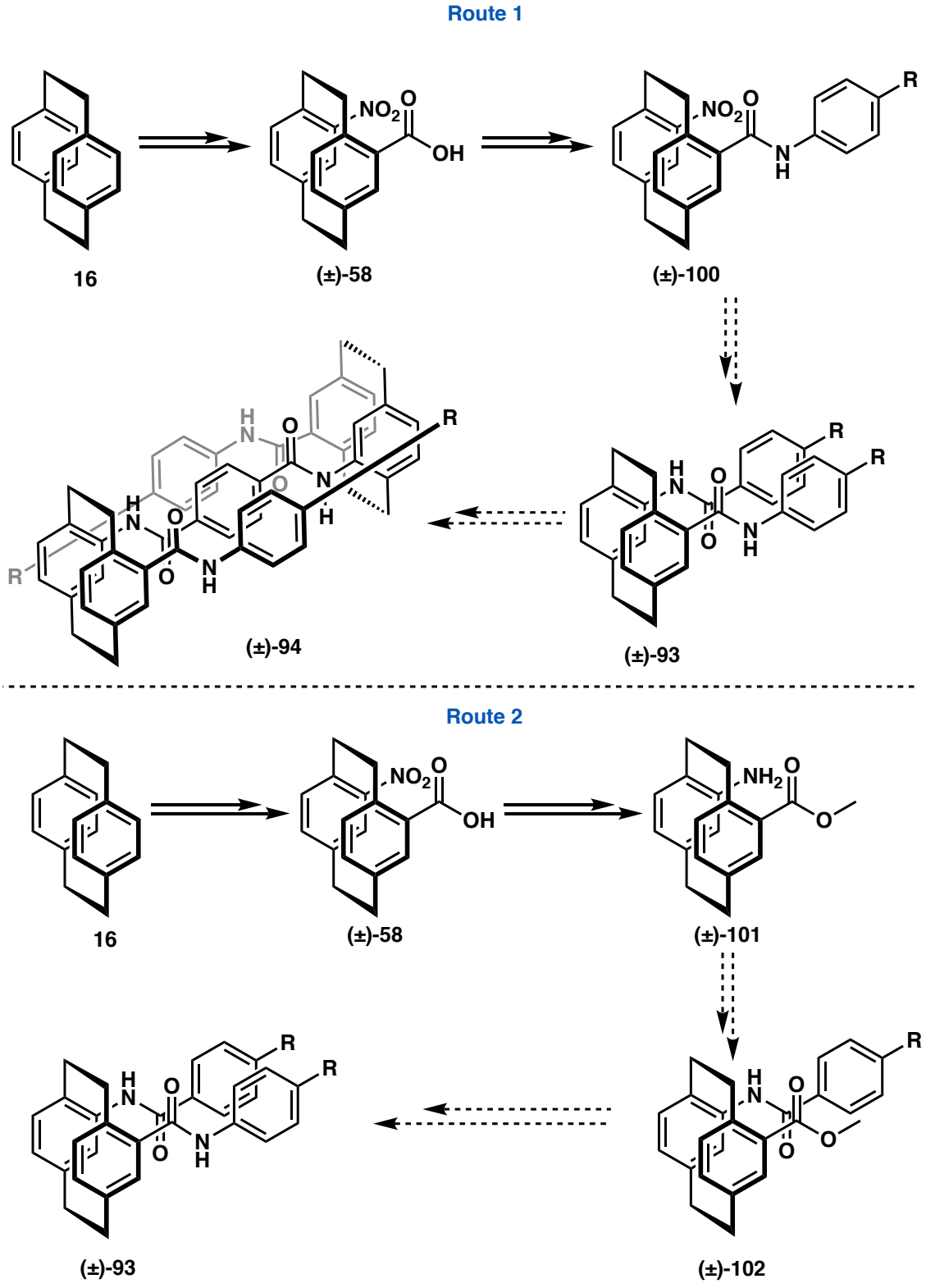


*Scheme 40 – Route 1 and 2 to produce a backbone sequence stabilised by aromatic interactions.*

## 2.3.2.1 Aromatic Linker – Route 1

The first route builds upon results obtained from our original experimental approach, along with some principals utilised in the literature. A common method for synthesising foldamers has been stacking electron-rich aromatic rings followed by an electron-poor aromatic ring, capitalising on the electrostatic interactions between rings. To mimic this design concept, we utilised the electron-poor aromatic ring of benzocaine as our first aniline derivative. We would then add an electron-rich aromatic ring to the amine.

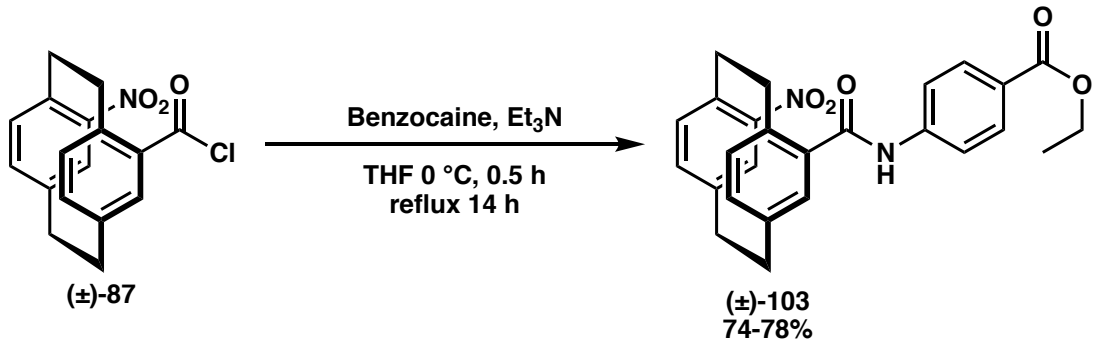


*Scheme 41 – Coupling of acyl chloride and benzocaine to furnish (±)-**103**.*

Synthesis of (±)-**103** was completed using the THF method and produced the desired product in 74-78% yield. Surprisingly, it was at this stage we started to see solubility issues with our compound, as (±)-**103** was only partially soluble in $CDCl_3$ and other common organic solvents. We had always known the compounds' solubility would eventually become an issue. As this project was aimed the linking together multiple partially soluble scaffolds, we did not have high hopes of the compounds being very soluble. However, we never anticipated the problem arising so soon. It is likely that in order to synthesise a [2.2]paracyclophane foldamer containing aromatic units in the future would require the aromatic to be further substituted with solubilising groups such as a long greasy chain. The mechanism of this reaction is the same as shown in Scheme 28.

The reduction of (±)-**103** was completed in EtOH rather than MeOH as we used before (Scheme 42). We wanted to prevent transesterification. Unfortunately, this reaction occurred poorly with yields ranging from 18-36%. There are many potential issues including amide cleavage and/or complexation of the Zn. However, without further investigation we cannot state which, if any, is occurring.

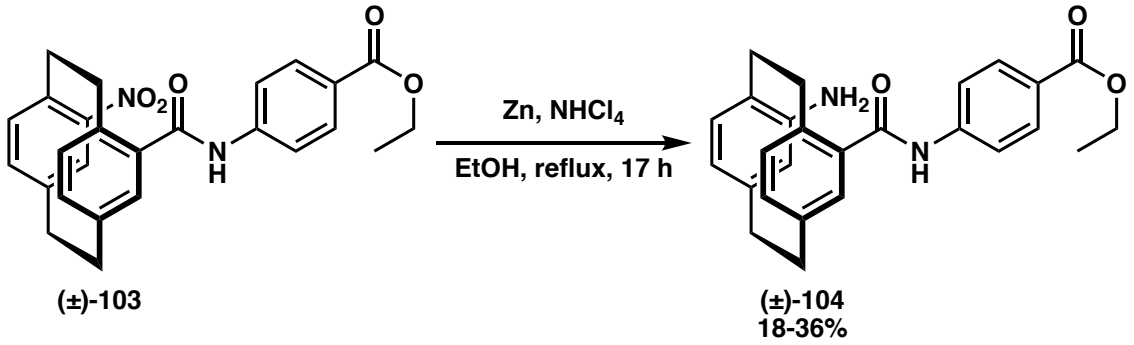


(±)-103 (±)-104 18-36%

*Scheme 42 – Attempted reduction of (±)-**103** to (±)-**104**.*

To synthesise a derivative of (±)-**93**, we first need to acquire **106**. By alkylating the amine of **105** we produce the cap for this foldamer and acts as a test reaction between the electron-rich and electron-poor aryl rings. The synthesis of **106** was achieved in 89-92% yield by reacting 4-aminobenzoic acid **105** with MeI. Standard methods for alkylation of **105** in literature utilised complicated procedures to form soley di-substituted **105**. We found that by merely monitoring the alkylation over 8 hours produced the desired product without any mono-substituted derivatives. The reaction occurs through a simple $S_N2$ mechanism.

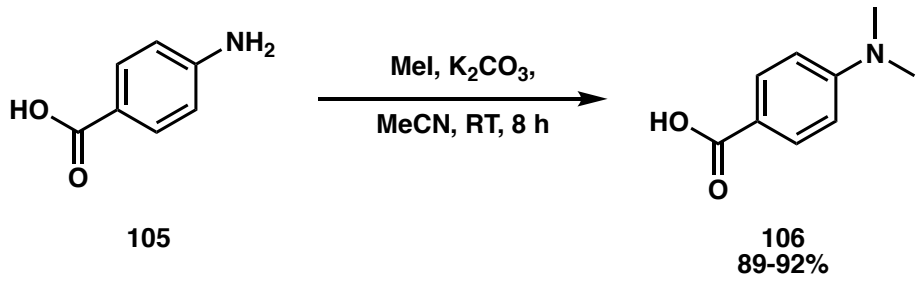


105 106 89-92%

*Scheme 43 – Alkylation of **105** to give **106**.*

Wanting a milder set of coupling conditions, we decided to look at classic peptide coupling reactions. A reaction of **106** with *N*-hydroxysuccinimide (NHS) and *N*,*N*'-dicyclohexylcarbodiimide (DCC) was completed to produce an active ester. Unsure of the stability of the activated intermediate, it was reacted with (±)-**104** immediately (Scheme 46).

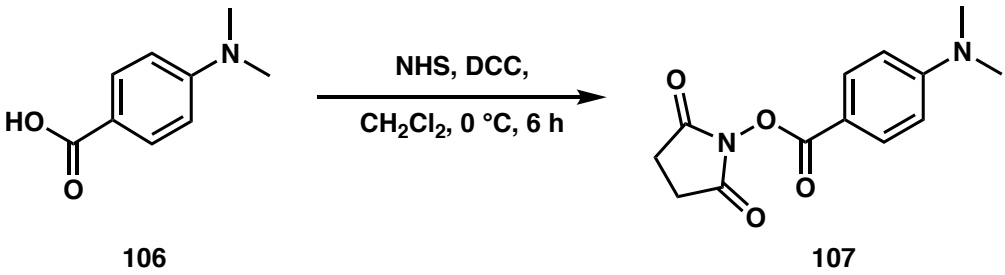


*Scheme 44 – Coupling conditions of **106** to give **107**.*

The mechanism for this reaction can be seen in Scheme 45. The reaction begins like a typical Steglich esterification with DCC acting as a base and deprotonating **106**. The resulting iminium-like cation and carboxylate combine to furnish an unstable *O*-acylisourea ester. Nucleophilic attack of NHS results in the production of dicyclohexylurea as a side product and formation of **107**.

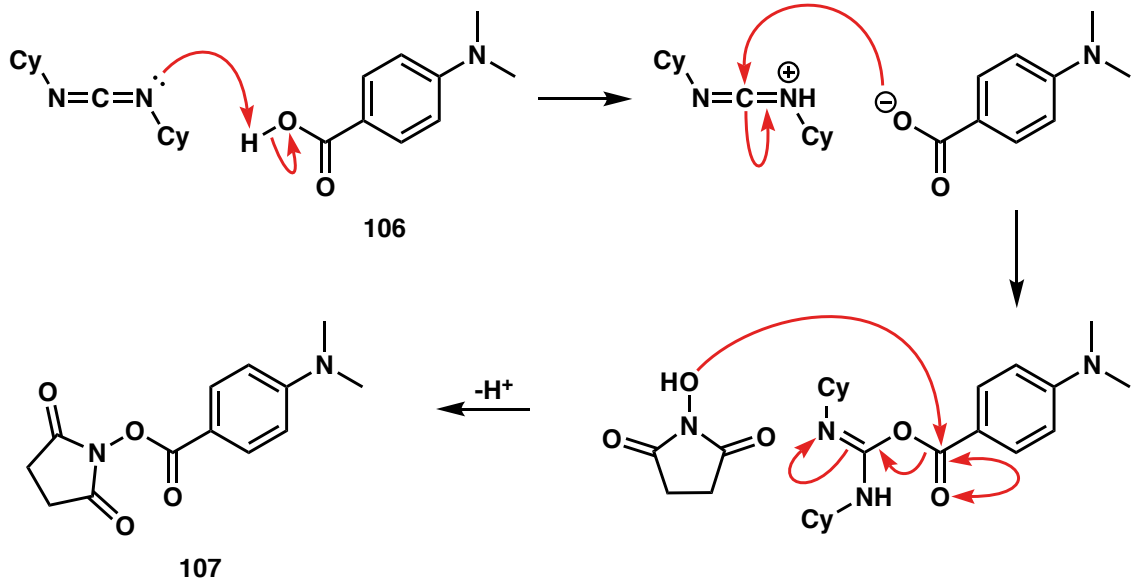


*Scheme 45 – The proposed mechanism to produce the active ester 4-aminobenzoic acid derivative **107**.*

With the active ester **107** and amine (±)-**104** in hand, coupling of the aromatic groups was attempted (Scheme 46). Analysis by TLC of the crude reaction mixture showed signs of starting material consumption along with the formation of considerable number of impurities. This caused interpretation of the $^{1}$H NMR spectrum of the crude reaction mixture to be problematic. The reaction was performed in a small scale as the previous step, the reduction, had been so inefficient. This meant we were unable to purify the mixture.

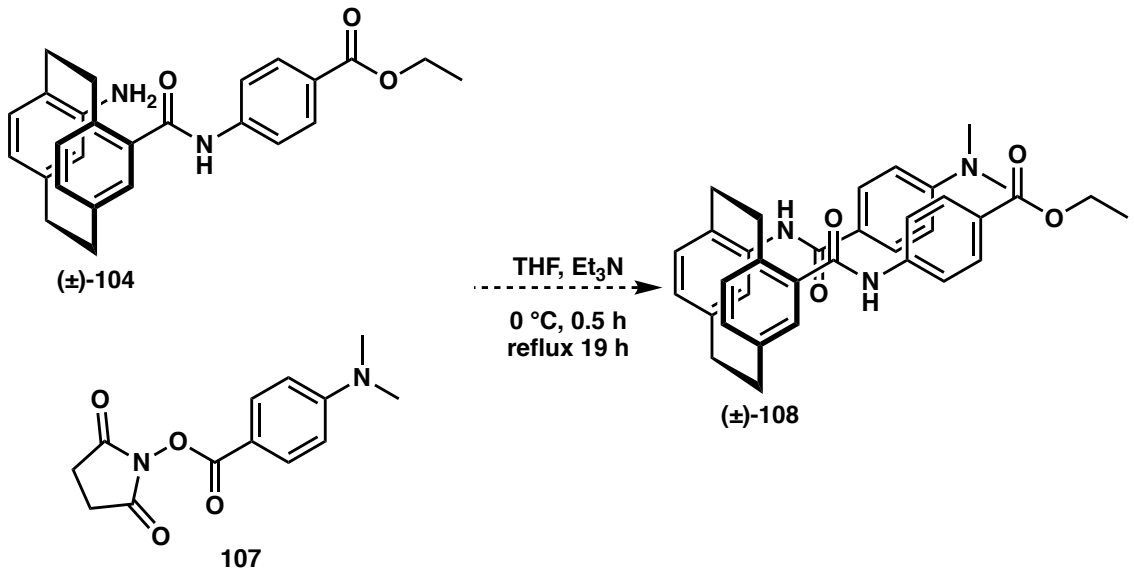


*Scheme 46 – Reaction conditions used to synthesise (±)-**108**.*

As the synthesis of (±)-**108** was not looking promising, a more direct method to link the [2.2]paracyclophane scaffolds was used. Synthesis of **110** was completed affording a mixture of diastereoisomers in 46% yield (Scheme 47). Like previous coupling reactions, a gel-like emulsion formed during the work-up. Filtration of the gel was completed, and $^{1}$H NMR analysis of the filtrate showed the presence of the product, suggesting the loss of material during washing. The $^{1}$H NMR spectrum of the crude reaction material showed the bulk of the material was 1,3-diaminobenzene **109**. To remove the excess starting material an acid-base work-up was completed. The work resulted in a 1:3 mixture of **110** diastereoisomers but some of desired product remained in aqueous phase. Although this route appears promising, we abandoned it due to a combination of time constraints and because we wanted to wait until we had resolved the [2.2]paracyclophane material.

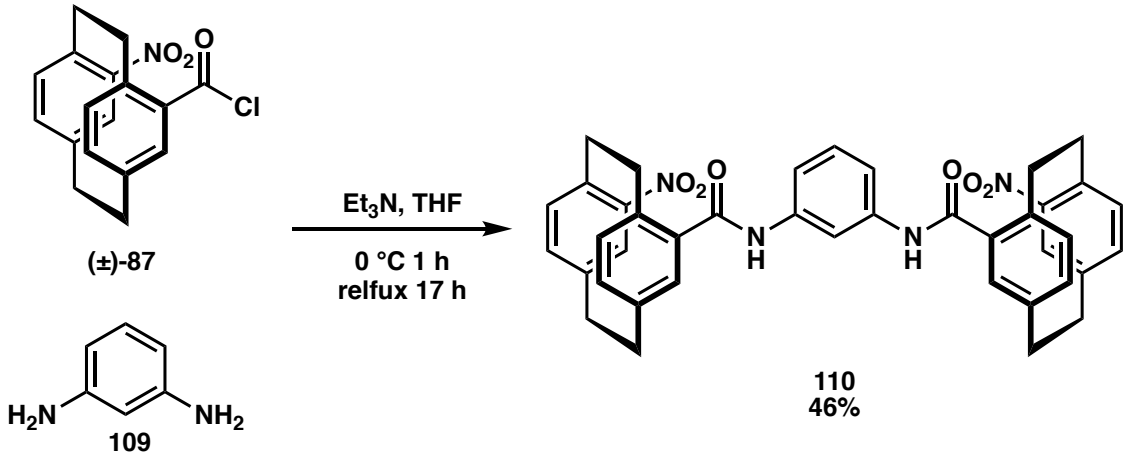


*Scheme 47 – Reaction conditions used to synthesise **110**.*

## 2.3.2.2 Aromatic Linker – Route 2

The problems encountered in the first route suggested a new plan was required. The second route was lengthier than the first as it involved formation of the methyl ester then reduction of nitro group and coupling of the amine. Typically, longer routes are not utilised as it results in a decreased overall yield of the end product. However, a longer route that gives the desired product is infinitely better than one that is shorter but fails. Members of the Rowlands group have had success in the past utilising this ester in coupling reactions, as such seemed like a logical starting point. With (±)-**58** in hand, the first step in this route was to make the methyl ester, (±)-**111**. As seen in the natural amino acid section, synthesis of a methyl ester can be achieved by refluxing (±)-**58** in excess MeOH and $SOCl_2$. This reaction occurred cleanly with yields ranging from 83-94%. The mechanism for this reaction is the same as Scheme 15. Conversion to the methyl ester was necessary as it prevented side reactions from occurring when coupling the aromatic units in future reactions. The reduction of (±)-**111** using Zn and $NH_4Cl$ occurred adequately, with yields ranging from 42-56% (Scheme 48). The mechanism for this reaction is the same as shown in Scheme 30.

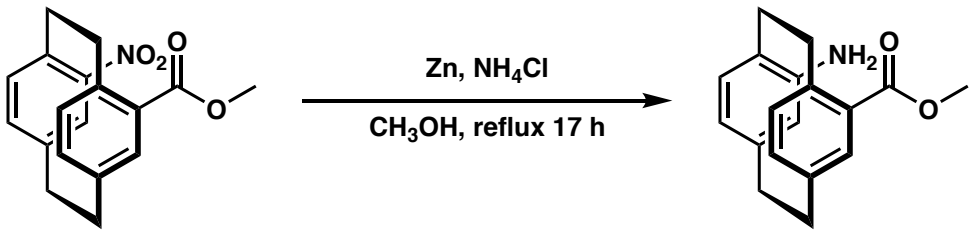


(±)-111 (±)-101 42-56%

*Scheme 48 – Reaction conditions used to synthesise (±)-**101**.*

With the amine (±)-**101** now in hand, conversion of **106** to **115** using $SOCl_2$ was completed and coupling of the two molecules was attempted (Scheme 49). Analysis of the $^1H$ NMR spectrum of the crude reaction mixture showed little promise of product formation, with the bulk of the material being (±)-**101**. Purification of the mixture failed to isolate any pure (±)-**113**.

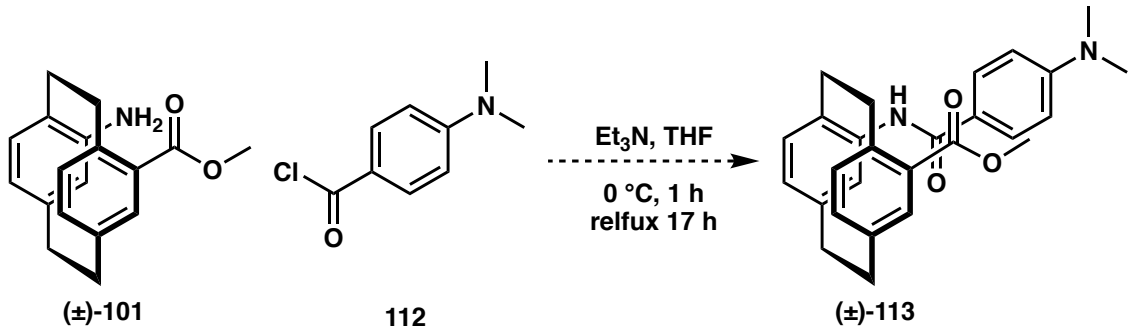


*Scheme 49 – Reaction conditions used to synthesise (±)-**113**.*

Although both routes showed promise, we started to notice flaws. Firstly, the solubility of these compounds was an issue. The benzocaine derivative (±)-**103** was only partially soluble in $CDCl_3$ or other common organic solvents. Secondly, coupling to the [2.2]paracyclophane amine is problematic. We suspect this due to the strong electron-withdrawing effect of the conjugated π-electron system. The nitrogen of an aniline is less nucleophilic than an amine due to the lone pair being delocalised over the ring. This effect is further exasperated due to the shared π-electron system seen in [2.2]paracyclophane and the electron withdrawing group on the other ring. In this instance, it could be argued that the nitrogen is deactivated by resonance between the rings (Figure 22).

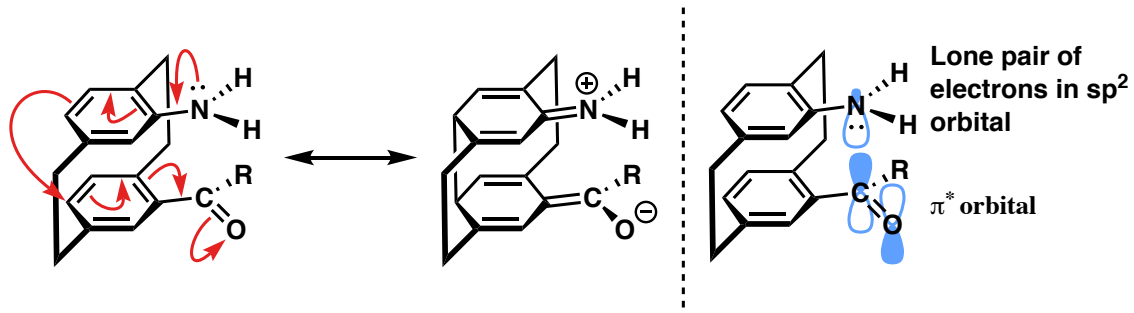


*Figure 22 – Aromatic resonance due to nitrogen's lone pair of electrons and the orbital overlap seen in the shared π-electron system.*

We suspect that the *pseudo-geminal* carbonyl could have two other effects. Firstly, it increases the steric bulk close to the amine. This is not helpful. Secondly, it is positioned so the lone pair of the amine interacts with the $\pi^*$ antibonding orbital of the carbonyl in a situation analogous to the Bürgi–Dunitz experiments. This can be seen in the X-ray crystal structure of (±)-**101**, acquired by slow evaporation of a 20% mixture of EtOAc in hexane. The X-ray crystal structure shows the pyramidal nitrogen has its lone pair of electrons orientated towards the carbonyl, suggesting the activity of the amine is

significantly decreased. Further evidence of this can be seen with our attempts to couple the amine to other groups, where we predominately regain (±)-**101**.

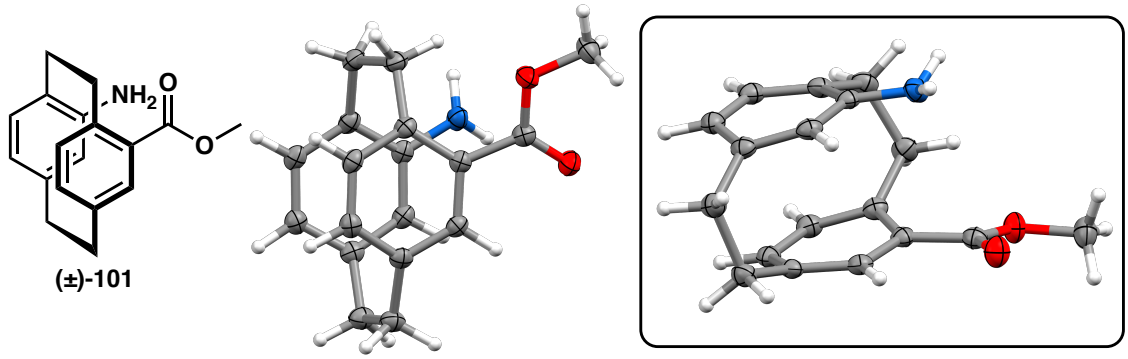


*Figure 23 – Molecular structure (left) and X-ray crystal (right) structure of (±)-**101** acquired through slow evaporation of EtOAc and hexane. C = grey, H = white N = blue O = red. Thermal ellipsoid probability level 50%.*

As these routes did not appear promising and each exhibited its own difficulties, a fourth route was explored. All the previous routes investigated the addition of an aromatic linker. An alkyl amine linker might be a lot more nucleophilic, less sterically demanding and could help with solubility. So, it was decided to investigate glycine based compounds. In addition to this, members of the Rowlands group have shown that glycine can be incorporated onto the [2.2]paracyclophane scaffold, or if required can be built off [2.2]paracyclophane through a longer series of reactions.[101]

Two glycine derivatives were synthesised prior to coupling to (±)-**87** or (±)-**101** (Scheme 50). The addition of the aromatic groups was not necessarily a required step for this route but were used for two main reasons. First, the addition of the phenyl ring made the compound more user-friendly, as it allowed for the reactions to be monitored through TLC. Secondly, if we were able to get the second glycine linker attached on the *pseudo-geminal* position, an interaction between the rings should have been visible by UV-Vis spectroscopy. A repulsive or an attractive interaction of the aromatic linkers should be distinguishable through shifts in the λ max and intensity.

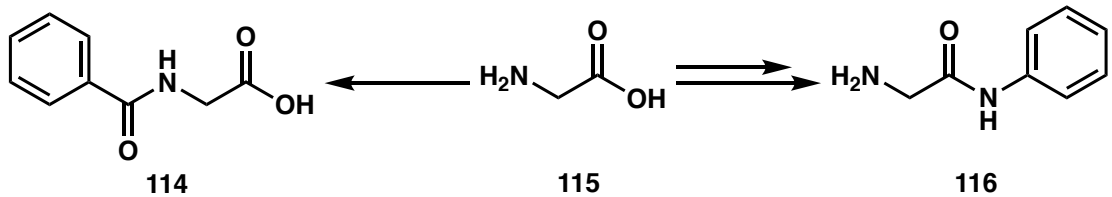


114 115 116

*Scheme 50 – Glycine target molecules to couple to [2.2]paracyclophane.*

The synthesis of the first desired compound, benzoylglycine **114**, was achieved in 86-90% yield, with only minor complications (Scheme 51). The $^1$H NMR of the crude reaction mixture showed the presence of benzoic acid as a minor side product, a result of excess benzoyl chloride reacting with $H_2O$. To prevent any side reactions from occurring in the following reactions the benzoic acid had to be removed as both products contained carboxylic acid groups. The purification of **114** was easily completed though a silica-gel plug. Mechanistically, the formation of **114** occurs through standard acyl substitution as previously discussed in alternative acyl chloride reactions (Scheme 28).

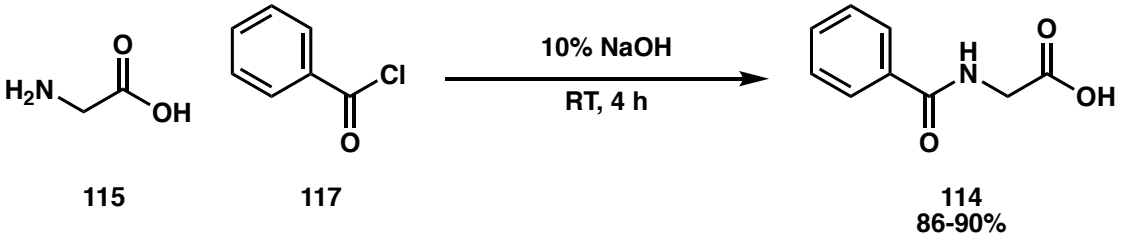


*Scheme 51 – Synthesis of N-benzoylglycine **114**.*

The Boc protection of glycine was much simpler than its fellow proteogenic amino acid arginine, seen in Section 1, with yields ranging from 93-95% (Scheme 52). The mechanism for this reaction can be seen in Scheme 17 of Section 1 of results and discussion.

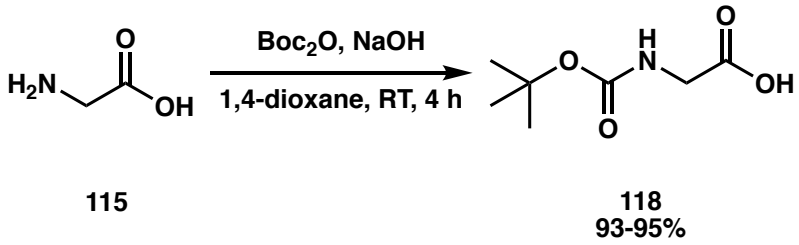


*Scheme 52 – Reaction conditions used to synthesise **118**.*

Having prepared **118**, activation of the carboxylic acid was required before the addition of aniline. The activation of the carboxylic acid has previously been achieved through two methods, conversion to an acyl chloride or an active ester. Transformation to an active ester was chosen in order to avoid Boc deprotection by the HCl byproduct formed in the $SOCl_2$ methodology. Unsure of the stability of the active ester **119**, it was used immediately after synthesis. The mechanism for this reaction can be seen in Scheme 45.

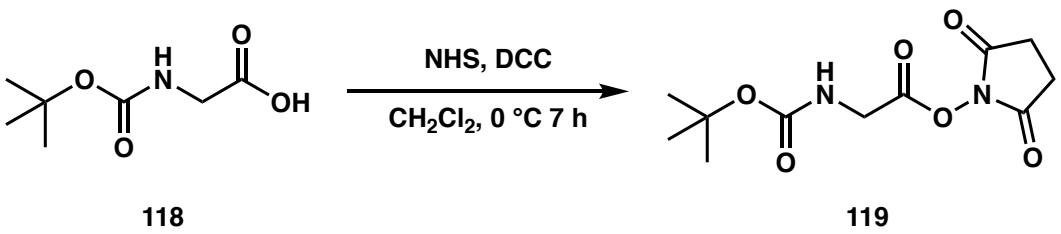


**118** **119**

*Scheme 53 – Activation of N-Boc glycine **118** to afford **119**.*

The synthesis of the Boc-glycine-aniline derivative **120** occurred affording a yield of 89% with no complications. We hoped this would bode well for coupling of **114** with the [2.2]paracyclophane aniline.

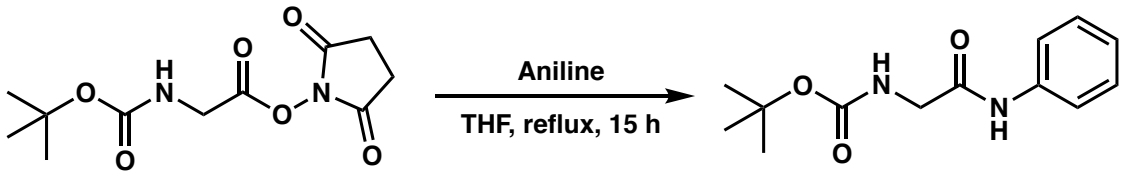


**119** **120**
**89%**

*Scheme 54 – Reaction conditions to synthesise the glycine amide **120**.*

The final step before reacting with [2.2]paracyclophane was the removal of the Boc protecting group from **120**, which is a acid mediated reaction that occurred near quantitively affording **116** in 96-98% yield (Scheme 55).

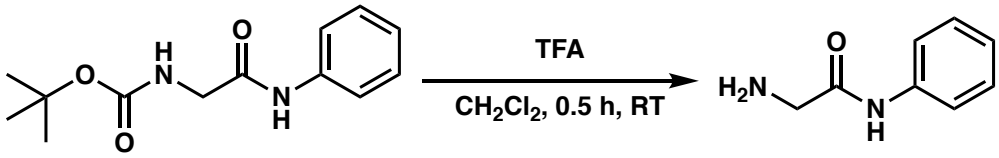


**120** **116**
**96-98%**

*Scheme 55 – Reactions conditions used to remove the Boc protecting group, affording **116**.*

The mechanism for this reaction (Scheme 56) begins with protonation of the *tert*-butyl carbonate producing a reactive oxonium ion. Decomposition of the oxonium species results in the release of a *tert*-butyl cation followed by carbon dioxide and formation of the amine. Protonation gives the salt.

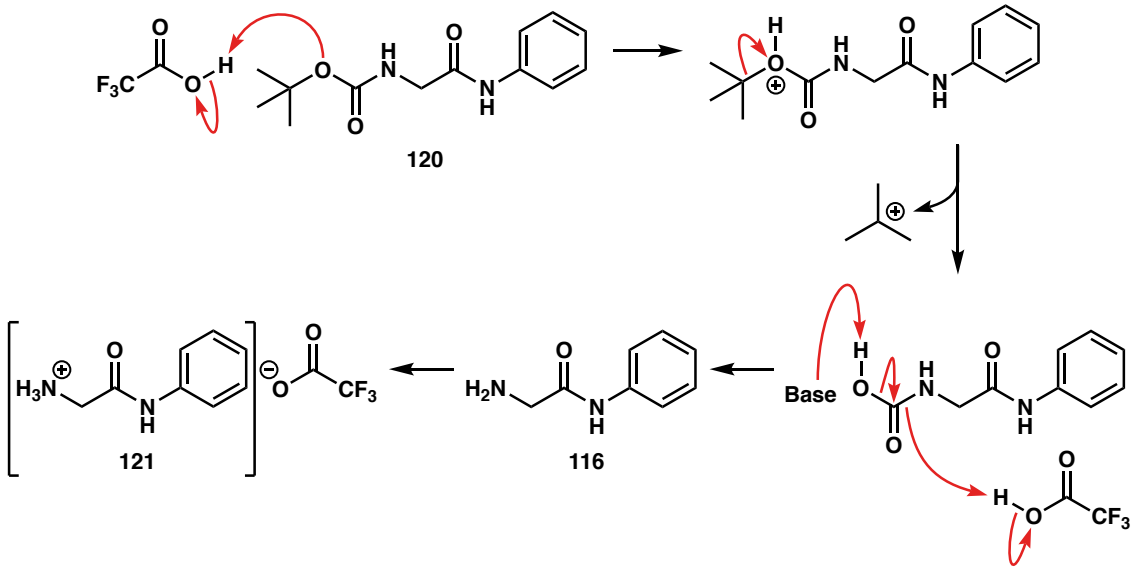


*Scheme 56 – Proposed mechanism for the Boc deprotection to afford the aniline-glycine derivative **116**.*

With the desired glycine derivative now in hand, we could start coupling to [2.2]paracyclophane the derivative (Scheme 57). Coupling to (±)-**87** shows a crude yield of 93%, with purification not attempted due to time constraints. Initial results are promising and show an increase in crude yield compared to the synthesis of the benzocaine derivative (±)-**103**. This is likely due to the increased nucleophilicity of the amine over an aniline derivative and the less cumbersome structure **116** provides.

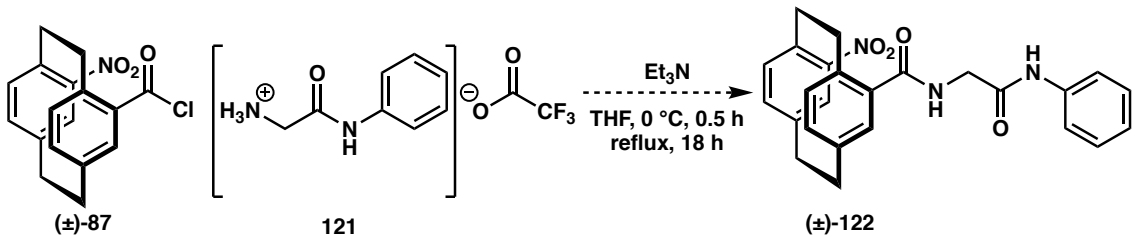


*Scheme 57 – Reaction conditions used to synthesise (±)-**122**.*

Unfortunately, further research for this section was not able to be completed to due time restrictions. However, the future potential for this research is promising and is further discussed in Chapter 3.

## 2.4 Section 4 – Synthesis of [2.2]Metaparacyclophane Derivatives

Earlier, in Section 2, we discussed the nitration of [2.2]paracyclophane. While we were able to optimise this reaction so that a satisfactory yield of 80-87% was obtained, we were curious as to the nature of the side product. It is often speculated that over nitration or the products of polymerisation and/or oxidation are obtained. In this section, we discuss our observations that the acidic conditions can cause rearrangement.

In order to obtain sufficient quantities of the amino acid precursor (±)-**58**, the nitration was conducted on a large scale and this permitted the various side products to be isolated in substantial quantities. The main-side product showed distinct peaks in its 1H NMR spectrum. Key were the peaks at 10.78 ppm and 5.80 ppm. The spectrum also showed both low field peaks associated with the aromatic region and high field peaks for the bridge head $CH_2$, although the latter had been shifted and spread out compared to most [2.2]paracyclophane derivatives we have isolated. This led us to speculate the product was (±)-**123**. An aromatic peak at 5.5 ppm is normally only observed in [2.2]paracyclophane with electron donating groups. The phenol derivative shows a peak for H-5 at 5.54 ppm while the amine is 5.39 pm. [102,103] Although the possibility of an amine could be ruled out by mass spectroscopy results. While the resonance at 10.78 ppm in $^{1}H$ NMR suggests the presence of a strongly deshielded proton, a distinguishing characteristic of a hydroxyl group participating in H-bonding. Infrared, mass spectroscopy, and $^{13}C$ NMR did not support the presence of an aldehyde, suggesting synthesis of (±)-**123** was correct and the peak at 10.78 ppm might be the OH internally hydrogen bonding.

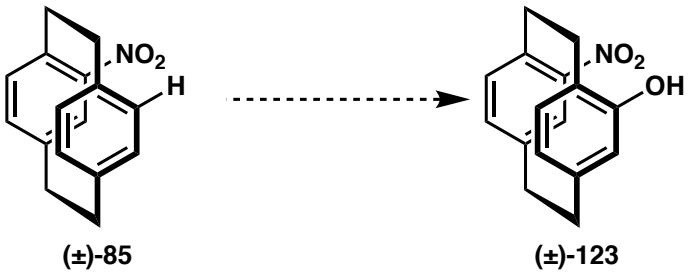


*Scheme 58 – Proposed transformations to produce (±)-**123**.*

While (±)-**123** was a potential structure, there were a number of problematic peaks that suggested we were wrong. The spreading of the bridge-head protons was unusual, as it hadn't been seen in other [2.2]paracyclophane derivatives synthesised by our group.

Fortunately, it was possible to grow a single crystal suitable for X-ray crystallographic analysis by the slow evaporation of $CH_2Cl_2$ and this gave us the structure. We were correct to assume disubstitution of the aromatic decks, but we had never considered the possibility of rearrangement of the cyclophane backbone. The product was a [2.2]metaparacyclophane derivative, 4-hydroxy-5-nitro[2.2]metaparacyclophane (±)-**124** (Scheme 62). The only time we had observed rearrangement was at high temperature.[104]

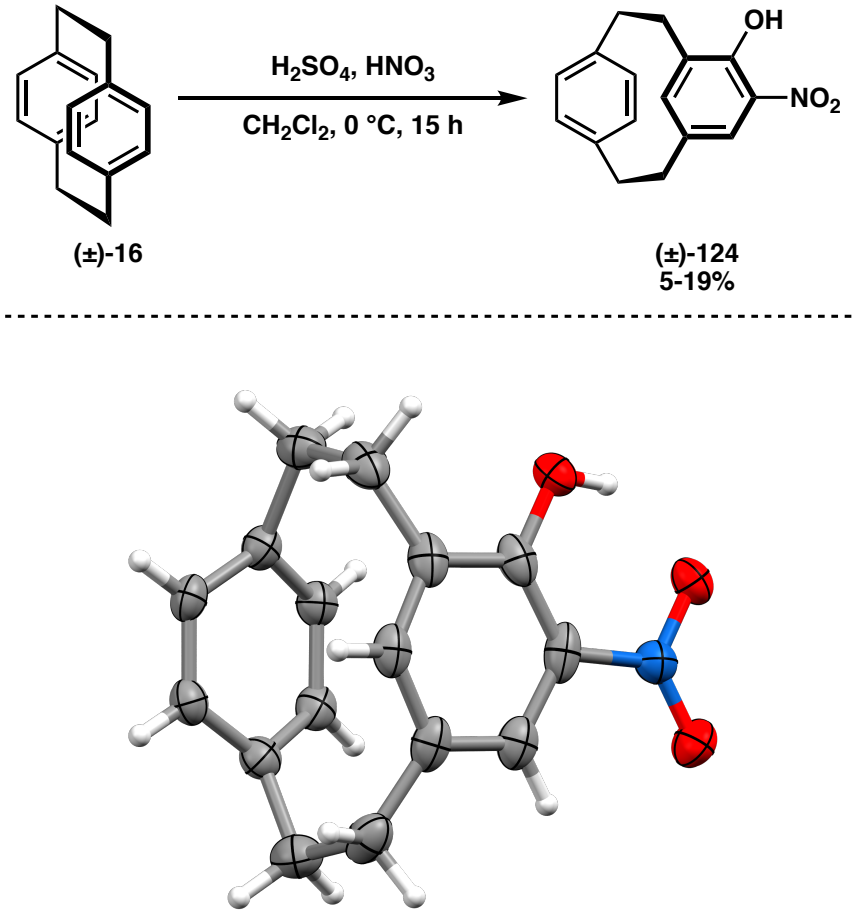


*Scheme 62 – Synthesis of 4-hydroxy-5-nitro[2.2]metaparacyclophane (±)-**124**, and X-ray crystal structure acquired through slow evaporation of $CH_2Cl_2$. C = grey, H = white, N = blue, O = red. Thermal ellipsoid probability level 50%.*

As always, once we knew the structure, the anomalous data made more sense. The peak at 10.78 ppm was from an OH internally hydrogen-bonded to the nitro group as predicted. The high field peak at 5.5 ppm caused from H-8 (see Figure 24 for numbering). This proton sits over the π system of the *para* substituted ring and is very shielded. We now use this peak as a diagnostic to indicate the presence of a meta substituted cyclophane.

The [2.2]metaparacyclophane framework itself is fascinating (Figure 24), as the *para* ring is forced into a shallow boat-like conformation and the *meta* ring is deformed into a chair-like conformation. The scaffold shares mixed characteristics of both [2.2]paracyclophane and [2.2]metacyclophane. Due to the conformation of **17**, the substituent of the carbon at the 8-position is forced over the top of the *para* ring, a unique characteristic of the scaffold. Studies have shown the *meta* ring undergoes conformation flipping with an energy barrier of 23 kcal $mol^{-1}$ (Figure 24).[105] This has been a key area of investigation of [2.2]metaparacyclophane with various derivatives synthesised focusing on the alterations of bridges have on the flipping and substitution at the C8 position to prevent ring flipping, thus producing chiral molecules.

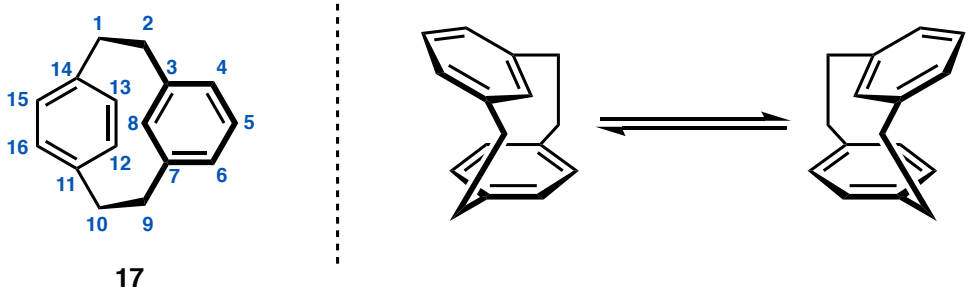


**17**

*Figure 24 – Molecular structure of [2.2]metaparacyclophane with conventional numbering of carbons (left) and conformational flipping (right).*

However, compared to [2.2]paracyclophane and [2.2]metacyclophane, research on [2.2]metaparacyclophane is scarce, with a single group routinely publishing in this area.[106–109] The group has published the vast majority of research involving [2.2]metaparacyclophane. Still, with exclusion to research looking at the ring flipping, most of the research lacks any imagination, with most reports treating the scaffold to traditional organic reactions, but then takes a step backwards and uses a substitution patterns that makes the scaffold achiral. In fact, most of the literature looking at [2.2]metaparacyclophane is simply how to produce the scaffold. After Donald Crams initial paper on the synthesis of [2.2]metaparacyclophane various other procedures were developed; with the most common route using 2,11-dithia[3.3]metaparacyclophane, which is followed by the extrusion of S or $SO_2$.[110] Even though various symmetrical substitution pattens have been reported, the substitution pattern of (±)-**124** is a novel discovery, with an asymmetric pattern not seen in the literature before, let alone acquired through a single reaction, highlighting that new routes to functionised [2.2]metaparacyclophanes has the potential to promote research in the field.

As we preform nitration at 0 °C, we hadn't considered the rearrangement of [2.2]paracyclophane. Unaware the pioneer of [2.2]cyclophane chemistry, Donald Cram, had already reported on the rearrangement to [2.2]metaparacyclophane, we were left puzzled and curious. As such, an in-depth investigation was completed to uncover the order of events, substitution or rearrangement first, and whether we would make other derivatives.

Initially we wanted to investigate the rearrangement, to see if it occurred before substitution. We first looked at the two acids separately to see if either would bring about rearrangement. A reaction between [2.2]paracyclophane and $H_2SO_4$ is believed to form an achiral disulfonic acid derivative **125**. However, the reaction did not go to completion, resulting in a mixture of **125** and [2.2]paracyclophane. Due to [2.2]paracyclophanes tendency to streak during silica-gel chromatography, isolation of **125** was unsuccessful.

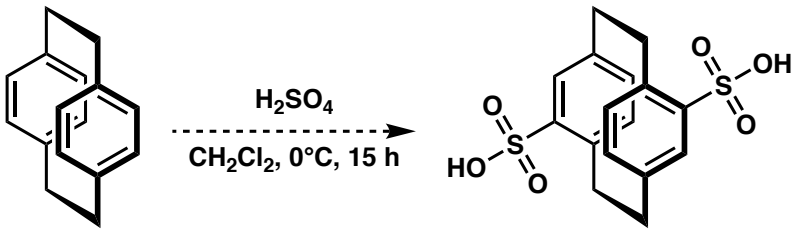


**16** **125**

*Scheme 59 – Reaction conditions thought to produce **125**.*

Treatment of [2.2]paracyclophane with $HNO_3$ gave a surprisingly clean nitration reaction acquiring the desired product in 97% yield. Oddly, there are limited reports of just $HNO_3$ being used to produce the nitronium ion. We assume that the equilibrium shown in Scheme 60 (bottom) exists and can provide the necessary electrophile. The reaction would be slower than normal as this is an equilibrium and the concentration of nitronium would be lower, but the reaction is clearly still possible.

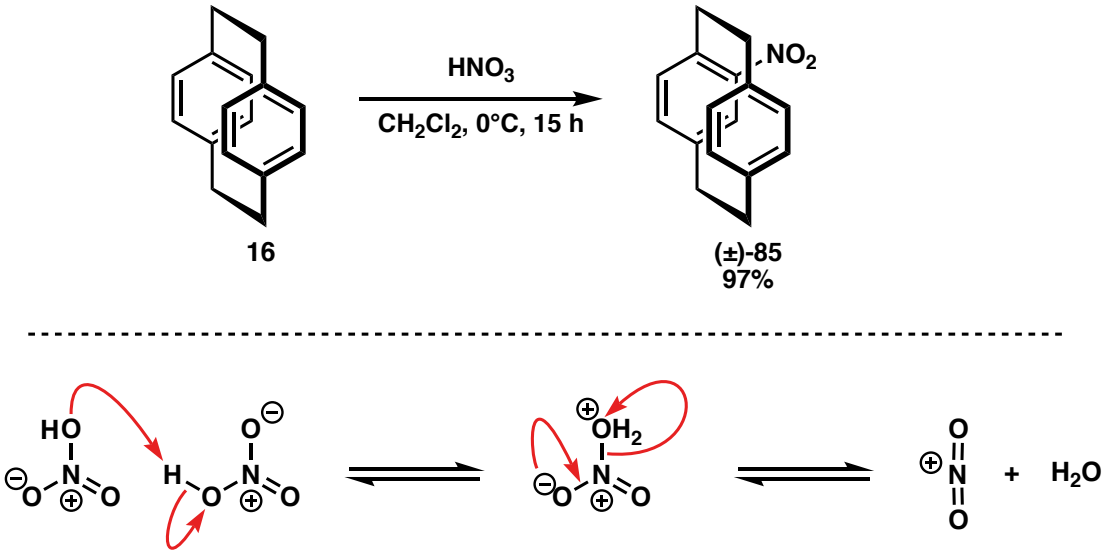


*Scheme 60 – Nitration of [2.2]paracyclophane $HNO_3$ to afford (±)-**85** (top) and the proposed mechanism, to produce a nitronium ion from $HNO_3$ with no additional acid (bottom).*

However, like previous nitration reactions of [2.2]paracyclophane, this reaction is unpredictable and frequently gave alternative side products along with a low yield of (±)-**124** (2.3%). This led us to believe both reagents are required to obtain good conversion to form (±)-**124**.

These results suggest that neither acid was capable of causing rearrangement and we assumed that substitution must occur first. Therefore, we investigated the rearrangement of the nitro substituted [2.2]paracyclophane(±)-**85**. Initially, we reacted (±)-**85** under nitration conditions (Scheme 61). From the $^1$H NMR spectrum and mass spectroscopy of the crude reaction mixture we believe we had obtained a dinitro compound. However, there were no signs of product formation. This was not surprising though, as the nitro substituent is strongly electron withdrawing, which deactivates the ring to protonation.

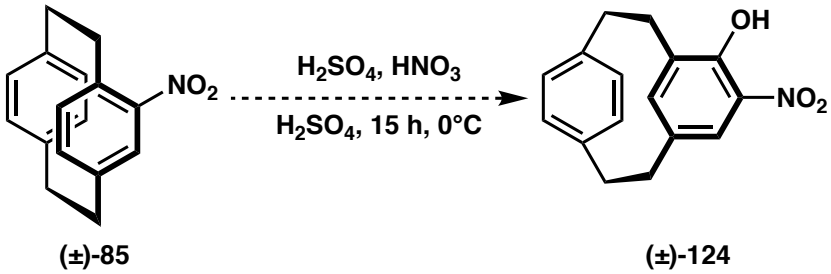


*Scheme 61 – Reaction conditions used to examine if (±)-**85** undergoes rearrangement.*

Since nitrating conditions are highly oxidising, we wanted to see if other oxidising conditions would cause rearrangement. A procedure in the literature has shown reliable

oxidation of nitrobenzene compounds using $K_2S_8O_2$. Once again, in hopes to see rearrangement, we applied these conditions to (±)-4-nitro[2.2]paracyclophane (Scheme 62). As $K_2S_8O_2$ is water soluble and (±)-**85** isn't we tried biphasic mixtures of $H_2O$ and acetone, THF, 1,4-dioxane, or *tert*-BuOH. All reactions failed to produce the desired product. In all examples, starting material was recovered. This led us to suspect the nitro compound wasn't the precursor to (±)-**124**. Next we looked at 4-hydroxy[2.2]paracyclophane (±)-**127** as this might activate the ring.

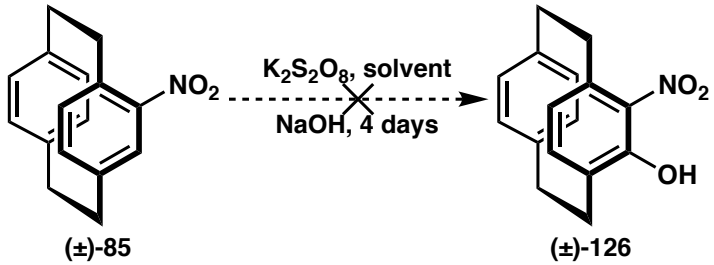


*Scheme 62 – Oxidation conditions utilised where the solvent is either water, or a mixture of water and acetone, THF, 1,4-dioxane, or tert-BuOH.*

As a colleague had already prepared 4-hydroxy[2.2]paracyclophane (±)-**127**, nitration of (±)-**127** using the standard procedure to obtain (±)-**124** or (±)-**126** was performed next (Scheme 63). Considering phenols are electron donating and thus are more active than unsubstituted benzene rings, we were surprised that no reaction was observed. No rearrangement and no nitration.

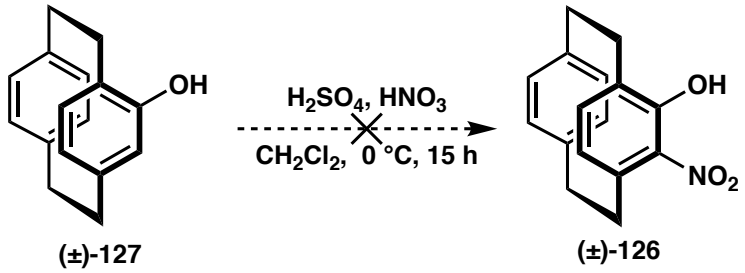


*Scheme 63 – The nitration conditions attempted for the formation of 4-hydroxy-5-nitro[2.2]paracyclophane (±)-**126**.*

We started to believe rearrangement was occurring through acid mediated carbocation intermediate. To confirm this idea, [2.2]paracyclophane was reacted under strongly acidic conditions. One of the reactions was completed in the presence of water while the other acted as a control (Scheme 64). If the suspected carbon cation was being produced in the rearrangement, the addition of a hydroxy group should be observable in the $^1$H NMR of the final product.

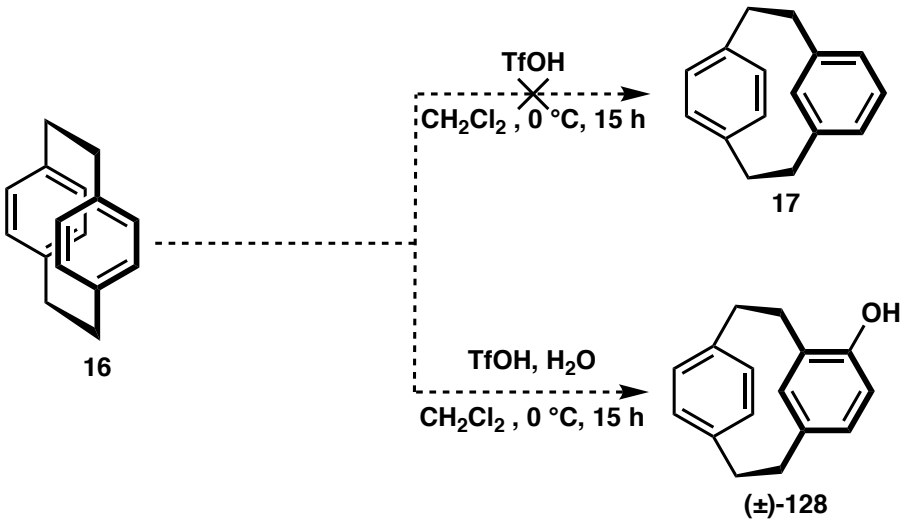


*Scheme 64 – The reaction conditions used to drive rearrangement.*

The reaction without water resulted in multiply products, which we suspect is simply the result of polymerisation of [2.2]paracyclophane. The addition of water, however, created more promising results. Mass spectrometry and $^1$H NMR of the crude reaction mixture indicated the formation of 4-hydroxy[2.2]metaparacyclophane (±)-**128**. Purification of (±)-**128** through silica-gel chromatography was unsuccessful. After further investigation, we believed this was due to the low stability of [2.2]metaparacyclophane derivatives on silica-gel resulting in decomposition, which is further discussed in later on. Further attempts to regain (±)-**128** were unsuccessful, with substitution only seen in one out of ten experiments.

Although the initial reaction using TfOH proved unsuccessful, a clear colour change was observed in the early minutes of the reaction, resulting in the undissolved white [2.2]paracyclophane changing to a blood-red colour. Therefore, a shorter reaction was attempted (Scheme 65). The $^1$H NMR spectrum of the crude reaction mixture showed promising signs as there were clear signs of a new aromatic species present with the resonance of the C-8 proton occurring at 5.42 ppm, a signature shift in [2.2]metaparacyclophane compounds.

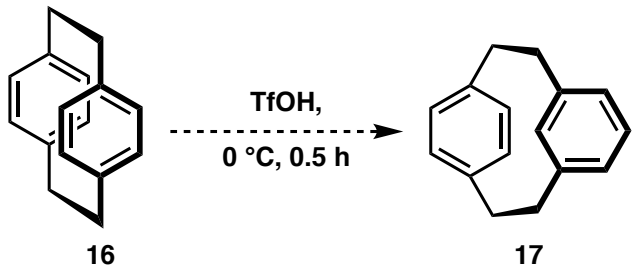


*Scheme 65 – Shorter reaction conditions implemented to form [2.2]metaparacyclophane.*

There were, however, two main issues with this reaction. First, complete conversion to [2.2]metaparacyclophane was not achieved. The highest percentage of conversion observed based on $^1$H NMR analysis was 21%, with an extended reaction time only resulting in increased formation of a polymerisation side product. Secondly, both [2.2]paracyclophane and [2.2]metaparacyclophane are non-polar compounds, they are just isomeric hydrocarbons, and there is no separation between them by standard chromatographical techniques.

Assuming that the reaction occurred by protonation of [2.2]paracyclophane and subsequent rearrangement of the resulting carbocation we wondered if it would be possible to trap the cation with a suitable nucleophile. The product would be polar and hence should be separable from unreacted [2.2]paracyclophane. Experiments using NaI or MeCN were attempted using the same conditions previously used to show rearrangement (Scheme 66). Both reactions to form (±)-**129** and (±)-**130** were unsuccessful, with the $^1$H NMR indicating the formation of [2.2]metaparacyclophane, 17% for the MeCN reaction, and 20% for NaI reaction.

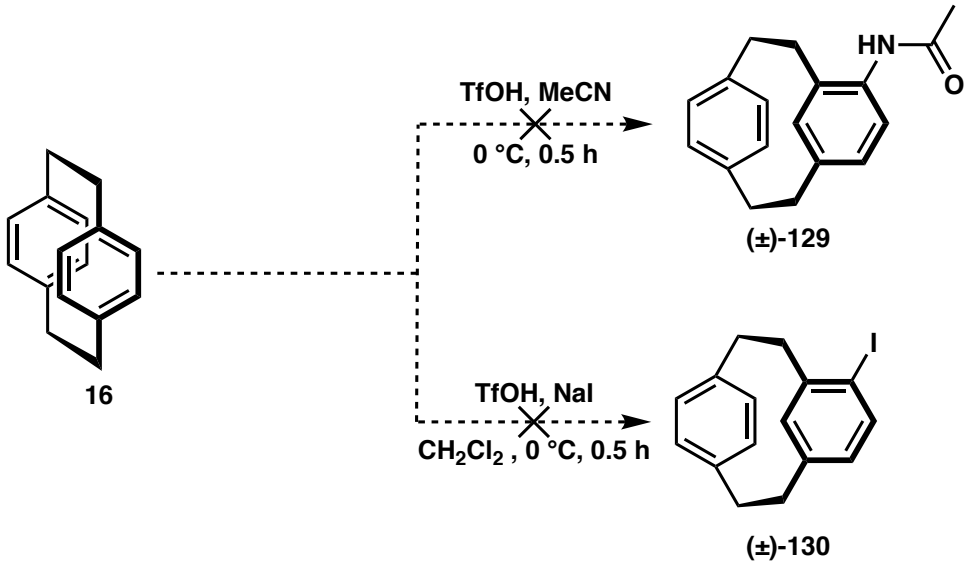


*Scheme 66 – Reaction conditions used to produce [2.2]metaparacyclophane derivatives.*

None of these reactions gave the desired compound but all showed [2.2]metaparacyclophane in the crude reaction mixture. A quick investigation of the strengths of acids required to cause rearrangement revealed that both TfOH ($pK_a$ = -14) and $HClO_4$ ($pK_a$ = -10) were sufficiently strong to cause rearrangement while $HNO_3$, $H_2SO_4$, and AcOH were all too weak. While these results seem to make sense, when we compare the $pK_a$ values they do not explain why a mixture of $H_2SO_4$ and $HNO_3$ can cause rearrangement. It is possible that we are comparing the wrong values. $pK_a$ measures acidity in $H_2O$. Under our reaction conditions it might better to compare the Hammett acidity function $H_0$. This measure works better for concentrated acids. On this scale TfOH = -14.1, $HClO_4$ = -13 and $H_2SO_4$ = -12.0 are more similar and might explain why nitration conditions cause rearrangement.[111]

Regardless, we can propose a mechanism for the formation of the hydroxy nitro [2.2]metaparacyclophane. The driving force for the reaction appears to be release of cyclophane strain. This causes the initial rearrangement and the subsequent addition reactions that will be discussed later (Scheme 67). The first step is protonation at the bridgehead to give the carbocation. Protonation here is thought to release the most strain.[112] Rearrangement to *meta* further releases strain to give a new carbocation. This is trapped by water generated by the mixture of acids. Although it is possible that the nitrate anion, the conjugate base of nitric acid adds and is subsequently hydrolysed. Either way, we believe the [2.2]metaparacyclophane phenol is formed. The electron donating hydroxy group activates the *meta* substituted ring. Substitution at the ortho position occurs as the *para* positions is blocked by the bridgehead. This gives the product (±)-**124**.

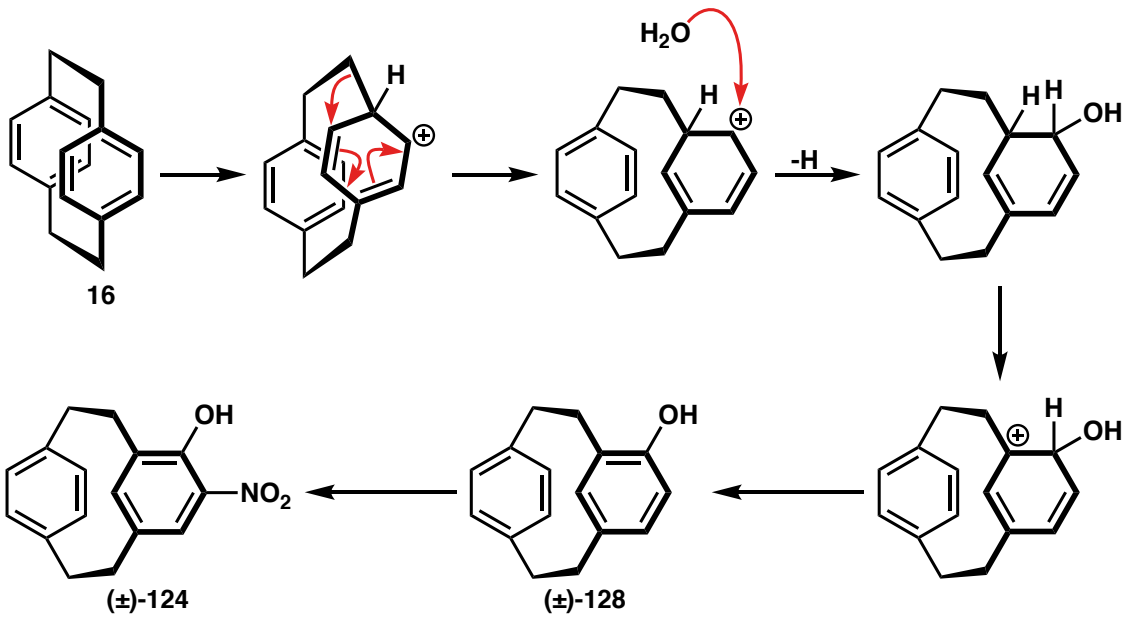


*Scheme 67 – Proposed sequence of transformations for rearrangement and to afford (±)-**124**.*

As research for Section 2 and 3 was being completed in parallel to this research, nitration of [2.2]paracyclophane to produce the amino acid precursor was required. As (±)-**85** had been cleanly afforded in high yields using only $HNO_3$, these conditions attempted again (Scheme 68). However, this reaction's fickle nature was shown again as the reaction did not occur cleanly and showed the presence of (±)-**124**. As the crystallisation of (±)-**124** was easily achieved, hot recrystallisation of the sample was performed, which caused a precipitate to form.

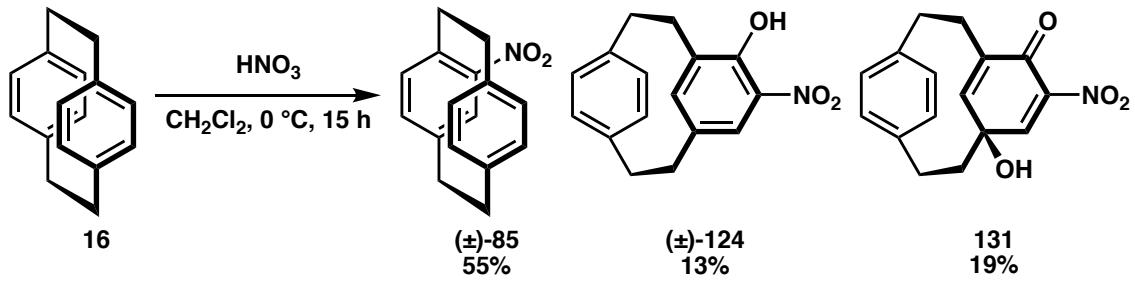


*Scheme 68 – Nitration of [2.2]paracyclophane to form (±)-**88** and two [2.2]metaparacyclophane derivatives (±)-**124**, **131**.*

The $^{1}H$ NMR spectrum of this precipitate showed the formation of an alternative [2.2]metaparacyclophane compound. Analysis of the $^{1}H$, $^{13}C$ NMR and other spectroscopic data was puzzling. Recrystallisation of the product from hot $CH_2Cl_2$ allowed a X-ray structure to be obtained and confirm the product. Surprisingly, we no longer had [2.2]paracyclophane or [2.2]metaparacyclophane, the aromaticity of the *meta*

ring had been broken resulting in the synthesis of a cyclohexadienone compound (Figure 25).

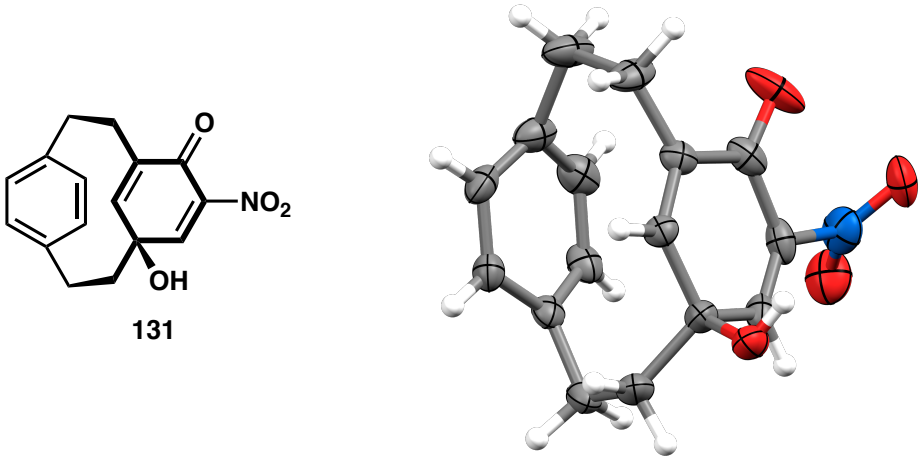


131

*Figure 25 – Molecular structure and X-ray of the newly acquired cyclohexadienone cyclophane derivative **134**. C = grey, H = white N = blue O = red. Thermal ellipsoid probability level 50%.*

Structural changes have occurred due to the dearomatisation of the *meta* ring. The additional $sp^3$-hybridised atom bonded to the bridge reduces the distortion to 7° compared to **124**. Also, due to the absence of a hydroxy group for hydrogen bonding, the repulsion between the lone pair of electrons on the dienone causes the nitro group to face out of the plane at 60°.

The literature has reported the oxidation of phenols to ketones is achievable using $HNO_3$, suggesting the cyclohexadienone cyclophane **131** is a product of the subsequent oxidation of (±)-**124**.[113,114] A proposed sequence of transformations is shown in Scheme 69. The initial step from (±)-**124** are unclear, however, there are two main possibilities. Firstly, electrophilic aromatic addition leads to the formation of *ipso*-substituted nitro, *meta* to the hydroxy group (red curly arrows). Alternatively, electrophilic addition may occur directly on the oxygen of the nitronium ion to produce a nitrite species that is then hydrolysed to afford **131** (blue curly arrows). Substitution at the C7 position results in the introduction of point chirality to the molecule. This along with the planar chirality the scaffold provides would normally produce a mixture of diastereoisomers. However, the nitronium ion is unable to approach from the *para* ring due to the restricted space, this results in the addition *anti* to the *para* ring, resulting in **131** as a single diastereoisomer. Planar chirality is then locked once oxidation has occurred, preventing flipping of the *meta* ring.

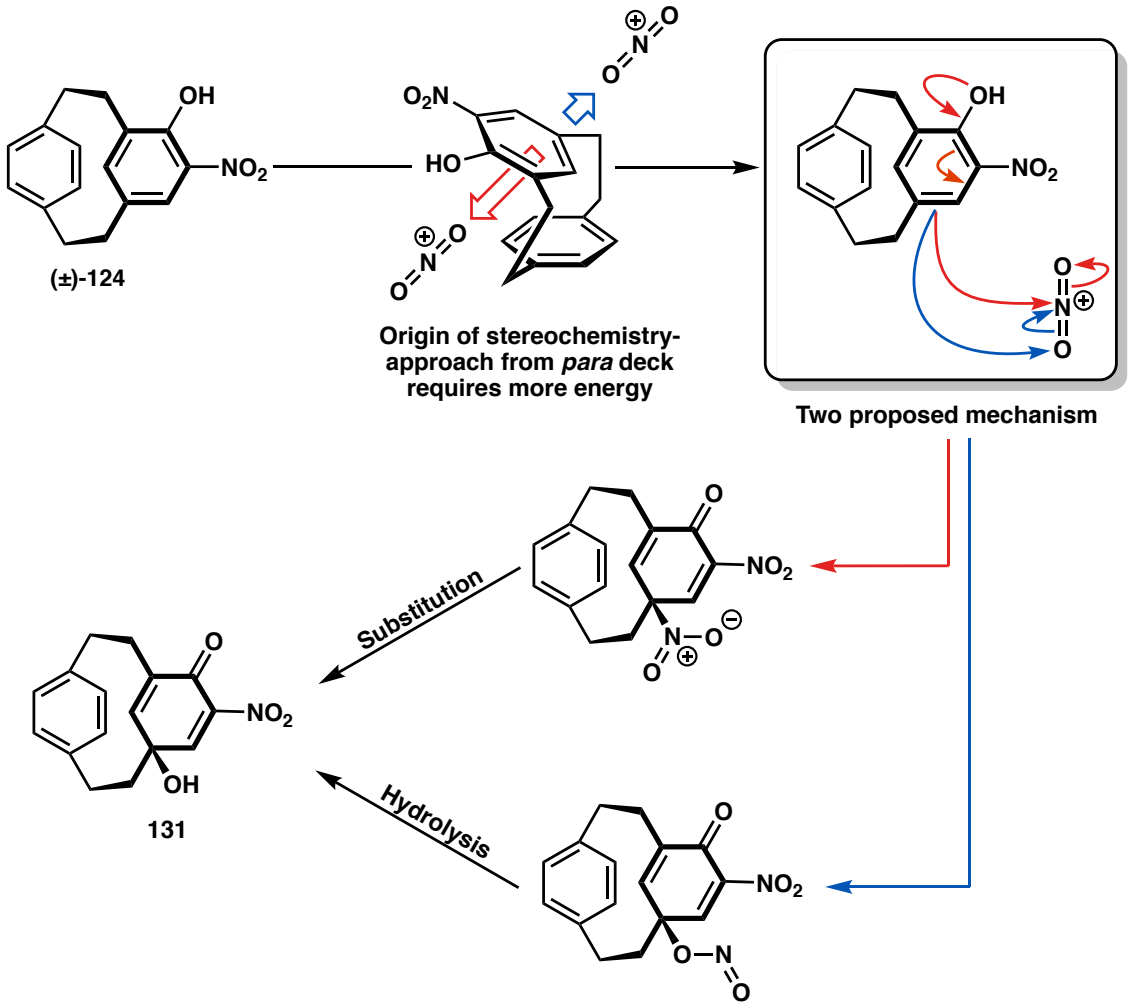


*Scheme 69 – Proposed steps to form **131**.*

We were unsure how stable this compound would be, believing that dehydration to reform the aromatic ring would occur. As a result, we thought the acidic nature of a silica column might be sufficient to cause the reaction. Surprisingly, in the presence of MeOH, conjugated addition to the activated alkene to form **132** was observed (Scheme 70). It is believed the addition of the methoxy group results in the release of yet more cyclophane strain. A X-ray crystal structure of **132** was obtained through hot recrystallisation in a mixture of MeOH and $CH_2Cl_2$.

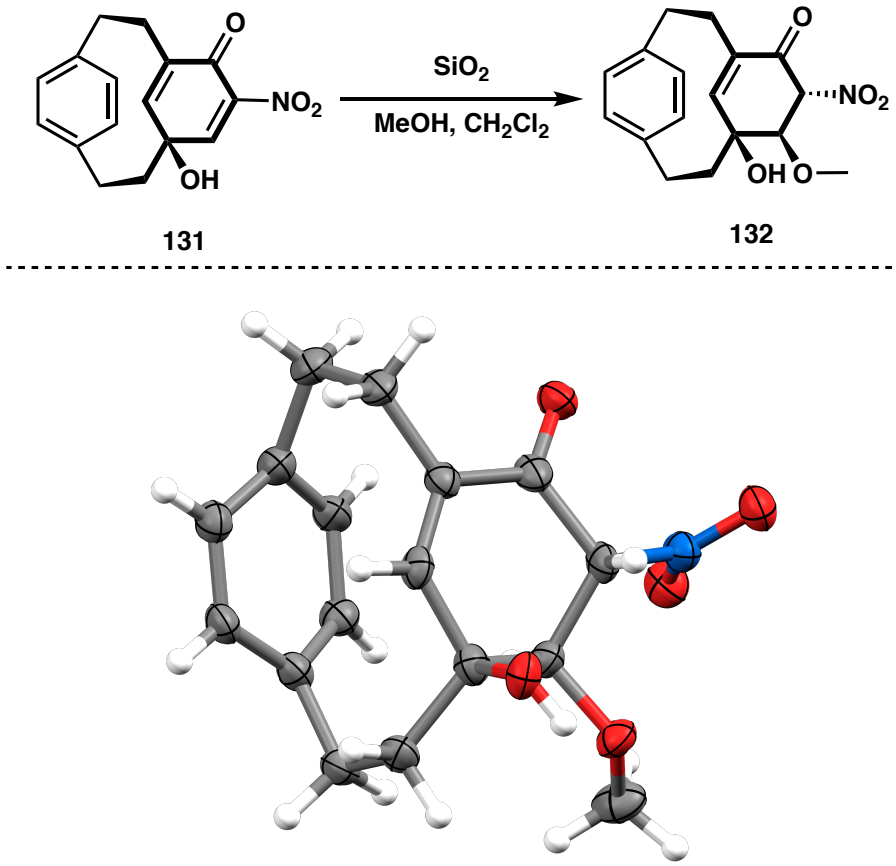


*Scheme 70 – X-Ray crystal structure of the newly acquired cyclohexadienone cyclophane derivative, C = grey, H = white, N = blue, O = red. Thermal ellipsoid probability level 50%.*

As **132** was obtained as a single fraction containing greasy impurities, further purification was required. Initial attempts found **132** to be highly reactive, decomposing on silica-gel into unknown products. As the purification of **132** was difficult, we tried to replicate the reaction through acid-mediated ether formation in MeOH, in the hope we could get full conversion to the product (Scheme 71). However, even with an extended period of time, transformation to the product was limited to 75%, with the remaining 25% to be starting material. As this provided a crude reaction mixture with a larger concentration of the desired product, we looked at hot recrystallisation in the hope of crystallising either compound. This would allow us to separate out the mother liquor and crystals with one or the other being the desired product. However, the subsequent $^{1}$H NMR spectrum of both the crystals and the mother liquor showed the presence of only starting material. Suggesting the **132** decomposes during the recrystallisation process.

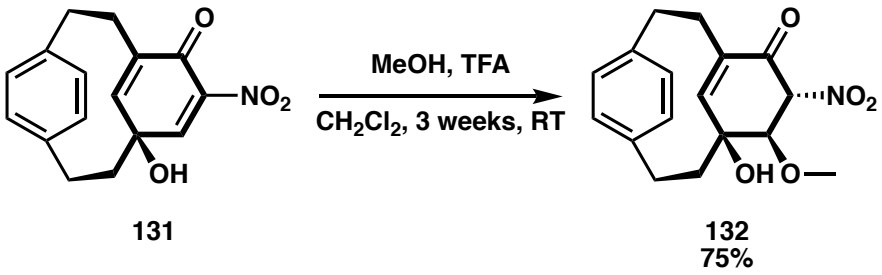


131 132 75%

*Scheme 71 – Reaction conditions used to obtain **132**.*

As formation of **132** through reaction conditions were limited, and still required purification, further attempts to purify **132** was trailed. A summary of the various purification efforts and methods can be seen in Scheme 72. It appears the rate of decomposition is proportional to time spent on the column.

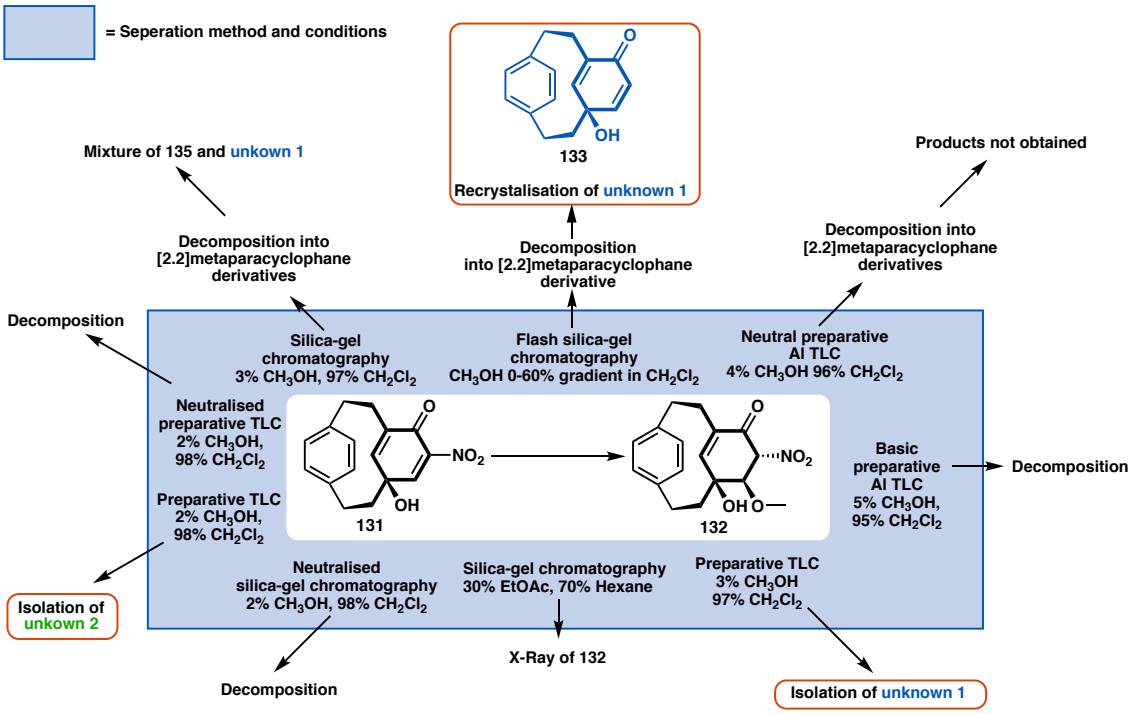


*Scheme 72 – Various purification methods and conditions attempted to isolate **132**.*

Isolation of **132** was finally achieved through slow evaporation of flash chromatography fractions containing a mixture of [2.2]metaparacyclophane derivatives (Scheme 73). Although the fractions were a mixture of compounds, **132** appears as transparent crystals which could be separated by hand and allowed further examination of the compound. First, the decomposition of compounds could be analysed through the use of TLC. Analysis of the plate showed **132** is the only compound that undergoes decomposition. The product of this decomposition also showed an $R_f$ value equal to **133**. This explains why isolation of **132** was difficult, as it breaks down to **133** during our attempts to isolate it. While on the other hand, $^1$H NMR analysis of **132** after heating for a short period of

time, like our hot recrystallisation attempts, resulted in full conversion to its predecessor **131**. This explained why our previous attempts at purification were unsuccessful.

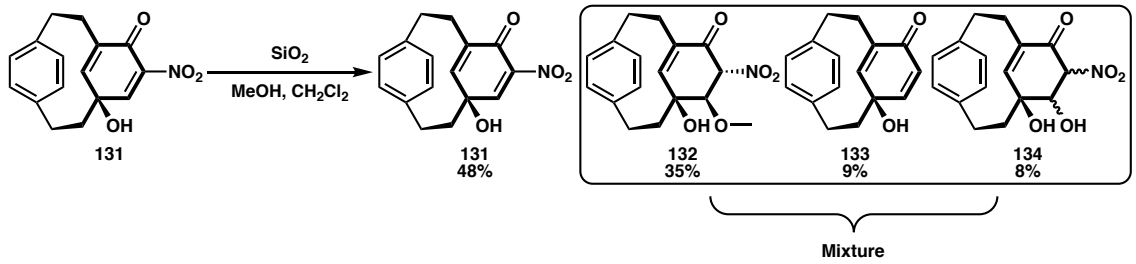


*Scheme 73 – Isolation of **132** completed by flash silica column chromatography using a gradient of 0-60% EtOAc in hexane. Acquiring a mixture of [2.2]metaparacyclophane derivatives contributing to 52% of the yield.*

During our attempts to isolate **132**, two alternative [2.2]metaparacyclophane derivatives were also isolated. Although we were familiar with [2.2]metaparacyclophane derivatives at this point the $^1$H NMR spectrum of the first compound showed a particular unique characteristic compared to previous compounds. The peaks corresponding to the *meta* ring had shifter closer together suggesting the ring had a more similar substitution pattern and conformation as to the *para* ring. Once again, it was only when an X-ray crystal structure of the compound was attained the results of the various spectroscopy analysis results became clear. Surprisingly, the crystal structure acquired by hot recrystallisation in $CH_2Cl_2$ and MeOH, showed the *meta* ring no longer contained a nitro group (Figure 26). The loss of the nitro group resulted in planarity of the *meta* ring being restored, hence the peaks in the $^1$H NMR spectrum showed similar characteristics to the *para* ring. Although, we had known of examples where the C-N bond is cleaved we had never anticipated the loss of the nitro group through column chromatography. In fact, to the best of our knowledge this is the first example reported.

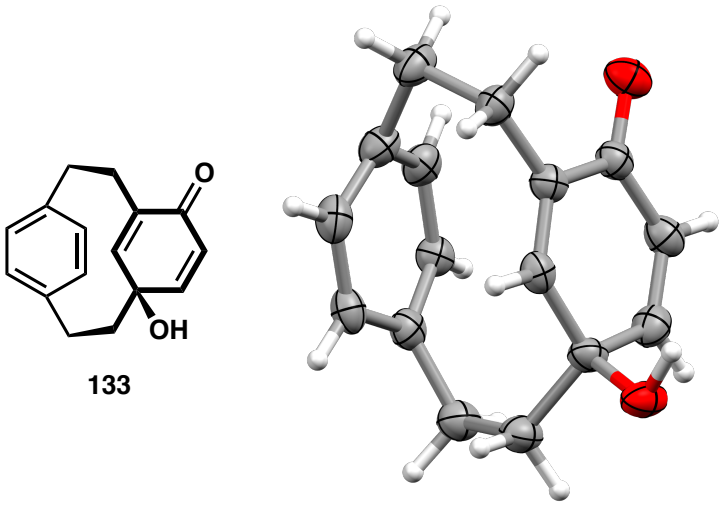


133

*Figure 26 – Molecular structure and X-ray of the newly acquired cyclohexadienone cyclophane derivative **133**. C = grey, H = white, N = blue, O = red. Thermal ellipsoid probability level 50%.*

While the structure of the second compound is undetermined, analysis of the $^{1}H$ and $^{13}C$ indicated that **134** was still a cyclophane derivative as shown by the distinctive splitting of the bridge head protons. The *para* ring showed no signs of alteration, with the protons being very similar to the previous [2.2]metaparacyclophane derivatives (**132** and **133**) shown by the DEPT 135 $^{13}C$ NMR spectrum containing peaks corresponding to four CH groups. Similarly, resonance of a hydrogen appearing as a singlet at 5.64 ppm and the distinctive roofing pattern seen in the doublets of the *para* ring suggest a [2.2]metaparacyclophane derivative was still present. Resonance of a quaternary carbon at 187.00 ppm in the $^{13}C$ and a carbonyl peak in the IR spectrum provided evidence of a ketone, analogous to **131** and **132**. This implies the remaining quaternary carbons are correlated to the bridgehead positions joining the rings together. The largest piece of evidence is the similarity in $^{1}H$ NMR spectrums of **132** and the unknown. From the similarities we believe the nitro and hydroxy group have remained intact at the C5 and C7. The $^{1}H$ and DEPT 135 $^{13}C$ NMR spectrum provide evidence of the absence of an alkene between the C5 and C6 atoms. Of particular interest is the quartet at 4.70 ppm of the unknown and the doublet at 4.45 ppm of **132** from the $^{1}H$ NMR spectrum. We suspect these peaks are correlated to the same hydrogen and has showed different splitting due to the surrounding substituents. For **132** this hydrogen corresponded to the hydrogen at C6, joined to the methoxy group. The slight increase in chemical shift suggested a stronger electron-withdrawing group has been added to the molecule but has increased the splitting. Analysis of the COSY NMR shows coupling to two protons, one belonging to

the proton showing resonance at 5.16 ppm, believed to be the hydrogen at the C5 position, while the other at 2.78 ppm. This suggests both positions contain substituents, as mentioned C5 is likely to be a nitro group, while the C6 we believe is a hydroxy group. Leading us to believe the structure of the unknown is **134** (Figure 27).

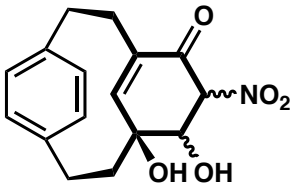


**134**

*Figure 27 – Proposed molecular structure of the unknown compound.*

Three reasons supported the presence of an alcohol at the C6 position. Firstly, this would explain the slight increase of chemical shift of the hydrogen attached to the carbon, as alcohols are more electron withdrawing than ethers. Secondly, there is clear similarity between the two NMRs of **131** and **134** with the only main difference being the lack of a $CH_3$ peak and splitting of the C6 carbon. However, this difference produces our third reason for believing a hydroxy group. In **131** the proton appears as a doublet due to splitting between the hydrogen and the hydroxy group present at C7, but with **134** splitting can occur between the hydroxy group at the C6 and C7 carbons, while the methoxy group in **131** is unable to participate in splitting. Further evidence of this splitting was seen in the COSY where the C6 is coupled to a broad peak at 2.78 integrating to 0.87, likely to be a result of deuterium hydrogen exchange causing the integration to be reduced. Analysis of mass spectrometry results support the isolation of **134** with peaks corresponding to the desired *m/z*.

Chapter 3

# Future perspective and conclusion

## 3.0 Future Perspective

The work completed in this thesis has only just begun to scratch the surface of each strand of research. Further investigation is required in each area. As in previous chapters, the future work will be broken into three Sections. In the first, the steps required to complete the natural amino acid stream of research will be discussed. This will be followed by a discussion on what is necessary to synthesise a foldamer from [2.2]paracyclophane. While the last section will look at the potential future of [2.2]metaparacyclophane compounds in our group.

## 3.1 Natural Amino Acid – Opiorphin

The largest issue in this line of research continues to be joining the hydrates **44** and **53** to the guanidine group. Various biologically friendly methods have been explored, with each being so far unsuccessful. Promising signs of acquiring the desired product have been found using a more straight-forward organic chemistry approach, but the isolation of the products has continued to be a problem. Further exploration of conditions is required to optimise the joining of arginine to the hydrate. If this is completed, we will provide a proof of concept before moving onto opiorphin. Another possibility would be to attempt the biologically friendly methodology on opiorphin as it is a peptide. Perhaps model studies are pointless.

Alternatively, as reactions between the arginine side chain and the hydrate did not show promise, there are two other routes we could explore. The first involves screening other groups that would selectively bind the arginine side chain. The second is targeting a different amino acid of opiorphin. Originally, arginine was targeted as it caused the largest issues for permeability to the BBB, but the serine residue is also a viable option. The esterification of serine has been reported in the literature, and therefore should be investigated first in future research (Scheme 74).[22] With additional time and study it

should be possible to mask one of the functional groups of opiorphin and alter its properties in a beneficial manner.

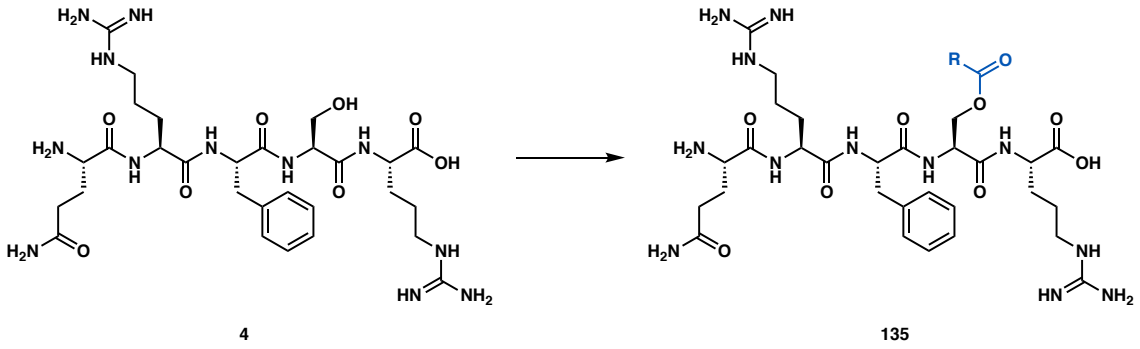

4 135

*Scheme 74 – Esterification of opiorphin to increase lipophilicity, where R is a nonpolar chain*

## 3.2 Unnatural Amino Acid – Foldamer

The synthesis of a foldamer using [2.2]paracyclophane still requires a large amount of work. Obviously, it would be worth while pursuing the investigation of glycine derivatives. Glycine linkers could potentially overcome the issues discussed earlier and synthesis of a dimer by linking (±)-**136** should be achievable (Scheme 75).

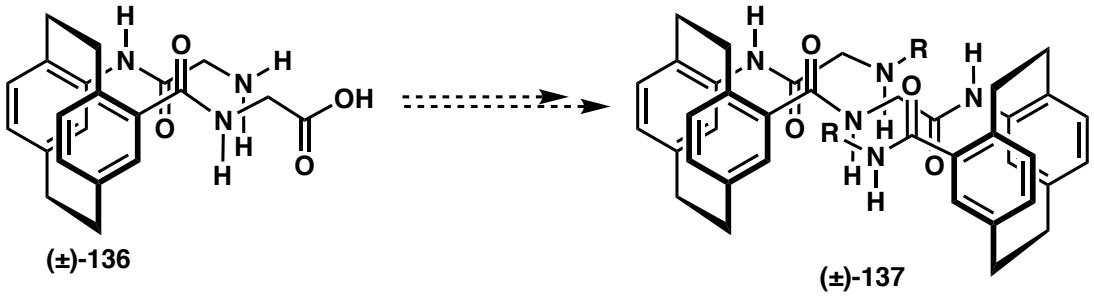

(±)-136 (±)-137

*Scheme 75 – Proposed route to produce glycine foldamer.*

The research reported in this thesis highlights the key issues that need to be addressed. Firstly, the resolution of [2.2]paracyclophane derivatives must be completed. This was investigated in this thesis but was abandoned due to lost time caused by the Covid-19 pandemic. Secondly, while the *pseudo-geminal* amino acid used in this strand is undoubtedly the easiest to form, we are concerned that is the less reactive than other isomers. Therefore, an alternative substitution pattern should be explored.

Both these issues can be addressed together. The resolution of [2.2]paracyclophane using oxazoline derivatives has been an area the Rowlands group have been exploring. They have incorporated various oxazoline derivatives at different [2.2]paracyclophane

positions, allowing two birds to be killed with one stone; different regioisomers can be obtained in enantiomerically pure form. Numerous substitution patterns have been accessed using oxazoline, including *pseudo-para*, *meta*, *ortho*, and even tetra substitution patterns (Scheme 76). Recent progress by the group has shown hydrolysis of the oxazoline is achievable allowing access to resolved carboxylic acid derivatives of [2.2]paracyclophane, making this avenue of research a promising route for future foldamer synthesis.

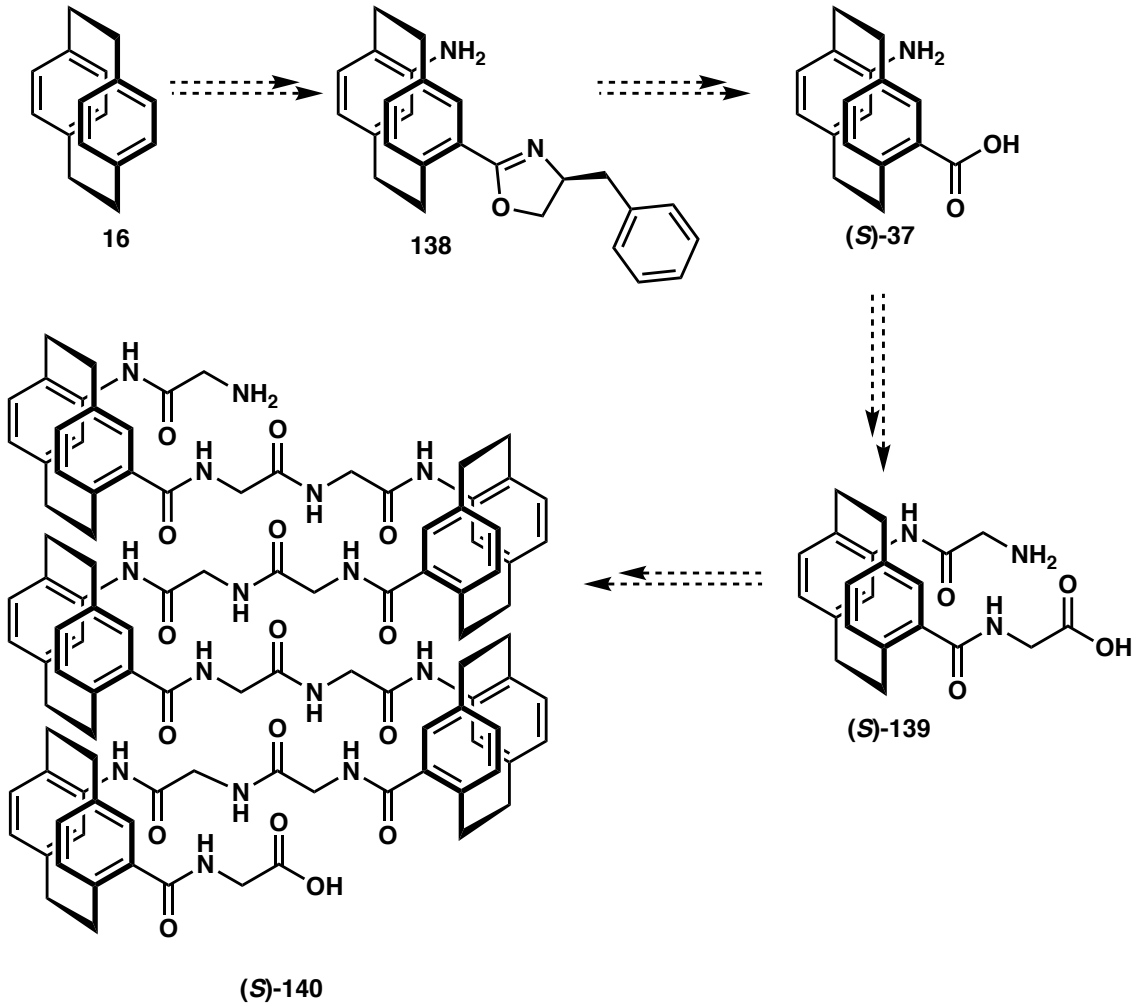


*Scheme 76 – Proposed glycine [2.2]paracyclophane foldamer synthesis utilising extended linkers causing greater separation of [2.2]paracyclophane components.*

## 3.3 [2.2]Metaparacyclophane Derivatives

The use of [2.2]metaparacyclophane in any synthetic setting, such as asymmetric synthesis or electronics have yet to be fully explored. The framework has been poorly researched with little experimental work reported, and this creates an area that is ripe for study. Of particular interest is the original 4-hydroxy-5-nitro[2.2]metaparacyclophane (±)-**124**, and its first derivative isolated in this project, **131**. The structure of (±)-**124** provides for an exciting scaffold with two versatile functional groups to build on. Esterification of the phenol group of (±)-**124** would allow us to explore a variety of interesting research. A study of particular interest would be to introduce an additional chiral group like Mosher's acid, which would allow us to examine the ring flipping of the *meta* ring through NMR experiments (Scheme 77).

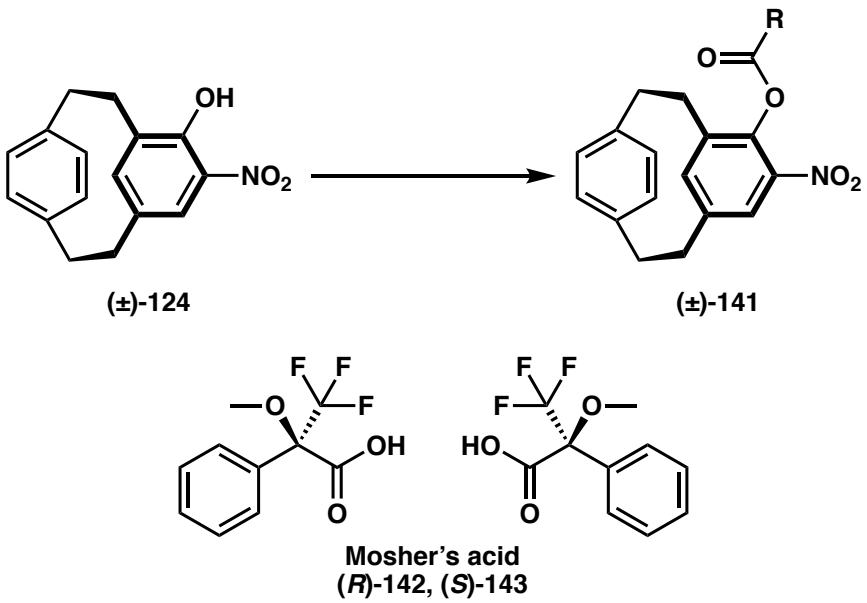


*Scheme 77 – Functional group interconversion to produce an ester derivative of (±)-**124** and the molecule structures of the two enantiomers of Mosher's acid (R)-**142**, (S)-**143**.*

Alternatively, reduction of the nitro group can be completed allowing (±)-**144** to act as a nucleophile. This allows (±)-**144** to produce peptide bonds and the possibility of forming a foldamer from [2.2]metaparacyclophane derivatives or a mixture of [2.2]paracyclophane and [2.2]metaparacyclophane.

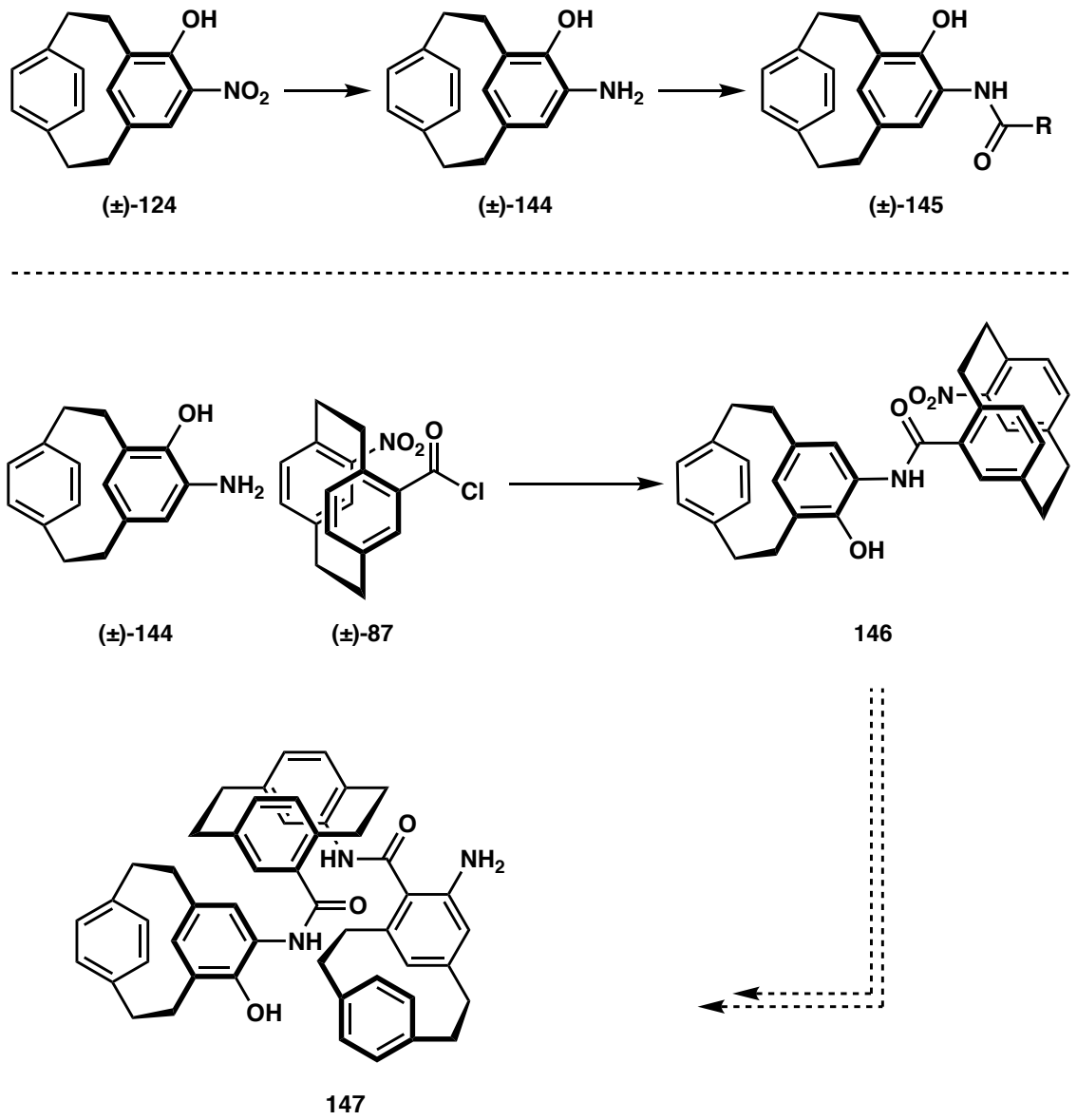


*Scheme 78 – Formation of peptide bonds using (±)-**144** (top), and the synthesis of a foldamer using (±)-**144** and (±)-**87** (bottom).*

Alternatively, **131** has the potential to be useful as well. Results reported earlier showed **131** undergoes ether formation in the presence of alcohol. Therefore, the synthesis of a dimer using **131** should be readily achievable using a diol and acidic conditions (Scheme 79). The reduction of the nitro group would give rise to an accessible nucleophile for growing the structure like **148**.

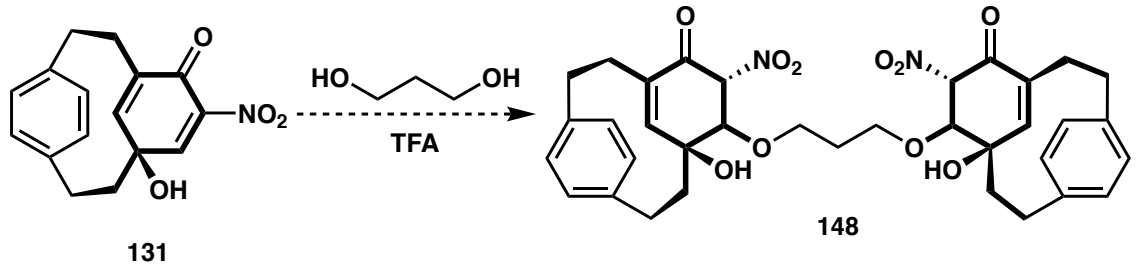


*Scheme 79 – Potential reaction conditions to produce a [2.2]metaparacyclophane derived dimer.*

In summation, the natural amino acid drug opiorphin was investigated, and a viable path for converting it to a prodrug was proposed. An enormous amount of research is still required before a viable biological moiety is produced. The unnatural amino acid stream of research to develop a foldamer has shown success by developing a [2.2]paracyclophane dimer from amino acid derivatives. Viable options in the form of a glycine [2.2]paracyclophane derivatives have begun and potential pathways in form of oxazolines have been highlighted. In addition, a novel and efficient route to functionalised [2.2]metaparacyclophane derivatives has been shown. Various compounds have been highlighted showing the compound needs to be stabilised before they can be explored for applicational reasons.

Originally, this thesis set out to answer one question: is it possible for a chemist to improve on nature. This is an enormous task requiring a vast amount of research. Although the research presented here doesn't even scratch the surface it provides the foundation for future work that could answer this question.

Chapter 4

# Experimental Methods

Solvents and reagents were received from commercial sources without additional purification unless otherwise stated. All reactions were performed in oven-dried glassware under atmospheric conditions unless otherwise stated. Column chromatography was carried out on silica gel (grade 60, mesh size 230-400, Scharlau). Visualisation techniques for TLC plates include using ultraviolet light (254 nm), potassium permanganate, iodine, *p*-anisaldehyde and cerium ammonium molybdate when applicable. NMR spectra were collected at room temperature (expect for variable temperature NMR experiments) on Bruker-400, Bruker-500, or Bruker-700. Mass spectra and high-resolution mass spectrometry were performed using a ThermoScientific Q Exactive Focus Hybrid Quadrupole-Orbitrap Mass Spectrometer. Infrared spectroscopy of compounds were completed on a ThermoFisher Nicolet iS5 with an iD7 ATR accessory. Melting points were analysed on a Gallenkamp melting point instrument.

Where applicable, mixtures of diastereoisomers have been reported as major or minor diastereoisomers with the ratio between them at the start of characterisations. When additional aromatic rings are present, peaks corresponding to the resonance shown by their hydrogens are represented as Ar-H; while the resonance associated with the aromatic protons for [2.2]paracyclophane are represented as Ar-$H_{22pc}$. When possible, resonance of a distinctive proton has been assigned to the appropriate number. Melting points have not been reported on mixture of diastereomers.

X-Ray crystallography was performed on a Bruker D8 Venture diffractometer equipped with a Photon III detector and an I$\mu$S Diamond microfocus X-ray source, emitting Cu $K_\alpha$ radiation ($\lambda$ = 1.54178 Å). Single crystals were mounted on MiTeGen mylar loops using Fomblin® Y oil and cooled to 100 K using an Oxford Cryostream 800. Data were collected, integrated, scaled, and averaged using the APEX3 software package. The space group was determined and data merged by XPREP.[116] All structures were solved by SHELXT [116] and refined with SHELXL,[115] as implements in Olex2.[117] All non-hydrogen atoms were found in the electron density difference map, and refined anisotropically. All hydrogen atoms were calculated to their ideal positions, unless otherwise stated, and refined using a riding model with fixed isotropic $U_{iso}$ values.

**Synthesis of 1-(4-(decyloxy)phenyl)ethan-1-one**

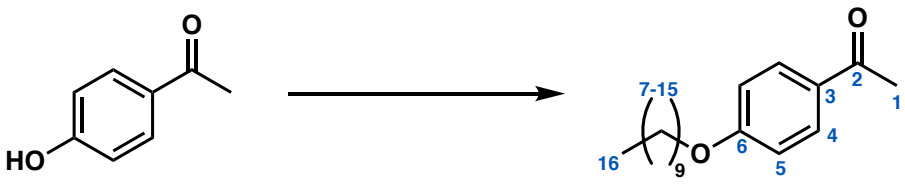


**43** **68**

To a solution of 1-(4-hydroxyphenyl)ethan-1-one **43** (5.00 g, 36.72 mmol, 1.00 eq) in DMF (92 mL, 0.40 M) was added $K_2CO_3$ (15.23 g, 110.17 mmol, 3.00 eq) followed by bromodecane (7.61 mL, 36.72 mmol, 1.00 eq). The reaction mixture was stirred at RT for 15 hours. The solution was diluted with $H_2O$ (150 mL) and extracted with EtOAc (250 mL) and then was washed with brine (150 mL). The organic layer was dried ($MgSO_4$) and concentrated under reduced pressure to furnish **68** as a cloudy-white liquid (9.85 g, 35.62 mmol, 97%).

$^1$H NMR (500 MHz, $CDCl_3$): δ (ppm) = 7.91 (2H, d, *J* = 8.8 Hz, H-4), 6.90 (2H, d, *J* = 8.7 Hz, H-5), 4.00 (2H, t, *J* = 6.7 Hz, H-7), 2.54 (3H, s, H-1), 1.82-176 (2H, m, H-8), 1.48-1.42 (m, 2H, H-9), 1.34-1.27 (12H, m, H-10, H-11, H-12, H-13, H-14, H-15), 0.875 (3H, t, *J* = 6.4 Hz, H-16).

$^{13}$C NMR (126 MHz, $CDCl_3$): δ (ppm) = 196.8, 163.1, 130.6, 130.1, 114.1, 68.3, 31.9, 29.5, 29.5, 29.4, 29.3, 29.1, 26.3, 26.0, 22.7, 14.1.

HRMS-EI: *m/z* found: $[M]^+$, 277.2161. $C_{18}H_{29}O_2$ requires $[M]^+$, 277.2229.

Mass spectrometry (ESI) $[M]^+$= 300.16, 277.24, 156.30, 140.24, 130.32, 122.16, 108.02, 59.94 *m/z*.

IR: 2922, 2853, 1677, 1601, 1254, 1172 $cm^{-1}$.

Mp: 21-23 °C.

$R_f$: 0.86 (15% EtOAc, 85% hexane).

**Synthesis of 2-(4-(decyloxy)phenyl)-2-oxoacetaldehyde and 1-(4-(decyloxy)phenyl)-2,2-dihydroxyethan-1-one**

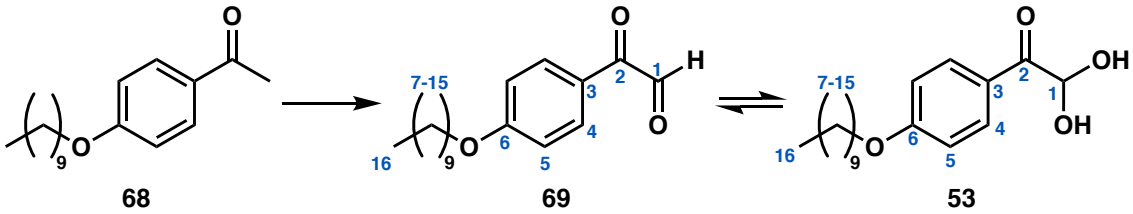


To a solution of 1-(4-(decyloxy)phenyl)ethan-1-one **68** (0.41 g, 1.483 mmol, 1.00 eq) in 1,4-dioxane (1.00 mL, 11.36 mmol, 0.10 eq) was added $SeO_2$ (0.33 g, 2.96 mmol, 2.00 eq) with $H_2O$ (2 drops). The reaction mixture was stirred at reflux for 8 hours. The solution was diluted with $CH_2Cl_2$ (5 mL) then filtered over celite and washed through with $CH_2Cl_2$ (3 × 8 mL). The combined organics were dried ($MgSO_4$) and concentrated under reduced pressure to furnish **53** as a pinkish-white powder, which changes to a green-white powder depending on the humidity (0.41 g, 1.32 mmol, 89%).

A mixture of **53** and **69** is seen in the $^1$H NMR in a 1.00:0.25 ratio respectively.

$^1$H NMR (400 MHz, DMSO-$d_6$): δ (ppm) = 9.53 (1H, s, H-1, **69**), 8.06 (2H, d, *J* = 8.7 Hz, H-4, **69**), 8.03 (2H, d, *J* = 8.5 Hz, H-4, **53**), 7.01 (2H, d, *J* = 8.5 Hz, H-5, **53**) 6.98 (2H, d, *J* = 9.0 Hz, H-5, **69**), 5.64 (1H, s, H-1, **53**) 4.04 (2H, t, *J* = 6.6 Hz H-7, **53**), 3.50 (2H, t, *J* = 6.6 Hz, H-7, **69**), 1.72 (4H, quint, *J* = 6.6 Hz, H-8, **53**, **69**), 1.43-1.37 (4H, m, H-9, **53**, **69**), 1.32-1.21 (24H, m, H-10, H-11, H-12, H-13, H-14, H-15, **53**, **69**), 0.85 (6H, t, *J* = 6.3 Hz, H-16, **53**, **69**).

$^{13}$C NMR (126 MHz, DMSO-$d_6$): δ (ppm) = 195.1, 190.7,187.1, 167.5, 164.2, 163.1, 133.1, 132.2, 131.8, 126.7, 125.0, 115.2, 114.6, 114.6, 89.4, 69.8, 68.5, 68.3, 68.2, 35.6, 32.7, 31.8, 29.5, 29.4, 29.4, 29.4, 29.2, 29.2, 29.1, 29.0, 28.9, 28.6, 28.0, 25.9, 22.6, 14.4.

IR: 3422, 2937, 2919, 3852, 1675, 1604, 1574, 1509, 12535, 1121, 1014 cm$^{-1}$.

Mp: 83-91°C.

$R_f$: 0.50 (15% EtOAc, 85% hexane).

**Synthesis of 1-(4(methoxy)phenyl)ethan-1-one**


**43** **70**

To a solution of 1-(4-hydroxyphenyl)ethan-1-one **43** (0.25 g, 1.84 mmol, 1.00 eq) in MeCN (0.20 M, 9.20 mL) was added $K_2CO_3$ (0.76 g, 5.51 mmol, 3.00 eq) followed by MeI (0.39 g, 2.75 mmol, 1.50 eq). The reaction mixture was stirred at RT for 12 hours. The solution was diluted with $H_2O$ and extracted with EtOAc (3 × 20 mL) then washed with brine (30 mL). The organic layer was dried ($MgSO_4$) and concentrated under reduced pressure to furnish **70** as a yellow solid (0.26 g, 1.73 mmol, 94%).

$^1$H NMR (500 MHz, $CDCl_3$): δ (ppm) = 7.90 (2H, d, *J* = 8.8 Hz, H-4), 6.90 (2H, d, *J* = 8.8 Hz, H-5), 3.84 (3H, s, H-7), 2.52 (3H, s, H-1).

$^{13}$C NMR (126 MHz, $CDCl_3$): δ (ppm) = 196.8, 163.5, 130.6, 130.3, 113.7, 55.4, 26.3.

Mass spectrometry (ESI) $[M]^+$= 151.14, 130.16, 122.19, 108.02 *m/z*.

IR: 3675, 2989, 1666, 1600, 1506, 1417, 1357, 1277, 1177, 1021, 835, 591 $cm^{-1}$.

Mp: 40-41 °C.

$R_f$: 0.50 (20% EtOAc, 80% hexane).

**Synthesis of 1-(4-(methoxy)phenyl)-2,2-dihydroxyethan-1-one**

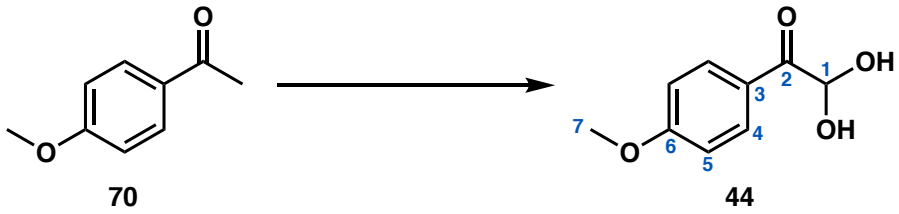


To a solution of 1-(4-(methoxy)phenyl)ethan-1-one (0.26 g, 1.73 mmol, 1.00 eq) in 1,4-dioxane (0.20 M, 8.65 mL) was added $SeO_2$ (0.39 g, 3.46 mmol, 2.00 eq) with $H_2O$ (15 drops). The reaction mixture was stirred at reflux for 9 hours. The solution was diluted with $CH_2Cl_2$ (5 mL) then filtered through celite and washed through with $CH_2Cl_2$ (3 × 8 mL). The combined organics were dried ($MgSO_4$) and concentrated under reduced pressure to yield a creamy yellow solid, which was purified by hot recrystallisation ($H_2O$), to furnish **43** as white crystals (0.279 g, 1.53 mmol, 89%).

$^{1}$H NMR (500 MHz, DMSO-$d_6$): δ (ppm) = 8.05 (2H, d, *J* = 8.7 Hz, H-4), 7.98 (1H, d, *J* = 9.60 Hz, OH), 7.02 (2H, d, *J* = 8.8 Hz, H-5), 5.97 (1H, d, *J* = 9.4 Hz, H-1), 3.84 (3H, s, H-7).

$^{13}$C NMR (126 MHz, DMSO-$d_6$): δ (ppm) = 192.5, 164.0, 132.4, 126.6, 114.3, 91.0, 56.0.

Mass spectrometry (ESI) $[M]^+$= 182, 115, 106, 74 *m/z*.

IR: 3437, 2942, 1680, 1599, 1512, 1472, 1259, 1170, 1104, 1007 $cm^{-1}$.

Mp: 137-138 °C.

$R_f$: 0.21 (25% EtOAc, 75% hexane).

**Synthesis of methyl L-arginine**

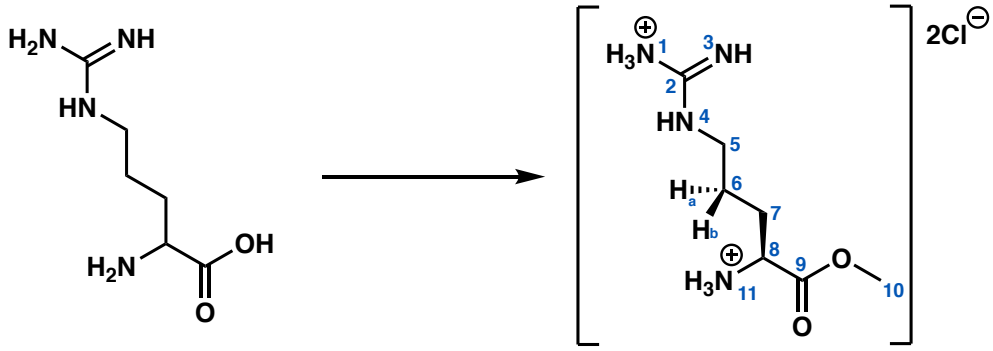


54 77

To a solution of L-arginine **54** (0.25 g, 1.44 mmol, 1.00 eq) in $CH_3OH$ (0.20 M, 7.18 mL) was added $SOCl_2$ (1.00 M, 1.44 mL). The reaction mixture was stirred at reflux for 14 hours. The solution was concentrated under reduced pressure to furnish **77** as white crystals (0.23 g, 1.24 mmol, 86%).

$^1$H NMR (400 MHz, DMSO-$d_6$): δ (ppm) = 8.69 (3H, s, NH-11), 7.96 (1H, t, $J$ = 5.8 Hz, NH-4), 7.71-6.90 (4H, bs, NH-1, NH-3) 4.04 (1H, t, $J$ = 6.4 Hz, H-8), 3.75 (3H, s, H-10), 3.14 (2H, q, $J$ = 6.0, 6.6 Hz, H-5), 1.90-1.77 (2H, m, H-7), 1.68-1.57 (1H, m, H-6$_a$), 1.56-1.47 (1H, m, H-6$_b$).

$^{13}$C NMR (126 MHz, DMSO-$d_6$): δ (ppm) = 170.2, 157.6, 53.3, 52.0, 27.6, 24.8, 24.7.

HRMS-EI: *m/z* found: $[M-2Cl]^+$, 189.1346. $C_7H_{17}N_4O_2$ requires $[M]^+$, 188.1346.

Mass spectrometry (ESI) $[M-2Cl]^+$= 189.16, 175.16, 129.80, 70.08 *m/z*.

IR: 3320, 3137, 2861, 2527, 1744, 1666, 1634, 1524, 1240 cm$^{-1}$.

Mp: 185-187 °C.

$R_f$: 0.11 (5% MeOH, 95% $CH_2Cl_2$).

**Synthesis of Boc L-arginine methyl ester**

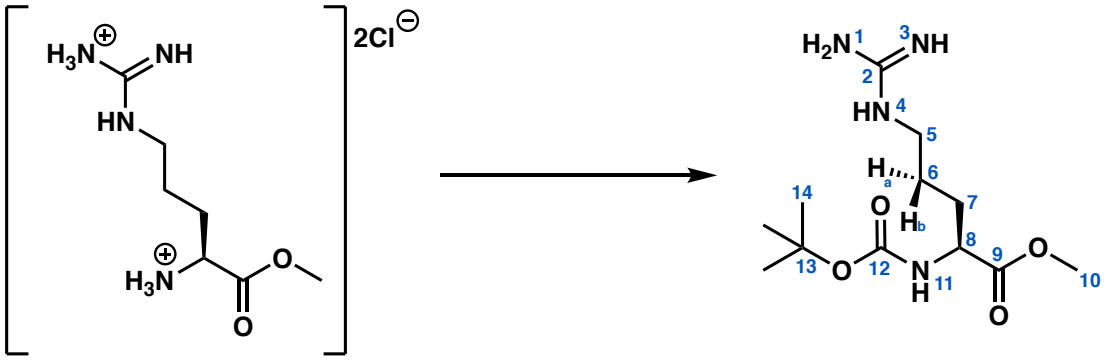

77 55

To a solution of methyl L-arginine **77** (1.00 g, 5.31 mmol, 1.00 eq) in MeCN (0.20 M, 11 mL) was added $Et_3N$ (0.44 g, 4.30 mmol, 0.80 eq). The reaction mixture was stirred at 25 °C for 13 hours. The solution was filtered and concentrated under reduced pressure. To a solution of the residue in MeCN (0.20 M, 11 mL) under Ar was added $Boc_2O$ (1.00 g, 4.584 mmol, 0.86 eq) dropwise over 20 minutes. The reaction mixture was stirred at 25 ˚C for 12 hours. An additional solution of MeCN (0.20 M, 11 mL) and $Boc_2O$ (1.00 g, 4.58 mmol, 0.86 eq) was added dropwise over a 20 min period and left to stir for 12 hours. The solution was concentrated under reduced pressure. The residue was dissolved in $H_2O$ (30 mL) and washed with EtOAc (3 × 15 mL) and $Et_2O$ (3 × 15 mL). The aqueous layer was freeze dried yielding the crude product as a white solid. The crude mixture was dissolved in $CH_2Cl_2$ and filtered. The resulting filtrate was concentrated under reduced pressure to furnish **55** as a hygroscopic white solid (0.47 g, 1.61 mmol, 30%).

$^1$H NMR (400 MHz, DMSO-$d_6$): δ (ppm) = 7.67 (1H, bs, NH-11), 7.29 (1H, d, *J* = 7.8 Hz, NH-4), 7.24-6.76 (3H, bs, NH-1, NH-3) 3.99-3.94 (1H, m, H-8), 3.63 (3H, s, H-10) 3.08 (2H, q, *J* = 6.3, H-5), 1.73-1.64 (1H, m, H-$6_a$), 1.62-1.54 (1H, m, H-$6_b$), 1.54-1.47 (2H, m, H-7), 1.39 (9H, s, H-14).

$^{13}$C NMR (126 MHz, DMSO-$d_6$): δ (ppm) = 173.4, 157.4, 156.0, 78.8, 53.6, 52.3, 28.6, 28.38, 28.3, 25.7.

HRMS-EI: *m/z* found: $[M]^+$, 289.1866. $C_{12}H_{25}N_4O_4$ requires $[M]^+$, 289.1870.

Mass spectrometry (ESI) $[M]^+$= 289.18, 233.15, 189.32, 172.22, 130.25, 69.97 *m/z*.

IR: 3675, 3347, 2969, 2972, 1716, 1651, 1634, 1511, 1362, 1227, 1162 $cm^{-1}$.

Mp: 155-158.4 °C.

$R_f$: 0.08 (10% MeOH, 90% $CH_2Cl_2$).

## 4.2 Unnatural Amino Acid

The following section of experimental work consist of the synthesis and analysis of [2.2]paracyclophane compounds. The numbering system adopted for naming compounds can been seen in the figure below. The plane with the highest level of substitution is considered the chiral plane with the highest priority chosen according to the Cahn-Ingold-Prelog (CIP) system. Position 1 is the closest out of plane atom to the chiral plane atom to the chiral plane (typically one of the ethyl bridge carbons). Substituents with additional carbons and hydrogens will be numbered following [2.2]paracyclophane, i.e. will start at 17, unless otherwise depicted.

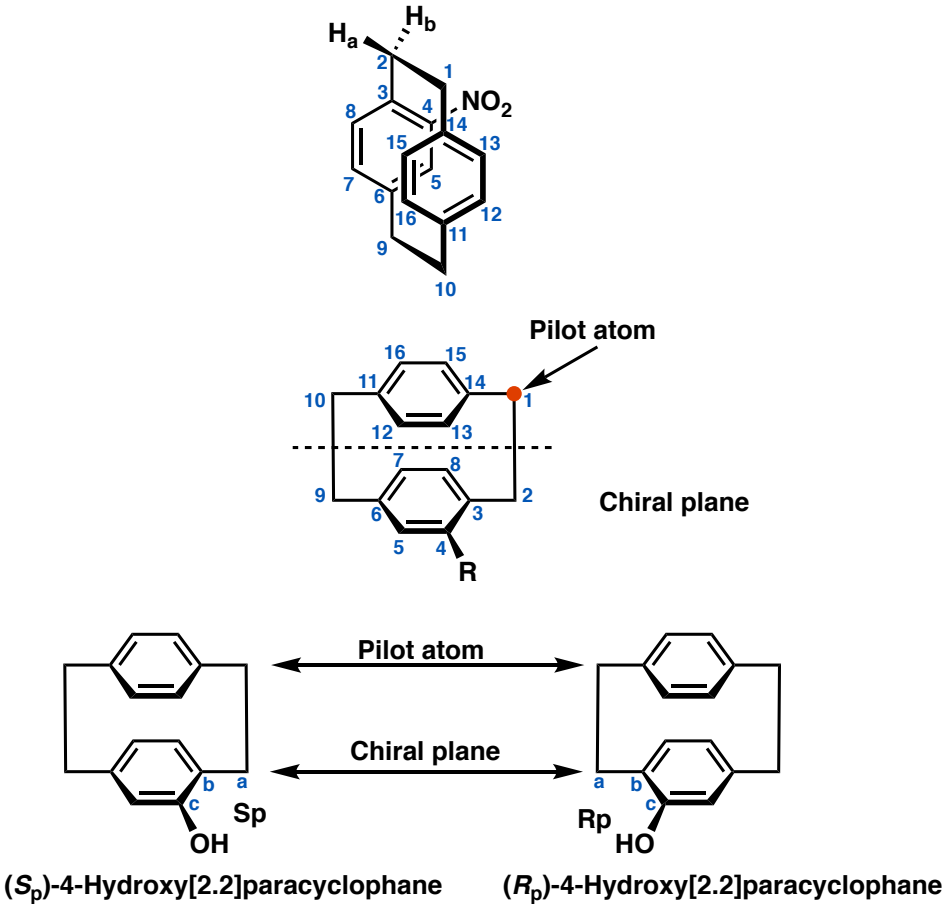

**Synthesis of (±)-4-nitro[2.2]paracyclophane**

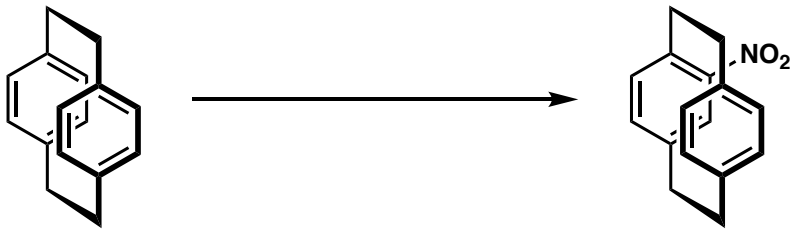


16 (±)-85

To a solution of [2.2]paracyclophane **16** (5.00 g, 24.03 mmol, 1.00 eq) in $CH_2Cl_2$ (0.20 M, 120 mL) at 0 °C was added a solution of $HNO_3$ (2.00 mL, 48.08 mmol, 2.00 eq) and $H_2SO_4$ (2.03 mL, 48.08 mmol 2.00 eq). The reaction mixture was stirred at 0 °C for 8 hours, observing a colour change from clear to yellow. The reaction was poured onto ice (100 g) through filter paper, and stirred until the ice had melted. The layers were separated and the aqueous layer was extracted with $CH_2Cl_2$ (5 × 40 mL). The combined organic layers were dried ($MgSO_4$) and concentrated under reduced pressure to yield an orange solid, which was purified by silica-gel chromatography (3% EtOAc, 97% hexane), to furnish (±)-**85** as a yellow solid (5.06 g, 19.98 mmol, 94%).

$^1$H NMR (500 MHz, $CDCl_3$): δ (ppm) = 7.24 (1H, d, *J* = 1.5 Hz, H-5), 6.81 (1H, dd, *J* = 1.3, 7.8 Hz, H-13), 6.62 (2H, d, *J* = 7.6 Hz, H-7, H-16), 6.57 (2H, ddd, *J* = 1.3, 7.8, 15.3 Hz, H-8, H-15), 6.48 (1H, d, *J* = 6.90, H-12), 4.02 (1H, ddd, *J* =1.3, 9.6, 13.4 Hz, H-$2_b$), 3.21-3.13 (4H, m, H-9, H-10), 3.10-3.03 (2H, m, H-$1_a$, H-$2_a$), 2.90 (1H, ddd, *J* = 7.2, 8.5, 13.3 Hz, H-$1_b$).

$^{13}$C NMR (126 MHz, $CDCl_3$): δ (ppm) = 149.0, 142.2, 139.9, 139.5, 137.9, 137.5, 136.6, 133.3, 133.3, 132.6, 130.1, 129.7, 36.2, 35.1, 35.0, 34.6.

IR: 3009, 2928, 1694, 1532, 1516, 1336, 808 $cm^{-1}$.

Mp: 158-160 °C.

$R_f$: 0.43 (10% EtOAc, 90% hexane).

**Synthesis of (±)-4-nitro-13-formyl[2.2]paracyclophane**

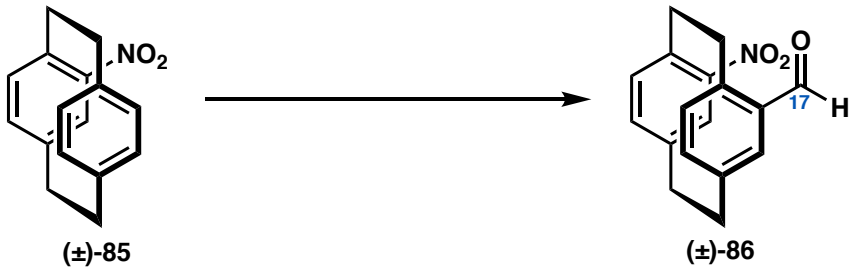


(±)-85 (±)-86

To a solution of (±)-4-nitro[2.2]paracyclophane (±)-**85** (1.00 g, 3.95 mmol, 1.00 eq) in $CH_2Cl_2$ (0.20 M, 19 mL) under Ar at -10 °C was added $CHCl_2OMe$ (0.39 mL, 4.35 mmol, 1.10 eq) followed by $TiCl_4$ (0.87, mL, 7.91 mol, 2.00 eq), observing a colour change from yellow to dark brown. The reaction mixture was stirred at -10 °C for 13 hours. The reaction was poured onto ice (50 g) and stirred until the ice melted. The layers were separated and the aqueous layer extracted with $CH_2Cl_2$ (3 × 25 mL). The combined organics were washed with saturated aqueous $NaHCO_3$ (50 mL) followed by $H_2O$ (50 mL) and brine (50 mL). The organic layer was dried ($MgSO_4$) and concentrated under reduced pressure to yield a dark brown solid, which was purified by silica-gel chromatography (25% EtOAc, 75% hexane), to furnish (±)-**86** as yellow crystals (0.93 g, 3.31 mmol, 84%).

$^1$H NMR (500 MHz, $CDCl_3$): δ (ppm) = 9.93 (1H, s, H-17), 7.14 (1H, s, H-5), 7.10 (1H, s, H-12), 6.82 (1H, d, *J* = 7.8 Hz, H-7), 6.77 (1H, d, *J* = 7.9 Hz, H-16), 6.73 (1H, d, *J* = 7.6 Hz, H-8), 6.67 (1H, d, *J* = 7.9 Hz, H-15), 4.23-4.17 (1H, m, H-$1_b$), 4.03-3.99 (1H, m, H-$2_b$), 3.22-3.11 (6H, m, H-$1_a$, H-$2_a$, H-9, H-10).

$^{13}$C NMR (126 MHz, $CDCl_3$): δ (ppm) = 190.4, 149.5, 142.6, 141.9, 140.2, 137.9, 137.5, 137.4, 136.2, 136.1, 135.6, 134.7, 128.2, 34.5 (C × 2), 34.1, 31.6.

HRMS-EI: *m/z* found: $[M]^+$, 282.1133. $C_{17}H_{16}NO_3$ requires $[M]^+$, 282.1125.

Mass spectrometry (ESI) $[M]^+$= 304 (+ Na), 282, 235, 206, 192, 104.

IR: 2969, 2934, 1679, 1575, 1339, 804, 720, 708, 695, 678 $cm^{-1}$.

Mp: 156 °C decomposes.

$R_f$: 0.20 (20% EtOAc, 80% hexane).

**Synthesis of (±)-4-nitro[2.2]paracyclophane-13-carboxylic acid**

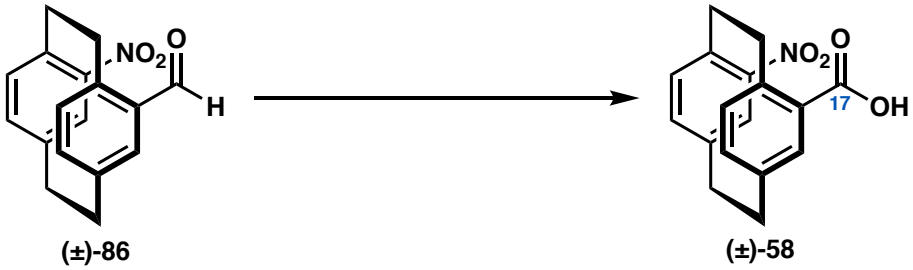


(±)-86 (±)-58

To a solution of (±)-4-nitro-13-formyl[2.2]paracyclophane (±)-**86** (13.00 g, 46.21 mmol, 1.00 eq) in acetone (920 mL) was added a solution of $KMnO_4$ (10.91 g, 69.05 mmol, 1.50 eq) in $H_2O$ (345 mL). The reaction mixture was stirred for 15 hours at RT. The solution was acidified to pH 2-3 with concentrated $HCl_{(aq)}$ (~37%; 3.0 mL) and extracted with EtOAc (3 × 175 mL). The combined organic layers were washed with $H_2O$ (2 × 250 mL) followed by brine (2 × 200 mL). The solution was concentrated under reduced pressure. The resulting solid was then partitioned between $NaOH_{(aq)}$ (2 M; 350 mL) and EtOAc (220 mL). The organic layer was collected and concentrated under reduced pressure yielding the starting material (±)-**86** as a dark brown solid. The aqueous layer was acidified to pH 1-2 with concentrated $HCl_{(aq)}$ (~37%, 5 mL) causing the formation of a precipitate. This material was collected by filtration and dried under reduced pressure, to furnish (±)-**58** as a white powder (6.46 g, 21.72 mmol, 47%).

$^1$H NMR (500 MHz, DMSO-$d_6$): δ (ppm) = 12.45 (1H, s, OH), 7.24 (1H, s, H-5), 7.09 (1H, s, H-12), 6.93 (1H, d, $J$ = 8.3 Hz, H-7), 6.87 (1H, d, $J$ = 7.6 Hz, H-8), 6.81 (1H, d, $J$ = 7.9 Hz, H-16), 6.74 (1H, d, $J$ = 7.1 Hz, H-15), 4.6-3.98 (1H, m, H-$2_b$), 3.85-3.78 (1H, m, H-$1_b$), 3.18-3.06 (6H, m, H-$1_a$, H-$2_a$, H-9, H-10).

HRMS-EI: *m/z* found: $[M]^-$, 296.0925 . $C_{17}H_{14}NO_4$ requires $[M]^-$, 296.0917.

Mass spectrometry (ESI) $[M]^-$= 319(+ Na), 296, 280, 252, 235, 206, 192, 100 *m/z*.

IR: 2933, 2857, 1678, 1549, 1516, 1338 $cm^{-1}$.

Mp: 163 °C (decomposes).

$R_f$: 0.10 (50% EtOAc, 50% hexane).

**Synthesis of (±)-4-nitro-*N*-((*S*)-1-phenylethyl)[2.2]paracyclophane-13-carboxamide**

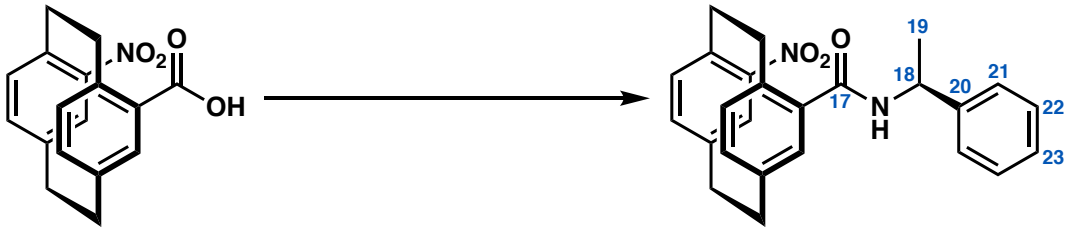


(±)-58 88a

To a solution of (±)-4-nitro[2.2]paracyclophane-13-carboxylic acid (±)-**58** (1.00 g, 3.37 mmol, 1.00 eq) in $CH_2Cl_2$ (0.20 M, 16 mL) under Ar was added $(COCl)_2$ (0.34 mL, 4.04 mmol, 1.2 eq) followed by DMF (2 drops in 1.00 mL of $CH_2Cl_2$ ). The reaction mixture was stirred until bubbling ceased (~35 minutes). The solvent was concentrated under reduced pressure with the crude acyl chloride yielding as a dark brown solid.

To a solution of the crude acyl chloride in $CH_2Cl_2$ (0.20 M, 15.84 mL) at 0 °C under Ar was added $Et_3N$ (0.35 g, 3.49 mmol, 1.10 eq) followed by (*S*)-1-phenylethylamine (0.76 g, 3.17 mmol, 2.00 eq). The reaction mixture was stirred at RT for 13 hours. The solution was washed with $H_2O$ (2 × 20 mL). The organic layer was dried ($MgSO_4$) and concentrated under reduced pressure yielding the crude product as a orange–brown solid, which was purified by silica-gel chromatography (40% EtOAc, 60% hexane), to furnish **88a** as a yellowy-green solid (0.87 g, 2.19 mmol, 69%).

Diastereoisomers are seen in a ratio of 1:0.6.

$^1$H NMR (400 MHz, $CDCl_3$): δ (ppm) = 7.39-7.24 (11H, m, 10 × Ar-H, Ar-$H_{22pc}$ mixture of diastereoisomers), 6.79-6.76 (5H, m, Ar-$H_{22pc}$, mixture of diastereoisomers), 6.68-6.61 (6H, m, Ar-$H_{22pc}$, mixture of diastereoisomers), 5.79 (1H, d, *J* = 7.3 Hz, NH, major diastereoisomers), 5.69 (1H, d, *J* = 7.3 Hz, NH, minor diastereoisomers), 5.26 (2H, quint, *J* = 7.0 Hz, H-18, mixture of diastereoisomers), 4.23-4.14 (2H, m , H-$2_b$, mixture of diastereoisomers), 3.95-3.89 (1H, m, H-$1_b$, minor diastereoisomers), 3.83-3.75 (1H, m, H-$1_b$, major diastereoisomers), 3.11-2.94 (12H, m, H-$2_a$, H-$1_a$, H-9, H-10), 1.61-1.59 (6H, m, H-19, mixture of diastereoisomers).

Mass spectrometry (ESI) $[M]^+$= 423 (+ $Na^+$), 401, 324, 281, 105 101, 77.

IR: 3345, 2920, 2900, 1650, 1567, 1285, 1240, 1071, 929, 750 $cm^{-1}$.

$R_f$: 0.81 (30% EtOAc, 70% hexane).

**Synthesis of (±)-4-nitro-*N*-((*R*)-1-phenylethyl)[2.2]paracyclophane-13-carboxamide**

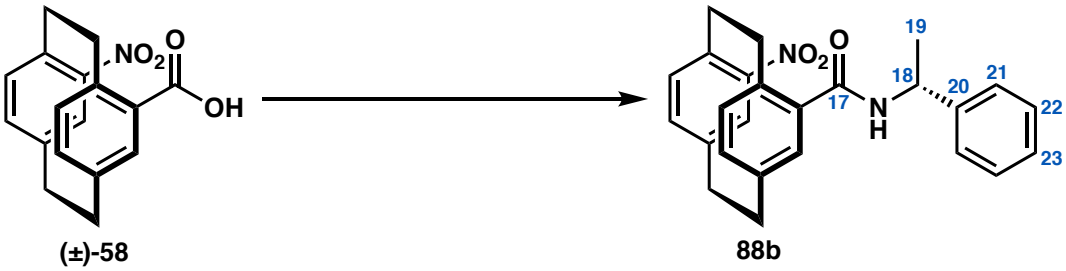


To a solution of (±)-4-nitro[2.2]paracyclophane-13-carboxylic acid (±)-**58** (1.00 g, 3.37 mmol, 1.00 eq) in $CH_2Cl_2$ (0.20 M, 16 mL) under Ar was added $(COCl)_2$ (0.34 mL, 4.04 mmol, 1.2 eq) and DMF (2 drops in 1 mL of $CH_2Cl_2$ ). The reaction mixture was stirred until bubbling ceased (~35 minutes). The solvent was concentrated under reduced pressure with the crude acyl chloride yielding as a dark brown solid.

To a solution of the crude acyl chloride in $CH_2Cl_2$ (0.20 M 15.84 mL,) at 0 °C under Ar was added $Et_3N$ (0.35 g, 3.49 mmol, 1.10 eq) followed by (*R*)-1-phenylethylamine (0.76 g, 3.17 mmol, 2.00 eq). The reaction mixture was stirred for 16 hours at RT. The solution was washed with $H_2O$ (2 × 20 mL). The organic layer was dried ($MgSO_4$) and concentrated under reduced pressure yielding the crude product as a orange–brown solid, which was purified by silica-gel chromatography (40% EtOAc, 60% hexane), to furnish **88b** as a yellowy-green solid (0.84 g, 2.09 mmol, 66%).

Diastereoisomers are seen in a ratio of 1:1.

$^1$H NMR (400 MHz, $CDCl_3$): δ (ppm) = 7.40-7.26 (12H, m, 10 × Ar-H, Ar-$H_{22pc}$), 6.77 (5H, d, *J* = 8.6 Hz, Ar-$H_{22pc}$), 6.70-6.63 (6H, m, Ar-$H_{22pc}$), 5.79 (1H, d, *J* = 7.0 Hz, NH), 5.69 (1H, d, *J* = 7.0 Hz, NH), 5.27 (2H, sext, 7.7 Hz, H-18), 4.25-4.16 (2H, m, CH), 3.98-3.89 (1H, m, CH), 3.85-3.78 (1H, m, CH), 3.23-2.93 (12H, m, 12 × CH), 1.61 (3H, d, *J* = 4.5 Hz, H-19), 1.60 (3H, d, *J* = 4.5 Hz, H-19).

Mass spectrometry (ESI) $[M]^+$= 423 (+ $Na^+$), 401, 324, 281, 105 101, 77 *m/z*.

IR: 3330, 2922, 2853,1738, 1677, 1601, 1576, 1358, 1254, 1172 $cm^{-1}$.

$R_f$: 0.81 (30% EtOAc, 70% hexane).

**Synthesis of (±)-4-nitro-*N*-isopropyl[2.2]paracyclophane-13-carboxamide**

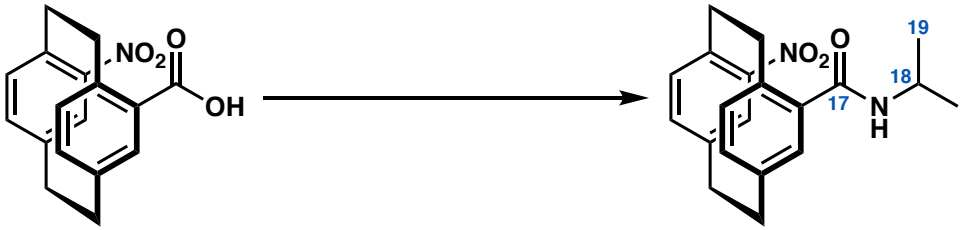


(±)-58 (±)-88c

To a solution of (±)-4-nitro[2.2]paracyclophane-13-carboxylic acid (±)-**58** (0.10 g, 0.34 mmol, 1.00 eq) in $SOCl_2$ (0.20 M, 1.68 mLwas stirred at reflux for 11 hours. The solution was then concentrated under reduced pressure to give the crude acyl chloride as a dark brown solid.

To a solution of the crude acyl chloride in $CH_2Cl_2$ (0.20 M, 7.92 mL) at 0 °C under Ar was added $Et_3N$ (0.24 mL, 0.24 mmol, 1.10 eq) followed by isopropylamine (0.27 mL, 3.17 mmol, 2.00 eq). The reaction mixture was stirred at RT for 16 hours. The solution was washed with $H_2O$ (2 × 20 mL). The organic layer was dried ($MgSO_4$) and concentrated under reduced pressure yielding the crude product as an orange brown solid, which was purified by silica-gel chromatography (20% EtOAc, 80% hexane), to furnish (±)-**88c** as a light yellow-orange solid (0.4063 g, 1.20 mmol, 76%).

$^1$H NMR (500 MHz, $CDCl_3$): δ (ppm) = 7.31 (1H, d, *J* = 1.3 Hz, H-5), 6.75 (1H, dd, *J* = 1.7, 7.9 Hz, H-7), 6.73 (1H, s, H-8), 6.66 (1H, s, H-16), 6.64 (1H, s, H-15), 6.63 (1H, s, H-12), 5.38 (1H, d, *J* = 6.9 Hz, NH), 4.20-4.06 (2H, m, H-$2_b$, H-18), 3.87-3.79 (1H, m, H-$1_b$), 3.13-2.99 (6H, m, H-$1_a$, H-$2_a$, H-9, H-10), 1.20 (6H, dd, *J* = 1.5, 6.5 Hz, H-19)

$^{13}$C NMR (700 MHz, $CDCl_3$): δ (ppm) = 198.3, 149.4, 142.1, 139.0, 167.2, 136.1, 134.72, 132.3, 129.2, 41.8, 35.4

Mass spectrometry (ESI) $[M]^+$= 361(+ $Na^+$), 338, 280, 194, 101

IR: 3305, 2970, 2932, 1639, 1521, 1385, 1340, 1171, 731 $cm^{-1}$.

Mp: 165 °C (decomposes)

$R_f$: 0.31 (20% EtOAc, 80% hexane)

**Synthesis of (±)-4-amino-*N*-((*S*)-1-phenylethyl)[2.2]paracyclophane-13-carboxamide**

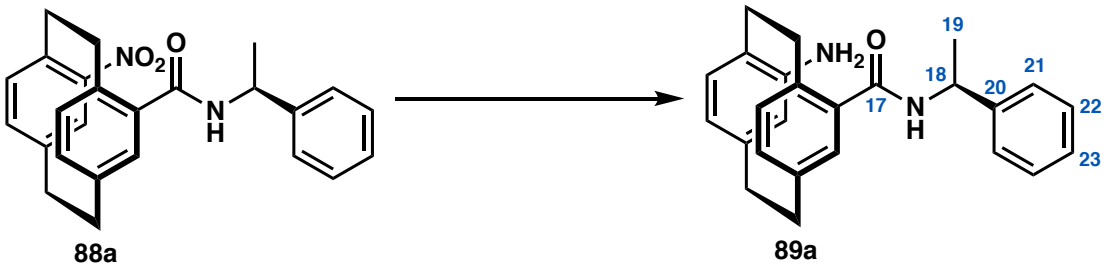


**88a** **89a**

To a solution of (±)-4-nitro-*N*-((*S*)-1-phenylethyl)[2.2]paracyclophane-13-carboxamide **88a** (0.87 g, 2.19 mmol, 1.00 eq) in MeOH (0.20 M, 10.86 mL) under Ar was added Zn powder (0.43 g, 6.51 mmol, 3.00 eq) followed by $NH_4Cl$ (0.39 g, 6.51 mmol, 3.00 eq). The reaction mixture was stirred at reflux for 11 hours. The solution was diluted with $CH_2Cl_2$ (10 mL) then filtered through celite and washed through with $CH_3OH$ (3 × 20 mL) followed by $CH_2Cl_2$ (2 × 15 mL). The combined organics were concentrated under reduced pressure yielding a dark green solid. The residue was dissolved in $CH_2Cl_2$ (100 mL) followed by the addition of $H_2O$ (150 mL). This solution stirred at RT for 1 hour. The organic layer was separated and aqueous layer was extracted with $CH_2Cl_2$ (2 × 15 mL). The combined organics were dried ($MgSO_4$) and concentrated under reduced pressure to furnish **89a** as an orange solid (0.50 g, 1.35 mmol, 62%).

Diastereoisomers are seen in a ratio of 1:1.

$^1$H NMR (400 MHz, $CDCl_3$): δ (ppm) = 7.44-7.26 (14H, m, 10 × Ar-H, Ar-$H_{22pc}$), 6.99 (1H, s, H-12), 6.91 (1H, s, H-12), 6.60-6.58 (2H, m, Ar-$H_{22pc}$), 6.34 (4H, td, *J* = 7.8, 13.2 Hz, Ar-$H_{22pc}$), 6.24 (1H, d, *J* = 7.5 Hz, Ar-$H_{22pc}$), 6.17-6.13 (2H, m, Ar-$H_{22pc}$), 5.9 (s, 2H, H-5), 5.30-5.21 (2H, m, H-18), 3.84 (1H, ddd, *J* = 6.1, 9.0, 13.5 Hz, CH), 3.61 (1H, ddd, *J* = 6.6, 8.7, 13.5 Hz, CH), 3.28 – 3.21 (1H, m CH) 3.12- 2.60 (13H, m, 13 × CH), 1.60 (3H, d, *J* = 6.8 Hz, H-19), 1.54 (3H, d, *J*, 6.8 Hz, H-19).

Mass spectrometry (ESI) $[M]^+$= 361(+ $Na^+$), 338, 280, 194, 101 *m/z*.

IR: 3305, 2970, 2932, 1639, 1521, 1385, 1340, 1171, 731 $cm^{-1}$.

$R_f$: 0.33 (3.5% MeOH, 96.5% $CH_2Cl_2$).

**Synthesis of (±)-4-amino-*N*-((*R*)-1-phenylethyl)[2.2]paracyclophane-13-carboxamide**

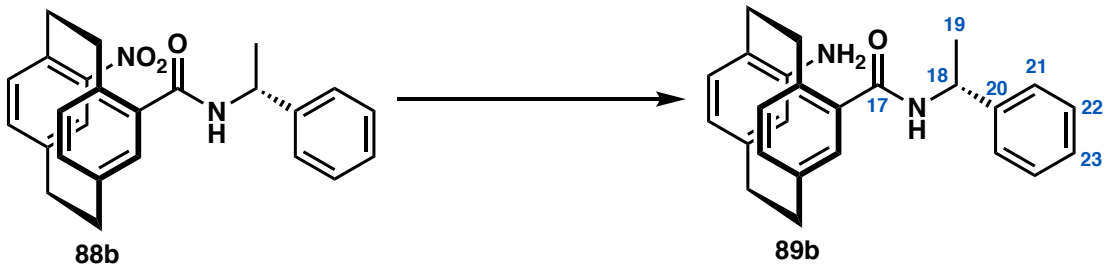


To a solution of (±)-4-nitro-*N*-((*R*)-1-phenylethyl)[2.2]paracyclophane-13-carboxamide **88b** (0.5 g, 1.25 mmol, 1.00 eq) in MeOH (0.20 M, 6.25 mL) under Ar was added Zn powder (0.25 g, 3.75 mmol, 3.00 eq) followed by $NH_4Cl$ (0.2 g, 3.75 mmol, 3.00 eq). The reaction mixture was stirred at reflux for 11 hours. The solution was diluted with $CH_2Cl_2$ (10 mL) then filtered through celite and washed through with $CH_3OH$ (2 × 15 mL) followed by $CH_2Cl_2$ (2 × 15 mL). The combined organics were concentrated under reduced pressure yielding a dark green solid. The residue was dissolved in $CH_2Cl_2$ (100 mL) followed by the addition of $H_2O$ (150 mL). This solution stirred at RT for 1 hour. The organic layer was separated and aqueous layer was extracted with $CH_2Cl_2$ (2 × 15 mL). The combined organics were dried ($MgSO_4$) and concentrated under reduced pressure to furnish **89b** as an orange solid (0.70 g, 1.88 mmol, 50%).

Diastereoisomers are seen in a ratio of 1:1.

$^1$H NMR (400 MHz, $CDCl_3$): δ (ppm) = 7.45-7.24 (12H, m, 10 × Ar-H, Ar-$H_{22pc}$), 7.00 (1H, d, *J* = 1.9 Hz, H-12), 6.91 (1H, d, *J* = 1.8 Hz, H-12), 6.61 (1H, dd, *J* = 1.8, 4.3 Hz, Ar-$H_{22pc}$), 6.59 (1H, dd, *J* = 1.6, 4.0 Hz, Ar-$H_{22pc}$), 6.39-6.60 (4H, m, Ar-$H_{22pc}$), 6.18-6.14 (4H, m, Ar-$H_{22pc}$), 5.50 (2H, t, *J* = 2.4 Hz, H-5), 5.29-5.22 (2H, m, H-18), 3.85 (1H, ddd, *J* = 6.2, 8.4, 13.4 Hz, CH), 3.62 (1H, ddd, *J* = 6.2, 8.0, 13.4 Hz, CH), 3.26 (1H, ddd, *J* = 2.1, 9.6, 13.8 Hz, CH), 3.13-2.86 (12H, m, 12 × CH), 2.80-2.72 (1H, m, CH), 2.72-2.63 (1H, m, CH), 1.61 (3H, d, *J* = 6.9 Hz, H-19), 1.56 (3H, d, *J* = 7.0 Hz, H-19).

Mass spectrometry (ESI) $[M]^+$= 361(+ $Na^+$), 338, 280, 194, 101 *m/z*.

IR: 3305, 2970, 2932, 1639, 1521, 1385, 1340, 1171, 731 $cm^{-1}$.

$R_f$: 0.31 (3.5% MeOH, 96.5% $CH_2Cl_2$).

**Synthesis of (±)-4-amino-*N*-isopropyl[2.2]paracyclophane-13-carboxamide**

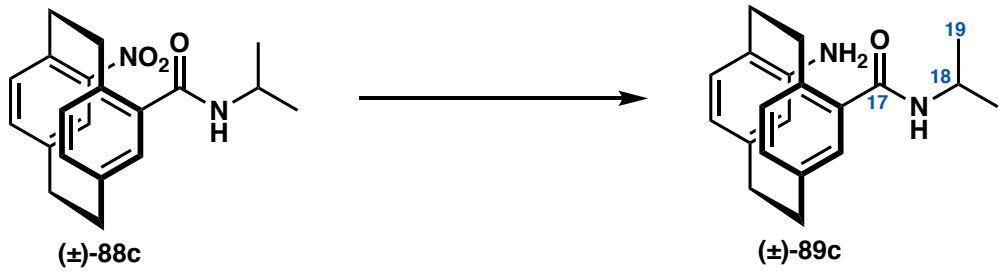


(±)-88c (±)-89c

To a solution of (±)-4-nitro-*N*-isopropyl[2.2]paracyclophane-13-carboxamide **88c** (0.030 g, 0.100 mmol, 1.00 eq) in MeOH (0.05 M, 1.94 mL) under Ar was added Zn powder (0.020 g, 0.29 mmol, 3.00 eq) followed by $NH_4Cl$ (0.020 g, 0.291 mmol, 3.00 eq). The solution was diluted with $CH_2Cl_2$ (10 mL) then filtered through celite and washed through with $CH_3OH$ (2 × 8 mL) followed by $CH_2Cl_2$ (2 × 8 mL). The combined organics were concentrated under reduced pressure yielding a dark green solid. The residue was dissolved in $CH_2Cl_2$ (25 mL) followed by the addition of $H_2O$ (30 mL). This solution stirred at RT for 1 hour. The organic layer was separated and aqueous layer was extracted with $CH_2Cl_2$ (2 × 15 mL). The combined organics were dried ($MgSO_4$) and concentrated under reduced pressure to yield a orange oil, which was purified by silica-gel chromatography (5% MeOH, 95% $CH_2Cl_2$), to furnish (±)-**89c** as a light brown solid (0.027 g, 0.086 mmol, 86%).

$^1$H NMR (400 MHz, $CDCl_3$): δ (ppm) = 6.84 (1H, d, *J* = 1.7 Hz, H-12), 6.63 (1H, dd, *J* = 1.7, 7.9 Hz, H-16), 6.49 (1H, d, *J* = 7.7 Hz, H-15), 6.44 (1H, d, *J* = 7.8 Hz, H-8), 6.40 (1H, dd, *J* = 1.3, 7.9 Hz, H-7), 6.19 (1H, s, H-5), 5.66 (1H, d, *J* = 7.9 Hz, NH), 4.23-4.18 (1H, m, H-18), 3.43-3.35 (1H, m, H-$1_b$), 3.67-3.60 (1H, m, H-$2_b$), 3.11-2.96 (6H, m, H-$1_a$, H-$2_a$, H-9, H-10), 1.20 (6H, d, *J* = 6.5 Hz, H-19).

$^{13}$C NMR (100 MHz, $CDCl_3$): δ (ppm) = 170.7, 141.4, 140.1, 137.2, 135.6, 135.2, 135.2, 134.3, 130.7, 128.8, 128.6, 125.5, 42.6, 34.7, 34.6, 31.8, 31.7, 22.6, 22.6.

Mass spectrometry (ESI) $[M]^+$= 309, 292, 263, 251, 118 *m/z*.

IR: 3297, 2965, 2922, 1647, 1531, 1350, 1342, 1151, 750 $cm^{-1}$.

Mp: 187-189 °C.

$R_f$: 0.28 (5% MeOH, 95% $CH_2Cl_2$).

**Synthesis of (±)-*N*-(13'-(isopropylcarbamoyl)[2.2]paracyclophane-4'-yl)-4-nitro[2.2]paracylophane-13-carboxamide**

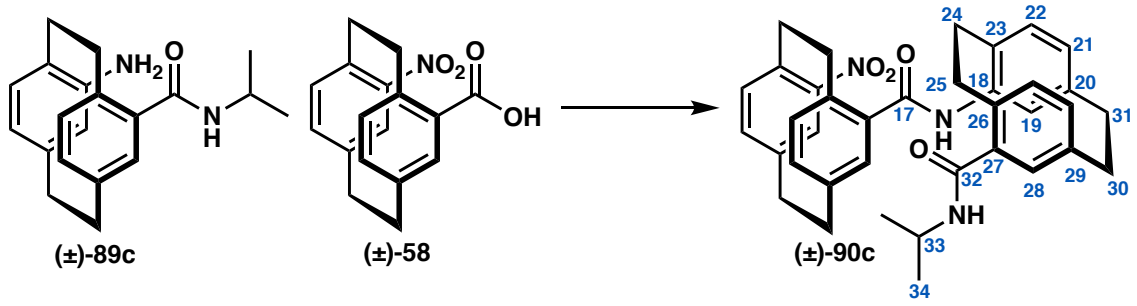


To a solution of (±)-4-nitro[2.2]paracyclophane-13-carboxylic acid (±)-**58** (0.03 g, 0.10 mmol, 1.17 eq) in $SOCl_2$ (0.05 M, 2.00 mL) was stirred at reflux for 11 hours. The solution was then concentrated under reduced pressure to give the crude acyl chloride as a dark brown solid.

To a solution of the crude acyl chloride in THF (0.02 M, 5.00 mL) under Ar at -10 °C was added $Et_3N$ (0.01 mL, 0.11 mmol, 1.10 eq) followed by 4-amino-*N*-isopropyl[2.2]paracyclophane-13-carboxamide (±)-**89c** (0.03 g, 0.09 mmol, 1.00 eq). The reaction mixture was stirred at -10 °C for 30 minutes followed by reflux for 14 hours. The solution was diluted with $H_2O$ (10 mL) and then extracted with EtOAc (3 × 15 mL). The combined organic phases were dried ($MgSO_4$) and concentrated under reduced pressure yielding as a light orange solid, which was purified by silica gel chromatography (40% EtOAc, 60% hexane), to furnish (±)-**90c** as a light yellow solid (0.02 g, 0.03 mmol, 37%).

1H NMR (500 MHz, CDCl3): δ (ppm) = 9.10 (1H, s, NH), 7.64 (1H, d, *J* = 1.3 Hz, Ar-H), 7.31 (1H, s, Ar-H), 6.92 (1H, d, *J* = 1.7 Hz, Ar-H), 6.84 (1H, dd, *J* = 1.4, 8.0 Hz, Ar-H), 6.73 (1H, d, *J* = 7.8 Hz, Ar-H), 6.69 (2H, s, 2 × Ar-H), 6.63 (1H, dd, *J* = 1.3, 7.7 Hz, Ar-H), 6.58 (1H, d, *J* = 8.3 Hz, Ar-H), 6.53 (2H, bs, 2 × Ar-H) 6.50 (1H, d, *J* = 7.8 Hz, Ar-H), 5.36 (1H, d, *J* = 8.0 Hz, NH), 4.24 (1H, ddd, *J* = 6.6, 13.1, 14.3 Hz, $CH_1$), 4.14-4.01 (3H, m, 3 × CH), 3.32-3.07 (12H, m, 12 × CH) 1.19 (3H, d, *J* = 6.7 Hz, $CH_3$), 1.11(3H, d, *J* = 6.5 Hz, $CH_3$).

Mass spectrometry (ESI) $[M]^+$= 588.17, 536.15, 319, 296, 239, 101 *m/z*.

$R_f$: 0.32 (40% EtOAc, 60% hexane).

**Synthesis of (±)-4-nitro-13-bromo[2.2]paracyclophane**

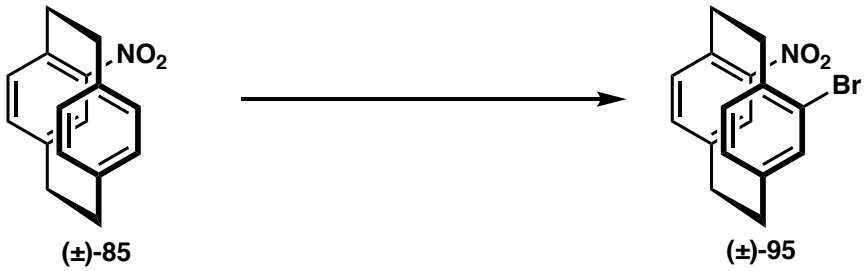


(±)-85 (±)-95

A stock solution of $Br_2$ (0.13 mL, 2.5 mmol, 1.3 eq) in $CH_2Cl_2$ (5.00 mL) was produced and added to an addition funnel covered in foil. A suspension of Fe fillings (0.01 g, 0.20 mmol, 0.10 eq) in stock solution (1.00 mL) was stirred at RT for 1 hour. To the Fe-$Br_2$ suspension was added (±)-4-nitro[2.2]paracyclophane (±)-**85** (0.50 g, 1.98 mmol, 1.00 eq) in $CH_2Cl_2$ (7.50 mL) followed by the remaining stock solution over 1 hour. After addition was completed, the solution was stirred at reflux for 9 hours. The solution was washed with $Na_2S_2O_3$ (15 mL) followed by brine (15 mL). The organic phase was dried ($MgSO_4$) and concentrated under reduced pressure to furnish (±)-**95** as a brown solid (0.57 g, 1.72 mmol, 86%).

$^1$H NMR (500 MHz, $CDCl_3$): $\delta$ (ppm) = 7.55 (1H, d, $J$ = 1.8 Hz, H-5), 6.76 (1H, dd, $J$ = 2.0, 7.5 Hz, H-7), 6.70 (1H, d, $J$ = 1.4 Hz, H-8), 6.65–6.60 (2H, m, H-16, H-15), 6.57 (1H, dd, $J$ = 1.4, 7.5 Hz, H-12), 4.37 (1H, dd, $J$ = 9.6, 13.7 Hz, H-$2_b$), 3.66 (1H, ddd, $J$ = 4.0, 9.3, 13.6 Hz, H-$1_b$), 3.20–3.04 (6H, m, H-$1_a$, H-$2_a$, H-9, H-10).

$^{13}$C NMR (126 MHz, $CDCl_3$): δ (ppm) = 147.7, 141.1, 138.8, 138.0 (C × 2), 137.7, 136.4, 136.2, 134.8, 131.5, 128.0, 127.4, 35.4, 34.7, 34.4, 32.7.

IR: 2934, 2855, 1547, 1475, 1451, 1335, 1033, 845, 710 $cm^{-1}$

$R_f$: 0.41 (20% EtOAc, 80% hexane).

**Synthesis of (±)-4-amino[2.2]paracyclophane**

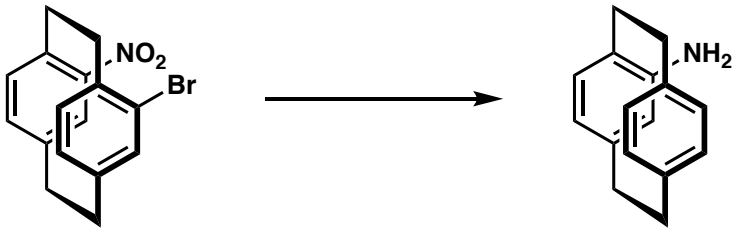


(±)-95 (±)-99

To a solution of (±)-4-nitro-13-bromo[2.2]paracyclophane **88c** (1.00 g, 3.01 mmol, 1.00 eq) in MeOH (0.20 M, 15.10 mL) under Ar was added Zn powder (0.590 g, 9.03 mmol, 3.00 eq) followed by $NH_4Cl$ (0.483 g, 9.03 mmol, 3.00 eq). The reaction mixture was stirred at reflux for 16 hours. The solution was diluted with $CH_2Cl_2$ (20 mL) then filtered through celite and washed through with $CH_3OH$ (2 × 15 mL) followed by $CH_2Cl_2$ (2 × 15 mL). The combined organics were concentrated under reduced pressure yielding a dark green solid. The residue was dissolved in $CH_2Cl_2$ (25 mL) followed by the addition of $H_2O$ (30 mL). This solution stirred at RT for 1 hour. The organic layer was separated and aqueous layer was extracted with $CH_2Cl_2$ (2 × 15 mL). The combined organics were dried ($MgSO_4$) and concentrated under reduced pressure to yield a orange oil, which was purified by silica-gel chromatography (10% EtOAc, 90% hexane), to furnish (±)-**89c** as a light brown solid (0.58 g, 2.62 mmol, 87%).

$^1$H NMR (500 MHz, $CDCl_3$): $\delta$ (ppm) = 7.19 (1H, ddd, $J$ = 1.9, 7.8 Hz, H-13), 6.61 (1H, ddd, $J$ = 1.6, 7.8 Hz, H-16), 6.42 (1H, s, H-12), 6.40 (1H, s, H-15), 6.29 (1H, d, $J$ = 7.8 Hz, H-7), 6.15 (1H, dd, $J$ = 1.6, 7.7 Hz, H-8), 5.40 (1H, d, $J$ = 1.5 Hz, H-5), 3.16-2.94 (6H, m, H-$1_a$ H-$2_a$, H-9, H-10), 2.88-2.82 (1H, m, H-$1_b$), 2.72-2.66 (1H, m, H-$2_b$).

Mass spectrometry (ESI) $[M]^+$= 224, 208, 117, 70.

$R_f$: 0.25 (10% EtOAc, 80% hexane).

**Synthesis of (±)-4-amino-13-bromo[2.2]paracyclophane**

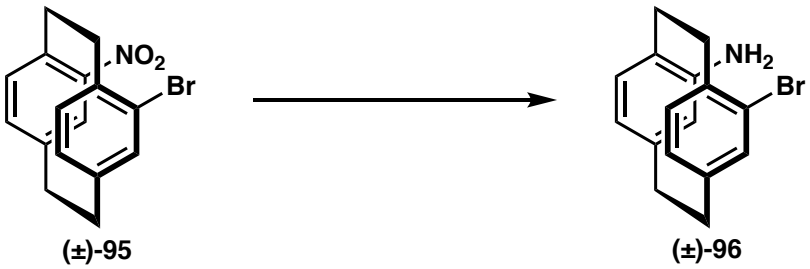


(±)-95 (±)-96

To a solution of (±)-4-nitro-13-bromo[2.2]paracyclophane (±)-**95** (1.00 g, 3.01 mmol, 1.00 eq) in EtOH/$H_2O$ (1:1, 0.1 M, 30.0 mL) was added Fe fillings (2.02 g, 36.12 mmol, 12.00 eq) followed by $HCl_{(aq)}$( 0.1 M, 30 mL). The reaction mixture was stirred at reflux for 16 hours. The solution was carefully added to saturated $NaHCO_3$ (100 mL). The solution was extracted with EtOAc (3 × 75 mL). The organic layer was washed with $H_2O$ (150 mL) followed by brine (150 mL). The organic phase was dried ($MgSO_4$) and concentrated under reduced pressure yielding a dark brown solid, which was purified by silica-gel chromatography (10% EtOAc, 90% hexane) to furnish (±)-**96** as a light orange solid (0.60 g 1.99 mmol, 66%).

NMR (500 MHz, $CDCl_3$): δ (ppm) = 6.83 (1H, s, H-12), 6.48 (1H, d, *J* = 7.8 Hz, H-16), 6.43 (1H, d, *J* = 7.7 Hz, H-15), 6.38 (1H, d, *J* = 7.8 Hz, H-8), 6.11 (1H, d, *J* = 7.4 Hz, H-7), 5.69 (1H, s, H-5), 3.70 (1H, ddd, *J* = 5.2, 9.1, 14.8 Hz, H-$1_b$), 3.33 (1H, ddd, *J* = 2.6, 10.6, 12.2 Hz, H-$2_b$), 3.14-3.09 (2H, m, H-$1_a$, H-$2_a$), 2.95-2.89 (4H, m, H-9, H-10).

$^{13}$C NMR (126 MHz, $CDCl_3$): δ (ppm) = 147.0, 140.9, 140.6, 138.1, 135.4, 135.3, 135.1, 132.7, 123.4, 123.1, 122.4, 121.1, 34.9, 34.7, 33.1, 31.5.

IR: 3392, 2926, 2851, 1611, 1423, 1260, 1032, 800 $cm^{-1}$.

Mass spectrometry (ESI) $[M]^+$= 303, 286, 222, 179 *m/z*.

Mp: 220 (decomposes).

$R_f$: 0.50 (20% EtOAc, 80% hexane).

**Synthesis of (*S*)-4-benzyl-4,5-dihydrooxazole**

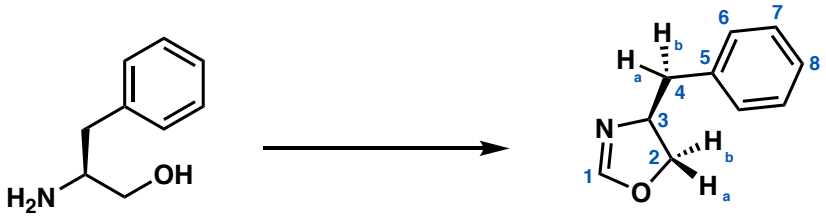


**97** **98**

To a solution of (*S*)-2-amino-3-phenylpropan-1-ol **97** (0.50 g, 3.31 mmol, 1.00 eq) in DCE (0.20 M, 6.6 mL) under Ar was added triethyl orthoformate (0.80 g, 4.960 mmol, 1.50 eq) followed by AcOH (0.02 g, 0.33 mmol, 0.10 eq). The reaction mixture was stirred at reflux for 12 hours and then concentrated under reduced pressure. The residue was dissolved with EtOAc (40 mL) and washed with $NaHCO_3$ (3 × 15 mL) and $H_2O$ (2 × 15 mL). The organic phase was dried ($MgSO_4$) and concentrated under reduced pressure to yielding a dark yellow oil, which was purified by Kugelrohr distillation (55 °C, 667 Pa), to furnish (*S*)-**98** as yellow-golden oil (0.33 g, 2.02 mmol, 61%).

$^1$H NMR (500 MHz, $CDCl_3$): δ (ppm) = 7.32 (2H, t, *J* = 7.4 Hz, H-7), 7.26-7.23 (3H, m, H-6, H-8), 6.83 (1H, s, H-1), 4.40 (1H, dq, *J* = 1.7, 7.7 Hz, H-3), 4.17 (1H, t, *J* = 9.0 Hz, H-$2_a$), 3.93 (1H, t, *J* = 7.9 Hz, H-$2_b$), 3.10 (1H, dd, *J* = 5.8, 13.8 Hz, H-$4_a$), 2.70 (1H, dd, *J* = 8.0, 13.7 Hz, H-$4_b$).

$^{13}$C NMR (126 MHz, $CDCl_3$): δ (ppm) = 154.8, 137.8, 129.2, 128.6, 126.6, 70.6, 66.5, 41.7.

Mass spectrometry (ESI) $[M]^+$= 162.24, 117.22, 90.97, 73.09 *m/z*.

IR: 3675, 2989, 2900, 1627, 1472, 1090, 931, 702 $cm^{-1}$.

$R_f$: 0.50 (10% MeOH, 90% $CH_2Cl_2$).

**Synthesis of (±)-4-nitro-*N*-(ethyl 4-benzoate)[2.2]paracyclophane-13-carboxamide**

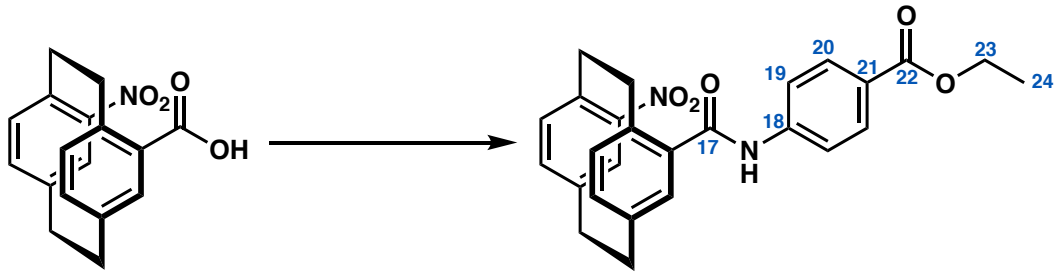


To a solution of (±)-4-nitro[2.2]paracyclophane-13-carboxylic acid (±)-**58** (0.250 g, 0.34 mmol, 1.00 eq) in $SOCl_2$ (2.00 M 4.20 mL) was stirred at reflux for 10 hours. The solution was then concentrated under reduced pressure to give the crude acyl chloride as a dark brown solid.

To a solution of the crude acyl chloride and ethyl 4-aminobenzoate (0.26 g, 1.587 mmol, 2.00 eq) in THF (0.20 M, 3.97 mL) at 0 °C under Ar was added $Et_3N$ (0.09 g, 0.87 mmol, 1.10 eq). The reaction mixture was stirred for 30 minutes at 0 °C followed by reflux for 15 hours. The solution was diluted with $H_2O$ (30 mL) and extracted with EtOAc (3 × 20 mL). The combined organics were dried ($MgSO_4$) and concentrated under reduced pressure to yield a dark brown solid, which was purified by silica-gel chromatography (30% EtOAc, 70% hexane), to furnish (±)-**103** as a light yellow solid (0.11 g, 0.242 mmol, 31%).

$^1$H NMR (500 MHz, DMSO-$d_6$): δ (ppm) = 10.10 (1H, s, NH), 7.93 (2H, d, *J* = 8.8 Hz, H-20), 7.78 (2H, d, *J* = 8.8 Hz, H-19), 7.31 (1H, d, *J* = 1.6 Hz, H-5), 6.96 (1H, dd, *J* = 1.5, 7.7 Hz, H-7) 6.93 (1H, d, *J* = 1.5 Hz, H-8), 6.89-6.85 (2H, m, H-16, H-15), 6.81 (1H, d, *J* = 7.8 Hz, H-12), 4.30 (2H, q, *J* = 7.0, H-23), 3.97 (1H, ddd, *J* = 3.5, 10.7, 12.8 Hz, H-$2_b$), 3.69 (1H, ddd, *J* = 2.7, 9.7, 12.2 Hz, H-$1_b$), 3.18-3.05 (6H, m, H-$1_a$, H-$2_a$ H-9, H-10), 1.32 (3H, t, *J* = 7.10, H-24).

$^{13}$C NMR (126 MHz, $CDCl_3$): δ (ppm) = 166.3, 166.3, 148.9, 142.1, 141.5, 140.2, 139.5, 137.5, 137.3, 136.2, 136.0, 135.7, 134.5, 131.4, 130.8, 128.2, 125.9, 119.4, 60.9, 34.7, 34.6, 34.5, 34.1, 14.4.

HRMS-EI: *m/z* found: $[M]^+$, 467.1575. $C_{26}H_{24}N_2O_5 + Na^+$ requires $[M]^+$, 467.1577 .

Mass spectrometry (ESI) $[M]^+$= 467, 445, 371 280, 253, 193, 161, 77 *m/z*.

IR: 3354, 2928, 2849, 1708, 1682, 1591, 1518, 1406, 1319, 1273, 1249, 1175, 770 $cm^{-1}$.

Mp: 166 °C (decomposes).

$R_f$: 0.25 (20% EtOAc, 80% hexane).

**Synthesis of (±)-ethyl 4-amino-*N*-benzoate[2.2]paracyclophane-13-carboxylate**

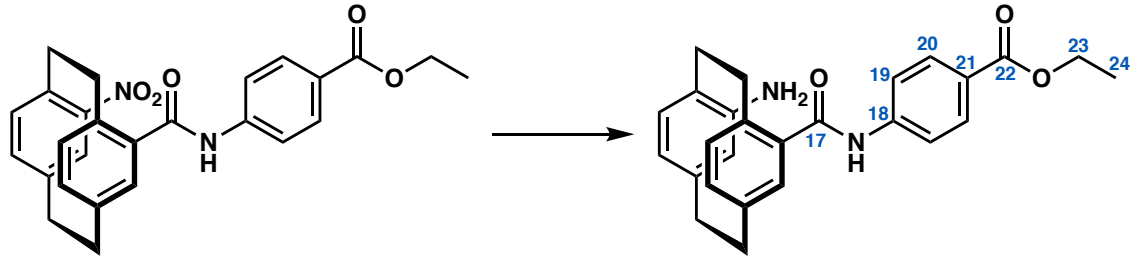


To a solution of (±)-ethyl 4-nitro-*N*-isopropyl[2.2]paracyclophane-13-benzoate (±)-**103** (0.108 g, 0.242 mmol, 1.00 eq) in EtOH (0.05 M, 4.84 mL) under Ar was added Zn powder (0.048 g, 0.727 mmol, 3.00 eq) followed by $NH_4Cl$ (0.039 g, 0.727 mmol, 3.00 eq). The reaction mixture was stirred at reflux for 13 hours. The solution was diluted with $CH_2Cl_2$ then filtered through celite and washed through with EtOH (30 mL) and then $CH_2Cl_2$ (2 × 20 mL). The combined organics were concentrated under reduced pressure yielding a dark green solid. The residue was dissolved in $CH_2Cl_2$ (50 mL) and stirred in $H_2O$ (50 mL) for one hour. The organic layer was separated and aqueous layer was extracted with $CH_2Cl_2$ (2 × 20 mL). The combined organics were dried ($MgSO_4$) and concentrated under reduced pressure to yield an orange solid, which was purified by silica gel-column chromatography (4% EtOH, 96% $CH_2Cl_2$), to furnish (±)-**104** as light orange solid (0.039 g, 0.087 mmol, 36%).

$^1$H NMR (400 MHz, $CDCl_3$): δ (ppm) = 8.05 (2H, d, *J* = 8.5 Hz, H-20), 7.98 (1H, bs, NH), 7.66 (2H, d, *J* = 8.7 Hz, H-19), 6.99 (1H, d, *J* = 1.4 Hz, H-12), 6.69 (1H, dd, *J* = 1.5, 7.7 Hz, H-16), 6.47 (2H, t, *J* = 7.8 Hz, H-15, H-8), 6.33 (1H, d, *J* = 7.4 Hz, H-7), 5.87 (1H, s, H-5), 4.38 (2H, q, *J* = 7.2 Hz, H-23), 3.80-3.73 (1H, m, H-$1_b$), 3.41-3.44 (1H, m, H-$2_b$), 3.18-3.02 (4H, m, H-9, H-10), 2.99-2.96 (1H, m, H-$2_a$), 2.87 (1H, ddd, *J* = 5.6, 11.0, 16.0 Hz, H-$1_a$), 1.40 (3H, t, *J* = 7.1 Hz, H-24).

Mass spectrometry (ESI) $[M]^+$= 415, 370, 342, 265,253, 223, 194, 166 78 *m/z*.

IR: 3423, 3267, 3153, 2827, 1698, 1686, 1550, 1498, 1320, 1260, 1170, 813, 793 $cm^{-1}$.

Mp: 176 °C (decomposes).

$R_f$: 0.25 (40% EtOAc, 60% hexane).

**Synthesis of *N*,*N*'-(1,3-phenylene)di(4-nitro[2.2]paracyclophane-13-carboxamide)**

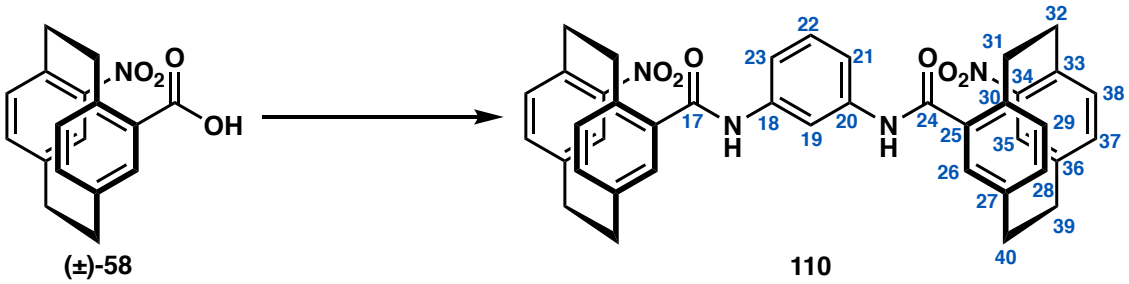


To a solution of (±)-4-nitro[2.2]paracyclophane-13-carboxylic acid (±)-**58** (0.250 g, 0.842 mmol, 1.00 eq) in $SOCl_2$ (2.00 M, 4.21 mL) was stirred at reflux for 10 hours. The solution was then concentrated under reduced pressure to give the crude acyl chloride as a dark brown solid.

To a solution of the crude acyl chloride in THF (0.200 M, 4.21 mL) at 0 °C under Ar was added, 1,3-diaminobenzene (0.100 g, 0.926 mmol, 1.10 eq) followed by $Et_3N$ (0.129 mL, 0.926, 1.10 eq). The reaction mixture was stirred for 30 minutes at 0 °C followed by reflux for 17 hours. The solution was diluted with $H_2O$ (30 mL) and extracted with EtOAc (3 × 50 mL). The combined organics were concentrated under reduced pressure yielding a black solid. The resulting residue was partitioned between $HCl_{(aq)}$ (2 M; 100 mL) and EtOAc (60 mL). The aqueous layer was separated was extracted with EtOAc (2 × 40 mL). The combined organics were dried ($MgSO_4$) and concentrated under reduced pressure to furnish a mixture of **110** diastereoisomers as a orange solid (0.258 g, 0.387 mmol, 46%).

Diastereoisomers are seen in a ratio of 1:03

$^1$H NMR (400 MHz, $CDCl_3$): δ (ppm) = 7.41 (2H, d, *J* = 1.8 Hz, Ar-$H_{22pc}$, mixture of diastereoisomers), 7.35-7.32 (4H, m, Ar-$H_{22pc}$, mixture of diastereoisomers), 7.24-7.20 (4H, m, NH, mixture of diastereoisomers), 7.08 (2H, t, *J* = 8.0 Hz, H-19, mixture of diastereoisomers), 6.96 (1H, d, *J* = 8.2 Hz, Ar-$H_{22pc}$, minor diastereoisomer), 6.90-6.86 (4H, m, Ar-$H_{22pc}$, mixture of diastereoisomers), 6.83 (1H, d, *J* = 1.7 Hz, Ar-$H_{22pc}$, minor diastereoisomer), 6.82-6.80 (3H, m, Ar-$H_{22pc}$, mixture of diastereoisomers), 6.78 (3H, d, *J* = 1.5 Hz, Ar-$H_{22pc}$, mixture of diastereoisomers), 6.72 (2H, d, *J* = 1.8 Hz, Ar-$H_{22pc}$, minor diastereoisomer) 6.74-6.66 (6H, m, Ar-H, H-21, H-19, Ar-$H_{22pc}$, mixture of diastereoisomers), 6.48 (4H, d, *J* = 8.2 Hz, Ar-$H_{22pc}$, mixture of diastereoisomers), 4.35 (2H, ddd, *J* = 2.1, 9.8, 13.6 Hz, H-$2_b$, minor diastereoisomer), 4.23-4.14 (2H, m, H-$2_b$, major diastereoisomer), 3.98-3.83 (2H, m, H-$1_b$, major diastereoisomer), 3.96 (2H, ddd, *J* = 6.5, 8.8, 13.6 Hz, minor diastereoisomer) 3.39-2.92 (24H, m, H-$1_a$,H-$2_a$, H-9, H-10, 24 × CH, mixture of diastereoisomers).

Mass spectrometry (ESI) $[M]^+$= 667, 414, 386, 371, 334, 295, 281, 106, 77 *m/z*.

$R_f$: 0.25, (1.5% MeOH, 98.5% $CH_2Cl_2$).

**Synthesis of (±)-methyl 4-nitro[2.2]paracyclophane-13-carboxylate**

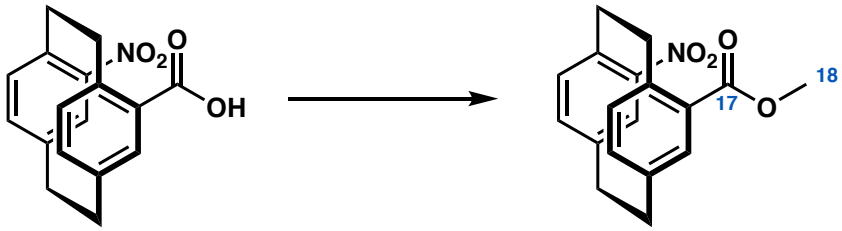


(±)-58 (±)-111

To a solution of (±)-4-nitro[2.2]paracyclophane-13-carboxylic acid (±)-**58** (0.67 g, 2.25 mmol 1.00 eq) in $SOCl_2$ (11.3 mL, 2 mol) was stirred at reflux for 10 hours. The solution was then concentrated under reduced pressure to give the crude acyl chloride as a dark brown solid.

To a solution of the crude acyl chloride in $CH_3OH$ (0.10 M, 22 mL) was stirred at RT for 11 hours. The solution was concentrated under reduced pressure to furnish (±)-**111** as a orange solid (0.70 g, 2.25 mmol, 94%).

$^1$H NMR (400 MHz, $CDCl_3$): δ (ppm) = 7.24 (1H, d, *J* = 1.9 Hz, H-12), 7.17 (1H, d, *J* = 2.0 Hz, H-16), 6.77 (1H, dd, *J* = 1.8, 7.9 Hz, H-15), 6.73 (1H, dd, *J* = 2.0, 7.9 Hz, H-8), 6.69 (1H, d, *J* = 5.9 Hz, H-7), 6.67 (1H, d, *J* = 6.0 Hz, H-5), 4.22-4.16 (1H, m, H-$2_b$), 4.08-4.02 (1H, m, H-$1_b$), 3.84 (3H, s, H-18), 3.19-3.01 (6H, m, H-$2_a$, H-$1_a$, H-9, H-10).

$^{13}$C NMR (126 MHz, $CDCl_3$): δ (ppm) = 167.0, 141.9, 141.6, 139.5, 137.7, 137.2, 136.1 (C × 2), 135.5, 134.2, 130.2, 128.0, 52.0, 51.9, 34.6, 34.5, 34.4, 33.6.

HRMS-EI: *m/z* found: $[M]^+$, 334.1045. $C_{18}H_{18}NO_4Na^+$ requires $[M]^+$, 334.1050.

Mass spectrometry (ESI) $[M]^+$= 312, 212, 280, 185, 115, 82 *m/z*.

IR: 32272, 2930, 1680, 1632, 1380, 1263, 1096 $cm^{-1}$.

Mp: 158 °C (decomposes).

$R_f$: 0.20 (20% EtOAc, 80 % hexane).

**Synthesis of (±)-methyl 4-amino[2.2]paracyclophane-13-carboxylate**

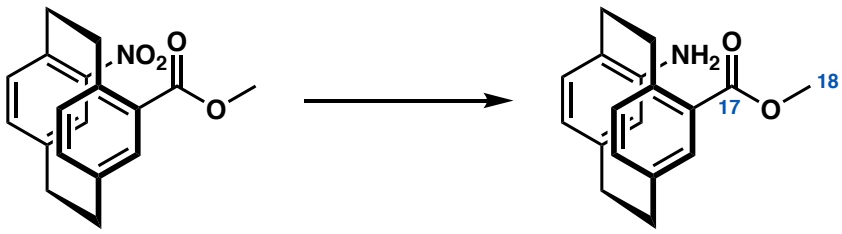


(±)-111 (±)-101

To a solution of (±)-methyl 4-nitro[2.2]paracyclophane-13-carboxylate (±)-**111** (0.047 g, 0.151 mmol, 1.00 eq) in MeOH (0.03 M, 5 mL) was added Zn powder (0.032 g, 0.604 mmol, 4.0 eq) followed by $NH_4Cl$ (0.039 g, 0.604mmol, 4.0 eq). The reaction mixture was stirred at reflux for 26 hours. The solution was diluted with $CH_2Cl_2$ (20 mL) then filtered through celite and washed with MeOH (3 × 10 mL) followed by $CH_2Cl_2$ (3 × 15 mL). The combined organic layers were concentrated under reduced pressure to yield a dark green solid. The residue was dissolved in $CH_2Cl_2$ (50 mL) and stirred in $H_2O$ for 1 hour. The organic layer was separated and the aqueous layer was extracted with $CH_2Cl_2$ (2 × 15 mL). The combined organics were dried ($MgSO_4$) and concentrated under reduced pressure yielding a light green solid, which was purified by silica gel-column chromatography (5% MeOH, 95% $CH_2Cl_2$), to furnish (±)-**101** as a light yellow solid (0.024 g, 0.077 mmol, 56%).

$^1$H NMR (500 MHz, $CDCl_3$): δ (ppm) = 7.24 (1H, s, H-12), 6.68 (1H, d, *J* = 7.7 Hz, H-16), 6.40 (1H, d, *J* = 7.7 Hz, H-15), 6.33 (1H, d, *J* = 7.7 Hz, H-8), 6.16 (1H, d, *J* = 7.6 Hz, H-7), 5.43 (1H, s, H-5), 4.29 (1H, ddd, *J* = 5.6, 9.9, 14.8 Hz, H-$1_b$), 3.88 (3H, s, H-18), 3.39 (2H, bs, $NH_2$), 3.14 (1H, ddd, *J* = 2.8, 10.2, 13.4 Hz, H-$2_b$), 3.07-2.96 (3H, m, H-$2_a$, H-10), 2.90 (2H, t, *J* = 7.2 Hz, H-9), 2.72 (1H, ddd, *J* = 5.5, 10.7, 14.4, H-$1_a$).

$^{13}$C NMR (126 MHz, $CDCl_3$): δ (ppm) = 169.0, 145.9, 142.0, 140.6, 138.7, 136.3, 135.3, 134.8, 133.7, 127.3, 124.4, 122.4, 120.9, 51.6, 34.8, 34.6, 31.8, 31.0.

HRMS-EI: *m/z* found: $[M]^+$, 282.1486. $C_{18}H_{20}NO_2Na$ requires $[M]^+$, 282.1489.

Mass spectrometry (ESI) $[M]^+$= 282, 273, 267, 266, 223, 207, 172, 152 *m/z*.

IR: 3438, 3349, 2954, 2931, 1691, 1629, 1440, 1272, 1182, 1082 $cm^{-1}$.

Mp: 168 °C (decomposes).

$R_f$: 0.40 (20% EtOAc, 80 % hexane).

**Synthesis of 4-(dimethylamino)benzoic acid**

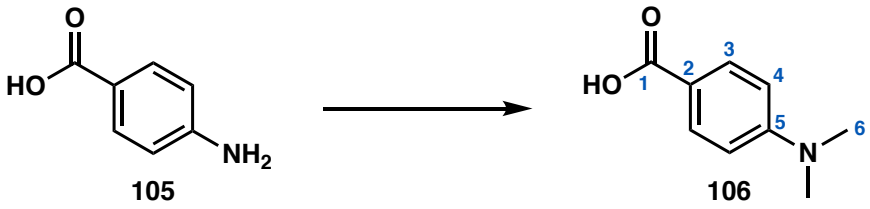


To a solution of 4-aminobenzoic acid **105** (1.00 g, 7.30 mmol, 1.00 eq) in MeCN (0.20 M, 36 mL) under Ar was added $K_2CO_3$ (3.03 g, 21.90 mmol, 3 eq) followed by MeI (1.55 g, 10.94 mmol, 1.50 eq) and stirred for 8 hours. The solution was diluted with $H_2O$ and extracted with EtOAc (2 × 50 mL). The combined organics were dried ($MgSO_4$) and concentrated under reduced pressure to furnish **106** as a light yellow solid (1.13 g, 6.84 mmol, 94%).

$^1$H NMR (500 MHz, $CDCl_3$): δ (ppm) = 7.98 (2H, d, *J* = 9.0 Hz, H-3), 6.68 (2H, d, *J* = 9.0 Hz, H-4), 3.06 (3H, s, H-6).

$^{13}$C NMR (126 MHz, $CDCl_3$): δ (ppm) = 172.0, 154.0, 132.2, 116.0, 110.8, 40.2.

HRMS-EI: *m/z* found: $[M]^+$, 166.0862 . $C_9H_{12}NO_2$ requires $[M]^+$, 166.0863.

Mass spectrometry (ESI) $[M]^-$= 164, 121, 120, 97 *m/z*.

IR: 2900, 1668, 1603, 1420, 1295, 1187, 830, 771 $cm^{-1}$.

Mp: 243-244 °C (decomposes).

$R_f$: 0.53 (3% MeOH, 97% $CH_2Cl_2$).

**Synthesis of *N*-benzoylglycine**

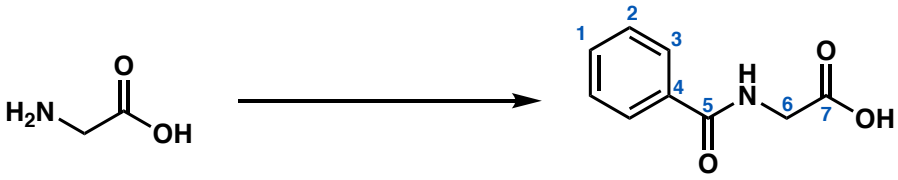


**115** **114**

To a solution of glycine **115** (1.00 g, 13.33 mmol, 1.00 eq) in $NaOH_{(aq)}$ (0.25 M, 10 mL). The reaction mixture was stirred at RT for 5 hours with the slow addition of benzoyl chloride (1.96 mL, 15.31 mmol, 1.15 eq). The solution was acidified with $HCl_{(aq)}$ (~37%, 5 mL) resulting in a precipitate that was filtered off. The solid was collected and recrystalised from $H_2O$ yielding white crystals, which was purified by a silica-gel plug (5% MeOH, 95% $CH_2Cl_2$) to furnish **114** as a white solid (2.15 g, 12.00 mmol, 90%).

NMR (500 MHz, DMSO-$d_6$): δ (ppm) = 8.78 (1H, t, *J* = 6.0 Hz, , NH), 7.87 (2H, d, *J* = 7.7 Hz, H-3), 7.54 (1H, t, *J* = 7.1 Hz, H-1), 7.47 (2H, t, *J* = 7.5 Hz, H-2), 3.92 (d, *J* = 5.9 Hz, 2H, H-6).

$^{13}C$ NMR (126 MHz, DMSO-$d_6$): δ (ppm) = 171.9, 166.9, 134.4, 131.9, 128.8, 127.7, 41.9.

HRMS-EI: *m/z* found: $[M]^-$, 178.0501. $C_9H_8NO_3$ requires $[M]^-$, 178.0499.

Mass spectrometry (ESI) $[M]^+$= 179, 135, 150, 105, 103 *m/z*.

IR: 3337, 2989, 1740, 1598, 1555, 1414, 1178, 1079, 722 $cm^{-1}$

Mp: 186-187 °C.

$R_f$: 0.09 (3% MeOH 97% $CH_2Cl_2$).

**Synthesis of Boc-glycine**

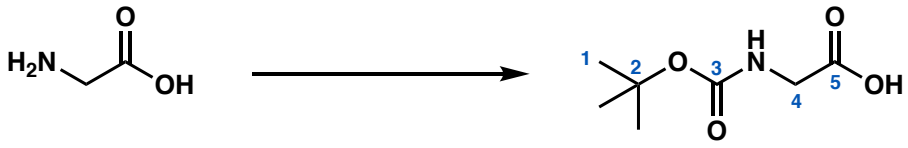


**115** **118**

To a solution of glycine **115** (0.50 g, 6.66 mmol, 1.00 eq) in MeCN (0.20 M, 33 mL) under Ar was added $Boc_2O$ (1.31 g, 5.99 mmol, 0.90 eq) dropwise over a 20 min period. The reaction mixture was stirred at 25 °C for 12 hours. The solution was concentrated under reduced pressure. The residue was dissolved in $H_2O$ (30 mL) and washed with EtOAc (3 × 15 mL) and $Et_2O$ (3 × 15 mL). The aqueous layer was freeze dried to furnish **118** as a white solid (1.11 g, 6.34 mmol, 95%).

NMR (500 MHz, DMSO-$d_6$): δ (ppm) = 12.43 (1H, bs, OH). 7.05 (1H, d, $J$ = 6.0, NH) 3.57 (2H, d, $J$ = 6.2, H-4), 1.38 (s, 9H, H-1).

$^{13}$C NMR (126 MHz, DMSO-$d_6$): δ (ppm) = 172.2, 156.3, 78.5, 42.3, 28.4.

Mass spectrometry (ESI) $[M]^+$= 174, 115, 101, 73 $m/z$.

IR: 3676, 3340, 2977, 2941, 1739, 1668, 1530, 1452, 1408, 1366, 1196, 1158, 957 $cm^{-1}$.

Mp: 87-88 °C.

$R_f$: 0.08 (30% EtOAc, 70% hexane).

**Synthesis of *tert*-butyl(2-oxo-2-(phenylamino)ethyl)carbamate**

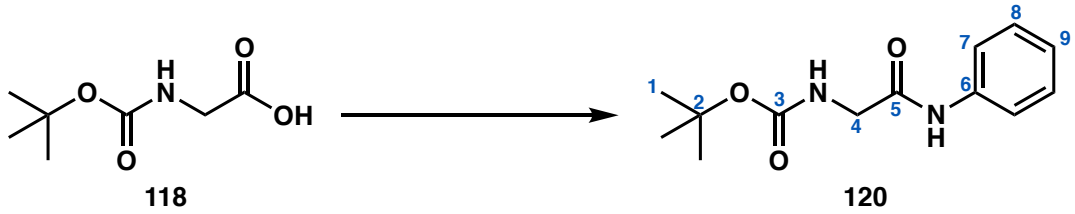


To a solution of (*tert*-butoxycarbonyl)glycine **118** (1.00 g, 5.71 mmol, 1.00 eq) in $CH_2Cl_2$ (0.20 M, 28.5 mL) under Ar at 0 °C was added NHS (0.72 g, 6.28 mmol, 1.10 eq) and stirred for 2 minutes, followed by the addition of DCC (1.30 g, 6.28 mmol, 1.10 eq). The reaction mixture was stirred for 4 hours, observing the formation of a white precipitate, which was filtered through cotton wool. The solution was concentrated under reduced pressure to ~5 mL and stored in the fridge for 2 hours, resulting in formation of additional precipitate that was filtered off. The solution was concentrated under reduced pressure yielding the active ester.

To a solution of the crude active ester in THF (0.3 M, 14.3 mL) was added aniline (0.75 mL, 7.42 mmol, 1.3 eq). The reaction mixture was stirred at reflux for 11 hours. The solution was diluted with $H_2O$ (15 mL) and extracted with EtOAc (3 × 15 mL). The combined organics were quickly washed with a cooled solution of $HCl_{(aq)}$ (2 M; 15 mL). The organic layer was dried ($MgSO_4$) and concentrated under reduced pressure to furnish **120** as a light purple solid (1.27 g, 5.08 mmol, 89%).

NMR (500 MHz, $CDCl_3$): δ (ppm) = 8.06 (1H, bs, NH), 7.51 (2H, d, $J$ = 8.0 Hz, H-7), 7.33 (2H, t, $J$ = 7.9 Hz, H-8), 7.12 (1H, t, $J$ = 7.3 Hz, H-9), 5.20 (1H, bs, NH), 3.92 (2H, d, $J$ = 6.1 Hz, H-4), 1.48 (9H, s, H-1).

Mass spectrometry (ESI) $[M]^+$= 251, 159, 151, 131, 121, 102 *m/z*.

Mp: 87-88 °C.

$R_f$: 0.37 (30% EtOAc, 70% hexane)

**Synthesis of 2-amino-*N*-phenylacetamide**

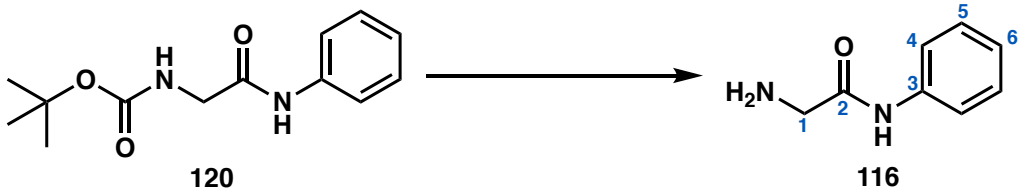


To a solution of the Boc-glycine-aniline **120** (0.150 g, 0.599 mmol, 1.00 eq) in $CH_2Cl_2$ (0.20 M, 3.0 mL) was added TFA (0.1 M, 1.5 mL). The reaction mixture was stirred at RT for 30 minutes. The solvent was concentrated under reduced pressure, furnishing **116** as a light yellow solid (0.088 g, 0.587 mmol, 98%).

NMR (500 MHz, $CD_3OD$): δ (ppm) = 7.58 (2H, d, *J* = 7.7 Hz, H-4), 7.33 (2H, t, *J* = 7.7 Hz, H-5), 7.12 (1H, t, 7.4 Hz, H-6), 3.85 (2H, s, H-1).

Mass spectrometry (ESI) $[M]^+$= 151, 121, 93, 78, 74 *m/z*.

IR: 3676, 3340, 2977, 2941, 1739, 1668, 1530, 1452, 1408, 1366, 1196, 1158, 957 $cm^{-1}$.

Mp: 86-90 °C.

$R_f$: 0. 18 (3% MeOH, 97% $CH_2Cl_2$).

**Synthesis of (±)-5-nitro-4-hydroxy[2.2]metaparacyclophane**

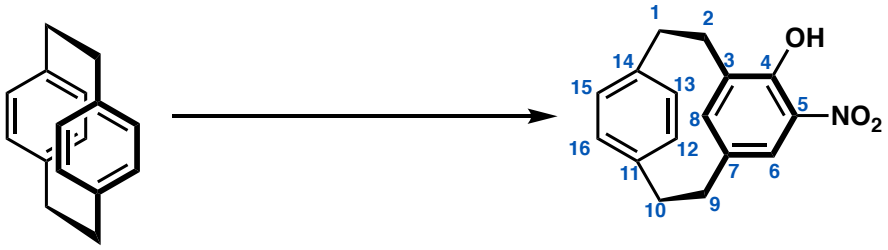


**16** (±)-**124**

To a solution of [2.2]paracyclophane **16** (10.00 g, 48.06 mmol, 1.00 eq) in $CH_2Cl_2$ (0.20 M, 240 mL) at 0 °C was added a solution of $HNO_3$ (4.00 mL, 96.16 mmol, 2.00 eq) and $H_2SO_4$ (10.10 mL, 192.32 mmol, 4.0 eq). The reaction mixture was stirred at 0 °C for 8 hours, observing a colour change from clear to yellow. The reaction was poured onto ice (100 g) through filter paper, and stirred until the ice had melted. The layers were separated and the aqueous layer was extracted with $CH_2Cl_2$ (5 × 80 mL). The combined organic layers were dried ($MgSO_4$) and concentrated under reduced pressure to yield an orange solid, which was purified by silica-gel chromatography (100% hexane), to furnish (±)-**124** as a yellow solid (2.46 g, 9.13 mmol, 19%).

$^1$H NMR (500 MHz, $CDCl_3$): δ (ppm) = 10.79 (1H, s, OH), 7.53 (1H, s, H-6), 7.22 (2H, q, *J* = 7.9, 12.7 Hz, H-15, H-16) 6.12 (1H, d, *J* = 7.9 Hz, H-13), 5.98 (1H, d, *J* = 7.9 Hz, H-12), 5.80 (1H, s, H-8), 3.23-3.12 (3H, m, 3 × CH), 2.85-2.76 (2H, m, 2 × CH), 2.52-2.46 (1H, m, CH), 2.19-2.12 (1H, m, CH), 1.99-1.93 (1H, m, CH).

$^{13}$C NMR (126 MHz, $CDCl_3$): δ (ppm) = 152.6, 141.2, 140.3, 138.6, 132.5, 132.3, 131.3, 130.8, 130.0 128.9, 128.1, 121.2, 37.1, 35.8, 35.0, 31.9.

152.6, 141.2, 140.0, 138.6, 132.5, 132.3, 131.3, 130.8, 130.0, 128.9, 128.1, 121.2

HRMS-EI: *m/z* found: $[M]^-$, 268.0981 . $C_{16}H_{14}NO_3$ requires $[M]^-$, 268.0968

Mass spectrometry (ESI) $[M]^+$= 264, 252, 223, 151, 89 *m/z*.

IR: 3306, 2917, 2850, 1739, 1534, 1261 $cm^{-1}$.

Mp: 152-155 °C.

$R_f$: 0.40, (10% EtOAc, 90% hexane).

**Synthesis of (4(16)Z)-8-hydroxy-6-nitrotricyclo[9.2.2.14,8]hexadeca-1(13),4,(16),6,11,14-pentaen-5-one**

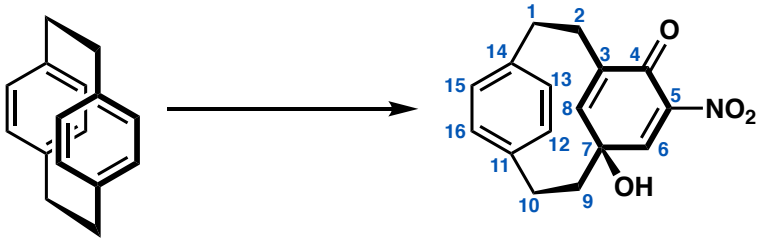


16 131

To a solution of [2.2]paracyclophane (10.00 g, 48.06 mmol, 1.00 eq) in $CH_2Cl_2$ (0.20 M, 240 mL), at 0°C was added a solution of $HNO_3$ (4.00 mL, 96.16 mmol, 2.00 eq) and $H_2SO_4$ (5.05 mL, 96.16 mmol, 2.00 eq). The reaction mixture was stirred at 0 °C for 8 hours, observing a colour change from clear to yellow. The reaction was poured onto ice (100 g) through filter paper and stirred until the ice had melted. The layers were separated and the aqueous layer was extracted with $CH_2Cl_2$ (5 × 80 mL). The combined organics layers were dried ($MgSO_4$) and concentrated under reduced pressure to produce an orange solid.

The residue was heated and dissolved in minimal amount of $CH_2Cl_2$ and allowed to come to RT resulting in the formation of a precipitate. The solvent was filtered yielding the desired product as a light yellow solid (3.35 g, 11.74 mmol, 14%).

$^1$H NMR (500 MHz, DMSO-$d_6$): δ (ppm) = 7.48 (1H, d, *J* = 8.1 Hz, H-15), 7.29 (1H, d, *J* = 2.5 Hz, H-6), 7.16 (1H, d, *J* = 8.1 Hz, H-16), 6.73 (1H, d, *J* = 7.8 Hz, H-13), 6.58 (1H, d, *J* = 7.7 Hz, H-12), 5.62 (2H, s, H-8, OH), 2.94-2.90 (1H, m, CH), 2.87-2.83 (1H, dd, *J* = 8.3, 12.0 Hz CH), 2.65-2.59 (1H, m, CH), 2.53-2.52 (1H, m, CH) 2.26-2.20 (1H, m, CH), 2.02-1.93 (2H, m, 2 × CH), 1.69-1.63 (1H, m, CH).

$^{13}$C NMR (126 MHz, DMSO-$d_6$): δ (ppm) = 177.3, 147.9, 147.4, 142.7, 141.1, 137.7, 130.6, 130.1, 130.1, 129.3, 129.2, 68.2, 43.4, 33.4, 32.2, 30.2.

HRMS-EI: *m/z* found: $[M]^-$, 284.0928. $C_{16}H_{16}NO_4$ requires $[M]^-$, 284.0917.

Mass spectrometry (ESI) $[M + Na]^+$= 309, 287, 269, 240, 215,194, 73 *m/z*.

IR: 3453, 2925, 1665, 1535, 1356, 1010, 729 $cm^{-1}$.

Mp: 206-213 °C.

$R_f$: 0.25 (20% EtOAc, 80% hexane).

**Synthesis of (4(16)Z)-8-hydroxy-7-methoxy-6-nitrocyclo[9.2.2.14,8]hexadeca-1(13),4(16),11,14-tetraen-5-one**

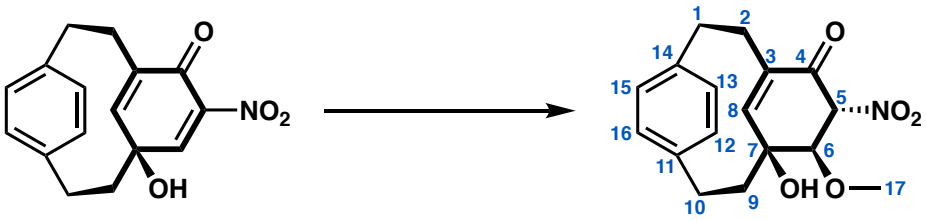


**131** **132**

To a solution of **131** (5.00 g, 17.53 mmol, 1.00 eq) in MeOH (0.20 M, 87.63 mL) was added TFA (1.00 M, 17.53 mL) and stirred at RT for 31 days. The solution was concentrated under reduced pressure yielding a light orange solid, which was purified by flash silica-gel chromatography (gradient of 0% to 60% EtOAc, Hexane over 1 hour). Slow evaporation of fractions containing **132**, **133** and **134**, furnished **132** as clear crystals that could be isolated to obtain pure characterisation (1.75 g, 6.14 mmol, 35%).

$^{1}$H NMR (500 MHz, $CDCl_3$): δ (ppm) 7.45 (1H, d, *J* = 8.2 Hz, H-15), 7.19 (1H, d, *J* = 8.6 Hz, H-16), 7.05 (1H, d, *J* = 8.0 Hz, H-13), 6.94 (1H, d, *J* = 8.0 Hz, H-12), 5.61 (1H, s, H-8), 5.17 (1H, d, *J* = 10.8 Hz, H-5), 4.40 (1H, d, *J* = 11.0 Hz, H-6), 3.62 (3H, s, H-17), 3.17 (1H, dd, *J* = 6.6, 14.1 Hz, CH), 2.94-2.86 (2H, m, 2 × CH), 2.58-2.47 (2H, m, 2 × CH), 1.99 (1H, dd, *J* = 6.1, 5.8 Hz, $CH_2$), 1.90 (1H, td, *J* = 6.7, 12.9, 19.9 Hz, CH), 1.68-1.61 (1H, m, CH).

$^{13}$C NMR (126 MHz, $CDCl_3$): δ (ppm) = 187.3, 145.2, 143.6, 132.0, 136.1, 130.8, 130.7, 130.5, 130.0, 92.7, 75.5, 72.0, 61.3, 42.3, 35.1, 33.3, 31.7.

HRMS-EI: *m/z* found: $[M + Na]^+$, 340.1172. $C_{16}H_{20}NO_5Na$ requires $[M + Na]^+$, 340.1152.

Mass spectrometry (ESI) $[M]^-$ = 316, 284, 255, 205, 145, 96.9

IR: 3525, 3455, 2934, 1683, 1557, 1367, 1074, 1056, 729.

Mp: 209-212 °C.

$R_f$: 0.25 (30% EtOAc, 70% hexane).

**Synthesis of (4(16)Z)-8-hyroxytricyclo[9.2.2.14,8]hexadeca-1(13),4(16),6,11,14-pentaen-5-one)**

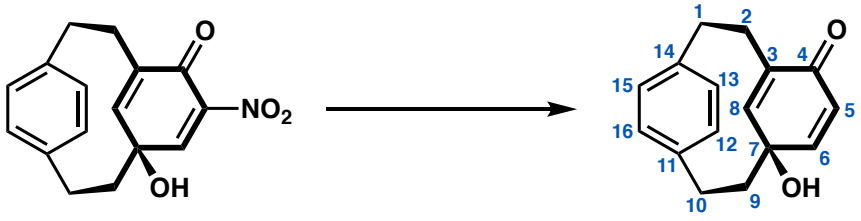


**131** **133**

To a solution of **131** (0.05 g, 0.18 mmol, 1.00 eq) in MeOH (0.10 M, 1.75 mL) was added TFA (0.10 M, 1.75 mL) and stirred at RT for 24 h. The solution was concentrated under reduced pressure yielding a light orange solid, which was purified by preparative TLC (3% MeOH, 97% $CH_2Cl_2$) to furnish **133** as a light yellow solid (0.013 g, 0.05, 30%).

$^1$H NMR (700 MHz, ($CdCl_3$): δ (ppm) = 7.36 (1H, d, *J* = 8.1 Hz, H-15), 7.09 (1H, dd, *J* = 1.2, 8.2 Hz, H-16), 6.69 (2H, AB q, *J* = 1.5, 8.0 Hz, H-12, H-13), 6.42 (1H, dd, *J* = 2.8, 9.9 Hz, H-5), 6.02 (1H, d, *J* = 9.9 Hz, H-6), 5.48 (1H, d, *J* = 2.9 Hz, H-8), 3.03-3.00 (1H, m, CH), 2.86 (1H, dd, *J* = 4.1, 9.5 Hz, CH), 2.70 (1H, td, *J* = 3.9, 12.5 Hz, CH), 2.27-2.22 (1H, m, CH), 1.99-1.96 (1H, m, CH), 1.54-1.49 (3H, m, 3 × CH).

$^{13}$C NMR (176 MHz, $CDCl_3$): δ (ppm) = 187.2, 145.8, 145.6, 143.4, 137.0, 132.1, 131.0, 129.9, 129.3, 129.1, 69.6, 42.9, 34.5, 33.1, 31.1.

$^1$H NMR (700 MHz, (Acetone-$d_6$): δ (ppm) 7.45 (1H, ddd, *J* = 0.8, 1.6, 8.0 Hz, H-15), 7.15 (1H, dd, *J* = 1.6, 7.7 Hz, H-16), 6.70 (1H, dd, *J* = 1.6, 7.7 Hz, H-13), 6.56 (1H, dd, *J* = 1.7, 7.7 Hz, H-12), 6.47 (1H, dd, *J* = 2.9, 10.0 Hz, H-5), 5.87 (1H, d, *J* = 10.0 Hz, H-6), 5.48 (1H, d, *J* = 2.8 Hz, H-8), 2.96 (1H, ddd, *J* = 2.7, 5.6, 13.8 Hz, CH), 2.73 (1H, dd, *J* = 7.4, 10.5 Hz, CH), 2.70 (1H, dd, *J* = 7.3, 10.6 Hz, CH), 2.57 (1H, dd, *J* = 7.4, 12.4 Hz, CH), 2.26 (1H, ddd, *J* = 6.5, 12.2, 18.5 Hz, CH), 2.00-1.93 (3H, m, 3 × CH).

$^{13}$C NMR (176 MHz, Acetone-$d_6$): δ (ppm) =186.8, 147.0, 146.6, 143.1, 137.7, 130.7, 130.0, 198.8, 194.4, 128.3, 128.3, 68.6, 43.2, 34.1, 32.8, 30.8.

HRMS-EI: *m/z* found: $[M + Na]^+$, 263.1054. $C_{16}H_{17}O_2Na$ requires $[M + Na]^+$, 263.1043.

Mass spectrometry (ESI) $[M]^+$= 241, 224, 118, 104 *m/z*.

IR: 3386, 2918, 2849, 1651, 1622, 1261, 1020, 829, 813 $cm^{-1}$.

Mp: 206-208 °C.

$R_f$: 0.25 (30% EtOAc, 70% hexane).

**Synthesis of (4(16)Z)-8-hydroxy-7-methoxy-6-nitrotricyclo[9.2.2.14,8]hexadeca-1(13),4(16),11,14-tetraen-5-one**

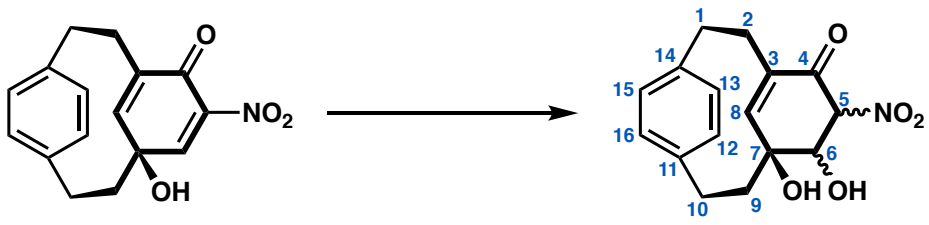


**131** **134**

To a solution of **133** (0.050 g, 0.18 mmol, 1.00 eq) in MeOH (0.10 M, 1.75 mL) was added TFA (0.10 M, 1.75 mL) and stirred at RT for 24 h. The solution was concentrated under reduced pressure yielding a light orange solid, which was purified by preparative TLC (2% MeOH, 98% $CH_2Cl_2$) to furnish **134** as a light yellow solid (0.013 g, 0.05 mmol, 30%).

$^1$H NMR (700 MHz, $CDCl_3$): δ (ppm) = 7.45 (1H, d, *J* = 7.9 Hz, H-15), = 7.19 (1H, d, *J* = 8.1 Hz, H-14), 7.03 (1H, dd, *J* = 1.5, 8.0, Hz, H-13), 6.91 (1H, dd, *J* = 1.3, 7.7, Hz, H-12), 5.67 (1H, s, H-8), 5.16 (1H, d, *J* = 10.9 Hz, H-5), 4.70 (1H, dd, *J* = 7.3, 10.7 Hz, H-6), 3.11 (1H, dd, *J* = 6.6, 14.3, Hz, CH), 2.95-2.86 (2H, m, 2 × CH), 2.78 (1H, d, *J* = 7.9 Hz, OH), 2.55-2.49 (2H, m, 2 × CH) 2.16 (2H, ddd, *J* = 1.3, 6.0, 14.1 Hz, 2 × CH), 1.78 (1H, td, *J* = 6.7, 13.2 Hz, CH), 1.65 (1H, td, *J* = 8.3, 16.4 Hz, CH).

$^{13}$C NMR (176 MHz, $CDCl_3$): δ (ppm) = 187.0, 145.0, 143.2, 136.6, 132.2, 130.8, 130.9, 130.3, 130.2, 93.7, 71.9, 66.0, 41.2, 35.0, 33.3, 31.1.

HRMS-EI: *m/z* found: $[M + Na]^+$, 326.0964. $C_{16}H_{18}NO_5Na$ requires $[M]^+$, 326.0999.

$R_f$: 0.15 (30% EtOAc, 70% hexane).

Chapter 5

# References


(1) Liu, X.; Dong, S.; Lin, L.; Feng, X. Chiral Amino Acids-Derived Catalysts and Ligands. *Chin. J. Chem.* **2018**, *36* (9), 791–797.

(2) Xu, L.-W.; Lu, Y. Primary Amino Acids: Privileged Catalysts in Enantioselective Organocatalysis. *Org. Biomol. Chem.* **2008**, *6* (12), 2047–2053.

(3) Mallakpour, S.; Dinari, M. Progress in Synthetic Polymers Based on Natural Amino Acids. *J. Macromol. Sci. A* **2011**, *48* (8), 644–679.

(4) Bischoff, R.; Schlüter, H. Amino Acids: Chemistry, Functionality and Selected Non-Enzymatic Post-Translational Modifications. *J. Proteom.* **2012**, *75* (8), 2275–2296.

(5) Goodman, C. M.; Choi, S.; Shandler, S.; DeGrado, W. F. Foldamers as Versatile Frameworks for the Design and Evolution of Function. *Nat. Chem. Biol.* **2007**, *3* (5), 252–262.

(6) Preciado, S.; Mendive-Tapia, L.; Albericio, F.; Lavilla, R. Synthesis of C-2 Arylated Tryptophan Amino Acids and Related Compounds through Palladium-Catalyzed C–H Activation. *J. Org. Chem.* **2013**, *78* (16), 8129–8135.

(7) Brosch, O.; Weyhermüller, T.; Metzler-Nolte, N. Synthesis of Alkynyl Amino Acids and Peptides and Their Palladium-Catalyzed Coupling to Ferrocene. *Inorg. Chem.* **1999**, *38* (23), 5308–5313.

(8) Guo, L.; Zhang, W.; Guzei, I. A.; Spencer, L. C.; Gellman, S. H. New Preorganized γ-Amino Acids as Foldamer Building Blocks. *Org. Lett.* **2012**, *14* (10), 2582–2585.

(9) Szórád, J. J.; Faragó, E. P.; Rágyanszki, A.; Cimino, F. A.; Fiser, B.; Owen, M. C.; Jójárt, B.; Morgado, C. A.; Szőri, M.; Jensen, S. J. K.; Csizmadia, I. G.; Viskolcz, B. Conformation Change of Opiorphin Derivates. A Theoretical Study of the Radical Initiated Epimerization of Opiorphin. *Chem. Phys. Lett.* **2015**, *626*, 29–38.

(10) Sarker, K.; Sen, D. D. J. Opiorphin as Endogenous Peptide of Human Saliva Acts as Inhibitor of Protease Enzymes of Enkephalins. *World J. Pharm. Res.* **2017**, *6* (03), 1727–1733.

(11) Rougeot, C.; Robert, F.; Menz, L.; Bisson, J.-F.; Messaoudi, M. Systemically Active Human Opiorphin Is a Potent yet Non-Addictive Analgesic without Drug Tolerance Effects. *J. Physiol. Pharmacol.* **2010**, *61* (4), 483–490.

(12) Wisner, A.; Dufour, E.; Messaoudi, M.; Nejdi, A.; Marcel, A.; Ungeheuer, M.-N.; Rougeot, C. Human Opiorphin, a Natural Antinociceptive Modulator of Opioid-Dependent Pathways. *Proc. Natl. Acad. Sci. U.S.A.* **2006**, *103* (47), 17979–17984.

(13) Singh, P.; Kongara, K.; Harding, D.; Ward, N.; Dukkipati, V. S. R.; Johnson, C.; Chambers, P. Comparison of Electroencephalographic Changes in Response to Acute Electrical and Thermal Stimuli with the Tail Flick and Hot Plate Test in Rats Administered with Opiorphin. *BMC Neurol.* **2018**, *18* (1), 43–53.

(14) Sweeney, M. D.; Zhao, Z.; Montagne, A.; Nelson, A. R.; Zlokovic, B. V. Blood-Brain Barrier: From Physiology to Disease and Back. *Physiol. Rev.* **2018**, *99* (1), 21–78.

(15) Daneman, R.; Prat, A. The Blood–Brain Barrier. *Cold Spring Harb. Perspect. Biol.* **2015**, *7* (1), a020412.

(16) Bocsik, A.; Darula, Z.; Tóth, G.; Deli, M. A.; Wollemann, M. Transfer of Opiorphin through a Blood-Brain Barrier Culture Model. *Arch. Med. Res.* **2015**, *46* (6), 502–506.

(17) Mehmood, Y.; Tariq, A.; Siddiqui, F. A. Brain Targeting Drug Delivery System: A Review. *Int. J. Basic Med. Sci. Pharm.* **2015**, *5* (1), 32–40.

(18) Seelig, A.; Gottschlich, R.; Devant, R. M. A Method to Determine the Ability of Drugs to Diffuse through the Blood-Brain Barrier. *Proc. Natl. Acad. Sci. U.S.A.* **1994**, *91* (1), 68–72.

(19) Rosa, M.; Marcelo, F.; Calle, L. P.; Rougeot, C.; Jiménez-Barbero, J.; Arsequell, G.; Valencia, G. Influence of Polar Side Chains Modifications on the Dual Enkephalinase Inhibitory Activity and Conformation of Human Opiorphin, a Pain Perception Related Peptide. *Bioorg. Med. Chem. Lett.* **2015**, *25* (22), 5190–5193.

(20) Rosa, M.; Arsequell, G.; Rougeot, C.; Calle, L. P.; Marcelo, F.; Pinto, M.; Centeno, N. B.; Jiménez-Barbero, J.; Valencia, G. Structure–Activity Relationship Study of Opiorphin, a Human Dual Ectopeptidase Inhibitor with Antinociceptive Properties. *J. Med. Chem.* **2012**, *55* (3), 1181–1188.

(21) Pinto, M.; Rougeot, C.; Gracia, L.; Rosa, M.; Garcı´a, A.; Arsequell, G.; Valencia, G.; Centeno, N. B. Proposed Boactive Conformations of Opiorphin, an Endogenous Dual APN/NEP Inhibitor. *ACS Med. Chem. Lett.* **2012**, *3* (1), 20–24.

(22) Bogeas, A.; Dufour, E.; Bisson, J.-F.; Messaoudi, M.; Rougeot, C. Structure-Activity Relationship Study and Function-Based Petidomimetic Design of Human Opiorphin with Improved Bioavailability Property and Unaltered Analgesic Activity. *Biochem Pharmacol* **2013**, *02* (03), 17–28.

(23) Rautio, J.; Meanwell, N. A.; Di, L.; Hageman, M. J. The Expanding Role of Prodrugs in Contemporary Drug Design and Development. *Nat. Rev. Drug Discov.* **2018**, *17* (8), 559–587.

(24) Rautio, J.; Kumpulainen, H.; Heimbach, T.; Oliyai, R.; Oh, D.; Järvinen, T.; Savolainen, J. Prodrugs: Design and Clinical Applications. *Nat. Rev. Drug Discov.* **2008**, *7* (3), 255–270.

(25) Sozio, P.; Cerasa, L. S.; Abbadessa, A.; Stefano, A. D. Designing Prodrugs for the Treatment of Parkinson's Disease. *Expert Opin. Drug Discov.* **2012**, *7* (5), 385–406.

(26) Ovallath, S.; Sulthana, B. Levodopa: History and Therapeutic Applications. *Ann. Indian Acad. Neurol.* **2017**, *20* (3), 185–189.

(27) Jones, A. X.; Cao, Y.; Tang, Y.-L.; Wang, J.-H.; Ding, Y.-H.; Tan, H.; Chen, Z.-L.; Fang, R.-Q.; Yin, J.; Chen, R.-C.; Zhu, X.; She, Y.; Huang, N.; Shao, F.; Ye, K.; Sun, R.-X.; He, S.-M.; Lei, X.; Dong, M.-Q. Improving Mass Spectrometry Analysis of Protein Structures with Arginine-Selective Chemical Cross-Linkers. *Nat. Commun.* **2019**, *10* (1), 3911–3922.

(28) Mendoza, V. L.; Vachet, R. W. Probing Protein Structure by Amino Acid-Specific Covalent Labeling and Mass Spectrometry. *Mass Spectrom. Rev.* **2009**, *28* (5), 785–815.

(29) Maffioli, S. I.; Zhang, Y.; Degen, D.; Carzaniga, T.; Del Gatto, G.; Serina, S.; Monciardini, P.; Mazzetti, C.; Guglierame, P.; Candiani, G.; Chiriac, A. I.; Facchetti, G.; Kaltofen, P.; Sahl, H.-G.; Dehò, G.; Donadio, S.; Ebright, R. H. Antibacterial Nucleoside-Analog Inhibitor of Bacterial RNA Polymerase. *Cell* **2017**, *169* (7), 1240–1248.

(30) Bui, T. P.; Li, Y.; Nunes, Q. M.; Wilkinson, M. C.; Fernig, D. G. Selective Labelling of Arginine Residues Engaged in Binding Sulfatedglycosaminoglycans. *bioRxiv* **2019**, 574947–575011.

(31) Sibbersen, C.; Palmfeldt, J.; Hansen, J.; Gregersen, N.; Jørgensen, K. A.; Johannsen, M. Development of a Chemical Probe for Identifying Protein Targets of α-Oxoaldehydes. *Chem. Commun.* **2013**, *49* (38), 4012–4014.

(32) Gauthier, M. A.; Klok, H.-A. Arginine-Specific Modification of Proteins with Polyethylene Glycol. *Biomacromolecules* **2011**, *12* (2), 482–493.

(33) Takahashi, K. The Reaction of Phenylglyoxal with Arginine Residues in Proteins. *J. Biol. Chem.* **1968**, *243* (23), 6171–6179.

(34) Klöpfer, A.; Spanneberg, R.; Glomb, M. A. Formation of Arginine Modifications in a Model System of Nα-Tert-Butoxycarbonyl (Boc)-Arginine with Methylglyoxal. *J. Agric. Food Chem.* **2011**, *59* (1), 394–401.

(35) El-Dahshan, A.; Nazir, S.; Ahsanullah; Ansari, F. L.; Rademann, J. Peptide–Heterocycle Chimera: New Classes of More Drug-like Peptidomimetics by Ligations of Peptide–Bis(Electrophiles) with Various Bis(Nucleophiles). *Eur. J. Org. Chem.* **2011**, *1* (4), 730–739.

(36) Biemel, K. M.; Reihl, O.; Conrad, J.; Lederer, M. O. Formation Pathways for Lysine-Arginine Cross-Links Derived from Hexoses and Pentoses by Maillard Processes: Unraveling the Structure of a Pentosidine Precursor. *J. Biol. Chem.* **2001**, *276* (26), 23405–23412.

(37) Bellier, J.; Nokin, M.-J.; Lardé, E.; Karoyan, P.; Peulen, O.; Castronovo, V.; Bellahcène, A. Methylglyoxal, a Potent Inducer of AGEs, Connects between Diabetes and Cancer. *Diabetes Res. Clin. Pract.* **2019**, *148*, 200–211.

(38) Galligan, J. J.; Wepy, J. A.; Streeter, M. D.; Kingsley, P. J.; Mitchener, M. M.; Wauchope, O. R.; Beavers, W. N.; Rose, K. L.; Wang, T.; Spiegel, D. A.; Marnett, L. J. Methylglyoxal-Derived Posttranslational Arginine Modifications Are Abundant Histone Marks. *Proc. Natl. Acad. Sci. U.S.A.* **2018**, *115* (37), 9228–9233.

(39) Hill, D. J.; Mio, M. J.; Prince, R. B.; Hughes, T. S.; Moore, J. S. A Field Guide to Foldamers. *Chem. Rev.* **2001**, *101* (12), 3893–4012.

(40) Oba, M. Cell-penetrating Peptide Foldamers: Drug-delivery Tools. *ChemBioChem* **2019**, *20* (16), 2041–2045.

(41) Prabhakaran, P.; Barnard, A.; Murphy, N. S.; Kilner, C. A.; Edwards, T. A.; Wilson, A. J. Aromatic Oligoamide Foldamers with a "Wet Edge" as Inhibitors of the α-Helix-Mediated P53- *h* DM2 Protein-Protein Interaction: Inhibitors of Protein-Protein Interactions. *Eur. J. Org. Chem.* **2013**, *2013* (17), 3504–3512.

(42) Bécart, D.; Diemer, V.; Salaün, A.; Oiarbide, M.; Nelli, Y. R.; Kauffmann, B.; Fischer, L.; Palomo, C.; Guichard, G. Helical Oligourea Foldamers as Powerful Hydrogen Bonding Catalysts for Enantioselective C–C Bond-Forming Reactions. *J. Am. Chem. Soc.* **2017**, *139* (36), 12524–12532.

(43) Mándity, I. M.; Fülöp, F. An Overview of Peptide and Peptoid Foldamers in Medicinal Chemistry. *Expert Opin. Drug Discov.* **2015**, *10* (11), 1163–1177.

(44) Mayoral, M. J.; Bilbao, N.; González-Rodríguez, D. Hydrogen-bonded Macrocyclic Supramolecular Systems in Solution and on Surfaces. *ChemistryOpen* **2015**, *5* (1), 10–32.

(45) Guichard, G.; Huc, I. Synthetic Foldamers. *Chem. Commun.* **2011**, *47* (21), 5933.

(46) Zhang, D.-W.; Zhao, X.; Hou, J.-L.; Li, Z.-T. Aromatic Amide Foldamers: Structures, Properties, and Functions. *Chem. Rev.* **2012**, *112* (10), 5271–5316.

(47) Sinnokrot, M. O.; Valeev, E. F.; Sherrill, C. D. Estimates of the Ab Initio Limit for π–π Interactions: The Benzene Dimer. *J. Am. Chem. Soc.* **2002**, *124* (36), 10887–10893.

(48) Ray, A. Solvophobic Interactions and Micelle Formation in Structure Forming Nonaqueous Solvents. *Nature* **1971**, *231*, 313–315.

(49) Zhao, Y.; Moore, J. S. Foldamers Based on Solvophobic Effects. In *Foldamers*; John Wiley & Sons, Ltd, 2007; pp 75–108.

(50) Rodnikova, M. N. Mechanism of Solvophobic Interactions. *Russ. J. Phys. Chem.* **2006**, *80* (10), 1605–1607.

(51) John, E. A.; Massena, C. J.; Berryman, O. B. Helical Anion Foldamers in Solution. *Chem. Rev.* **2020**, *120* (5), 2759–2782.

(52) Rinaldi, S. The Diverse World of Foldamers: Endless Possibilities of Self-Assembly. *Molecules* **2020**, *25* (14), 3276.

(53) Martinek, T. A.; Fülöp, F. Peptidic Foldamers: Ramping up Diversity. *Chem. Soc. Rev.* **2012**, *41* (2), 687–702.

(54) Saraogi, I.; Hamilton, A. D. Recent Advances in the Development of Aryl-Based Foldamers. *Chem. Soc. Rev.* **2009**, *38* (6), 1726–1743.

(55) Gellman, S. H. Foldamers: A Manifesto. *Acc. Chem. Res.* **1998**, *31* (4), 173–180.

(56) Girvin, Z. C.; Gellman, S. H. Exploration of Diverse Reactive Diad Geometries for Bifunctional Vatalysis via Foldamer Backbone Variation. *J. Am. Chem. Soc.* **2018**, *140* (39), 12476–12483.

(57) Girvin, Z. C.; Andrews, M. K.; Liu, X.; Gellman, S. H. Foldamer-Templated Catalysis of Macrocycle Formation. *Science* **2019**, *366* (6472), 1528–1531.

(58) Ziach, K.; Chollet, C.; Parissi, V.; Prabhakaran, P.; Marchivie, M.; Corvaglia, V.; Bose, P. P.; Laxmi-Reddy, K.; Godde, F.; Schmitter, J.-M.; Chaignepain, S.; Pourquier, P.; Huc, I. Single Helically Folded Aromatic Oligoamides That Mimic the Charge Surface of Double-Stranded B-DNA. *Nat. Chem.* **2018**, *10* (5), 511–518.

(59) Corvaglia, V.; Carbajo, D.; Prabhakaran, P.; Ziach, K.; Mandal, P. K.; Santos, V. D.; Legeay, C.; Vogel, R.; Parissi, V.; Pourquier, P.; Huc, I. Carboxylate-Functionalized Foldamer Inhibitors of HIV-1 Integrase and Topoisomerase 1: Artificial Analogues of DNA Mimic Proteins. *Nucleic Acids Res.* **2019**, *47* (11), 5511–5521.

(60) Gopalakrishnan, R.; Frolov, A. I.; Knerr, L.; Drury, W. J.; Valeur, E. Therapeutic Potential of Foldamers: From Chemical Biology Tools to Drug Candidates? *J. Med. Chem.* **2016**, *59* (21), 9599–9621.

(61) M. Grison, C.; Robin, S.; J. Aitken, D. 13-Helix Folding of a β/γ-Peptide Manifold Designed from a "Minimal-Constraint" Blueprint. *Chem. Commun.* **2016**, *52* (50), 7802–7805.

(62) Lamouroux, A.; Sebaoun, L.; Wicher, B.; Kauffmann, B.; Ferrand, Y.; Maurizot, V.; Huc, I. Controlling Dipole Orientation through Curvature: Aromatic Foldamer

Bent β-Sheets and Helix–Sheet–Helix Architectures. *J. Am. Chem. Soc.* **2017**, *139* (41), 14668–14675.

(63) Ikkanda, B. A.; Iverson, B. L. Exploiting the Interactions of Aromatic Units for Folding and Assembly in Aqueous Environments. *Chem. Commun.* **2016**, *52* (50), 7752–7759.

(64) Tanatani, A.; Mio, M. J.; Moore, J. S. Chain Length-Dependent Affinity of Helical Foldamers for a Rodlike Guest. *J. Am. Chem. Soc.* **2001**, *123* (8), 1792–1793.

(65) Cram, D. J.; Steinberg, H. Macro Rings. I. Preparation and Spectra of the Paracyclophanes. *J. Am. Chem. Soc.* **1951**, *73* (12), 5691–5704.

(66) Zhang, X.; Lu, G.; Sun, M.; Mahankali, M.; Ma, Y.; Zhang, M.; Hua, W.; Hu, Y.; Wang, Q.; Chen, J.; He, G.; Qi, X.; Shen, W.; Liu, P.; Chen, G. A General Strategy for Synthesis of Cyclophane-Braced Peptide Macrocycles via Palladium-Catalysed Intramolecular $Sp^3$ C–H Arylation. *Nat. Chem.* **2018**, *10* (5), 540–548.

(67) Baran, P. S.; Burns, N. Z. Total Synthesis of (±)-Haouamine A. *J. Am. Chem. Soc.* **2006**, *128* (12), 3908–3909.

(68) Nicolaou, K. C.; Sun, Y.-P.; Korman, H.; Sarlah, D. Asymmetric Total Synthesis of Cylindrocyclophanes A and F through Cyclodimerization and a Ramberg–Bäcklund Reaction. *Angew. Chem. Int. Ed.* **2010**, *49* (34), 5875–5878.

(69) Brown, C. J.; Farthing, A. C. Preparation and Structure of Di-*p*-Xylylene. *Nature* **1949**, *164* (4178), 915–916.

(70) Gibson, S. E.; Knight, J. D. [2.2]Paracyclophane Derivatives in Asymmetric Catalysis. *Org. Biomol. Chem.* **2003**, *1* (8), 1256–1269.

(71) Vorontsova, N. V.; Rozenberg, V. I.; Vorontsov, E. V.; Tok, O. L.; Bubnov, Yu. N. Stereoselective Synthesis of Homoallylic Alcohols of the [2.2]Paracyclophane Series and Their Use as Auxiliaries in Asymmetric Allylboration of Aldehydes. *Russ Chem Bull* **2000**, *49* (5), 912–919.

(72) Xie, F.; Deng, X.; Kratzer, D.; Cheng, K. C. K.; Friedmann, C.; Qi, S.; Solorio, L.; Lahann, J. Backbone-Degradable Polymers Prepared by Chemical Vapor Deposition. *Angew. Chem. Int. Ed.* **2017**, *56* (1), 203–207.

(73) Cram, D. J.; Cram, J. M. Cyclophane Chemistry: Bent and Battered Benzene Rings. *Acc. Chem. Res.* **1971**, *4* (6), 204–213.

(74) Dodziuk, H.; Szymański, S.; Jaźwiński, J.; Ostrowski, M.; Demissie, T. B.; Ruud, K.; Kuś, P.; Hopf, H.; Lin, S.-T. Structure and NMR Spectra of Some [2.2]Paracyclophanes. The Dilemma of [2.2]Paracyclophane Symmetry. *J. Phys. Chem. A* **2011**, *115* (38), 10638–10649.

(75) Dyson, P. J.; Humphrey, D. G.; McGrady, J. E.; Mingos, D. M. P.; Wilson, D. J. Comparison of the Reactivity of [2.2]Paracyclophane and *p*-Xylene. *Dalton Trans*. **1995**, No. 24, 4039–4043.

(76) Wolf, H.; Leusser, D.; Jørgensen, M. R. V.; Herbst-Irmer, R.; Chen, Y.-S.; Scheidt, E.-W.; Scherer, W.; Iversen, B. B.; Stalke, D. Phase Transition of [2,2]-Paracyclophane – An End to an Apparently Endless Story. *Chem. Eur. J.* **2014**, *20* (23), 7048–7053.

(77) Hassan, Z.; Spuling, E.; Knoll, D. M.; Lahann, J.; Bräse, S. Planar Chiral [2.2]Paracyclophanes: From Synthetic Curiosity to Applications in Asymmetric Synthesis and Materials. *Chem. Soc. Rev.* **2018**, *47* (18), 6947–6963.

(78) König, B.; Knieriem, B.; Rauch, K.; Meijere, A. D. 4,5,12,13-Tetrabromo[2.2]Paracyclophane – A New Bis(Aryne) Equivalent. *Chem. Ber.* **1993**, *126* (11), 2531–2534.

(79) Morisaki, Y.; Gon, M.; Sasamori, T.; Tokitoh, N.; Chujo, Y. Planar Chiral Tetrasubstituted [2.2]Paracyclophane: Optical Resolution and Functionalization. *J. Am. Chem. Soc.* **2014**, *136* (9), 3350–3353.

(80) Rowlands, G. J. Planar Chiral Phosphines Derived from [2.2]Paracyclophane. *Isr. J. Chem* **2012**, *52* (1–2), 60–75.

(81) Dahmen, S.; Bräse, S. The Asymmetric Dialkylzinc Addition to Imines Catalyzed by [2.2]Paracyclophane-Based N,O-Ligands. *J. Am. Chem. Soc.* **2002**, *124* (21), 5940–5941.

(82) Masterson, D. S.; Shirley, C.; Glatzhofer, D. T. *N*-(4-[2.2]Paracyclophanyl)-2′-Hydroxyacetophenone Imine: An Effective Paracyclophane Schiff-Base Ligand for Use in Catalytic Asymmetric Cyclopropanation Reactions. *J. Mol. Catal. A Chem.* **2012**, *361–362*, 111–115.

(83) Pye, P. J.; Rossen, K.; Reamer, R. A.; Tsou, N. N.; Volante, R. P.; Reider, P. J. A New Planar Chiral Bisphosphine Ligand for Asymmetric Catalysis: Highly Enantioselective Hydrogenations Under Mild Conditions. *J. Am. Chem. Soc.* **1997**, *119* (26), 6207–6208.

(84) Griffith, J. A.; Withers, J. M.; Martin, D. J.; Rowlands, G. J.; Filichev, V. V. Ligand Assembly and Chirality Transfer Guided by DNA Modified with Enantiomerically Pure [2.2]Paracyclophanes. *RSC Adv.* **2013**, *3* (24), 9373–9380.

(85) Henderson, W. R.; Fagnani, D. E.; Grolms, J.; Abboud, K. A.; Castellano, R. K. Transannular Hydrogen Bonding in Planar-Chiral [2.2]Paracyclophane-Bisamides. *Helv. Chim. Acta* **2019**, *102* (4), e1900047.

(86) Morisaki, Y.; Hifumi, R.; Lin, L.; Inoshita, K.; Chujo, Y. Through-Space Conjugated Polymers Consisting of Planar Chiral Pseudo-Ortho-Linked [2.2]Paracyclophane. *Polym. Chem.* **2012**, *3* (10), 2727–2730.

(87) Jagtap, S. P.; Collard, D. M. 2D Multilayered π-Stacked Conjugated Polymers Based on a U-Turn Pseudo-Geminal [2.2]Paracyclophane Scaffold. *Polym. Chem.* **2012**, *3* (2), 463–471.

(88) Ma, X.; Zhang, Y.; Zhang, Y.; Peng, C.; Che, Y.; Zhao, J. Stepwise Formation of Photoconductive Nanotubes through a New Top-down Method. *Adv. Mater.* **2015**, *27* (47), 7746–7751.

(89) Kazemi, F.; Massah, A. R.; Javaherian, M. Chemoselective and Scalable Preparation of Alkyl Tosylates under Solvent-Free Conditions. *Tetrahedron* **2007**, *63* (23), 5083–5087.

(90) He, G.-X.; Yuan, J.-M.; Zhu, H.-M.; Wei, K.; Wang, L.-Y.; Kong, S.-L.; Mo, D.-L.; Pan, C.-X.; Su, G.-F. Synthesis and Antitumor Evaluation of 2,3-Diarylbenzofuran Derivatives on HeLa Cells. *Bioorg. Med. Chem. Lett.* **2017**, *27* (8), 1660–1664.

(91) Kunieda, K.; Yamauchi, H.; Kawaguchi, M.; Ieda, N.; Nakagawa, H. Development of a Fluorescent Probe for Detection of Citrulline Based on Photo-Induced Electron Transfer. *Bioorg. Med. Chem. Lett.* **2018**, *28* (5), 969–973.

(92) Fantini, M.; Rivara, M.; Zuliani, V.; Kalmar, C. L.; Vacondio, F.; Silva, C.; Baheti, A. R.; Singh, N.; Merrick, E. C.; Katari, R. S.; Cocconcelli, G.; Ghiron, C.; Patel, M. K. 2,4(5)-Diarylimidazoles as Inhibitors of $HNa_v1.2$ Sodium Channels: Pharmacological Evaluation and Structure–Property Relationships. *Bioorg. Med. Chem.* **2009**, *17* (10), 3642–3648.

(93) Jahani, F.; Tajbakhsh, M.; Khaksar, S.; Azizi, M. R. An Efficient and Highly Chemoselective N-Boc Protection of Amines, Amino Acids, and Peptides under Heterogeneous Conditions. *Monatsh. Chem.* **2011**, *142* (10), 1035.

(94) Alfei, S.; Castellaro, S. *N,N,N*-Tris(Tert-Butoxycarbonyl)-l-Arginine: Five Isoforms Whose Obtainment Depends on Procedure and Scrupulous NMR Confirmation of Their Structures. *Res. Chem. Intermed.* **2018**, *44* (3), 1811–1832.

(95) Dračínský, M.; Jansa, P.; Bouř, P. Computational and Experimental Evidence of Through-Space NMR Spectroscopic *J* Coupling of Hydrogen Atoms. *Chem. Eur. J.* **2012**, *18* (3), 981–986.

(96) Lahann, J.; Höcker, H.; Langer, R. Synthesis of Amino[2.2]Paracyclophanes—Beneficial Monomers for Bioactive Coating of Medical Implant Materials. *Angew. Chem. Int. Ed.* **2001**, *40* (4), 726–728.

(97) Rahimi Razin, S. Synthesis of Functionalized [2.2]Paracyclophane Precursors for Functional Poly(Para-Xylylene) Thin Film Deposition. Thesis, 2015.

(98) Rieche, A.; Gross, H.; Höft, E. Über α-Halogenäther, IV. Synthesen aromatischer Aldehyde mit Dichlormethyl-alkyläthern. *Ber. Dtsch. Chem. Ges.* **1960**, *93* (1), 88–94.

(99) Das, T.; Häring, M.; Haldar, D.; Díaz, D. D. Phenylalanine and Derivatives as Versatile Low-Molecular-Weight Gelators: Design, Structure and Tailored Function. *Biomater. Sci.* **2017**, *6* (1), 38–59.

(100) Kodama, K.; Kawamata, R.; Hirose, T. Synthesis and Evaluation of Chiral β-Amino Acid-Based Low-Molecular-Weight Organogelators Possessing a Methyl/Trifluoromethyl Side Chain. *New J. Chem.* **2019**, *43* (7), 2882–2887.

(101) Leonie Etheridge. The Synthesis and Chemistry of [2.2]Paracyclophane Amino Acid Derivatives, Massey University, New Zealand, 2020.

(102) Moorthy, J. N.; Mandal, S.; Kumar, A. Photochromism of Novel Chromenes Constrained to Be Part of [2.2]Paracyclophane: Remarkable 'Phane' Effects on the Colored o-Quinonoid Intermediates. *New J. Chem.* **2012**, *37* (1), 82–88.

(103) Kreis, M.; Friedmann, C. J.; Bräse, S. Diastereoselective Hartwig–Buchwald Reaction of Chiral Amines with Rac-[2.2]Paracyclophane Derivatives. *Chem. Eur. J.* **2005**, *11* (24), 7387–7394.

(104) Hodgson, A. Enatioselective Nucleophillic Catalysis with [2.2]Paracyclophane-Based Heterocycles. Ph.D., University of Sussex, 2008.

(105) Shieh, C.-F.; McNally, D.; Boyd, R. H. The Heats of Combustion and Strain Energies of Some Cyclophanes. *Tetrahedron* **1969**, *25* (17), 3653–3665.

(106) Sharma, B.; Tazoe, K.; Feng, X.; Matsumoto, T.; Tanaka, J.; Yamato, T. Synthesis and Photoreaction of Polymethyl Substituted [2.2]Metaparacyclophanes. *J. Mol. Struct.* **2013**, *1037*, 271–275.

(107) Shimizu, T.; Hita, K.; Paudel, A.; Tanaka, J.; Yamato, T. Synthesis of Polymethyl Substituted [2.2]Metaparacyclophanes and Their Lewis-Acid Induced Isomerisation to [2.2]Metacyclophanes. *J. Chem. Res.* **2009**, *2009* (4), 244–247.

(108) Yamato, T.; Tokuhisa, K.; Tsuzuki, H. Medium-Sized Cyclophanes. Part 51. Acylation of [2.2]Metaparacyclophanes: Through-Space Electronic Interactions between Two Benzene Rings. *Can. J. Chem.* **2011**.

(109) Yamato, T.; Matsumoto, J.; Tokuhisa, K.; Tsuji, K.; Suehiro, K.; Tashiro, M. Medium-Sized Cyclophanes. Part 18. 5-Tert-Butyl-8-Substituted [2.2]Metaparacyclophanes: Preparation, X-Ray Diffraction Studies, and Their Treatment with Lewis Acids in Benzene. *J. Chem. Soc. Perkin Trans. 1* **1992**, No. 20, 2675–2682.

(110) Mitchell, R. H.; Otsubo, T.; Boekelheide, V. The Wittig Rearrangement of Some Thiacyclophanes. *Tetrahedron Lett.* **1975**, *16* (3), 219–222.

(111) Dawber, J. G.; Wyatt, P. a. H. The Hammett Acidity Function in Aqueous Nitric Acid. *J. Chem. Soc.* **1960**, No. 0, 3589–3593.

(112) Cram, D. J.; Helgeson, R. C.; Lock, D.; Singer, L. A. [2.2]Metaparacyclophane, a Highly Strained Ring System. *J. Am. Chem. Soc.* **1966**, *88* (6), 1324–1325.

(113) Gray, M. J.; Hartshorn, M. P.; Vaughan, J.; Wright, G. J. Some Rearrangements of 2,3,5,6-Tetrachloro-4-Methyl-4-Nitrocyclohexa-2,5-Dienone and 3,5-Dibromo-2,4,6-Trimethyl-4-Nitrocyclohexa-2,5-Dienone. *Aust. J. Chem.* **1984**, *37* (10), 2027–2036.

(114) Shestak, O. P.; Novikov, V. L.; Ivanova, E. P.; Gorshkova, N. M. Synthesis and Antimicrobial Activity of [3,5-Dibromo(Dichloro)-1-Hydroxy-4-Oxocyclohexa-2,5-Dien-1-Yl]Acetic Acids and Their Derivatives. *Pharm. Chem. J.* **2001**, *35* (7), 366–369.

(115) Sheldrick, G. M. Crystal Structure Refinement with SHELXL. *Acta Crystallogr.* **2015**, *71* (1), 3–8.

(116) Sheldrick, G. M. Acta Crystallogr., Sect. B. 2008, 64, 112

(117) Dolomanov, O. V.; Bourhis, L. J.; Gildea, R. J.; Howard, J. a. K.; Puschmann, H. OLEX2: A Complete Structure Solution, Refinement and Analysis Program. *J. Appl. Cryst.* **2009**, *42* (2), 339–341.

Chapter 6

# Appendix

$^{1}$H NMR spectrum of **68** in $CDCl_3$

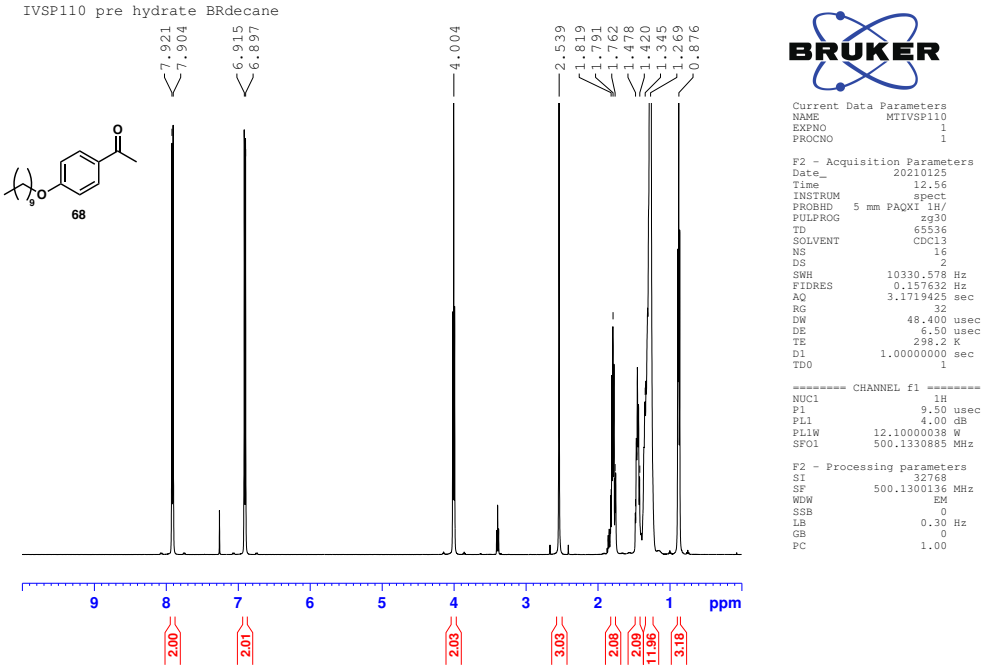


$^{13}$C NMR spectrum of **68** in $CDCl_3$

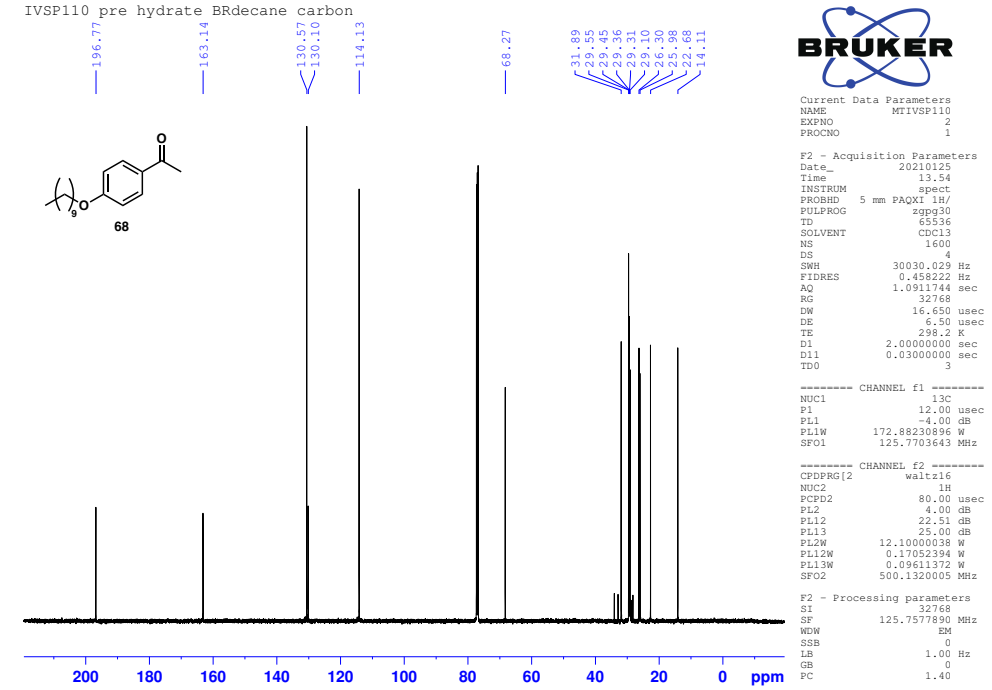

[1]H NMR spectrum of **53** (in equilibrium with **69**) in DMSO-$d_6$

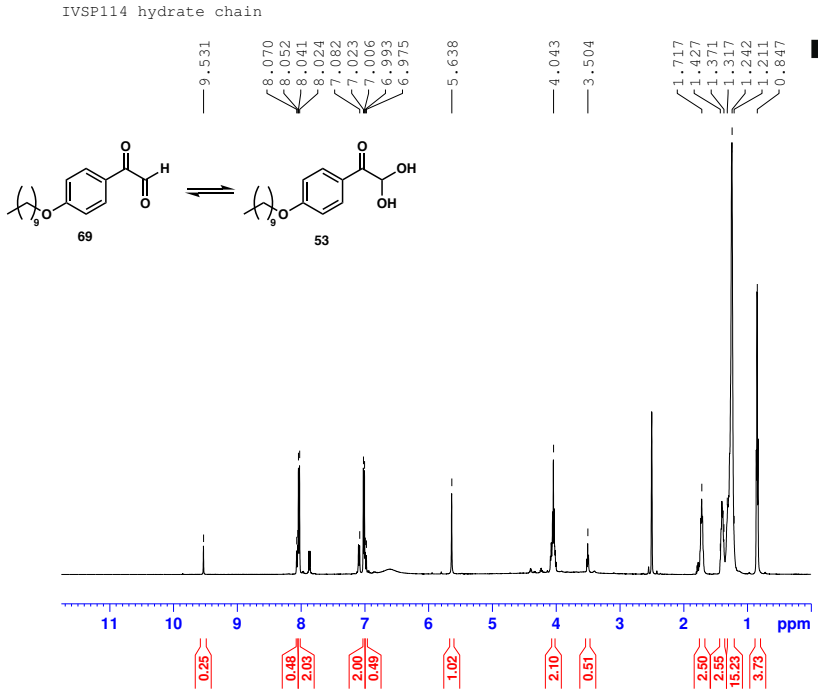


```
Current Data Parameters
NAME            0IVSP114
EXPNO                  1
PROCNO                 1

F2 - Acquisition Parameters
Date_           20210130
Time               11.37
INSTRUM            spect
PROBHD  5 mm PAQXI 1H/
PULPROG            zg30
TD                65536
SOLVENT            DMSO
NS                   16
DS                    2
SWH           10330.578 Hz
FIDRES        0.157632 Hz
AQ            3.1719425 sec
RG                 40.3
DW               48.400 usec
DE                6.50 usec
TE                298.0 K
D1           1.00000000 sec
TD0                    1

======== CHANNEL f1 ========
NUC1                  1H
P1                  9.50 usec
PL1                 4.00 dB
PL1W         12.10000038 W
SFO1        500.1330885 MHz

F2 - Processing parameters
SI                 32768
SF          500.1300053 MHz
WDW                   EM
SSB                    0
LB                  0.30 Hz
GB                     0
PC                  1.00
```

[13]C NMR spectrum of **53** (in equilibrium with **69**) in DMSO-$d_6$

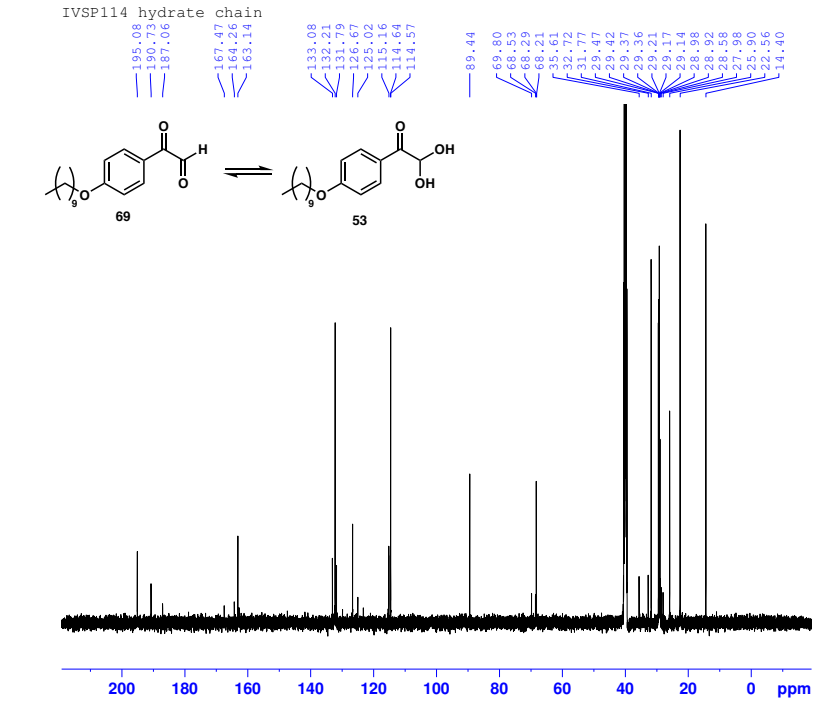


```
Current Data Parameters
NAME          MTIVSP114
EXPNO                 2
PROCNO                1

F2 - Acquisition Parameters
Date_           20210130
Time               12.33
INSTRUM            spect
PROBHD  5 mm PAQXI 1H/
PULPROG         zgpg30
TD                65536
SOLVENT            DMSO
NS                 1128
DS                    4
SWH           30030.029 Hz
FIDRES        0.458222 Hz
AQ            1.0911744 sec
RG                32768
DW               16.650 usec
DE                6.50 usec
TE                298.0 K
D1           2.00000000 sec
D11          0.03000000 sec
TD0                    4

======== CHANNEL f1 ========
NUC1                 13C
P1                 12.00 usec
PL1                -4.00 dB
PL1W        172.88230896 W
SFO1        125.7703643 MHz

======== CHANNEL f2 ========
CPDPRG[2         waltz16
NUC2                 1H
PCPD2              80.00 usec
PL2                 4.00 dB
PL12               22.51 dB
PL13               25.00 dB
PL2W         12.10000038 W
PL12W         0.17052394 W
PL13W         0.09611372 W
SFO2        500.1320005 MHz

F2 - Processing parameters
SI                 32768
SF          125.7577890 MHz
WDW                   EM
SSB                    0
LB                  1.00 Hz
GB                     0
PC                  1.40
```

$^{1}$H NMR spectrum of **70** in $CDCl_3$

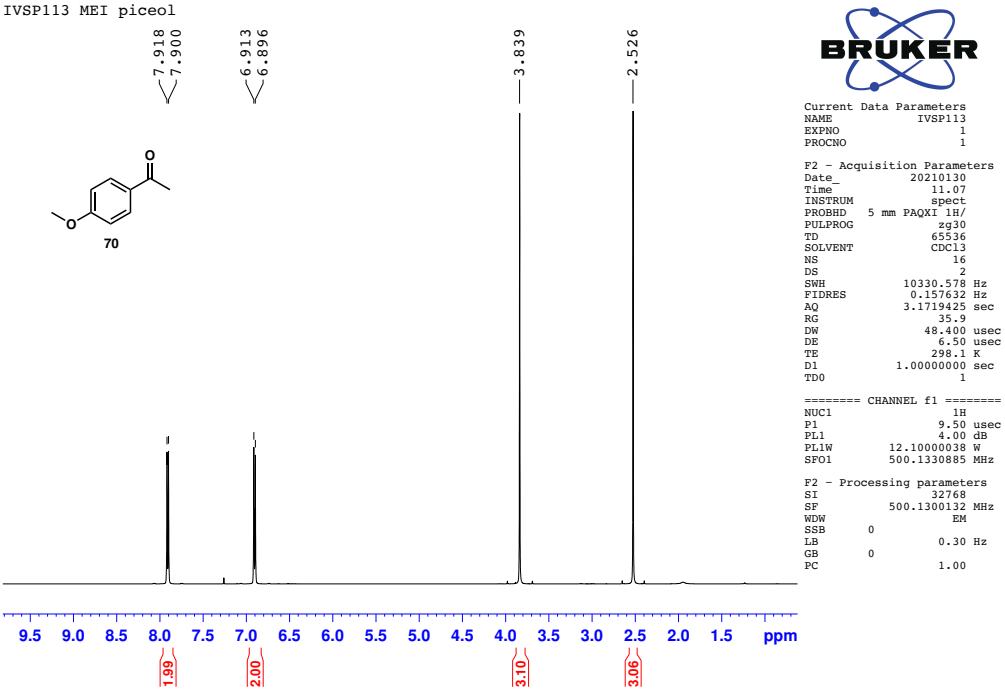


$^{13}$C NMR spectrum of **70** in $CDCl_3$

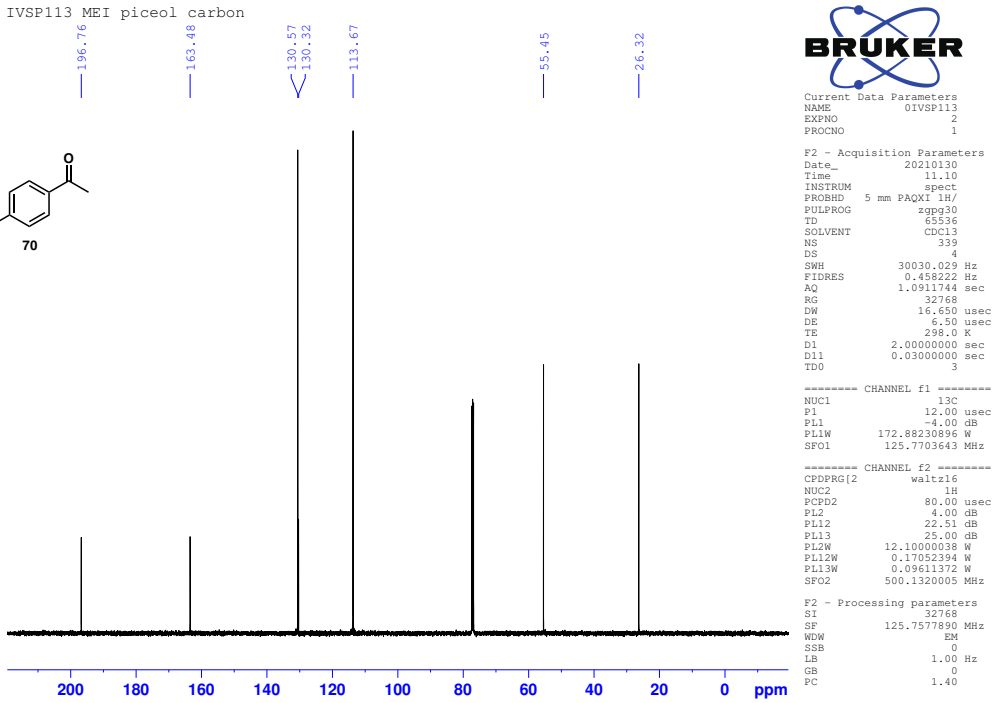

$^{1}$H NMR spectrum of **43** in DMSO-$d_6$

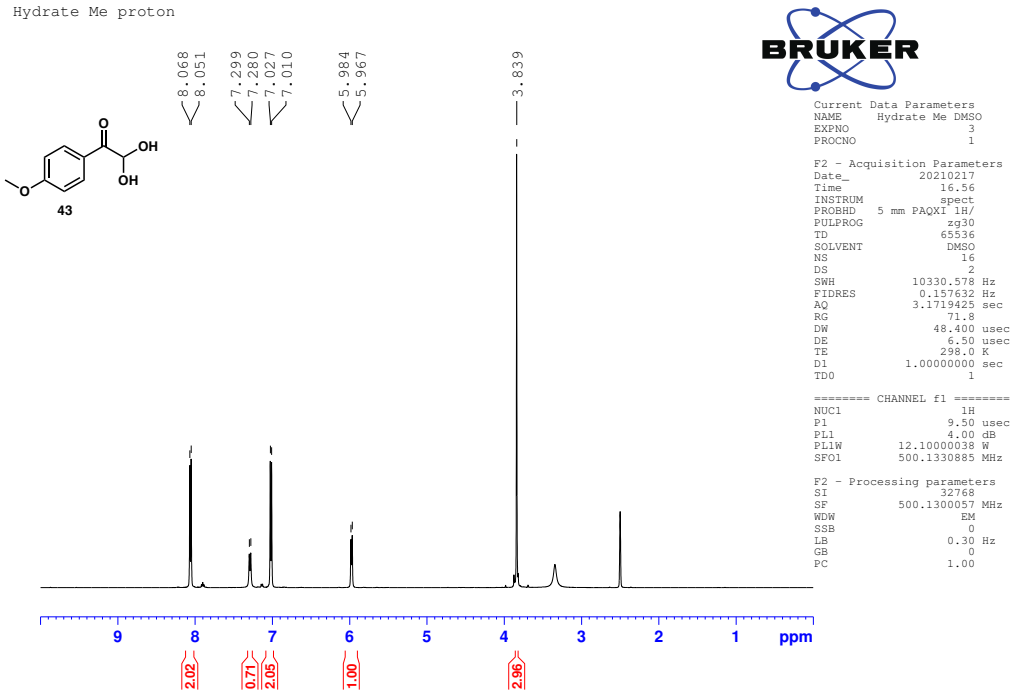


$^{13}$C NMR spectrum of **43** in DMSO-$d_6$

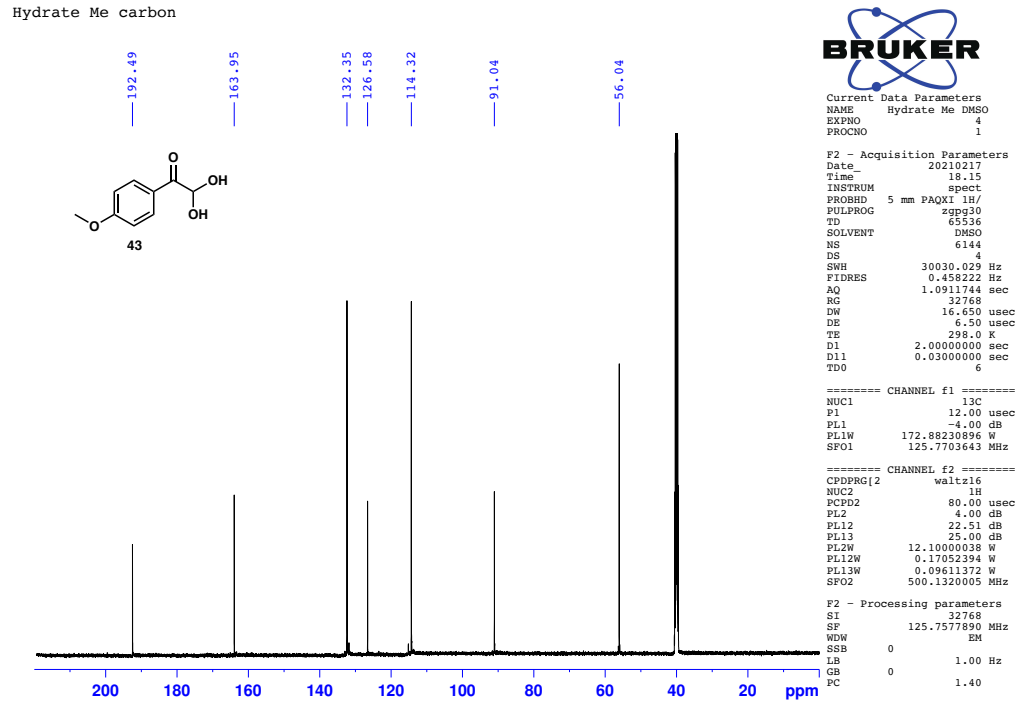

HMQC spectrum of **43** in DMSO-$d_6$

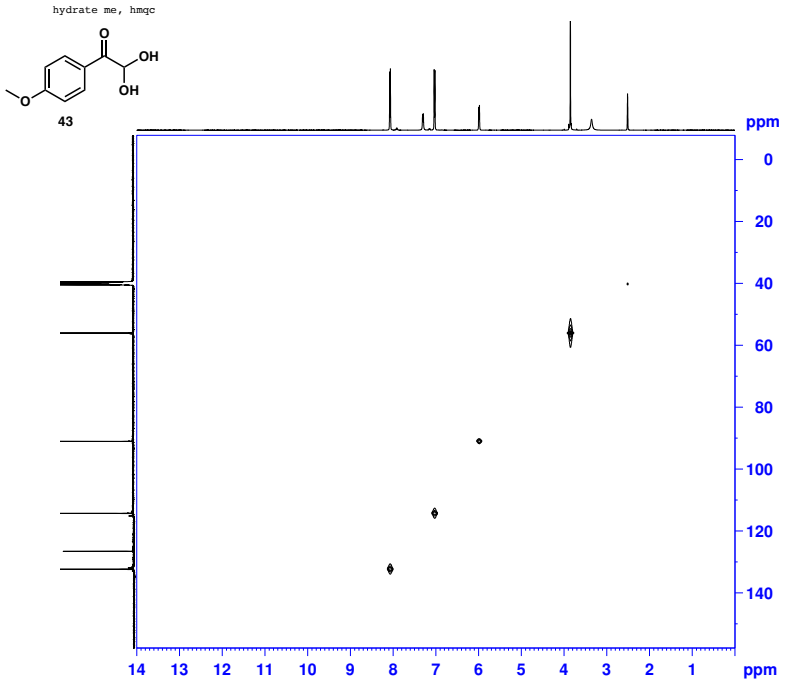



```
Current Data Parameters
NAME        Hydrate Me DMSO
EXPNO                    6
PROCNO                   1

F2 - Acquisition Parameters
Date_              20210218
Time                   0.42
INSTRUM               spect
PROBHD   5 mm PAQXI 1H/
PULPROG          hmqcgpqf
TD                     1024
SOLVENT                DMSO
NS                       32
DS                       16
SWH                7002.801 Hz
FIDRES             6.838673 Hz
AQ                 0.0731136 sec
RG                      4096
DW                   71.400 usec
DE                    6.50 usec
TE                   298.0 K
CNST2              145.0000000
D0                 0.00000300 sec
D1                 1.50000000 sec
D2                 0.00344828 sec
D12                0.00002000 sec
D13                0.00000400 sec
D16                0.00010000 sec
IN0                0.00002400 sec

======== CHANNEL f1 ========
NUC1                       1H
P1                       9.50 usec
P2                      19.00 usec
PL1                      4.00 dB
PLIW            12.10000038 W
SFO1           500.1335009 MHz

======== CHANNEL f2 ========
CPDPRG[2                 garp
NUC2                       13C
P3                      12.00 usec
PCPD2                   70.00 usec
PL2                     -4.00 dB
PL12                    11.32 dB
PLIW            172.88230896 W
PL12W             5.07867718 W
SFO2           125.7672198 MHz

====== GRADIENT CHANNEL =====
GPNAM[1]           SINE.100
GPNAM[2]           SINE.100
GPNAM[3]           SINE.100
GPZ1                  50.00 %
GPZ2                  30.00 %
GPZ3                  40.10 %
P16                 1000.00 usec

F1 - Acquisition parameters
TD                       256
SFO1           125.7672 MHz
FIDRES          81.374924 Hz
SW                165.639 ppm
FnMODE                   QF

F2 - Processing parameters
SI                      1024
SF             500.1300000 MHz
WDW                   QSINE
SSB          0
LB           0 Hz
GB           0
PC                      1.40

F1 - Processing parameters
SI                      1024
MC2                       QF
SF             125.7577890 MHz
WDW                   QSINE
SSB                       2
LB           0 Hz
GB           0
```

HMBC spectrum of **43** in DMSO-$d_6$

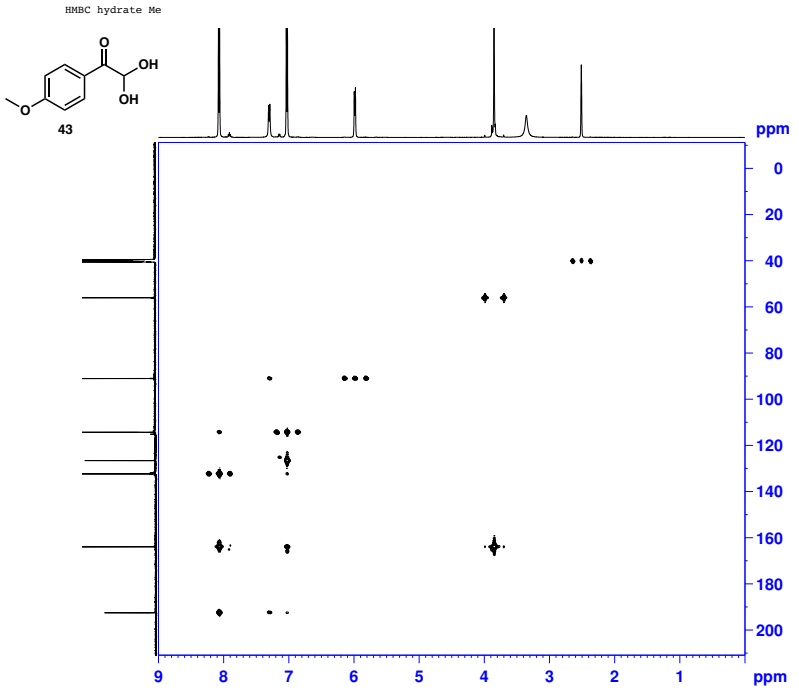



```
NAME        Hydrate Me DMSO
EXPNO                    7
PROCNO                   1

F2 - Acquisition Parameters
Date_              20210218
Time                   4.20
INSTRUM               spect
PROBHD   5 mm PAQXI 1H/
PULPROG        hmbcgpndqf
TD                     4096
SOLVENT                DMSO
NS                        8
DS                       16
SWH                7002.801 Hz
FIDRES             1.709668 Hz
AQ                 0.2924544 sec
RG                      4096
DW                   71.400 usec
DE                    6.50 usec
TE                   298.0 K
CNST13             8.0000000
D0                 0.00000300 sec
D1                 1.50000000 sec
D6                 0.06250000 sec
D16                0.00010000 sec
IN0                0.00001790 sec

======== CHANNEL f1 ========
NUC1                       1H
P1                       9.50 usec
P2                      19.00 usec
PL1                      4.00 dB
PLIW            12.10000038 W
SFO1           500.1335009 MHz

======== CHANNEL f2 ========
NUC2                       13C
P3                      12.00 usec
PL2                     -4.00 dB
PLIW            172.88230896 W
SFO2           125.7703443 MHz

====== GRADIENT CHANNEL =====
GPNAM[1]           SINE.100
GPNAM[2]           SINE.100
GPNAM[3]           SINE.100
GPZ1                  50.00 %
GPZ2                  30.00 %
GPZ3                  40.10 %
P16                 1000.00 usec

F1 - Acquisition parameters
TD                       256
SFO1           125.7703 MHz
FIDRES          109.113174 Hz
SW                222.095 ppm
FnMODE                   QF

F2 - Processing parameters
SI                      1024
SF             500.1300000 MHz
WDW                    SINE
SSB          0
LB           0 Hz
GB           0
PC                      1.40

F1 - Processing parameters
SI                      1024
MC2                       QF
SF             125.7577890 MHz
WDW                    SINE
SSB          0
LB           0 Hz
GB           0
```

$^{1}$H NMR spectrum of **77** in DMSO-$d_6$

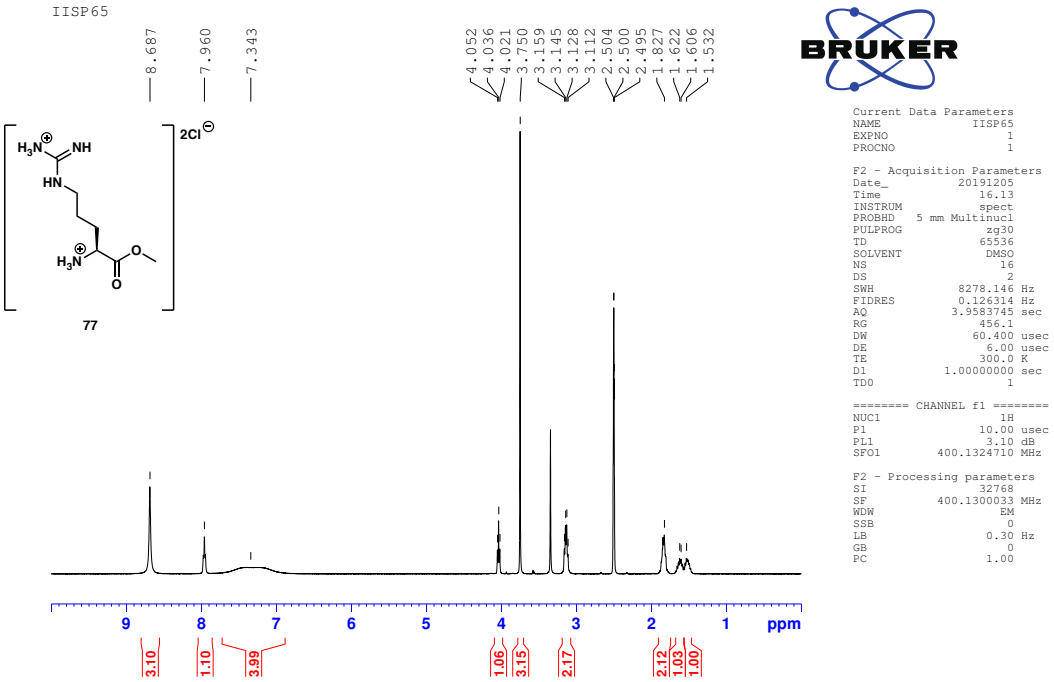


Current Data Parameters
NAME IISP65
EXPNO 1
PROCNO 1

F2 - Acquisition Parameters
Date_ 20191205
Time 16.13
INSTRUM spect
PROBHD 5 mm Multinucl
PULPROG zg30
TD 65536
SOLVENT DMSO
NS 16
DS 2
SWH 8278.146 Hz
FIDRES 0.126314 Hz
AQ 3.9583745 sec
RG 456.1
DW 60.400 usec
DE 6.00 usec
TE 300.0 K
D1 1.00000000 sec
TD0 1

======== CHANNEL f1 ========
NUC1 1H
P1 10.00 usec
PL1 3.10 dB
SFO1 400.1324710 MHz

F2 - Processing parameters
SI 32768
SF 400.1300033 MHz
WDW EM
SSB 0
LB 0.30 Hz
GB 0
PC 1.00

$^{13}$C NMR spectrum of **77** in DMSO-$d_6$

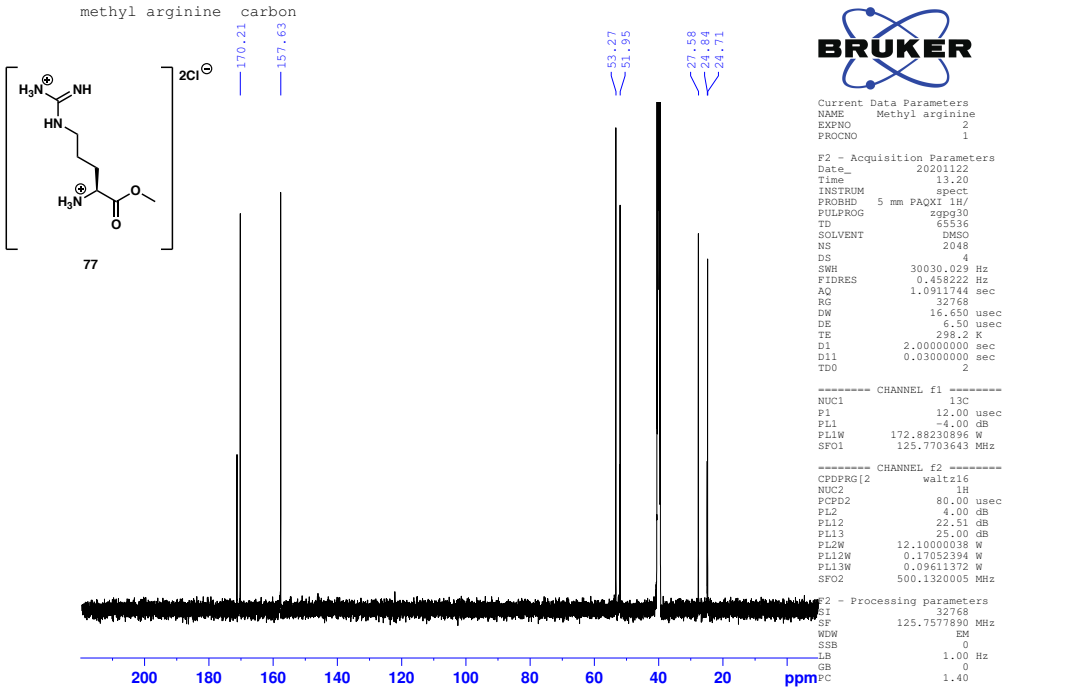


Current Data Parameters
NAME Methyl arginine
EXPNO 2
PROCNO 1

F2 - Acquisition Parameters
Date_ 20201122
Time 13.20
INSTRUM spect
PROBHD 5 mm PAQXI 1H/
PULPROG zgpg30
TD 65536
SOLVENT DMSO
NS 2048
DS 4
SWH 30030.029 Hz
FIDRES 0.458222 Hz
AQ 1.0911744 sec
RG 32768
DW 16.650 usec
DE 6.50 usec
TE 298.2 K
D1 2.00000000 sec
D11 0.03000000 sec
TD0 2

======== CHANNEL f1 ========
NUC1 13C
P1 12.00 usec
PL1 -4.00 dB
PL1W 172.88230896 W
SFO1 125.7703643 MHz

======== CHANNEL f2 ========
CPDPRG[2 waltz16
NUC2 1H
PCPD2 80.00 usec
PL2 4.00 dB
PL12 22.51 dB
PL13 25.00 dB
PL2W 12.10000038 W
PL12W 0.17052394 W
PL13W 0.09611372 W
SFO2 500.1320005 MHz

F2 - Processing parameters
SI 32768
SF 125.7577890 MHz
WDW EM
SSB 0
LB 1.00 Hz
GB 0
PC 1.40

$^{1}$H NMR spectrum of **55** in DMSO-$d_6$

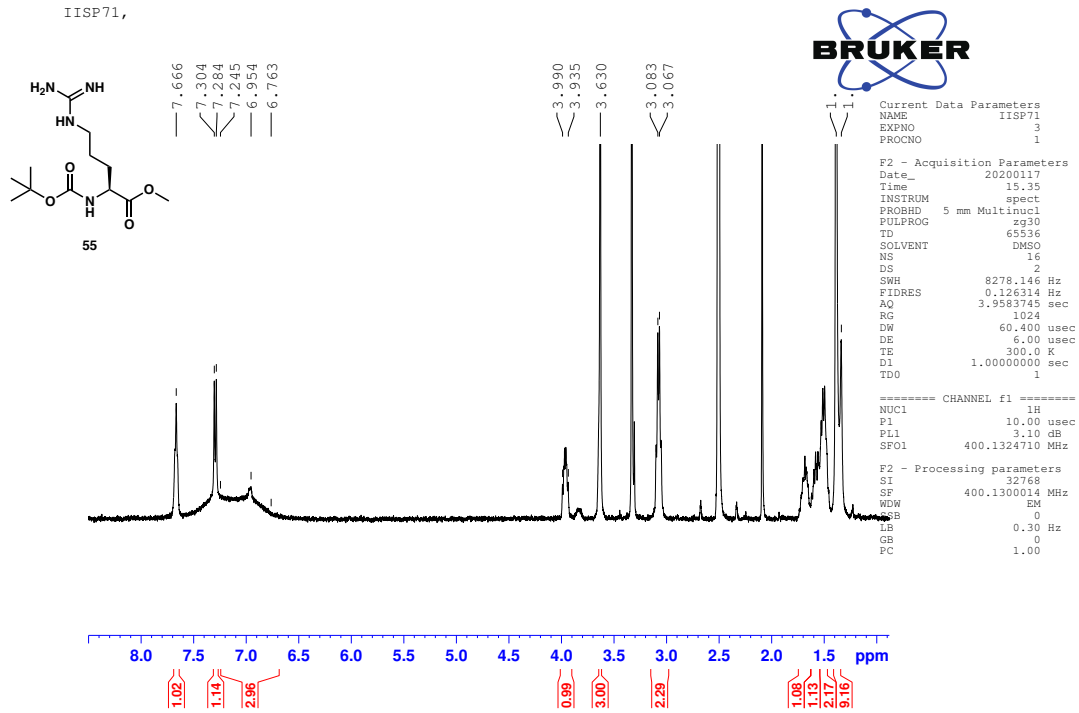


$^{13}$C NMR spectrum of **55** in DMSO-$d_6$

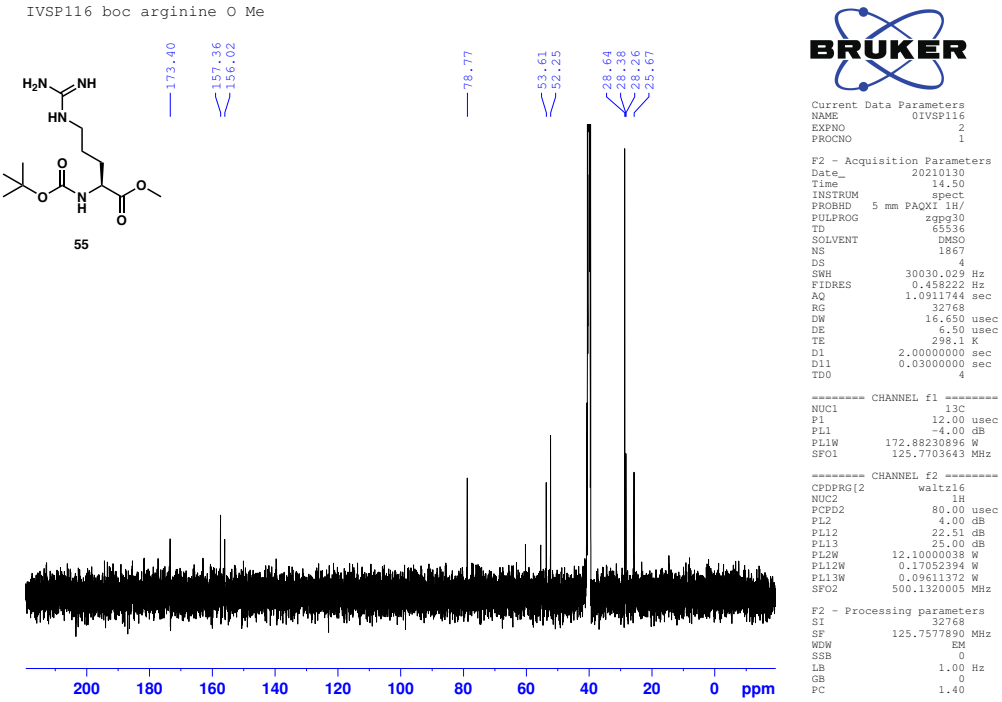

$^{1}$H NMR spectrum of (±)-**85** in $CDCl_3$

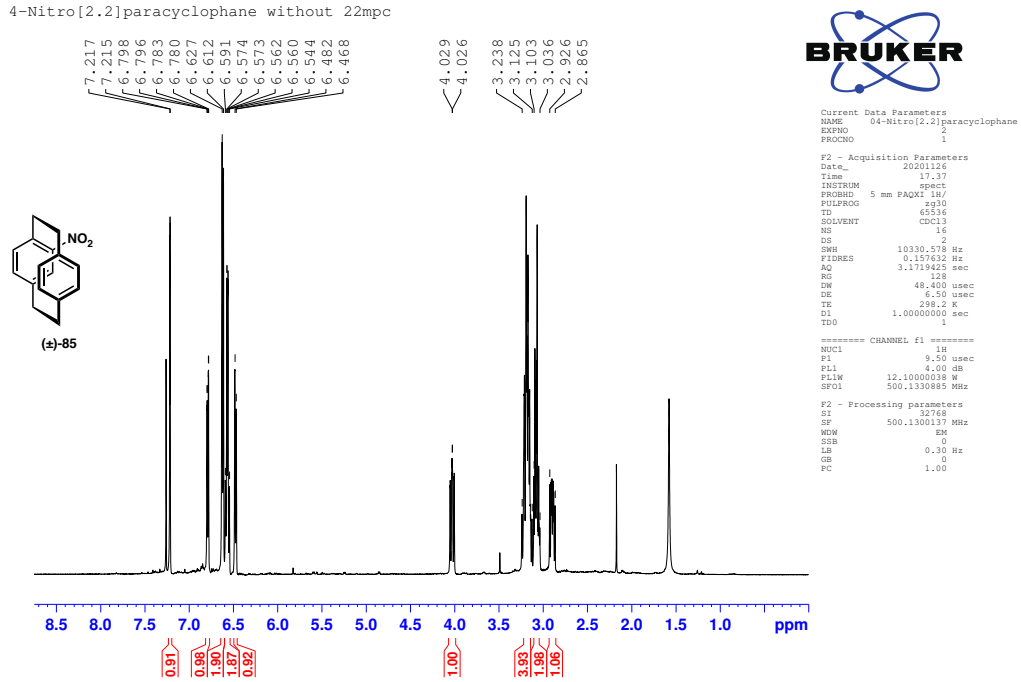


$^{13}$C NMR spectrum of (±)-**85** in $CDCl_3$

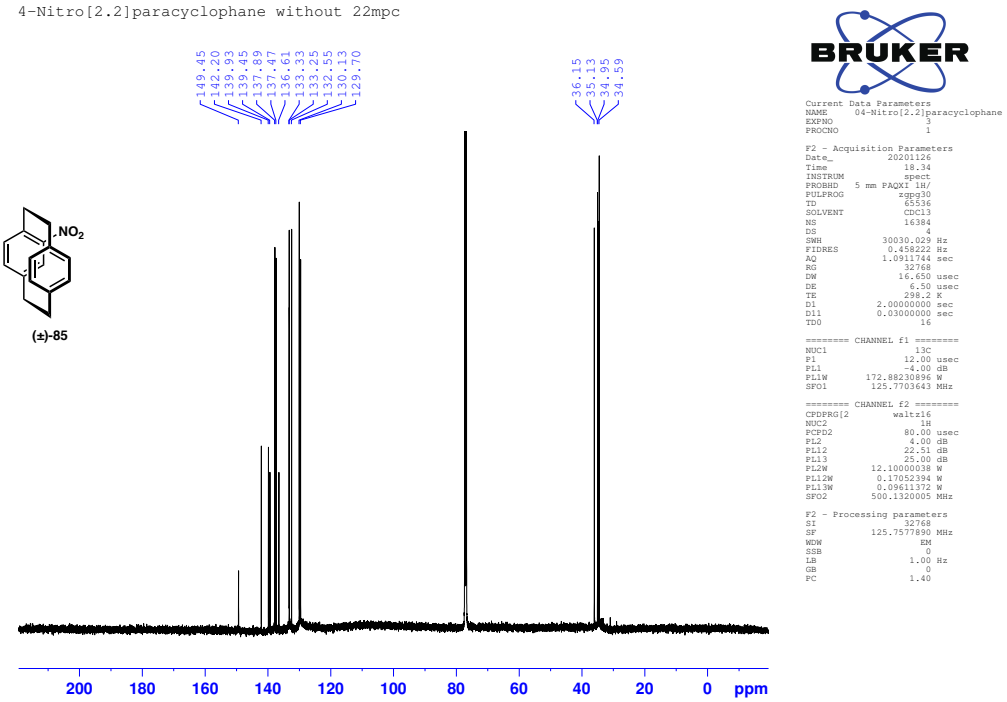

$^{1}$H NMR spectrum of (±)-**86** in $CDCl_3$

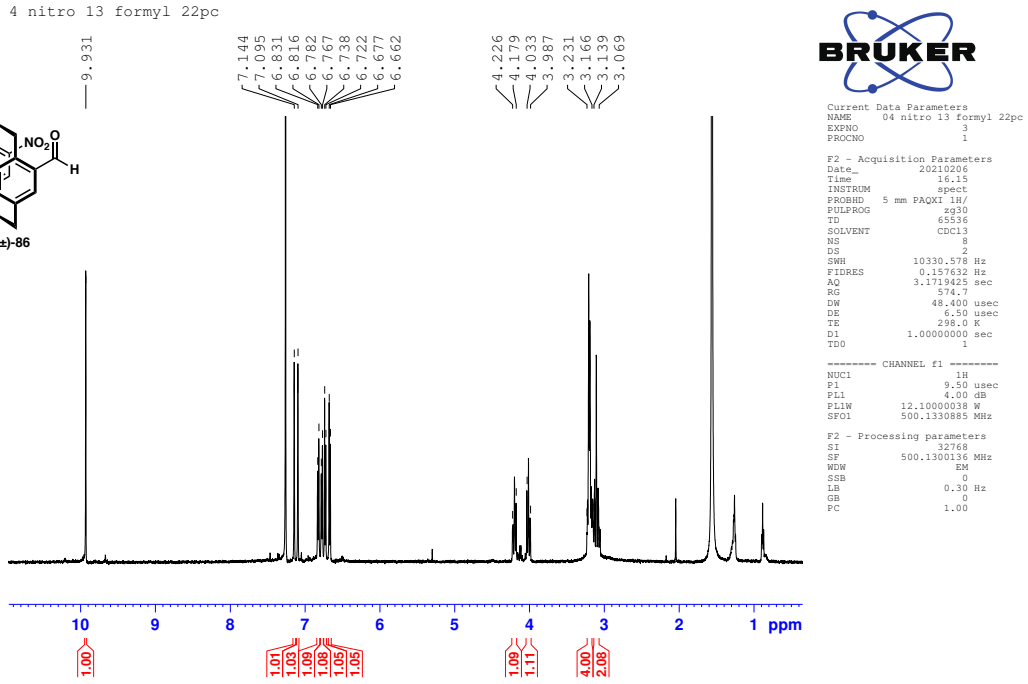


$^{13}$C NMR spectrum of (±)-**86** in $CDCl_3$

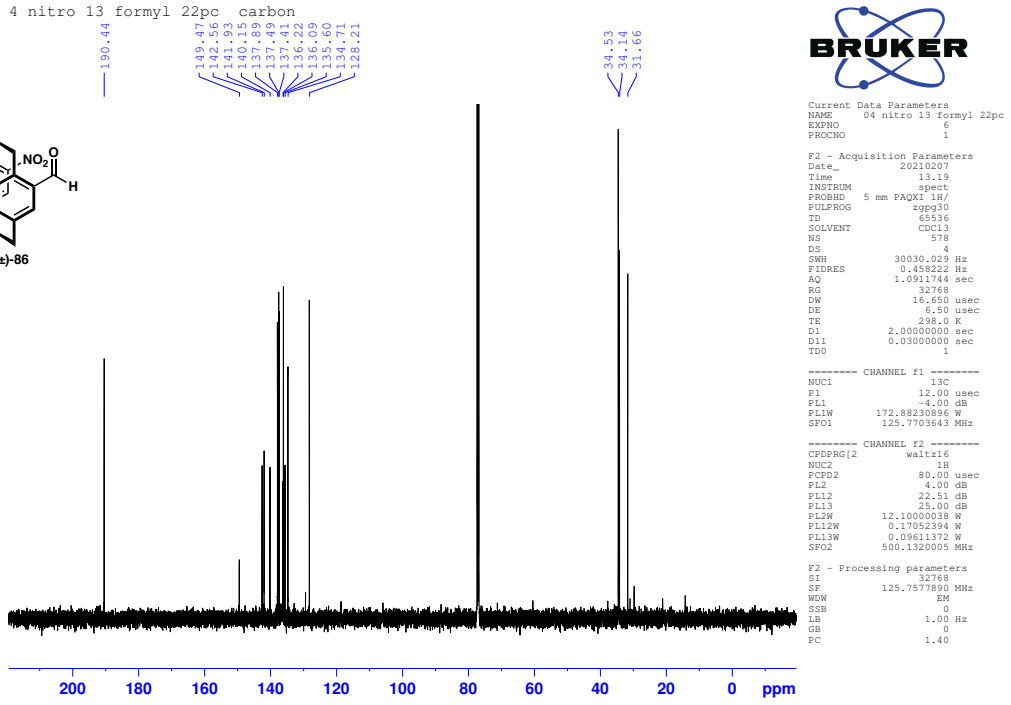

$^{1}$H NMR spectrum of (±)-**58** in DMSO-$d_6$

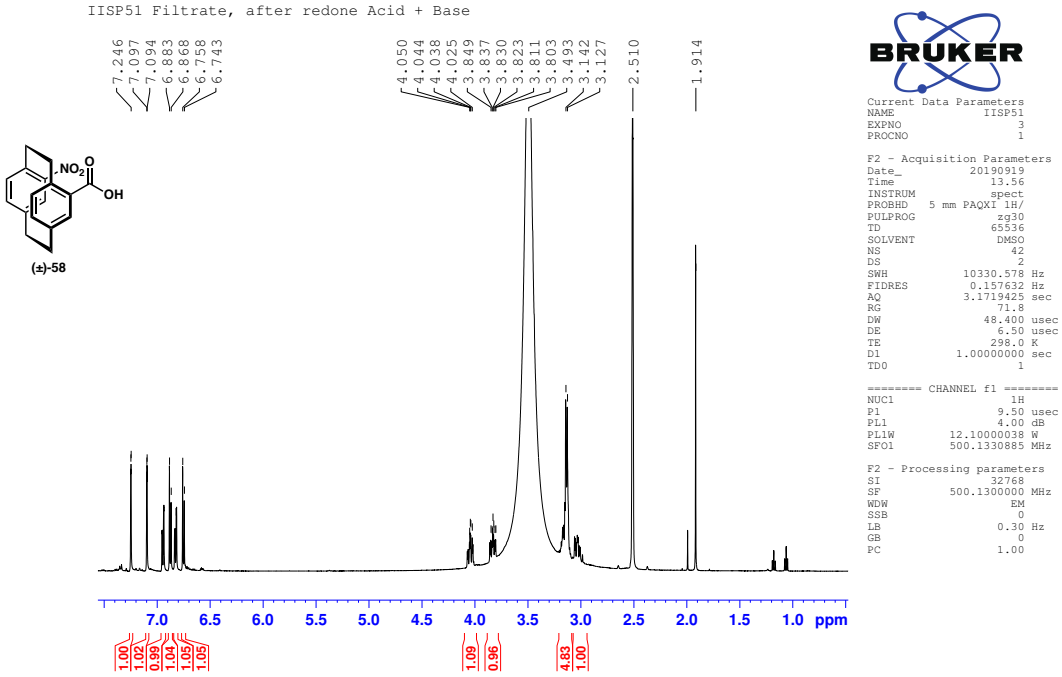

$^1$H NMR spectrum of **88a** in $CDCl_3$

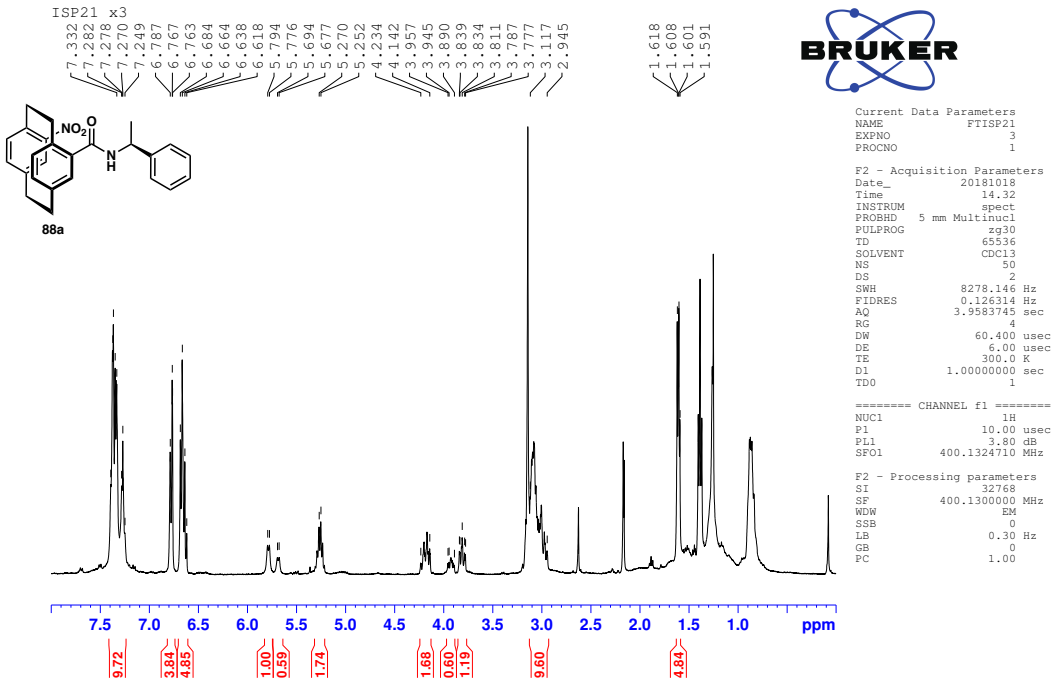


$^1$H NMR spectrum of **88b** in $CDCl_3$

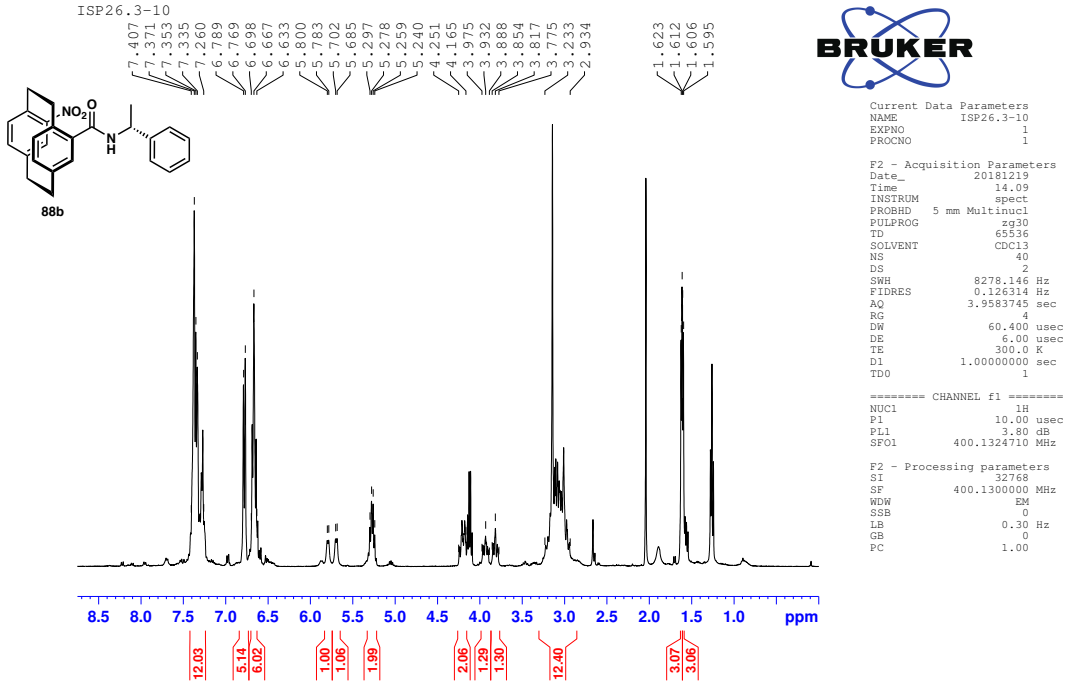

$^{1}$H NMR spectrum of **88c** in $CDCl_3$

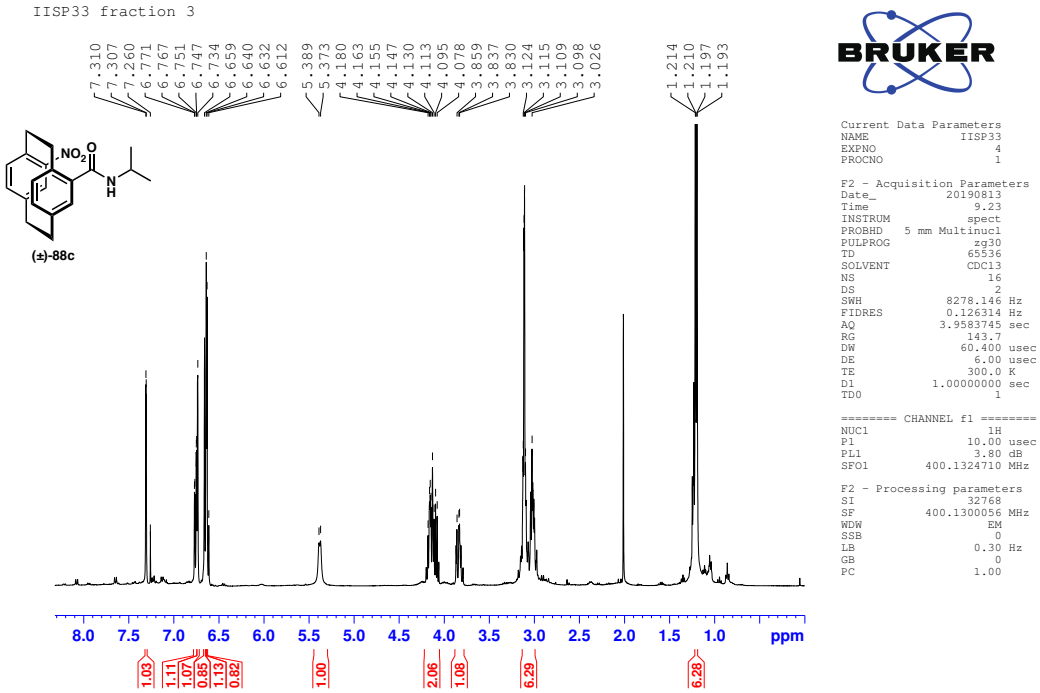


BRUKER

```
Current Data Parameters
NAME                 IISP33
EXPNO                     4
PROCNO                    1

F2 - Acquisition Parameters
Date_              20190813
Time                   9.23
INSTRUM               spect
PROBHD    5 mm Multinuc1
PULPROG               zg30
TD                   65536
SOLVENT              CDCl3
NS                      16
DS                       2
SWH               8278.146 Hz
FIDRES            0.126314 Hz
AQ                3.9583745 sec
RG                    143.7
DW                   60.400 usec
DE                    6.00 usec
TE                   300.0 K
D1              1.00000000 sec
TD0                       1

======== CHANNEL f1 ========
NUC1                    1H
P1                   10.00 usec
PL1                   3.80 dB
SFO1          400.1324710 MHz

F2 - Processing parameters
SI                    32768
SF            400.1300056 MHz
WDW                      EM
SSB                       0
LB                     0.30 Hz
GB                        0
PC                     1.00
```

$^1$H NMR spectrum of **89a** in $CDCl_3$

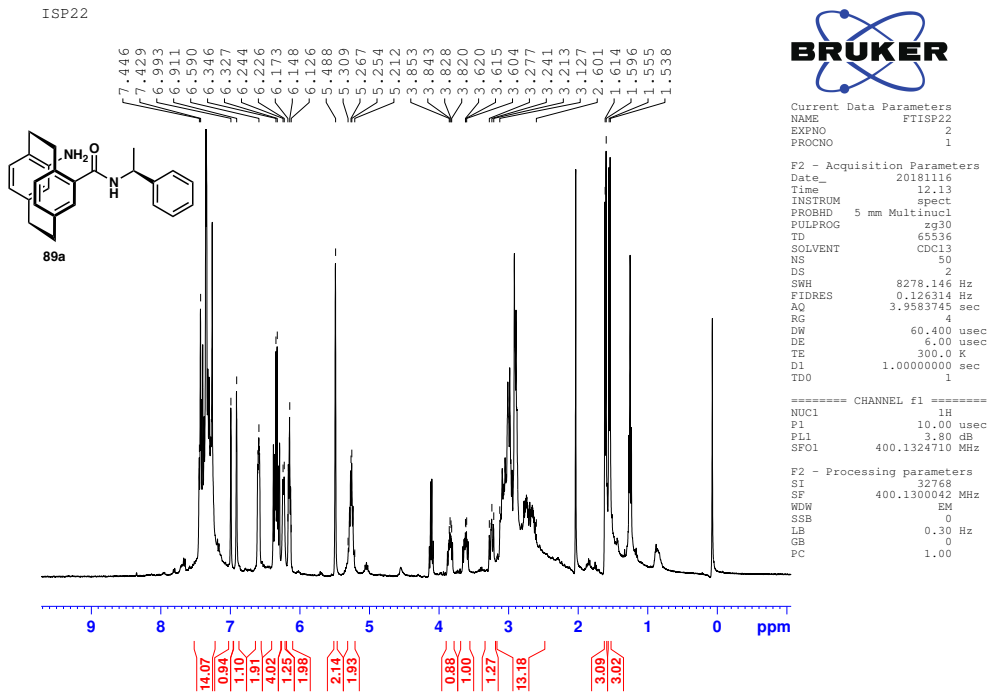


$^1$H NMR spectrum of **89b** in $CDCl_3$

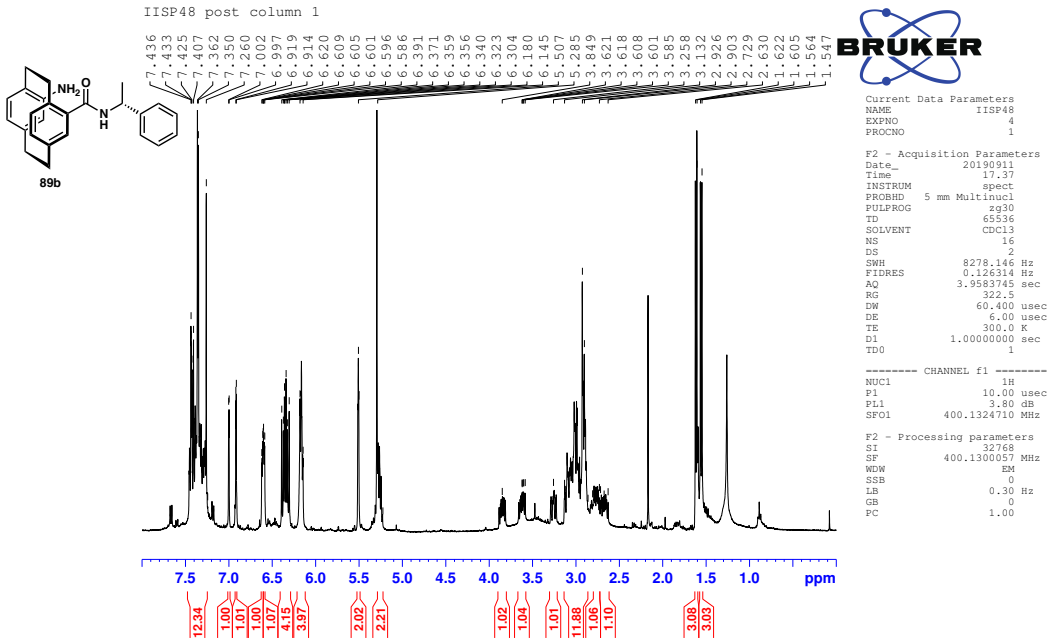

$^{1}$H NMR spectrum of (±)-**89c** in $CDCl_3$

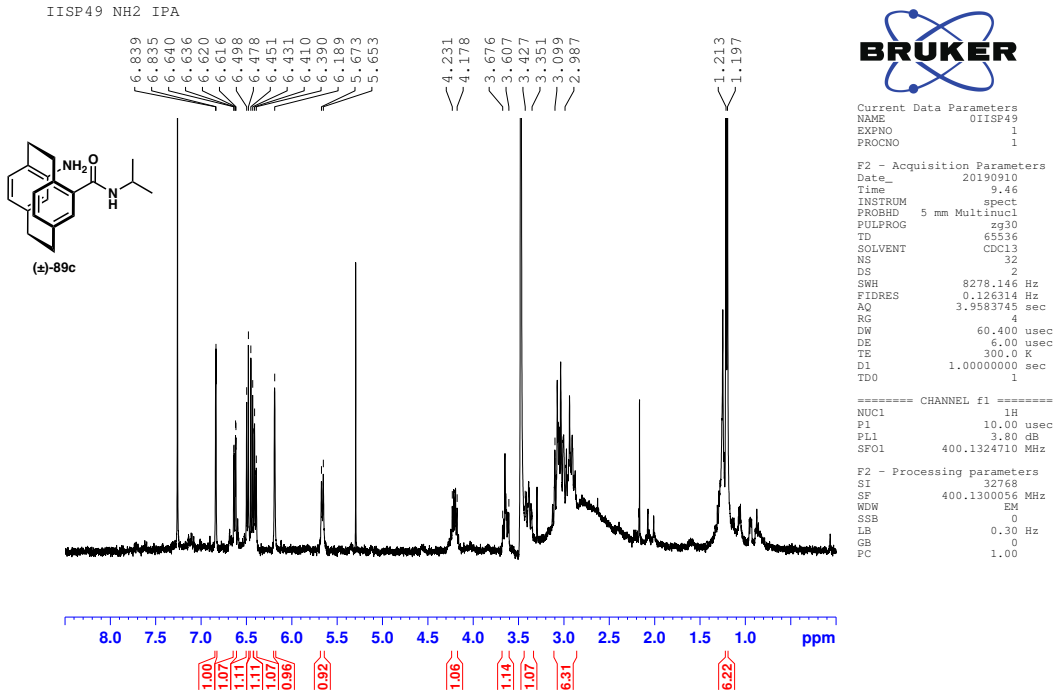



Current Data Parameters
NAME 0IISP49
EXPNO 1
PROCNO 1

F2 - Acquisition Parameters
Date_ 20190910
Time 9.46
INSTRUM spect
PROBHD 5 mm Multinucl
PULPROG zg30
TD 65536
SOLVENT CDCl3
NS 32
DS 2
SWH 8278.146 Hz
FIDRES 0.126314 Hz
AQ 3.9583745 sec
RG 4
DW 60.400 usec
DE 6.00 usec
TE 300.0 K
D1 1.00000000 sec
TD0 1

======== CHANNEL f1 ========
NUC1 1H
P1 10.00 usec
PL1 3.80 dB
SFO1 400.1324710 MHz

F2 - Processing parameters
SI 32768
SF 400.1300056 MHz
WDW EM
SSB 0
LB 0.30 Hz
GB 0
PC 1.00


$^{13}$C NMR spectrum of (±)-**89c** in $CDCl_3$

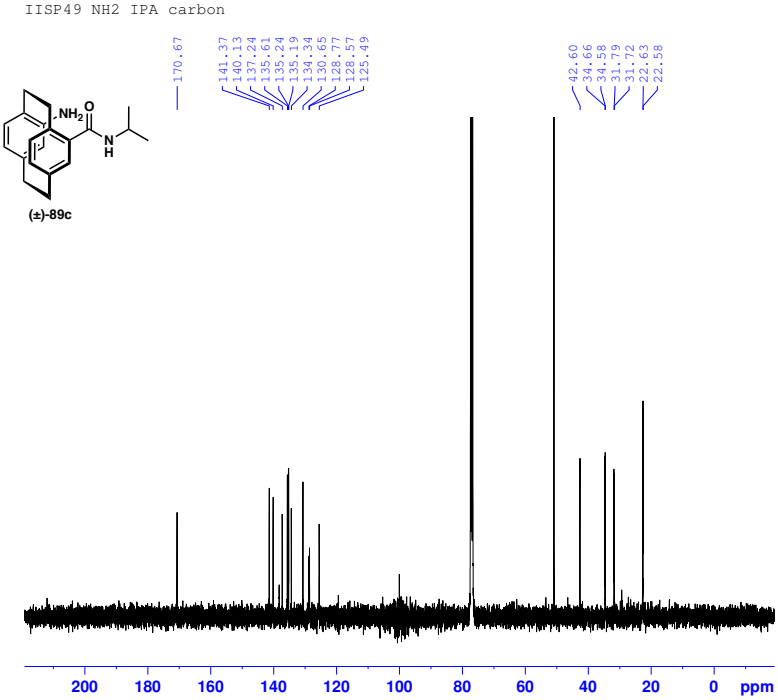



Current Data Parameters
NAME 0IISP49
EXPNO 2
PROCNO 1

F2 - Acquisition Parameters
Date_ 20190910
Time 18.06
INSTRUM spect
PROBHD 5 mm Multinucl
PULPROG zgpg30
TD 65536
SOLVENT CDCl3
NS 16384
DS 4
SWH 23980.814 Hz
FIDRES 0.365918 Hz
AQ 1.3664256 sec
RG 32768
DW 20.850 usec
DE 6.00 usec
TE 300.0 K
D1 2.00000000 sec
d11 0.03000000 sec
DELTA 1.89999998 sec
TD0 16

======== CHANNEL f1 ========
NUC1 13C
P1 20.00 usec
PL1 -6.00 dB
SFO1 100.6228298 MHz

======== CHANNEL f2 ========
CPDPRG[2 waltz16
NUC2 1H
PCPD2 80.00 usec
PL2 4.00 dB
PL12 20.50 dB
PL13 25.00 dB
SFO2 400.1316005 MHz

F2 - Processing parameters
SI 32768
SF 100.6127690 MHz
WDW EM
SSB 0
LB 1.00 Hz
GB 0
PC 1.40

$^{1}$H NMR spectrum of (±)-**90c** in $CDCl_3$

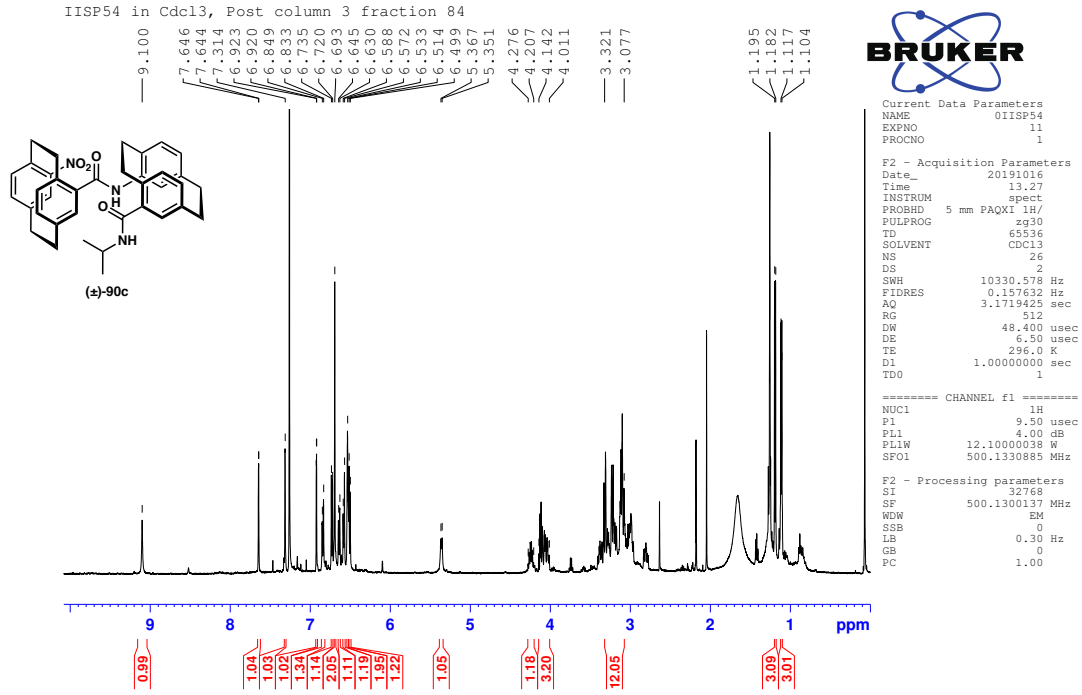

$^{1}$H NMR spectrum of (±)-**95** in $CDCl_3$

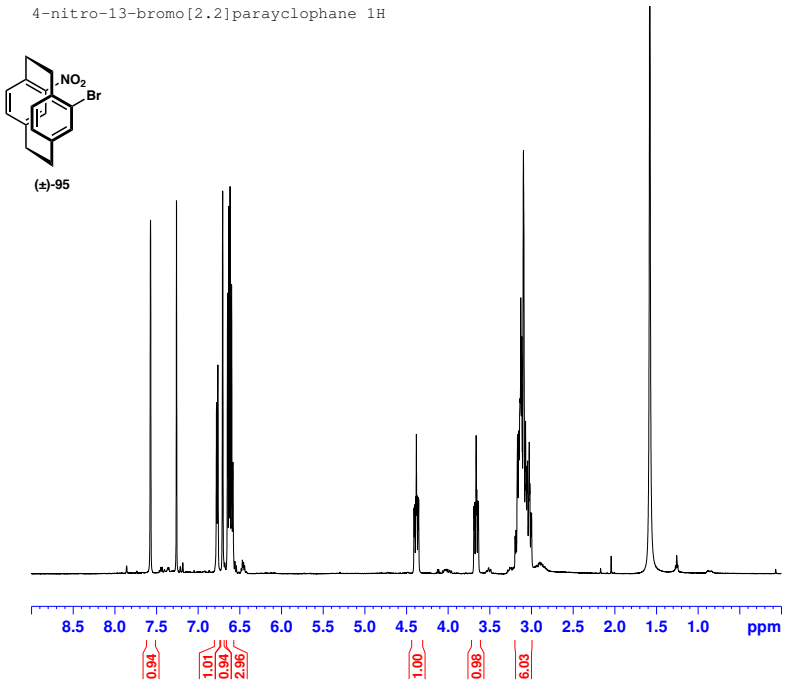


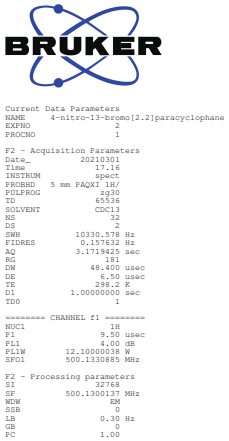


$^{13}$C NMR spectrum of (±)-**95** in $CDCl_3$

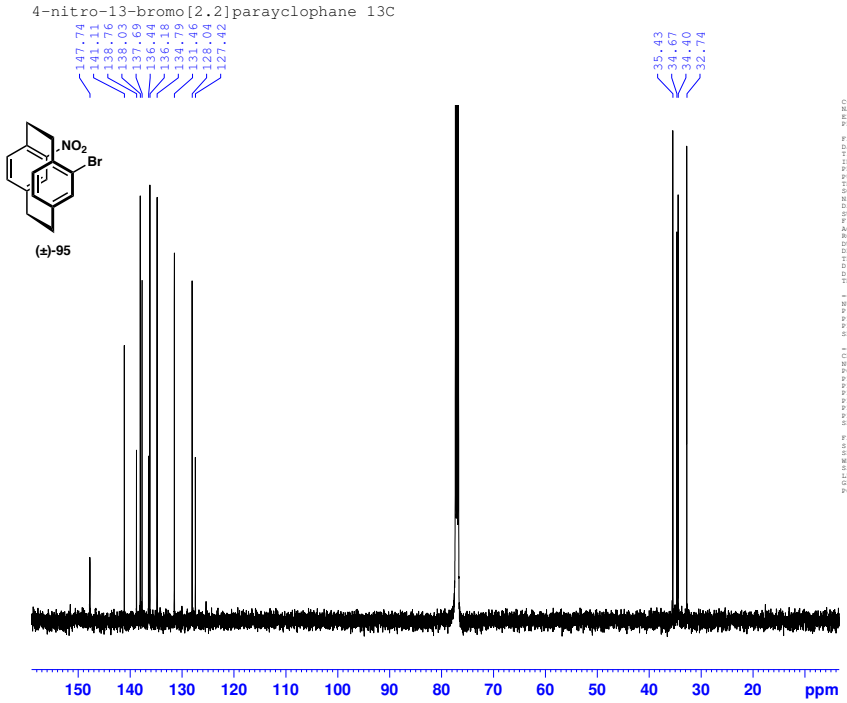


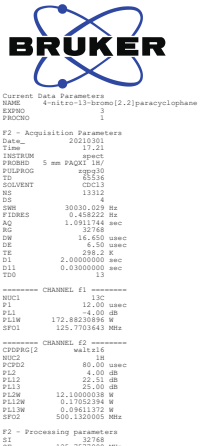

$^{1}$H NMR spectrum of (±)-**99** in $CDCl_3$

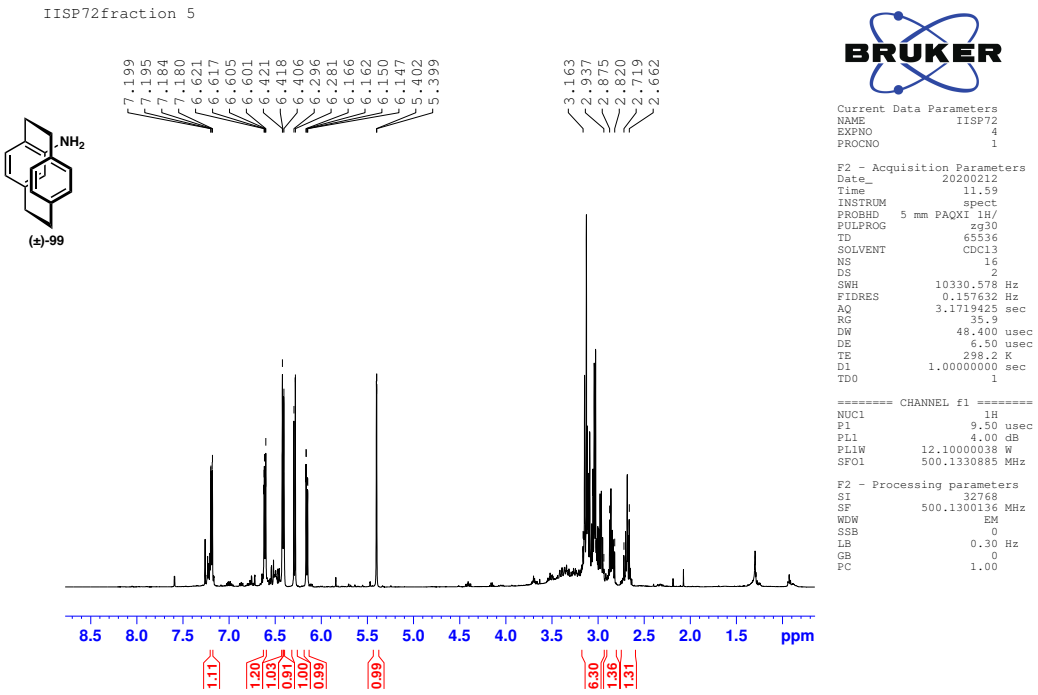

$^{1}$H NMR spectrum of (±)-**96** in $CDCl_3$

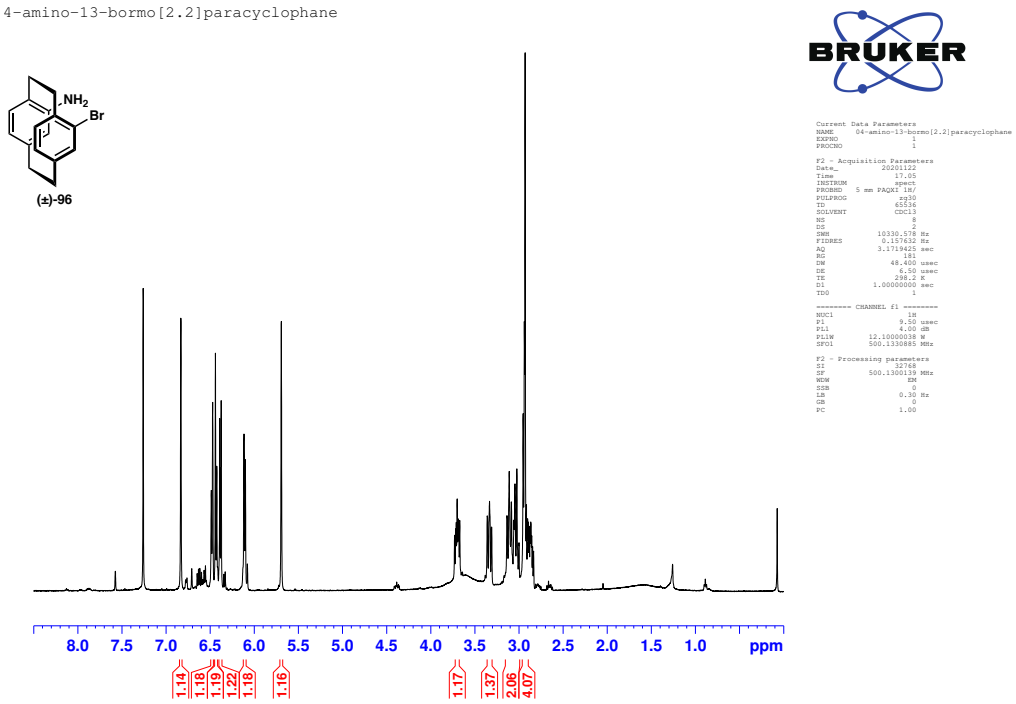


$^{13}$C NMR spectrum of (±)-**96** in $CDCl_3$

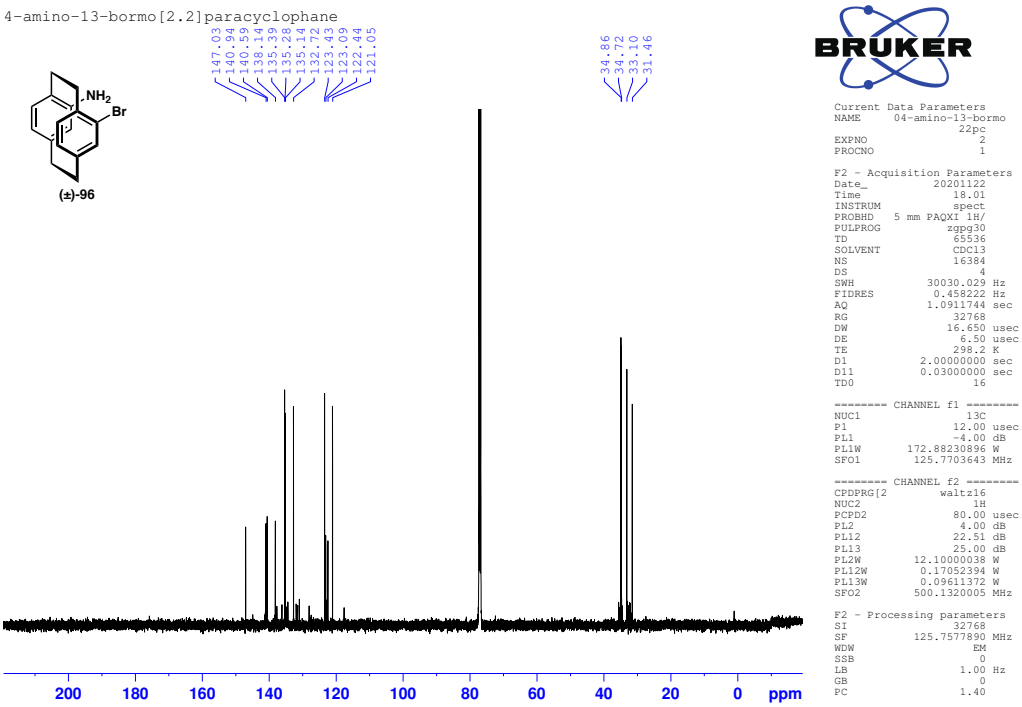

$^{1}$H NMR spectrum of (*S*)-**98** in $CDCl_3$

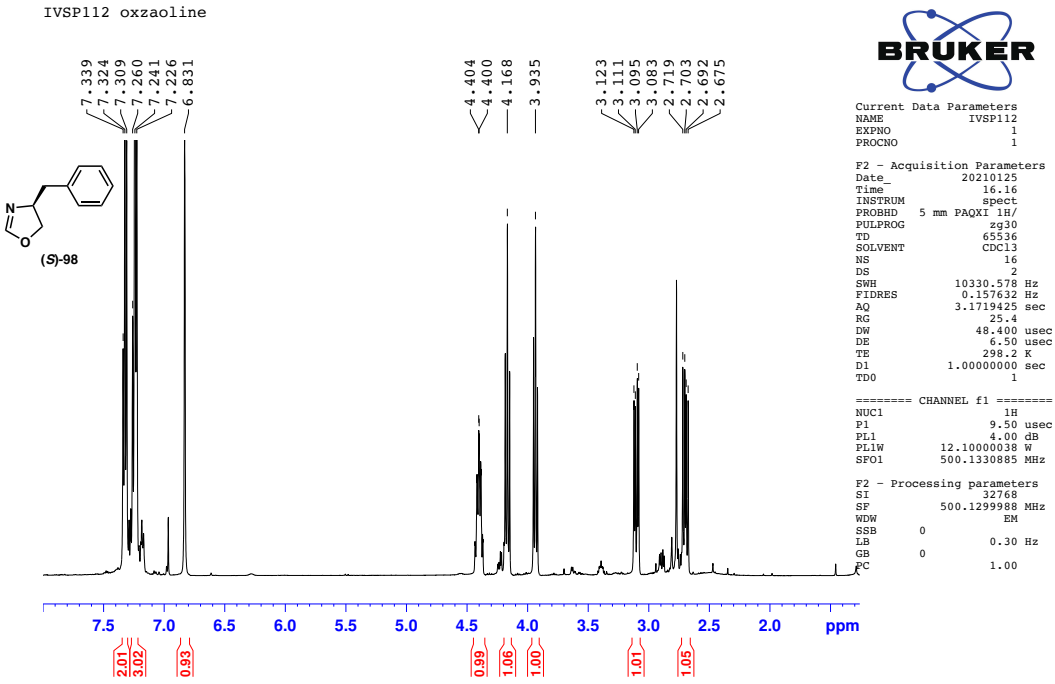


$^{13}$C NMR spectrum of (*S*)-**98** in $CDCl_3$

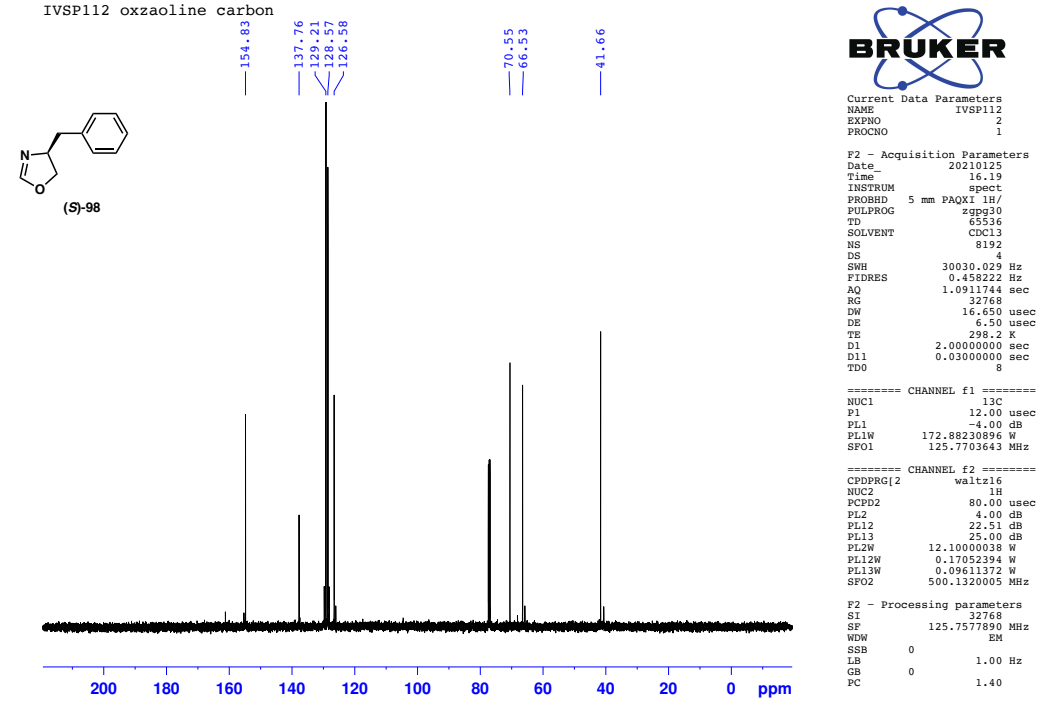

$^{1}$H NMR spectrum of (±)-**103** in DMSO-$d_6$

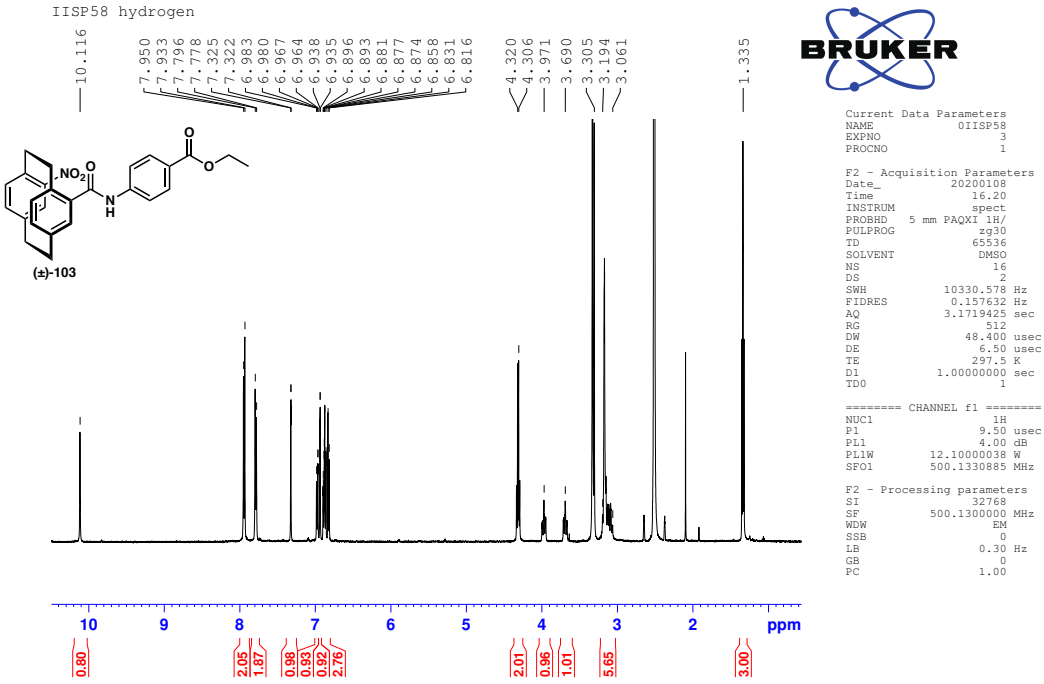



Current Data Parameters
NAME 0IISP58
EXPNO 3
PROCNO 1

F2 - Acquisition Parameters
Date_ 20200108
Time 16.20
INSTRUM spect
PROBHD 5 mm PAQXI 1H/
PULPROG zg30
TD 65536
SOLVENT DMSO
NS 16
DS 2
SWH 10330.578 Hz
FIDRES 0.157632 Hz
AQ 3.1719425 sec
RG 512
DW 48.400 usec
DE 6.50 usec
TE 297.5 K
D1 1.00000000 sec
TD0 1

======== CHANNEL f1 ========
NUC1 1H
P1 9.50 usec
PL1 4.00 dB
PL1W 12.10000038 W
SFO1 500.1330885 MHz

F2 - Processing parameters
SI 32768
SF 500.1300000 MHz
WDW EM
SSB 0
LB 0.30 Hz
GB 0
PC 1.00


$^{13}$C NMR spectrum of (±)-**103** in DMSO-$d_6$

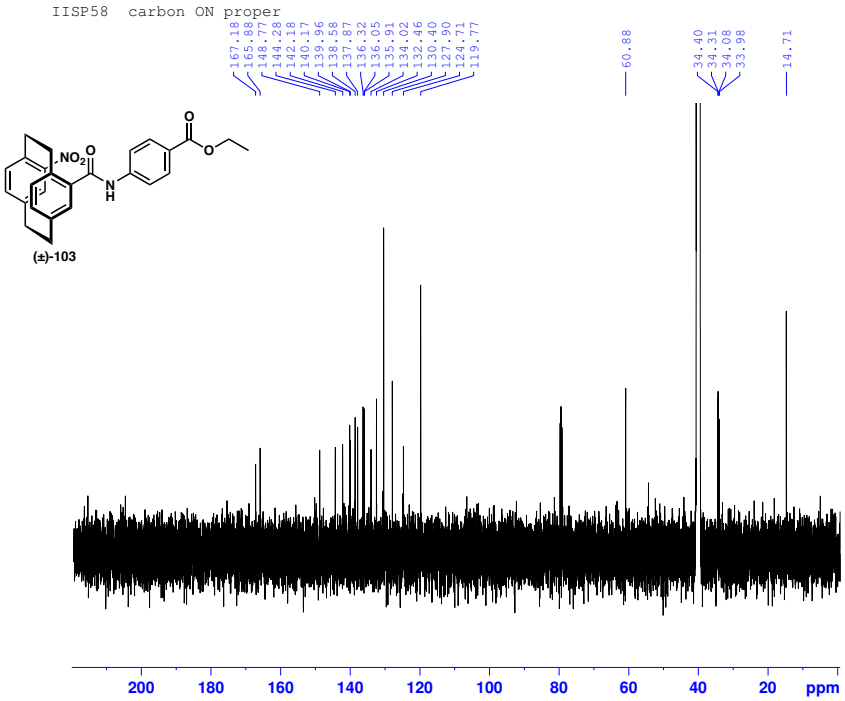



Current Data Parameters
NAME 0IISP58
EXPNO 11
PROCNO 1

F2 - Acquisition Parameters
Date_ 20200110
Time 5.14
INSTRUM spect
PROBHD 5 mm PAQXI 1H/
PULPROG zgpg30
TD 65536
SOLVENT DMSO
NS 14336
DS 4
SWH 30030.029 Hz
FIDRES 0.458222 Hz
AQ 1.0911744 sec
RG 32768
DW 16.650 usec
DE 6.50 usec
TE 297.5 K
D1 2.00000000 sec
D11 0.03000000 sec
TD0 1

======== CHANNEL f1 ========
NUC1 13C
P1 12.00 usec
PL1 -4.00 dB
PL1W 172.88230896 W
SFO1 125.7703643 MHz

======== CHANNEL f2 ========
CPDPRG[2 waltz16
NUC2 1H
PCPD2 80.00 usec
PL2 4.00 dB
PL12 22.51 dB
PL13 25.00 dB
PL2W 12.10000038 W
PL12W 0.17052394 W
PL13W 0.09611372 W
SFO2 500.1320005 MHz

F2 - Processing parameters
SI 32768
SF 125.7577890 MHz
WDW EM
SSB 0
LB 1.00 Hz
GB 0
PC 1.40

$^1$H NMR spectrum of (±)-**104** in $CDCl_3$

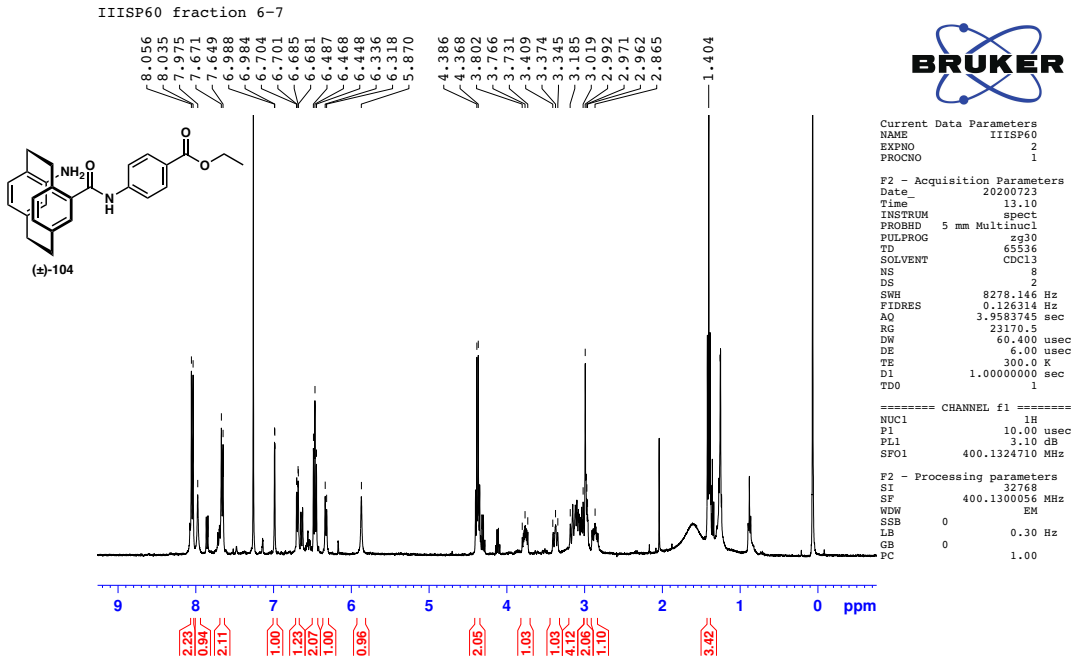


$^1$H NMR spectrum of **110** (1:3 mixture of diastereoisomers) in $CDCl_3$

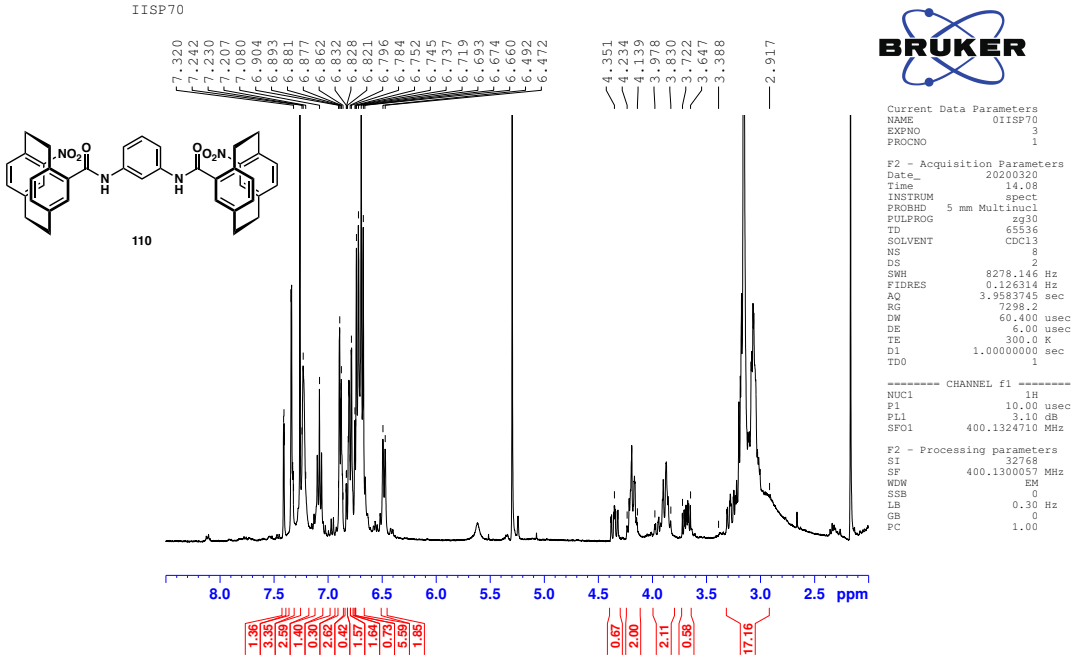

$^{1}$H NMR spectrum of **106** in $CDCl_3$

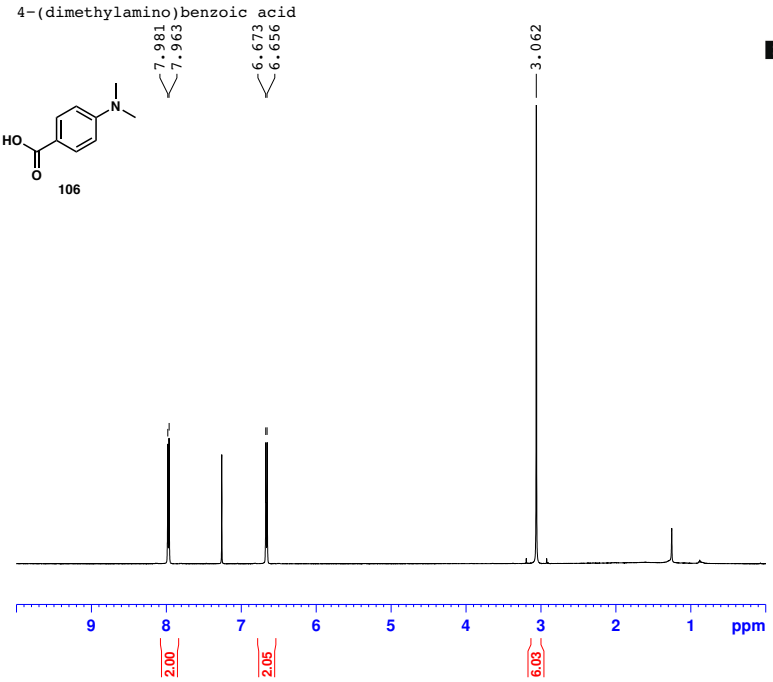


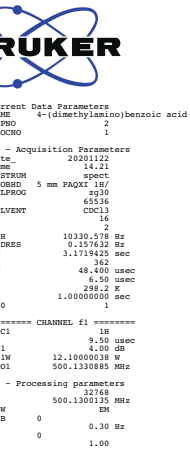


$^{13}$C NMR spectrum of **106** in $CDCl_3$

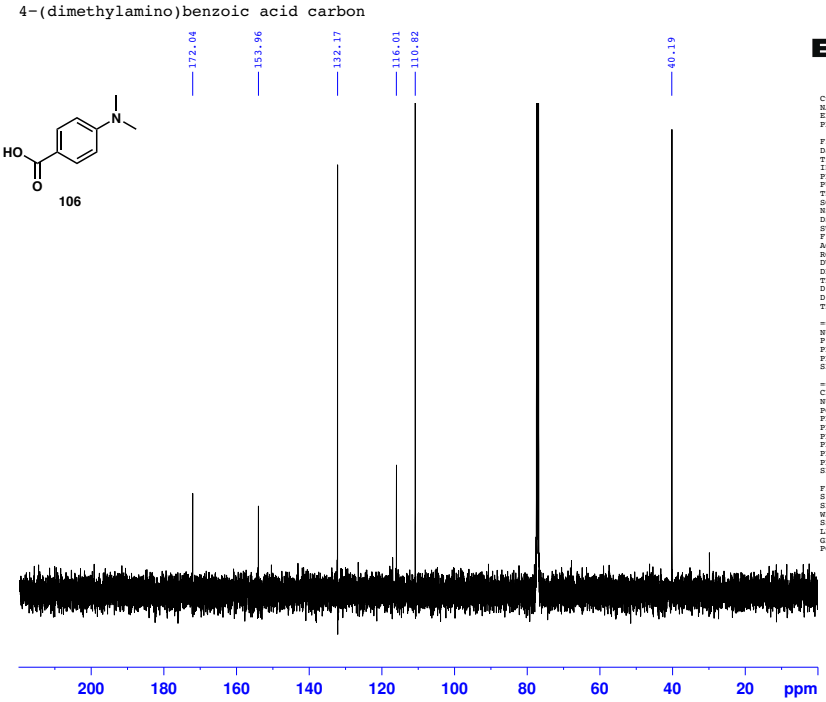


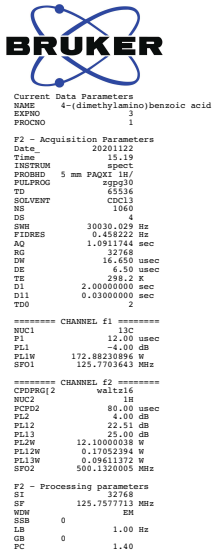

$^{1}$H NMR spectrum of (±)-**111** in $CDCl_3$

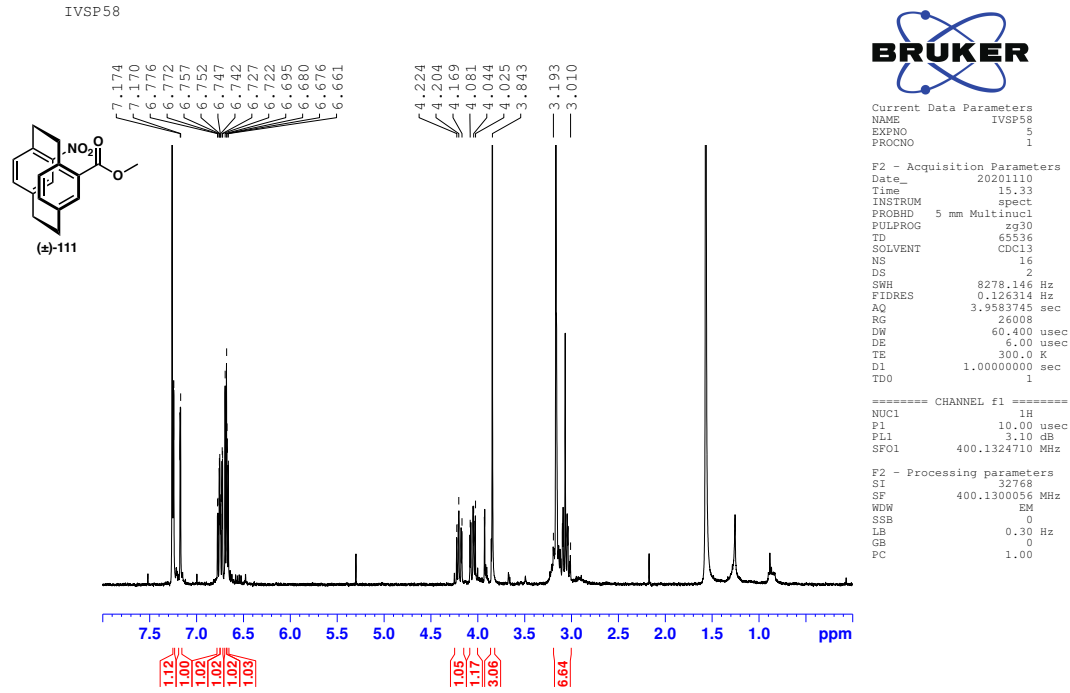


BRUKER

```
Current Data Parameters
NAME                  IVSP58
EXPNO                      5
PROCNO                     1

F2 - Acquisition Parameters
Date_              20201110
Time                  15.33
INSTRUM               spect
PROBHD    5 mm Multinucl
PULPROG                zg30
TD                    65536
SOLVENT               CDCl3
NS                       16
DS                        2
SWH                8278.146 Hz
FIDRES            0.126314 Hz
AQ                3.9583745 sec
RG                    26008
DW                   60.400 usec
DE                    6.00 usec
TE                   300.0 K
D1              1.00000000 sec
TD0                       1

======== CHANNEL f1 ========
NUC1                    1H
P1                   10.00 usec
PL1                   3.10 dB
SFO1           400.1324710 MHz

F2 - Processing parameters
SI                    32768
SF             400.1300056 MHz
WDW                      EM
SSB                       0
LB                    0.30 Hz
GB                        0
PC                     1.00
```

$^{13}$C NMR spectrum of (±)-**111** in $CDCl_3$

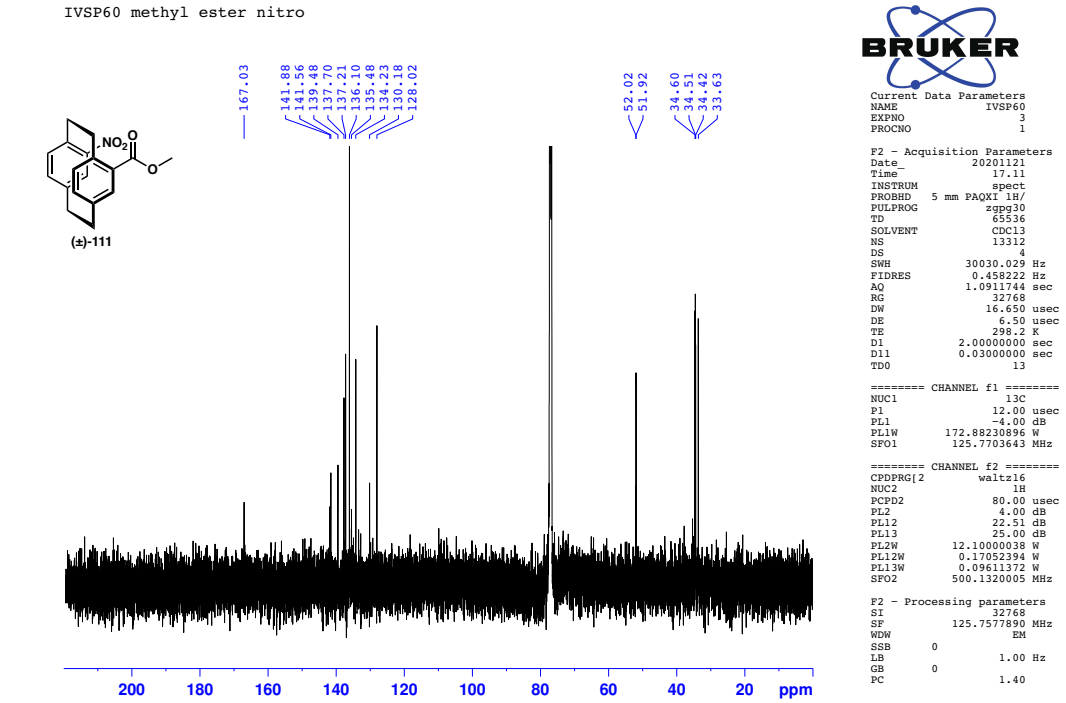


BRUKER

```
Current Data Parameters
NAME                  IVSP60
EXPNO                      3
PROCNO                     1

F2 - Acquisition Parameters
Date_              20201121
Time                  17.11
INSTRUM               spect
PROBHD    5 mm PAQXI 1H/
PULPROG              zgpg30
TD                    65536
SOLVENT               CDCl3
NS                    13312
DS                        4
SWH               30030.029 Hz
FIDRES            0.458222 Hz
AQ                1.0911744 sec
RG                    32768
DW                   16.650 usec
DE                    6.50 usec
TE                   298.2 K
D1              2.00000000 sec
D11             0.03000000 sec
TD0                      13

======== CHANNEL f1 ========
NUC1                   13C
P1                   12.00 usec
PL1                  -4.00 dB
PL1W          172.88230896 W
SFO1           125.7703643 MHz

======== CHANNEL f2 ========
CPDPRG[2          waltz16
NUC2                    1H
PCPD2                80.00 usec
PL2                   4.00 dB
PL12                 22.51 dB
PL13                 25.00 dB
PL2W          12.10000038 W
PL12W          0.17052394 W
PL13W          0.09611372 W
SFO2           500.1320005 MHz

F2 - Processing parameters
SI                    32768
SF             125.7577890 MHz
WDW                      EM
SSB       0
LB                    1.00 Hz
GB        0
PC                    1.40
```

$^{1}$H NMR spectrum of (±)-**101** in $CDCl_3$

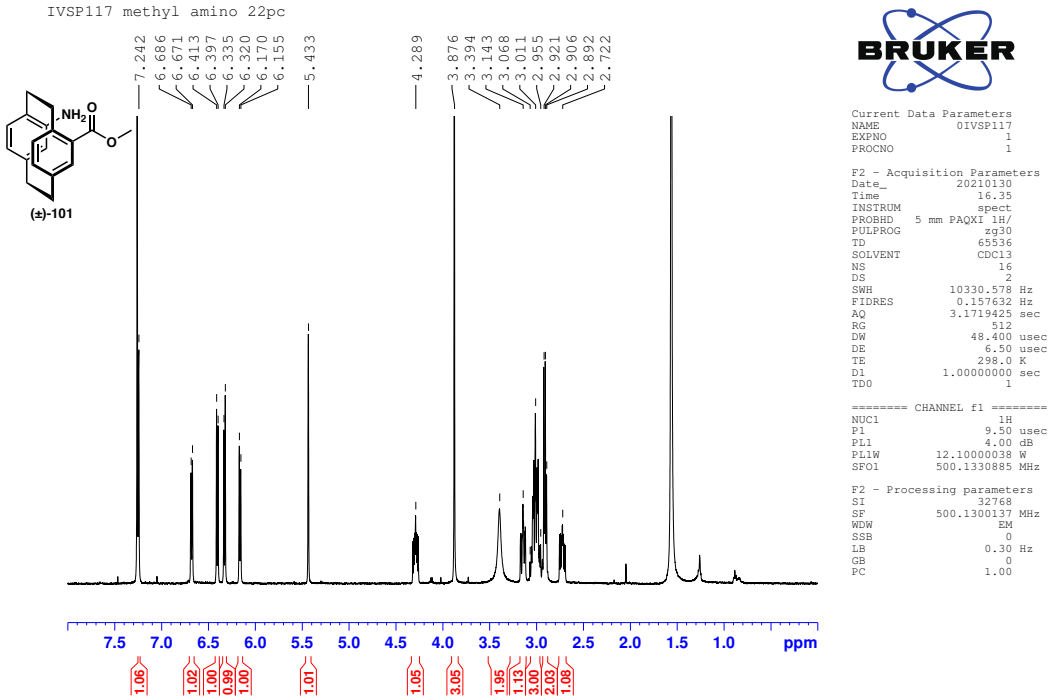


BRUKER

```
Current Data Parameters
NAME                  0IVSP117
EXPNO                        1
PROCNO                       1

F2 - Acquisition Parameters
Date_              20210130
Time                    16.35
INSTRUM                 spect
PROBHD    5 mm PAQXI 1H/
PULPROG                 zg30
TD                     65536
SOLVENT                CDC13
NS                        16
DS                         2
SWH                10330.578 Hz
FIDRES             0.157632 Hz
AQ                 3.1719425 sec
RG                       512
DW                    48.400 usec
DE                     6.50 usec
TE                    298.0 K
D1                 1.00000000 sec
TD0                          1

======== CHANNEL f1 ========
NUC1                       1H
P1                       9.50 usec
PL1                      4.00 dB
PL1W              12.10000038 W
SFO1              500.1330885 MHz

F2 - Processing parameters
SI                       32768
SF                500.1300137 MHz
WDW                         EM
SSB                          0
LB                        0.30 Hz
GB                           0
PC                        1.00
```

$^{13}$C NMR spectrum of (±)-**101** in $CDCl_3$

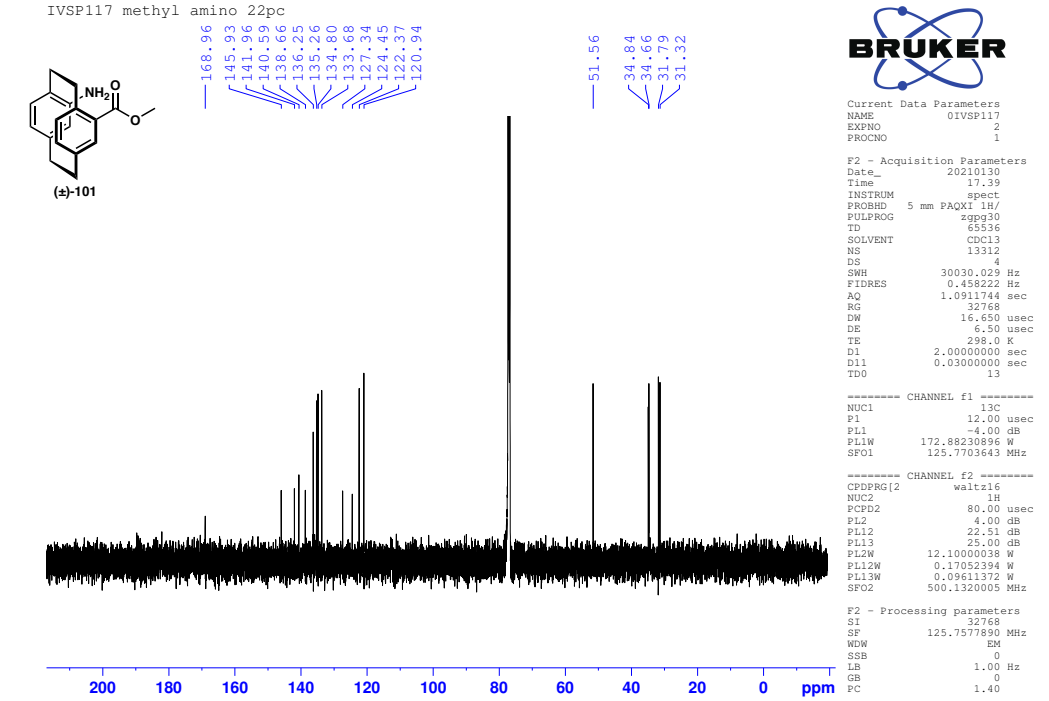


BRUKER

```
Current Data Parameters
NAME                  0IVSP117
EXPNO                        2
PROCNO                       1

F2 - Acquisition Parameters
Date_              20210130
Time                    17.39
INSTRUM                 spect
PROBHD    5 mm PAQXI 1H/
PULPROG              zgpg30
TD                     65536
SOLVENT                CDC13
NS                     13312
DS                         4
SWH                30030.029 Hz
FIDRES             0.458222 Hz
AQ                 1.0911744 sec
RG                       32768
DW                    16.650 usec
DE                     6.50 usec
TE                    298.0 K
D1                 2.00000000 sec
D11                0.03000000 sec
TD0                         13

======== CHANNEL f1 ========
NUC1                      13C
P1                      12.00 usec
PL1                     -4.00 dB
PL1W             172.88230896 W
SFO1             125.7703643 MHz

======== CHANNEL f2 ========
CPDPRG[2             waltz16
NUC2                       1H
PCPD2                  80.00 usec
PL2                     4.00 dB
PL12                   22.51 dB
PL13                   25.00 dB
PL2W              12.10000038 W
PL12W              0.17052394 W
PL13W              0.09611372 W
SFO2              500.1320005 MHz

F2 - Processing parameters
SI                       32768
SF                125.7577890 MHz
WDW                         EM
SSB                          0
LB                        1.00 Hz
GB                           0
PC                        1.40
```

$^{1}$H NMR spectrum of **114** in DMSO-$d_6$

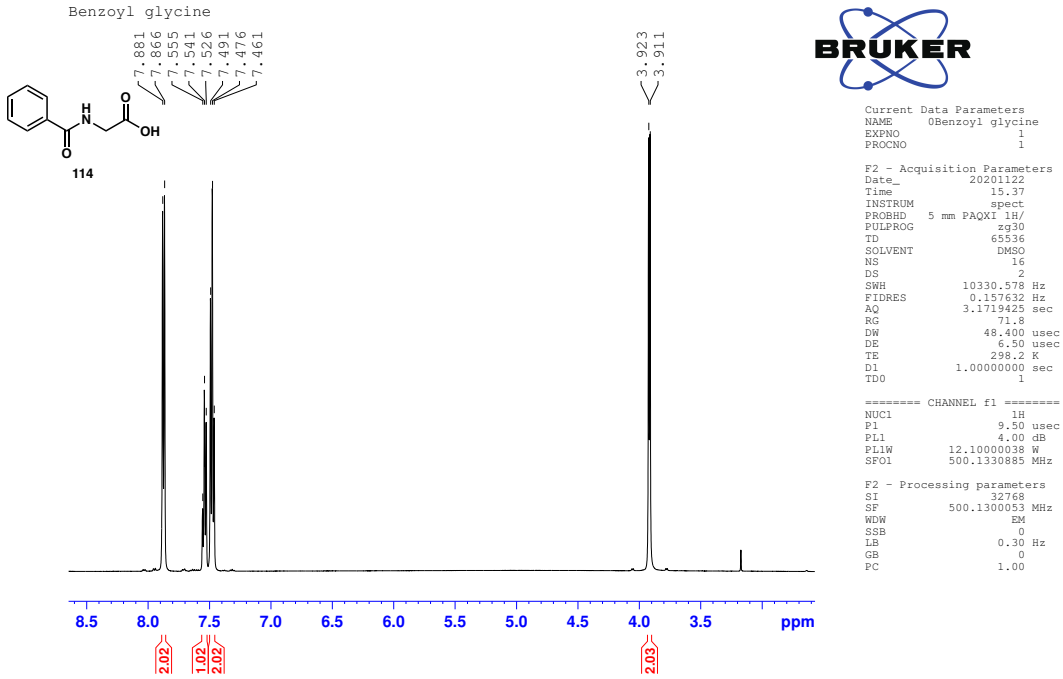


$^{13}$C NMR spectrum of **114** in DMSO-$d_6$

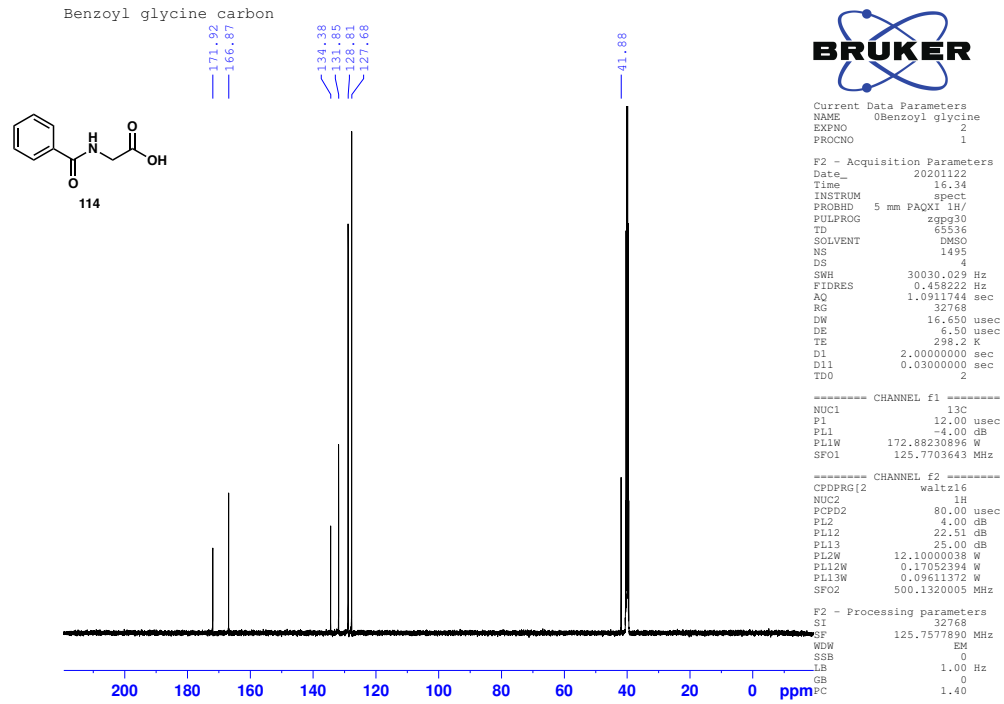

$^{1}$H NMR spectrum of **118** in DMSO-$d_6$

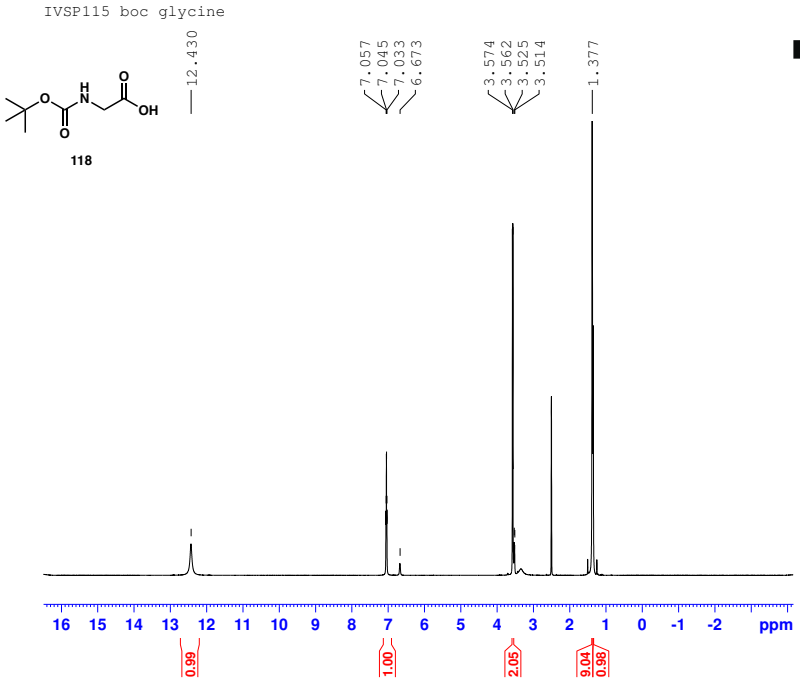


```
Current Data Parameters
NAME              0IVSP115
EXPNO                    1
PROCNO                   1

F2 - Acquisition Parameters
Date_              20210130
Time                 12.46
INSTRUM              spect
PROBHD   5 mm PAQXI 1H/
PULPROG              zg30
TD                  65536
SOLVENT              DMSO
NS                     16
DS                      2
SWH             10330.578 Hz
FIDRES          0.157632 Hz
AQ              3.1719425 sec
RG                     57
DW                48.400 usec
DE                 6.50 usec
TE                298.0 K
D1             1.00000000 sec
TD0                     1

======== CHANNEL f1 ========
NUC1                   1H
P1                  9.50 usec
PL1                 4.00 dB
PL1W          12.10000038 W
SFO1         500.1330885 MHz

F2 - Processing parameters
SI                  32768
SF            500.1300054 MHz
WDW                    EM
SSB                     0
LB                 0.30 Hz
GB                      0
PC                   1.00
```

$^{13}$C NMR spectrum of **118** in DMSO-$d_6$

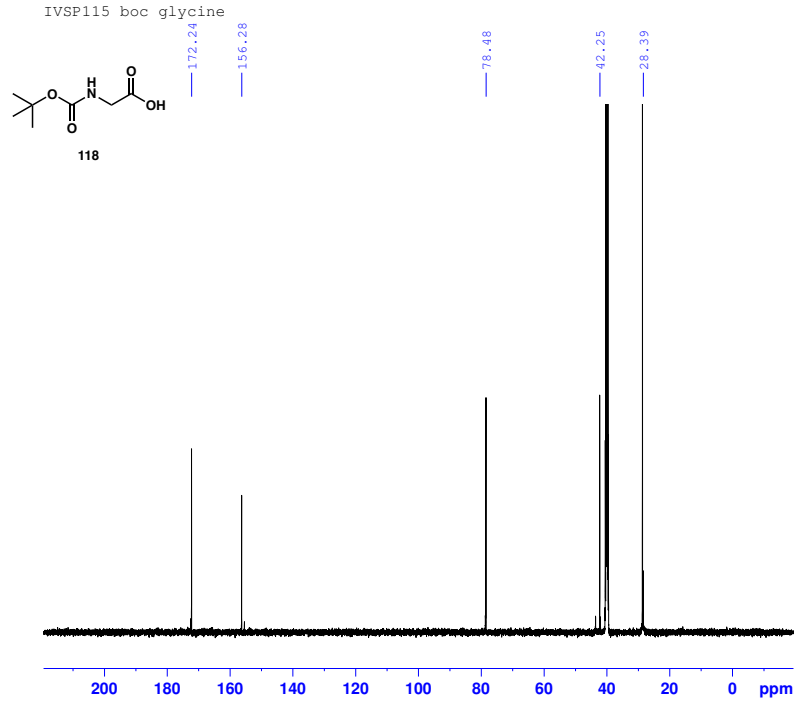


```
Current Data Parameters
NAME              0IVSP115
EXPNO                    2
PROCNO                   1

F2 - Acquisition Parameters
Date_              20210130
Time                 13.44
INSTRUM              spect
PROBHD   5 mm PAQXI 1H/
PULPROG           zgpg30
TD                  65536
SOLVENT              DMSO
NS                   2097
DS                      4
SWH             30030.029 Hz
FIDRES          0.458222 Hz
AQ              1.0911744 sec
RG                  32768
DW                16.650 usec
DE                 6.50 usec
TE                298.1 K
D1             2.00000000 sec
D11            0.03000000 sec
TD0                     4

======== CHANNEL f1 ========
NUC1                  13C
P1                 12.00 usec
PL1                -4.00 dB
PL1W         172.88230896 W
SFO1         125.7703643 MHz

======== CHANNEL f2 ========
CPDPRG[2          waltz16
NUC2                   1H
PCPD2              80.00 usec
PL2                 4.00 dB
PL12               22.51 dB
PL13               25.00 dB
PL2W          12.10000038 W
PL12W          0.17052394 W
PL13W          0.09611372 W
SFO2         500.1320005 MHz

F2 - Processing parameters
SI                  32768
SF            125.7577890 MHz
WDW                    EM
SSB                     0
LB                 1.00 Hz
GB                      0
PC                   1.40
```

$^1$H NMR spectrum of **120** in $CDCl_3$

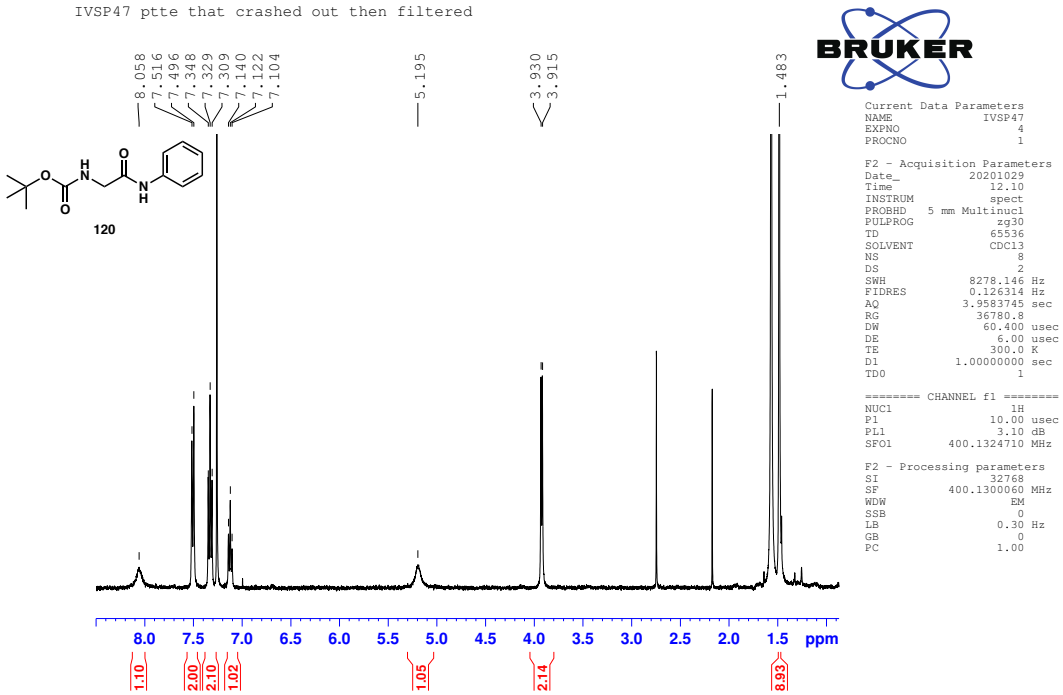


$^1$H NMR spectrum of **116** in $CD_3OD$

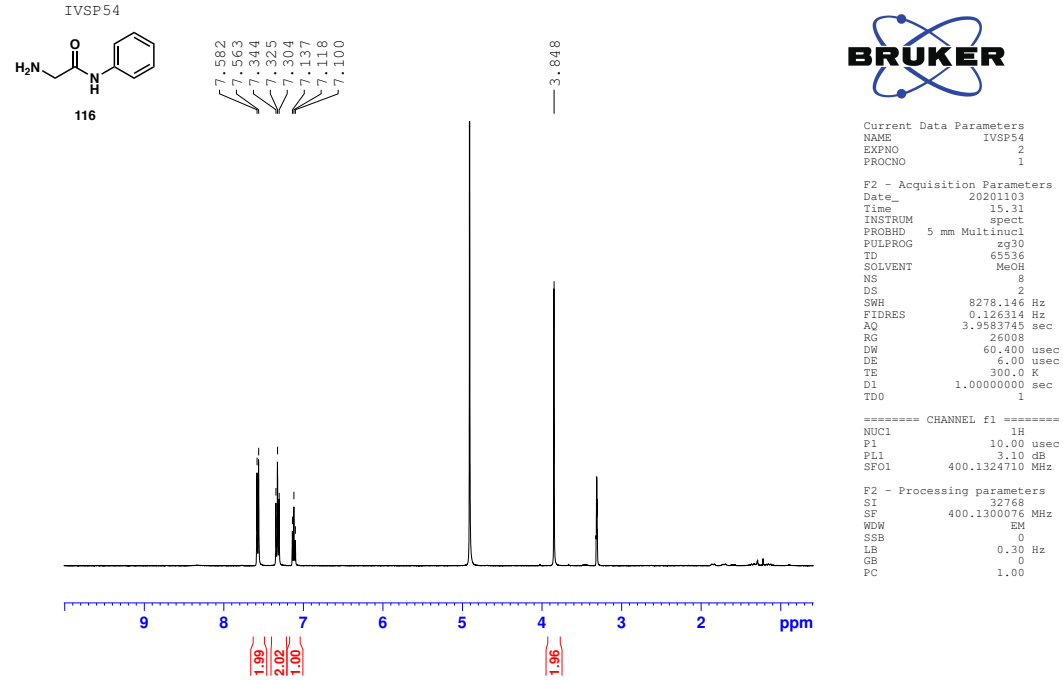

$^{1}$H NMR spectrum of (±)-**124** in $CDCl_3$

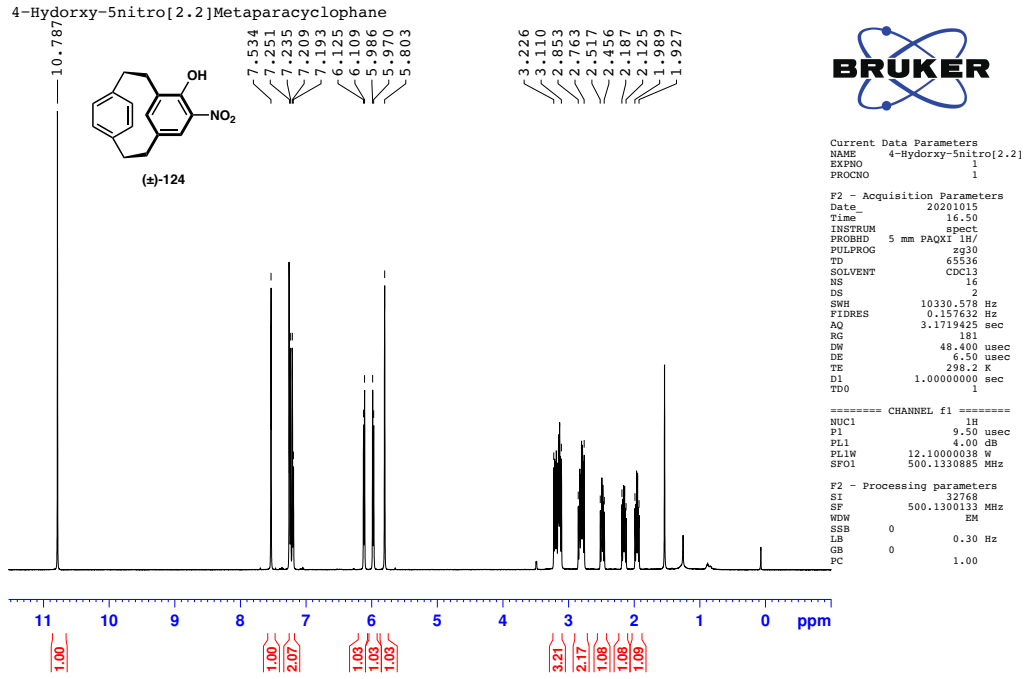


$^{13}$C NMR spectrum of (±)-**124** in $CDCl_3$

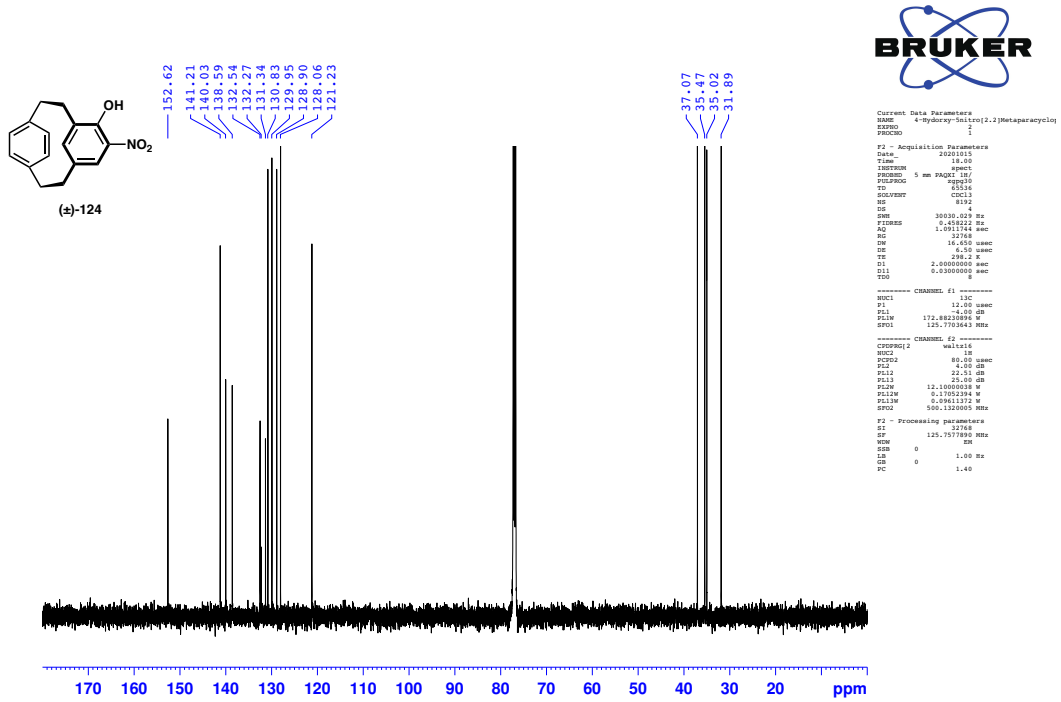

DEPT NMR spectrum of (±)-**124** in $CDCl_3$

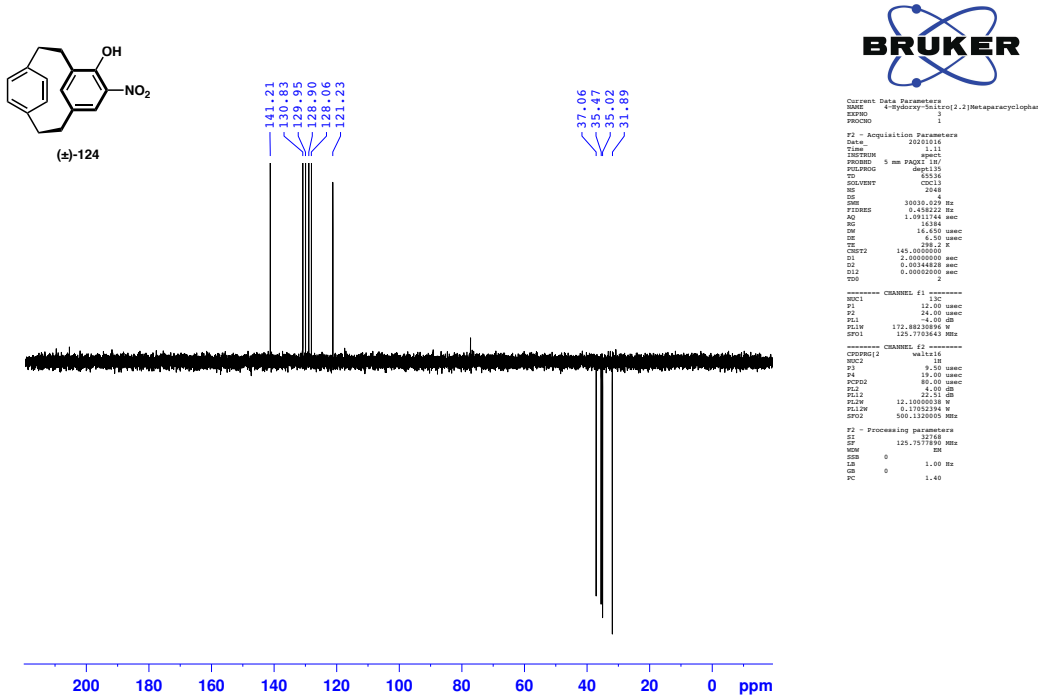


NOSEY spectrum of (±)-**124** in $CDCl_3$

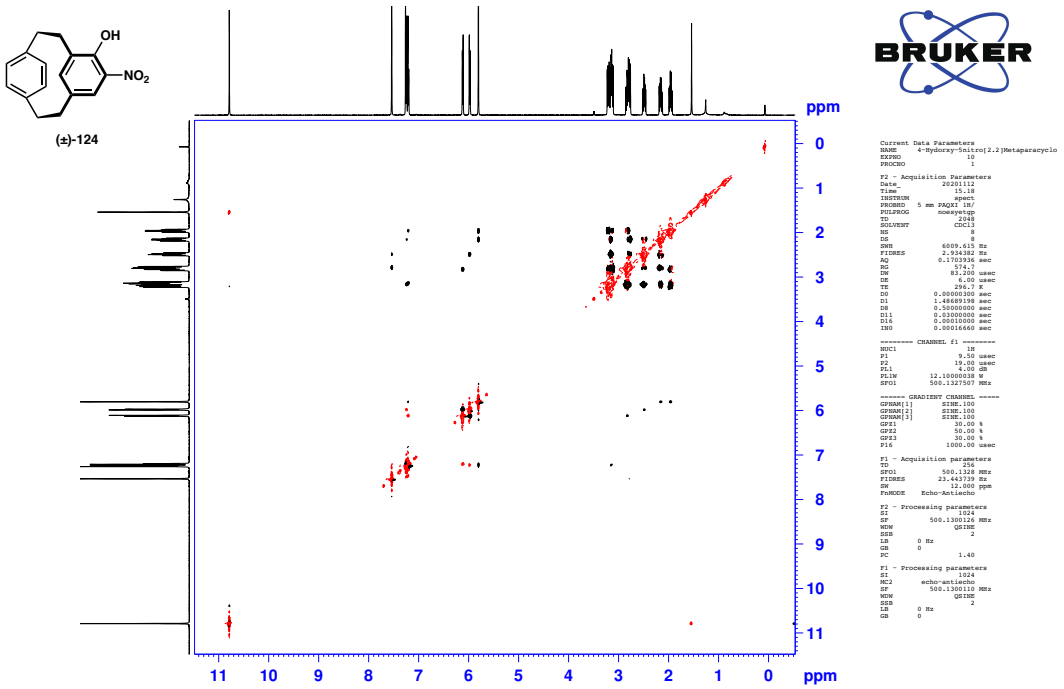

COSY NMR spectrum of (±)-**124** in $CDCl_3$

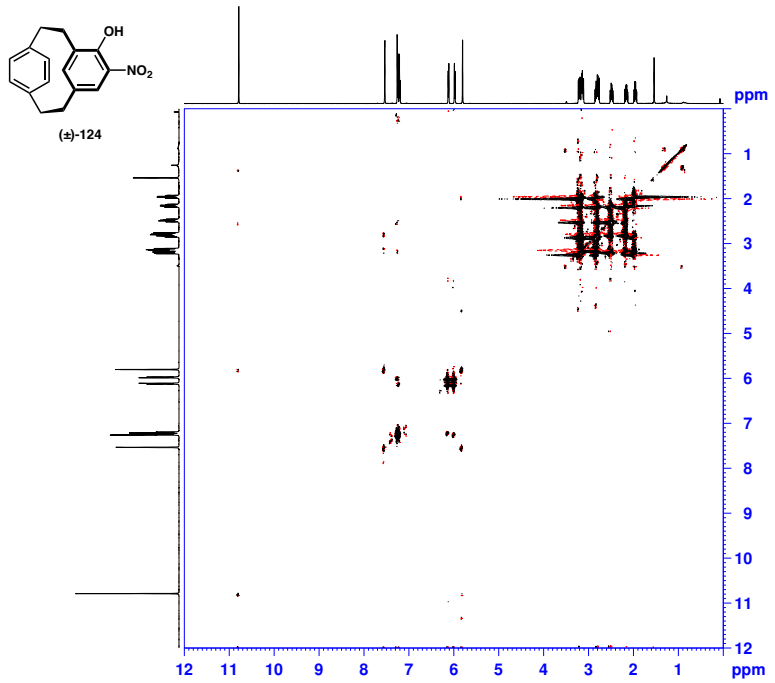



```
Current Data Parameters
NAME      4-Hydoroxy-5nitro[2.2]Metaparacyclopha
EXPNO                 4
PROCNO                1

F2 - Acquisition Parameters
Date_          20201016
Time                2.55
INSTRUM            spect
PROBHD   5 mm PAQXI 1H/
PULPROG      cosygpmfph
TD                 2048
SOLVENT            CDCl3
NS                    8
DS                    4
SWH             6510.417 Hz
FIDRES          3.178914 Hz
AQ              0.1572864 sec
RG                  256
DW                76.800 usec
DE                 6.50 usec
TE                298.2 K
D0           0.00006481 sec
D1           2.00000000 sec
D13          0.00000400 sec
D16          0.00010000 sec
IN0          0.00015380 sec

======== CHANNEL f1 ========
NUC1                1H
P1                 9.50 usec
P2                19.00 usec
PL1               4.00 dB
PLIW        12.10000038 W
SFO1       500.1327507 MHz

====== GRADIENT CHANNEL =====
GPNAM[1]        SINE.100
GPNAM[2]        SINE.100
GPZ1              10.00 %
GPZ2              20.00 %
P16             1000.00 usec

F1 - Acquisition parameters
TD                  400
SFO1       500.1328 MHz
FIDRES     16.254314 Hz
SW             13.000 ppm
FnMODE      States-TPPI

F2 - Processing parameters
SI                 1024
SF         500.1300000 MHz
WDW                QSINE
SSB                   2
LB        0 Hz
GB        0
PC                1.40

F1 - Processing parameters
SI                 1024
MC2         States-TPPI
SF         500.1300000 MHz
WDW                QSINE
SSB                   2
LB        0 Hz
GB        0
```

Long range COSY NMR spectrum of (±)-**124** in $CDCl_3$

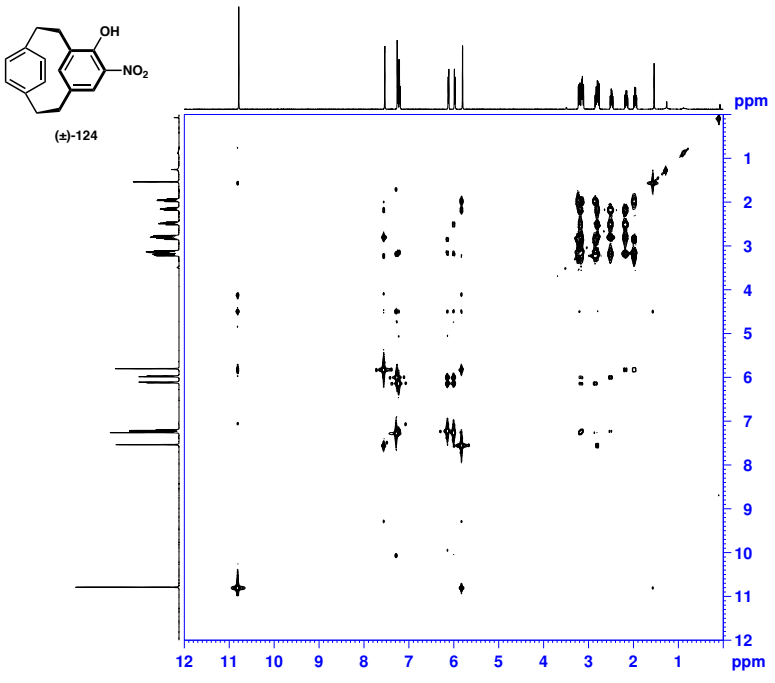



```
Current Data Parameters
NAME      4-Hydoroxy-5nitro[2.2]Metaparacyclophane
EXPNO                 5
PROCNO                1

F2 - Acquisition Parameters
Date_          20201016
Time                4.01
INSTRUM            spect
PROBHD   5 mm PAQXI 1H/
PULPROG          cosylrqf
TD                 2048
SOLVENT            CDCl3
NS                    8
DS                    4
SWH             6510.417 Hz
FIDRES          3.178914 Hz
AQ              0.1572864 sec
RG                 1024
DW                76.800 usec
DE                 6.50 usec
TE                298.2 K
D0           0.00000300 sec
D1           2.00000000 sec
D6           0.20000000 sec
IN0          0.00015380 sec

======== CHANNEL f1 ========
NUC1                1H
P1                 9.50 usec
PL1               4.00 dB
PLIW        12.10000038 W
SFO1       500.1322566 MHz

F1 - Acquisition parameters
TD                  400
SFO1       500.1323 MHz
FIDRES     16.254297 Hz
SW             13.000 ppm
FnMODE              QF

F2 - Processing parameters
SI                 1024
SF         500.1300000 MHz
WDW                SINE
SSB                   0
LB        0 Hz
GB        0
PC                1.40

F1 - Processing parameters
SI                 1024
MC2                 QF
SF         500.1300000 MHz
WDW                SINE
SSB                   0
LB        0 Hz
GB        0
```

HMQC NMR spectrum of (±)-**124** in $CDCl_3$

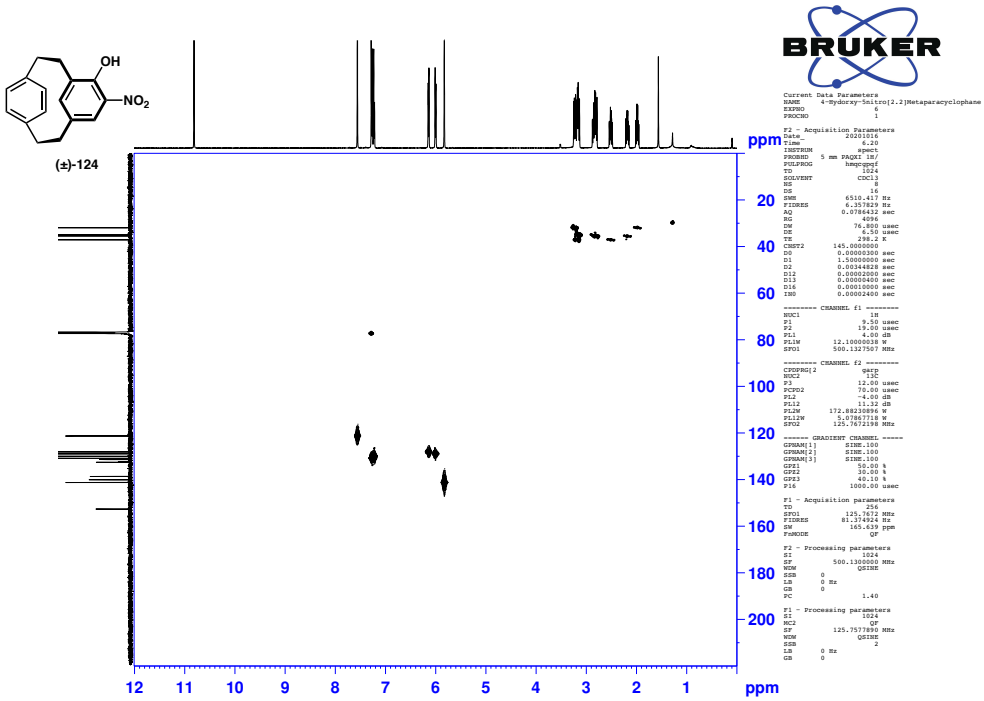


HMBC spectrum of (±)-**124** in $CDCl_3$

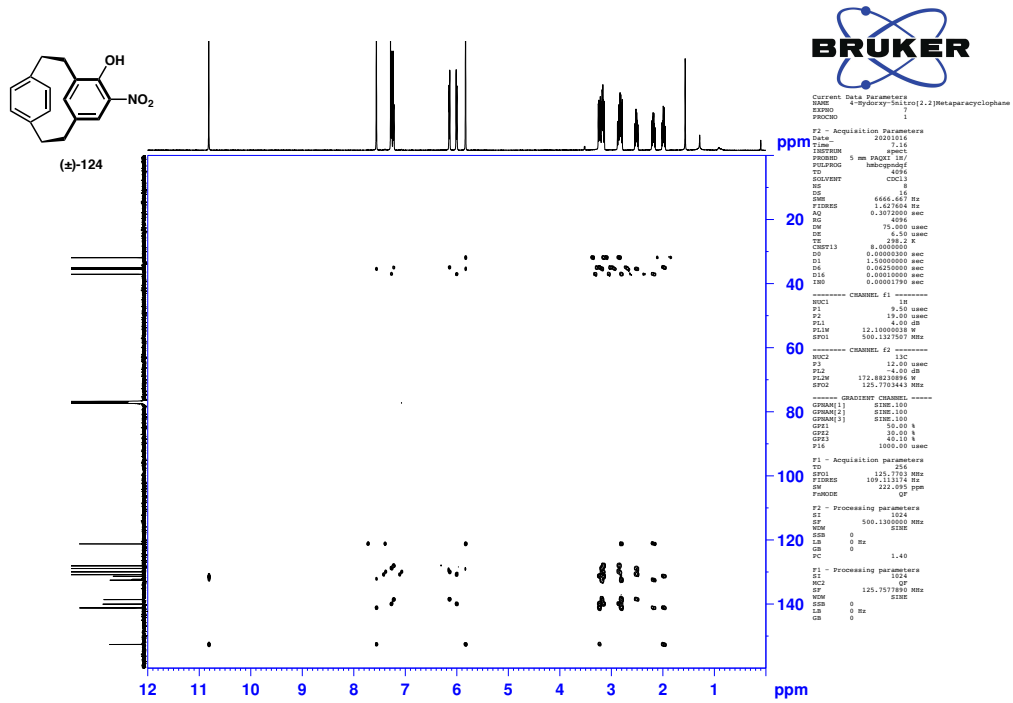

$^{1}$H NMR spectrum of **131** in DMSO-$d_6$

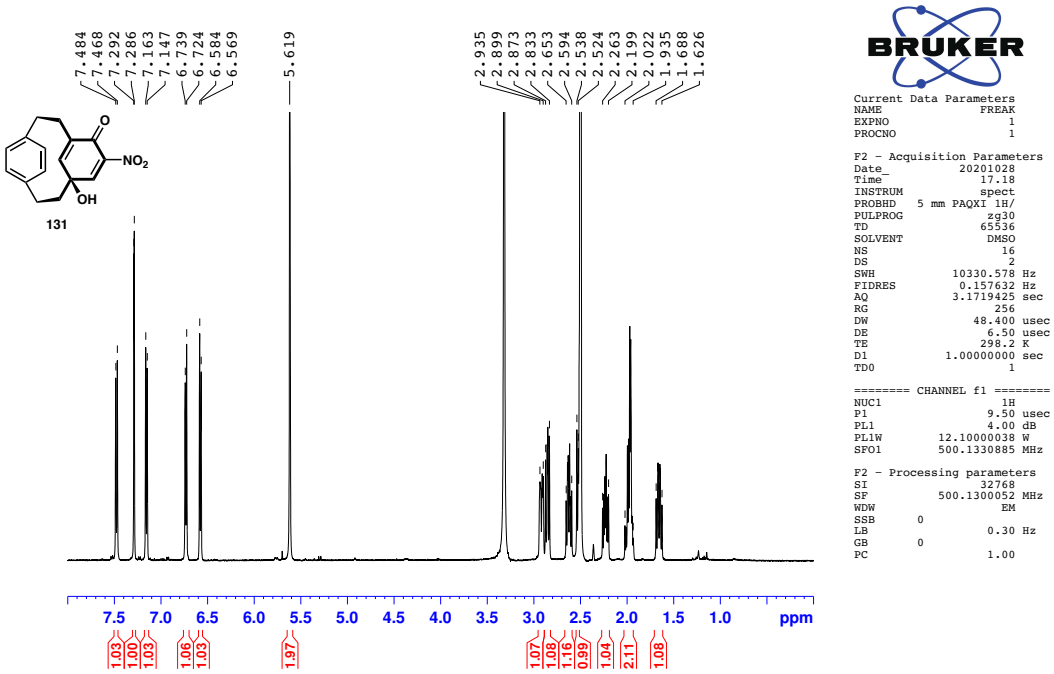


```
Current Data Parameters
NAME                  FREAK
EXPNO                     1
PROCNO                    1

F2 - Acquisition Parameters
Date_              20201028
Time                 17.18
INSTRUM              spect
PROBHD    5 mm PAQXI 1H/
PULPROG              zg30
TD                  65536
SOLVENT               DMSO
NS                       16
DS                        2
SWH              10330.578 Hz
FIDRES            0.157632 Hz
AQ                3.1719425 sec
RG                      256
DW                 48.400 usec
DE                  6.50 usec
TE                  298.2 K
D1              1.00000000 sec
TD0                       1

======== CHANNEL f1 ========
NUC1                    1H
P1                   9.50 usec
PL1                  4.00 dB
PL1W          12.10000038 W
SFO1          500.1330885 MHz

F2 - Processing parameters
SI                    32768
SF              500.1300052 MHz
WDW                      EM
SSB       0
LB                0.30 Hz
GB        0
PC                1.00
```

$^{13}$C NMR spectrum of **131** in DMSO-$d_6$

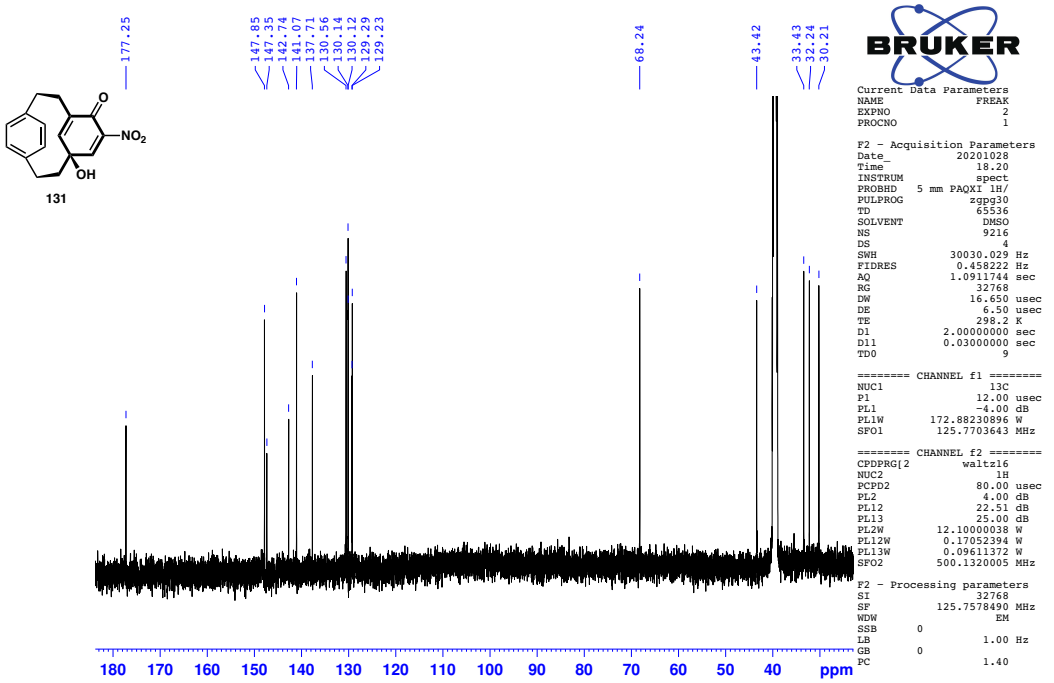


```
Current Data Parameters
NAME                  FREAK
EXPNO                     2
PROCNO                    1

F2 - Acquisition Parameters
Date_              20201028
Time                 18.20
INSTRUM              spect
PROBHD    5 mm PAQXI 1H/
PULPROG           zgpg30
TD                  65536
SOLVENT               DMSO
NS                     9216
DS                        4
SWH              30030.029 Hz
FIDRES            0.458222 Hz
AQ                1.0911744 sec
RG                    32768
DW                 16.650 usec
DE                  6.50 usec
TE                  298.2 K
D1              2.00000000 sec
D11             0.03000000 sec
TD0                       9

======== CHANNEL f1 ========
NUC1                   13C
P1                  12.00 usec
PL1                 -4.00 dB
PL1W         172.88230896 W
SFO1          125.7703643 MHz

======== CHANNEL f2 ========
CPDPRG[2           waltz16
NUC2                    1H
PCPD2               80.00 usec
PL2                  4.00 dB
PL12                22.51 dB
PL13                25.00 dB
PL2W          12.10000038 W
PL12W         0.17052394 W
PL13W         0.09611372 W
SFO2          500.1320005 MHz

F2 - Processing parameters
SI                    32768
SF              125.7578490 MHz
WDW                      EM
SSB       0
LB                1.00 Hz
GB        0
PC                1.40
```

DEPT NMR spectrum of **131** in DMSO-$d_6$

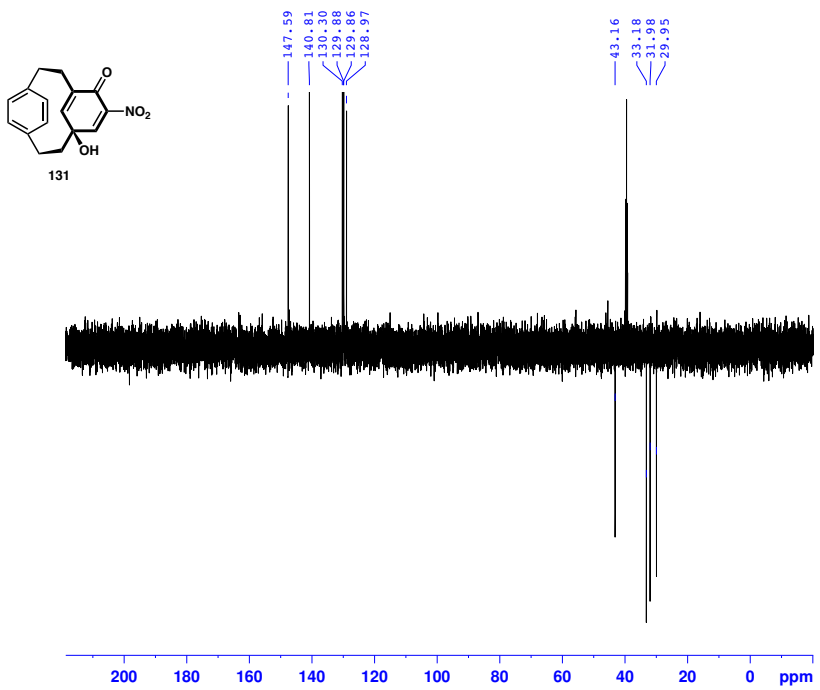


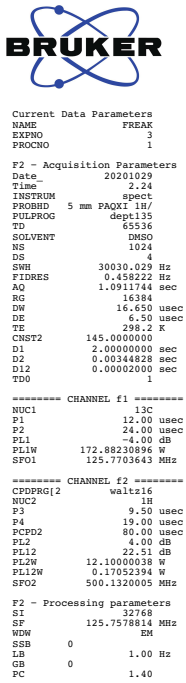


NOSEY spectrum of **131** in DMSO-$d_6$

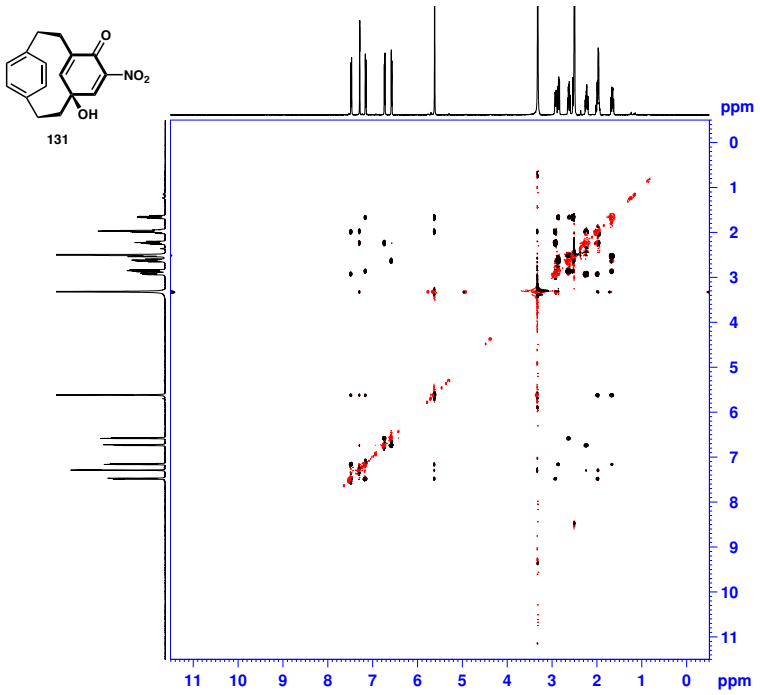


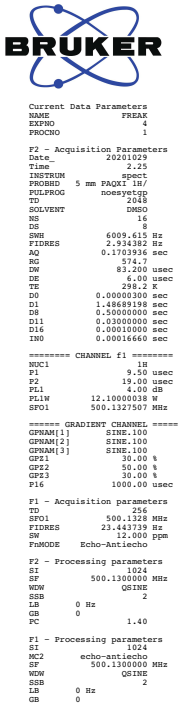

COSY NMR spectrum of **131** in DMSO-$d_6$

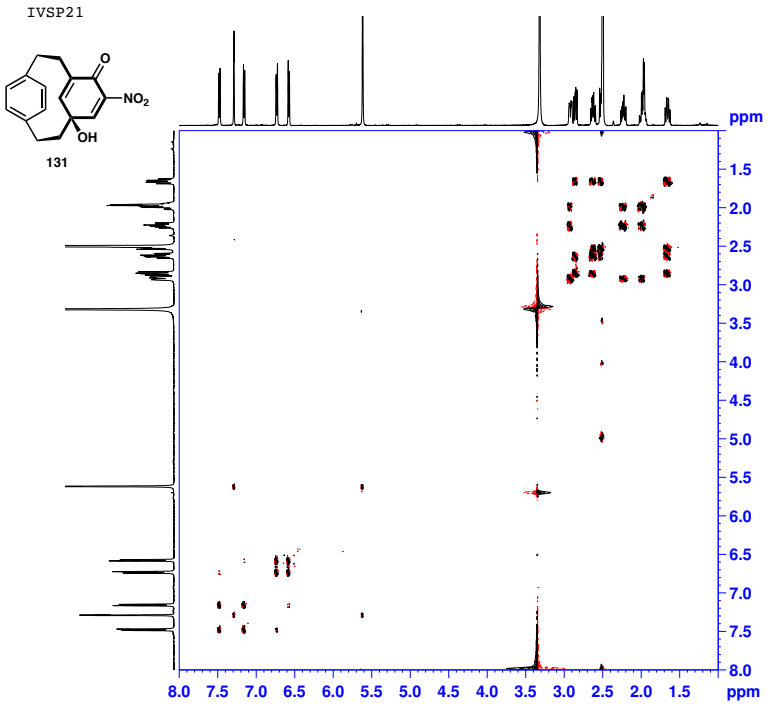


Long range COSY NMR spectrum of **131** in DMSO-$d_6$

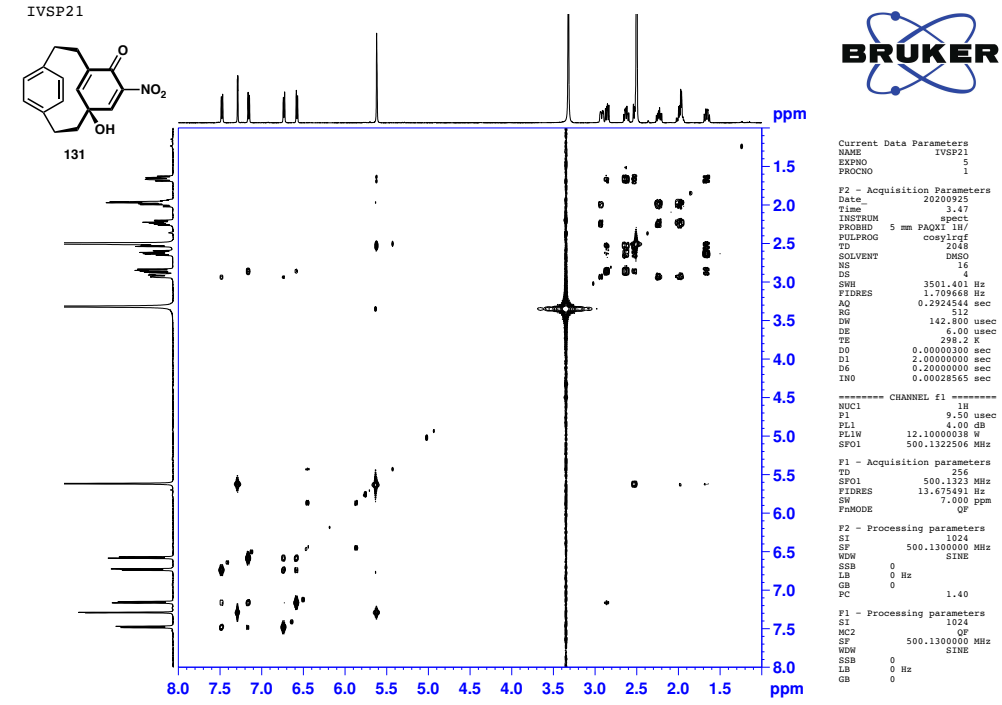

HMQC NMR spectrum of **131** in DMSO-$d_6$

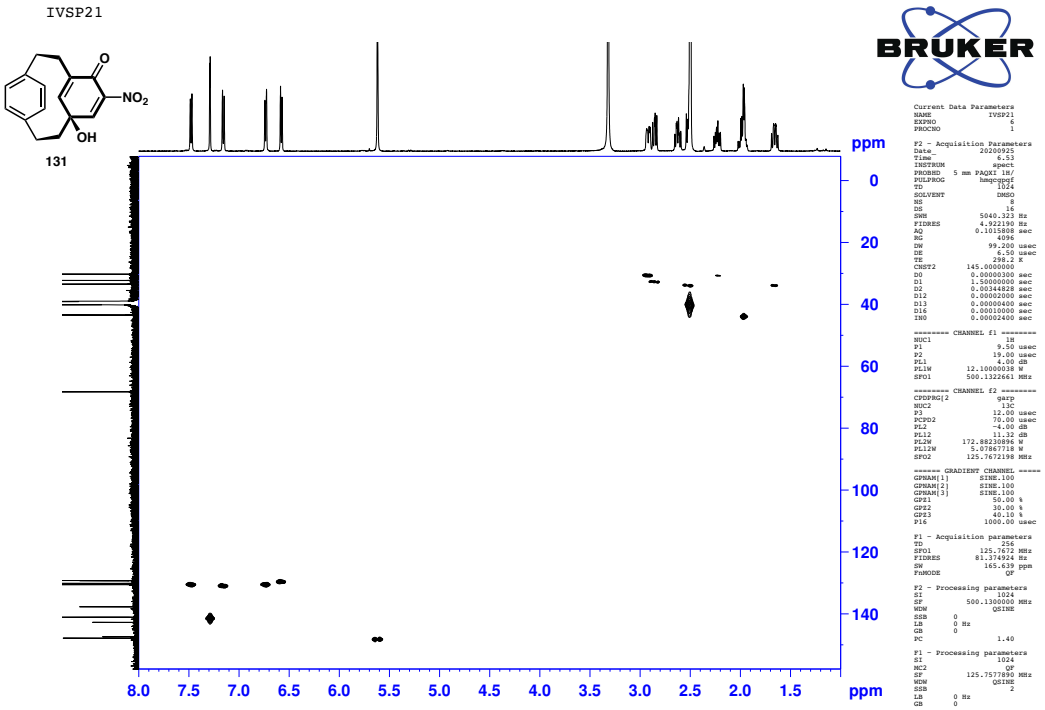


HMBC NMR spectrum of **131** in DMSO-$d_6$

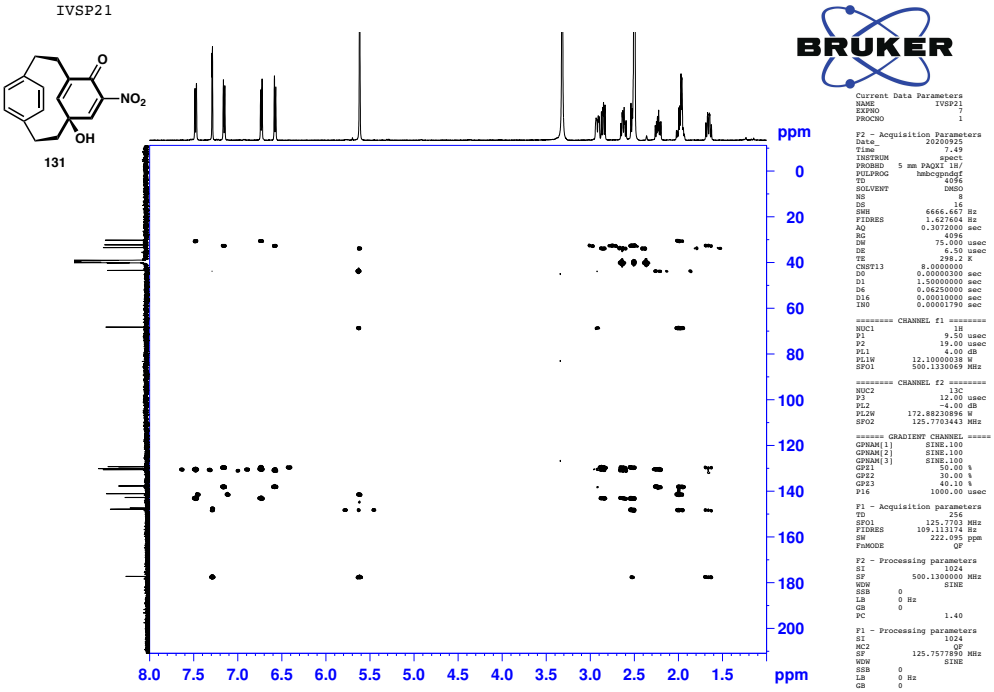

$^{1}$H NMR spectrum of **132** in $CDCl_3$

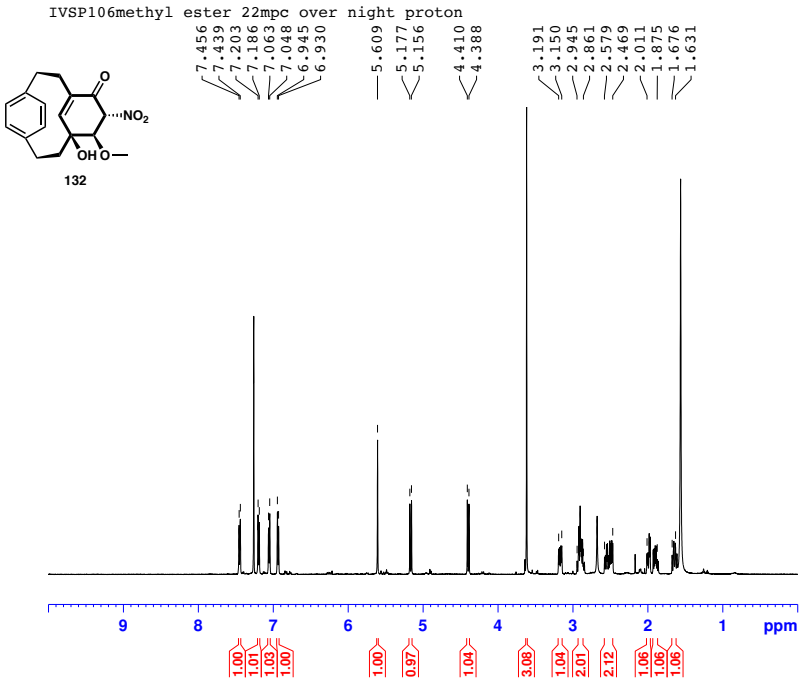


```
Current Data Parameters
NAME                  IVSP106
EXPNO                       1
PROCNO                      1

F2 - Acquisition Parameters
Date_                20210114
Time                    16.45
INSTRUM                 spect
PROBHD    5 mm PAQXI 1H/
PULPROG                 zg30
TD                     65536
SOLVENT                CDCl3
NS                        16
DS                         2
SWH                10330.578 Hz
FIDRES              0.157632 Hz
AQ                  3.1719425 sec
RG                      456.1
DW                     48.400 usec
DE                      6.50 usec
TE                     298.0 K
D1                 1.00000000 sec
TD0                         1

======== CHANNEL f1 ========
NUC1                       1H
P1                       9.50 usec
PL1                      4.00 dB
PL1W              12.10000038 W
SFO1              500.1330885 MHz

F2 - Processing parameters
SI                      32768
SF                500.1300138 MHz
WDW                        EM
SSB          0
LB                       0.30 Hz
GB           0
PC                       1.00
```

$^{13}$C NMR spectrum of **132** in $CDCl_3$

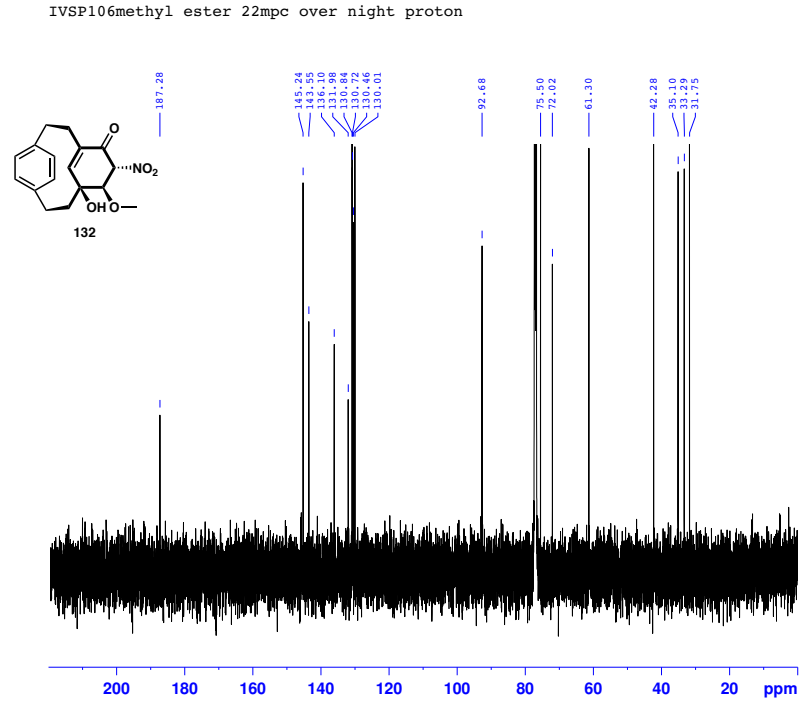


```
Current Data Parameters
NAME                  IVSP106
EXPNO                       2
PROCNO                      1

F2 - Acquisition Parameters
Date_                20210114
Time                    17.49
INSTRUM                 spect
PROBHD    5 mm PAQXI 1H/
PULPROG              zgpg30
TD                     65536
SOLVENT                CDCl3
NS                       6144
DS                          4
SWH                30030.029 Hz
FIDRES              0.458222 Hz
AQ                  1.0911744 sec
RG                      32768
DW                     16.650 usec
DE                      6.50 usec
TE                     298.0 K
D1                 2.00000000 sec
D11                0.03000000 sec
TD0                         6

======== CHANNEL f1 ========
NUC1                      13C
P1                      12.00 usec
PL1                     -4.00 dB
PL1W             172.88230896 W
SFO1              125.7703643 MHz

======== CHANNEL f2 ========
CPDPRG[2             waltz16
NUC2                       1H
PCPD2                  80.00 usec
PL2                     4.00 dB
PL12                   22.51 dB
PL13                   25.00 dB
PL2W              12.10000038 W
PL12W              0.17052394 W
PL13W              0.09611372 W
SFO2              500.1320005 MHz

F2 - Processing parameters
SI                      32768
SF                125.7577890 MHz
WDW                        EM
SSB          0
LB                       1.00 Hz
GB           0
PC                       1.40
```

DEPT spectrum of **132** in $CDCl_3$

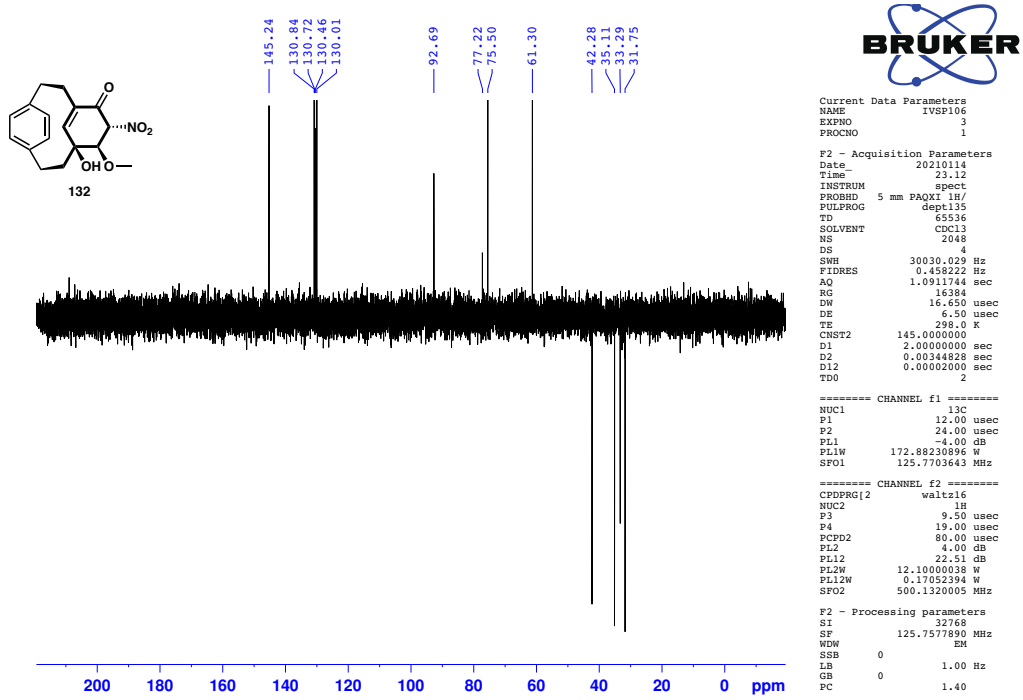


NOSEY spectrum of **132** in $CDCl_3$

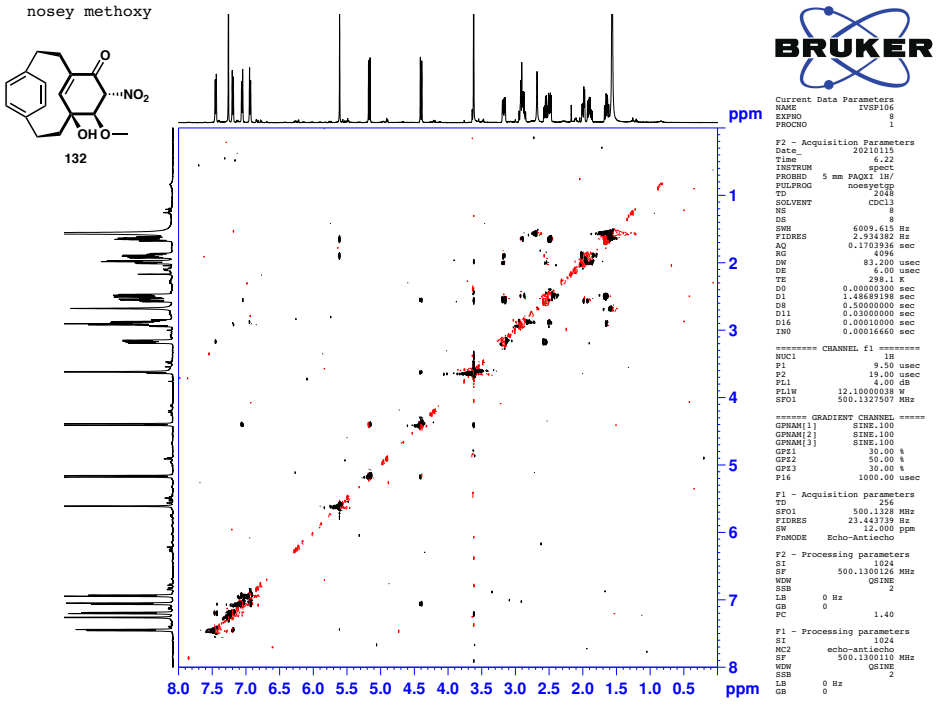

COSY spectrum of **132** in $CDCl_3$

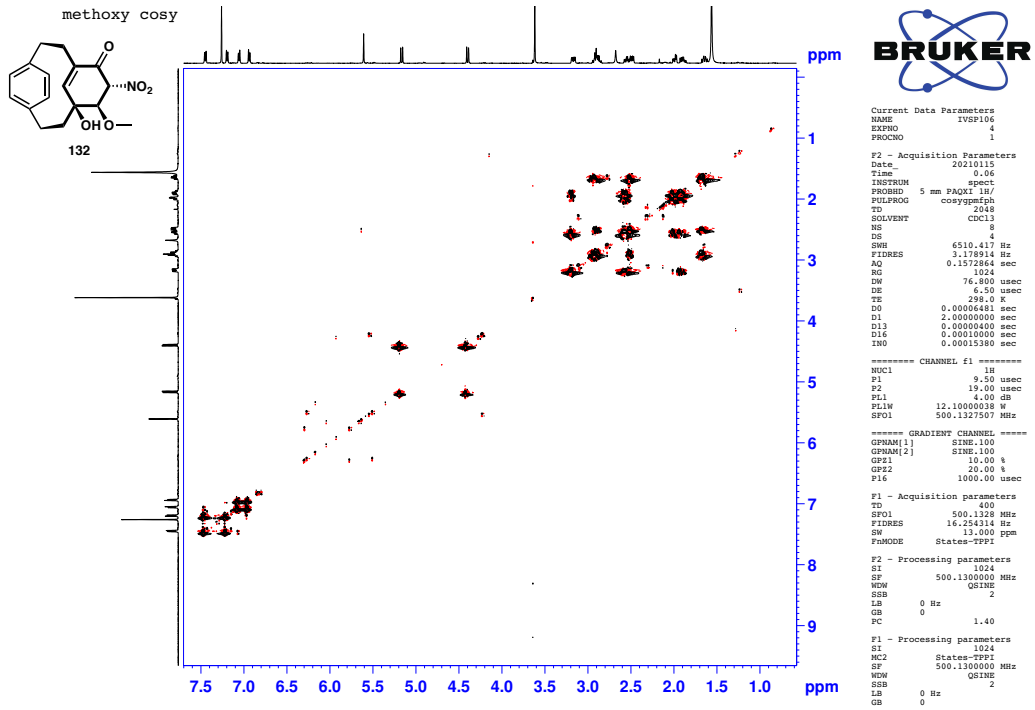


Long range COSY spectrum of **132** in $CDCl_3$

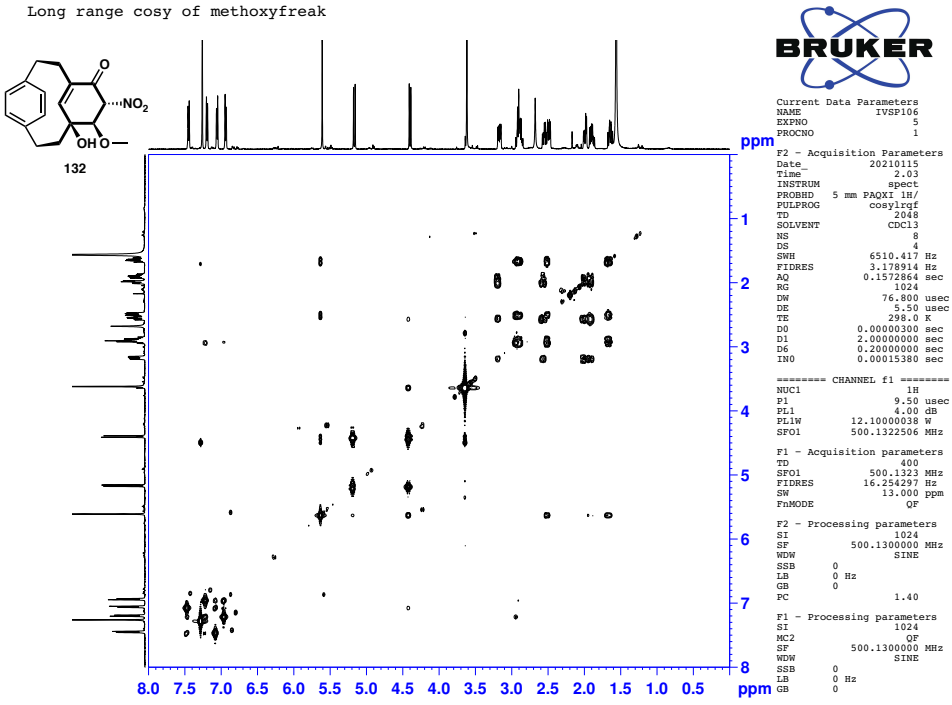

HMQC spectrum of **132** in $CDCl_3$

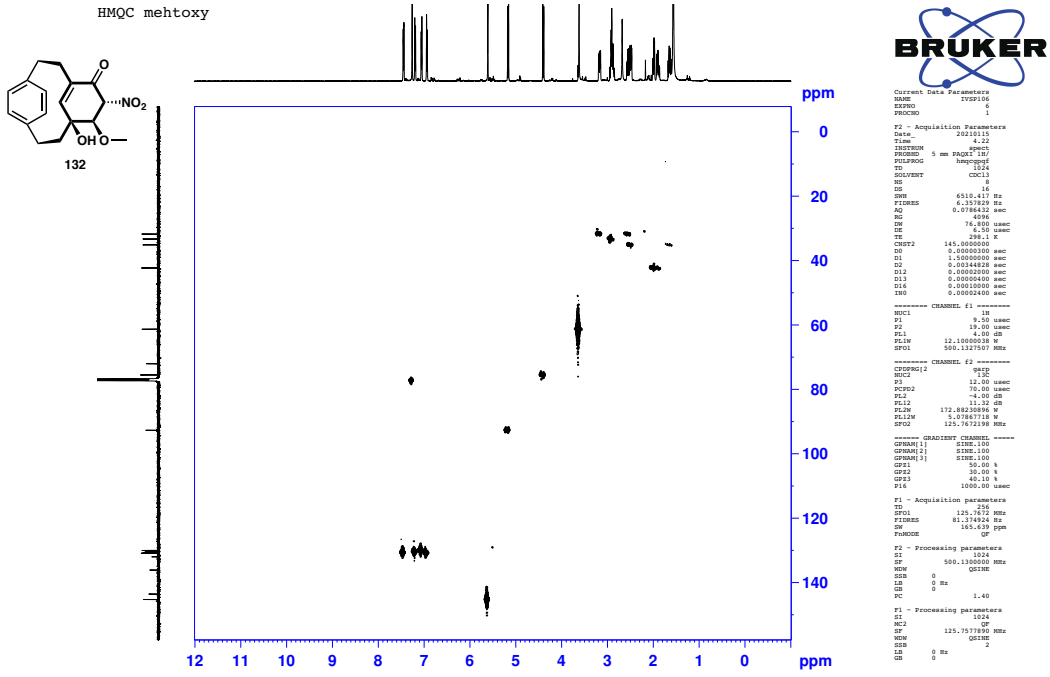


HMBC spectrum of **132** in $CDCl_3$

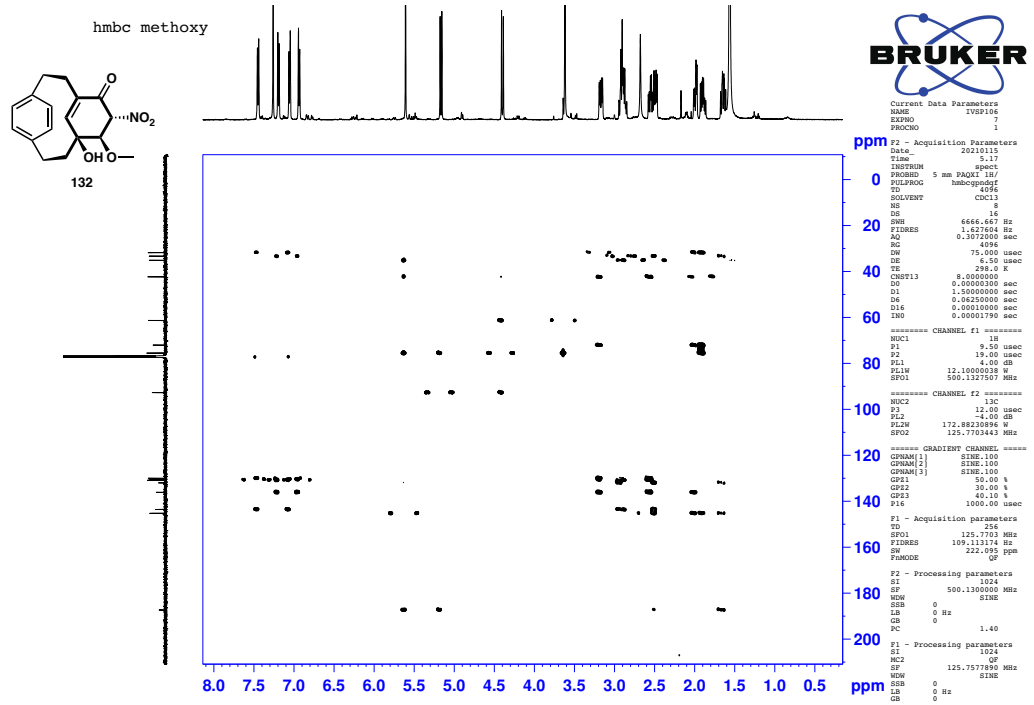

$^{1}$H NMR spectrum of **133** in $CDCl_3$

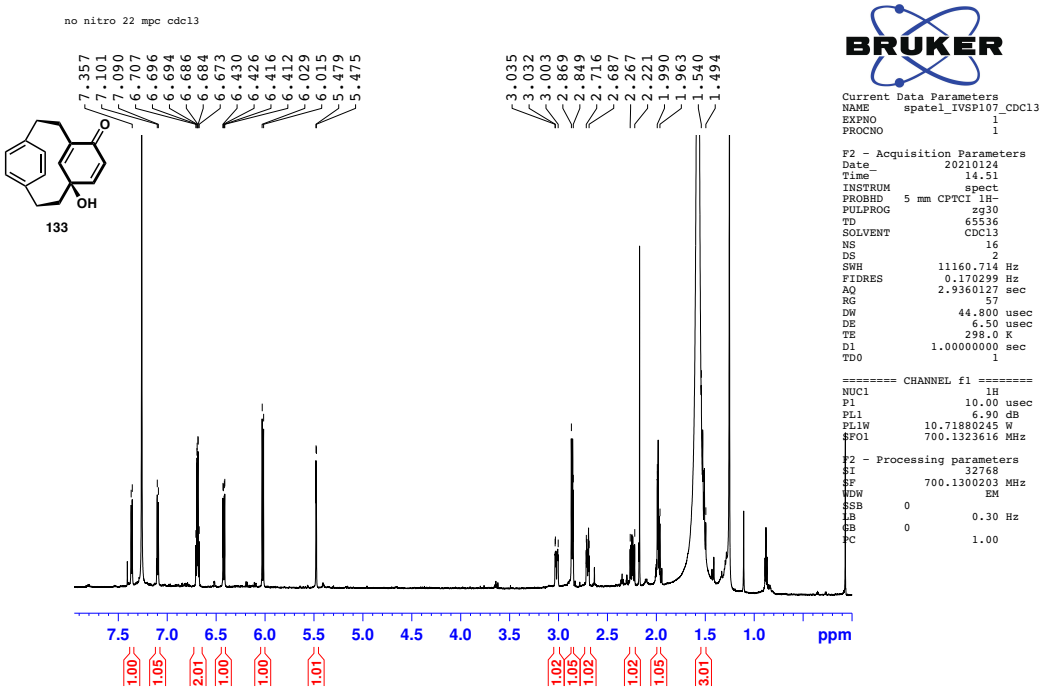


$^{13}$C NMR spectrum of **133** in $CDCl_3$

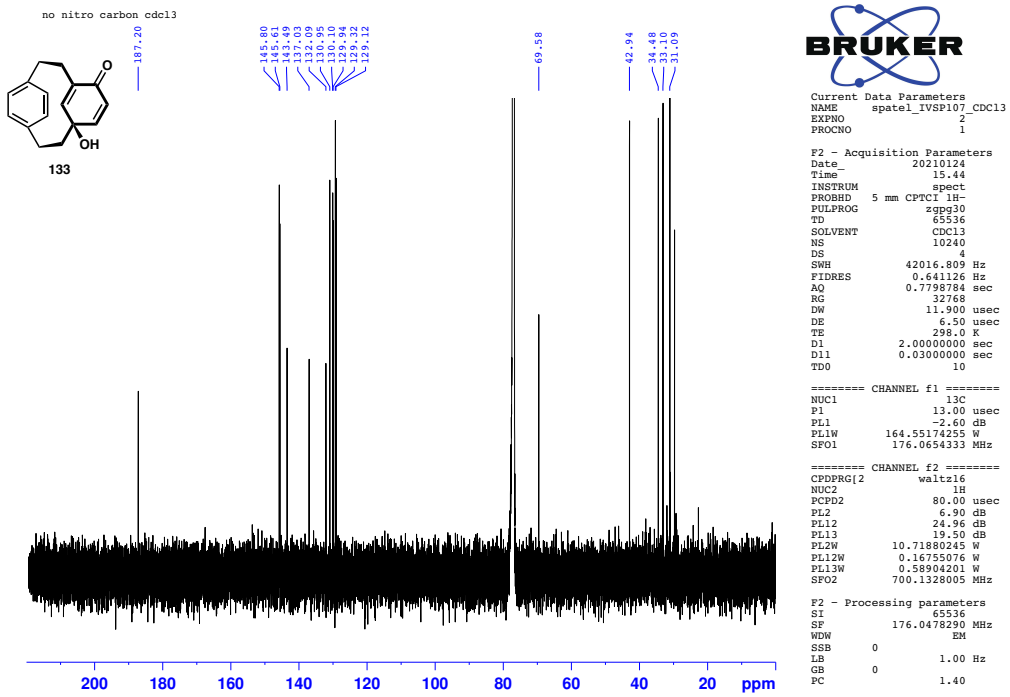

DEPT spectrum of **133** in $CDCl_3$

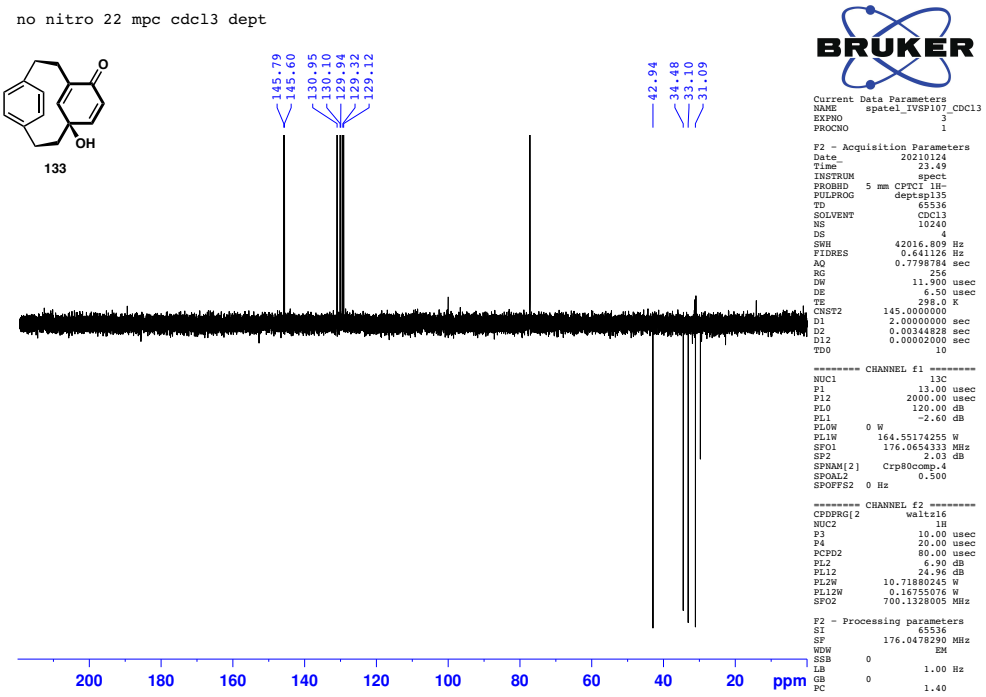


NOSEY spectrum of **133** in $CDCl_3$

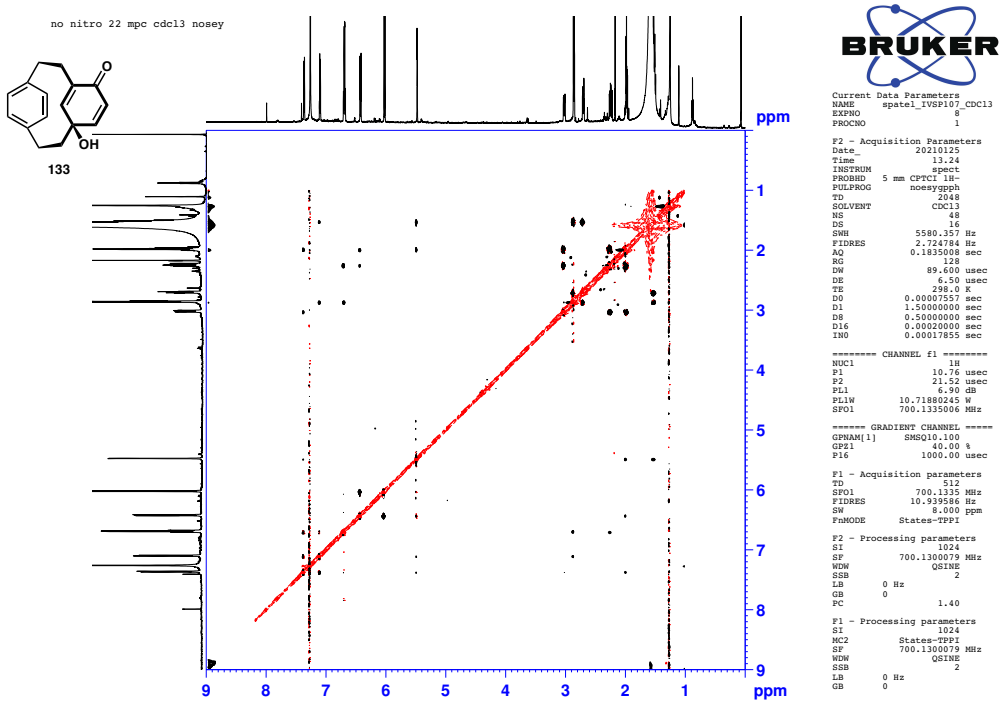

COSY spectrum of **133** in $CDCl_3$

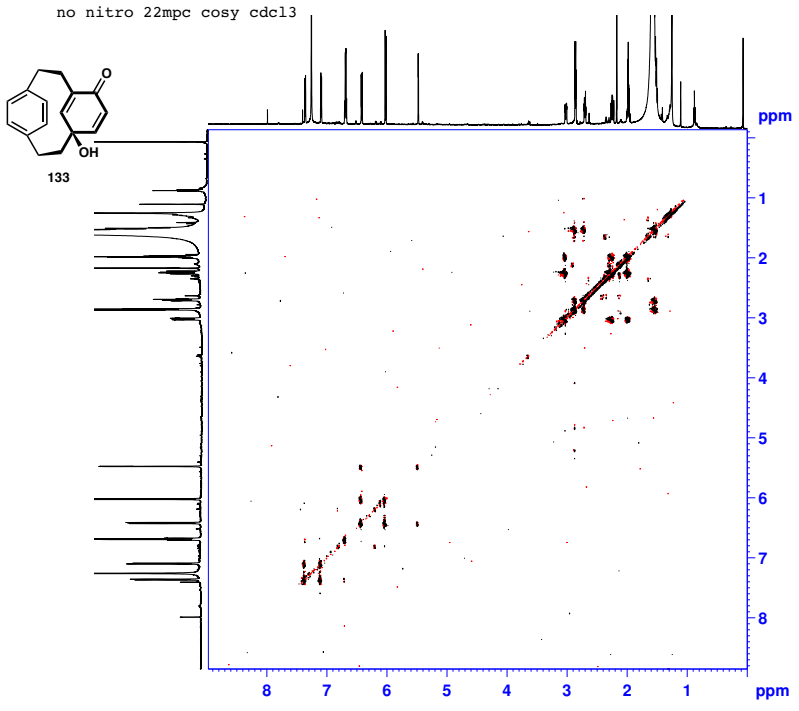


```
Current Data Parameters
NAME      spatel_IVSP107_CDCl3
EXPNO                4
PROCNO               1

F2 - Acquisition Parameters
Date_            20210125
Time                7.03
INSTRUM            spect
PROBHD    5 mm CPTCI 1H-
PULPROG       cosygpmfph
TD                  2048
SOLVENT             CDCl3
NS                     4
DS                     8
SWH              5580.357 Hz
FIDRES           2.724784 Hz
AQ               0.1835008 sec
RG                    64
DW                 89.600 usec
DE                  6.50 usec
TE                298.0 K
D0              0.00007557 sec
D1              1.48689198 sec
D13             0.00000400 sec
D16             0.00020000 sec
IN0             0.00017855 sec

======== CHANNEL f1 ========
NUC1                  1H
P1                 10.76 usec
P2                 21.52 usec
PL1                 6.90 dB
PL1W          10.71880245 W
SFO1         700.1335006 MHz

====== GRADIENT CHANNEL =====
GPNAM[1]       SMSQ10.100
GPNAM[2]       SMSQ10.100
GPZ1                10.00 %
GPZ2                20.00 %
P16               1000.00 usec

F1 - Acquisition parameters
TD                   256
SFO1          700.1335 MHz
FIDRES         21.879171 Hz
SW                8.000 ppm
FnMODE       States-TPPI

F2 - Processing parameters
SI                  1024
SF           700.1300079 MHz
WDW                 QSINE
SSB                    2
LB         0 Hz
GB         0
PC                  1.40

F1 - Processing parameters
SI                  1024
MC2          States-TPPI
SF           700.1300079 MHz
WDW                 QSINE
SSB                    2
LB         0 Hz
GB         0
```

Long range COSY spectrum of **133** in $CDCl_3$

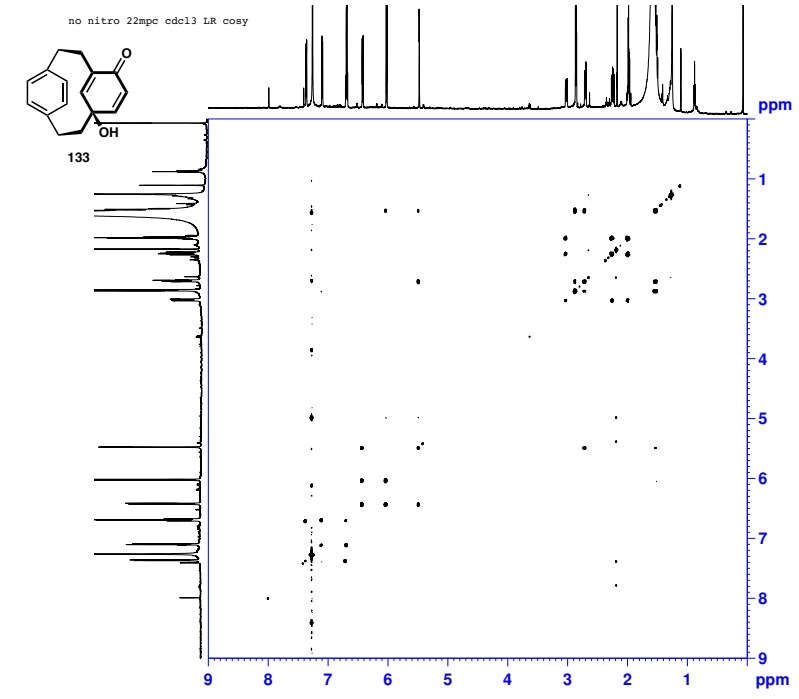


```
Current Data Parameters
NAME      spatel_IVSP107_CDCl3
EXPNO                5
PROCNO               1

F2 - Acquisition Parameters
Date_            20210125
Time                7.33
INSTRUM            spect
PROBHD    5 mm CPTCI 1H-
PULPROG         cosylrqf
TD                  2048
SOLVENT             CDCl3
NS                     8
DS                    16
SWH              5580.357 Hz
FIDRES           2.724784 Hz
AQ               0.1835008 sec
RG                   512
DW                 89.600 usec
DE                  6.50 usec
TE                298.0 K
D0              0.00000300 sec
D1              1.50000000 sec
D6              0.20000000 sec
IN0             0.00017855 sec

======== CHANNEL f1 ========
NUC1                  1H
P1                 10.76 usec
PL1                 6.90 dB
PL1W          10.71880245 W
SFO1         700.1335006 MHz

F1 - Acquisition parameters
TD                   512
SFO1          700.1335 MHz
FIDRES        10.939586 Hz
SW                8.000 ppm
FnMODE                QF

F2 - Processing parameters
SI                  1024
SF           700.1300079 MHz
WDW                 SINE
SSB                    0
LB         0 Hz
GB         0
PC                  1.40

F1 - Processing parameters
SI                  1024
MC2                   QF
SF           700.1300079 MHz
WDW                 SINE
SSB                    0
LB         0 Hz
GB         0
```

HMQC spectrum of **133** in $CDCl_3$

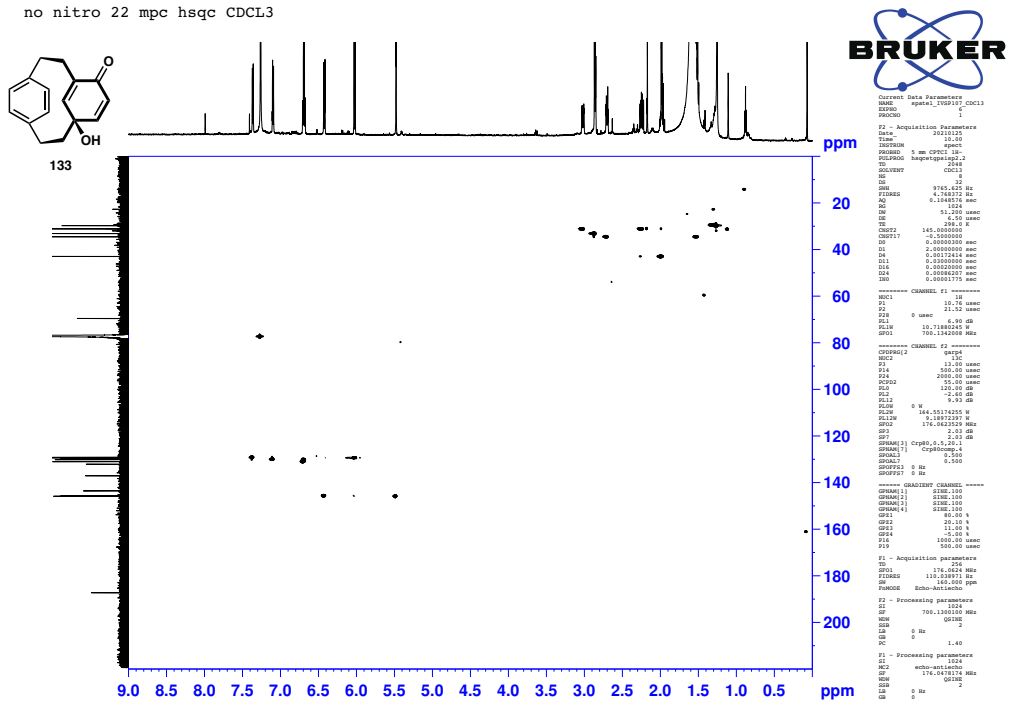


HMBC spectrum of **133** in $CDCl_3$

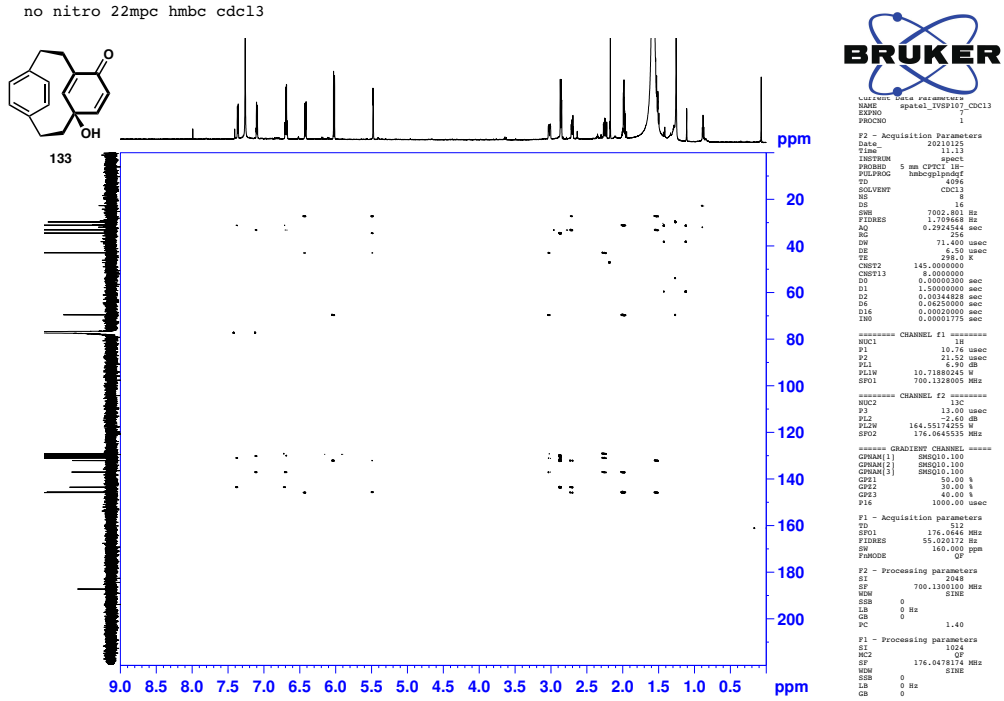

$^{1}$H NMR spectrum of **133** in $(CD_3)_2CO$

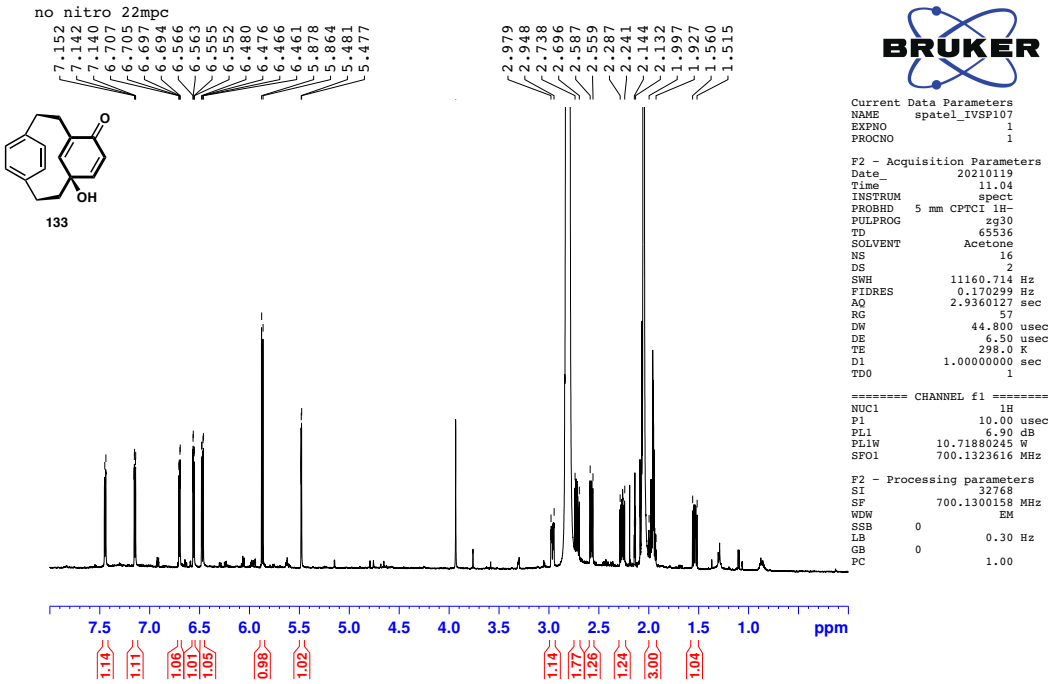


BRUKER

```
Current Data Parameters
NAME      spatel_IVSP107
EXPNO                  1
PROCNO                 1

F2 - Acquisition Parameters
Date_           20210119
Time              11.04
INSTRUM           spect
PROBHD   5 mm CPTCI 1H-
PULPROG           zg30
TD               65536
SOLVENT        Acetone
NS                  16
DS                   2
SWH          11160.714 Hz
FIDRES        0.170299 Hz
AQ           2.9360127 sec
RG                  57
DW              44.800 usec
DE               6.50 usec
TE              298.0 K
D1           1.00000000 sec
TD0                  1

======== CHANNEL f1 ========
NUC1                1H
P1               10.00 usec
PL1               6.90 dB
PL1W       10.71880245 W
SFO1      700.1323616 MHz

F2 - Processing parameters
SI                32768
SF        700.1300158 MHz
WDW                  EM
SSB       0
LB              0.30 Hz
GB        0
PC                1.00
```

$^{13}$C NMR spectrum of **133** in $(CD_3)_2CO$

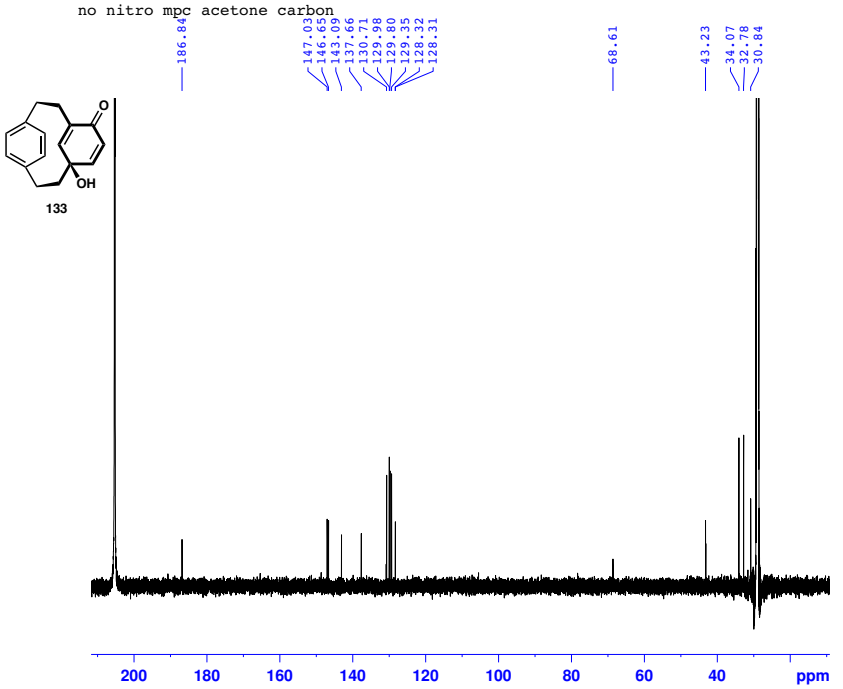


BRUKER

```
Current Data Parameters
NAME      spatel_IVSP107
EXPNO                  2
PROCNO                 1

F2 - Acquisition Parameters
Date_           20210118
Time              18.42
INSTRUM           spect
PROBHD   5 mm CPTCI 1H-
PULPROG         zgpg30
TD               65536
SOLVENT        Acetone
NS               10240
DS                   4
SWH          42016.809 Hz
FIDRES        0.641126 Hz
AQ           0.7798784 sec
RG                32768
DW              11.900 usec
DE               6.50 usec
TE              298.0 K
D1           2.00000000 sec
D11          0.03000000 sec
TD0                 10

======== CHANNEL f1 ========
NUC1                13C
P1               13.00 usec
PL1              -2.60 dB
PL1W       164.55174255 W
SFO1      176.0654333 MHz

======== CHANNEL f2 ========
CPDPRG[2         waltz16
NUC2                1H
PCPD2            80.00 usec
PL2               6.90 dB
PL12             24.96 dB
PL13             19.50 dB
PL2W       10.71880245 W
PL12W       0.16755076 W
PL13W       0.58904201 W
SFO2      700.1328005 MHz

F2 - Processing parameters
SI                65536
SF        176.0478290 MHz
WDW                  EM
SSB       0
LB              1.00 Hz
GB        0
PC                1.40
```

DEPT spectrum of **133** in $(CD_3)_2CO$

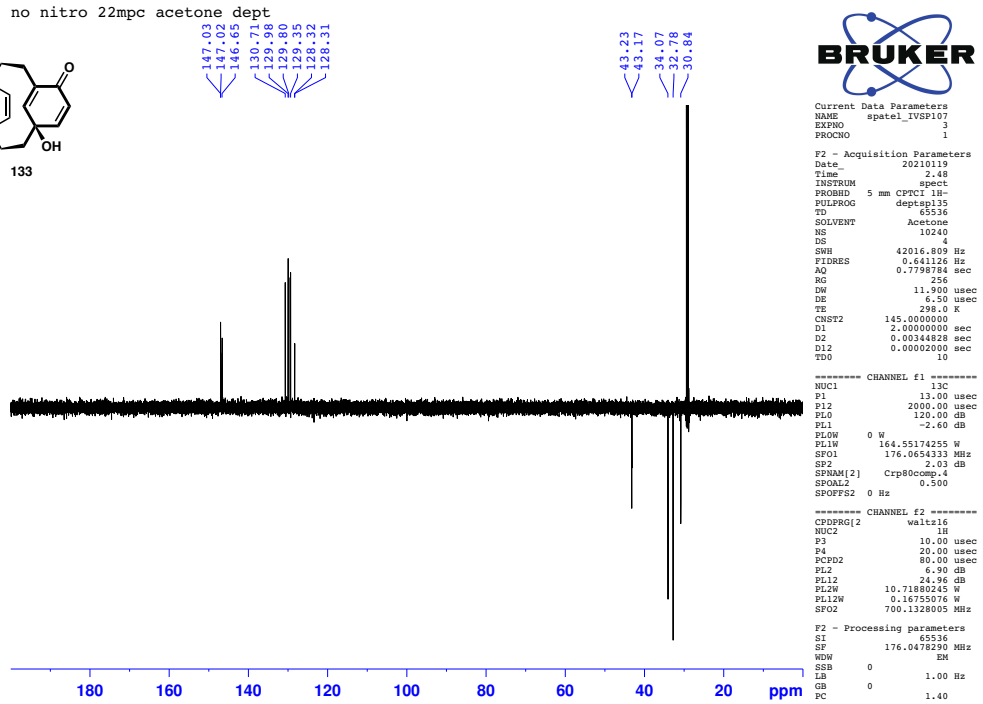


NOSEY spectrum of **133** in $(CD_3)_2CO$

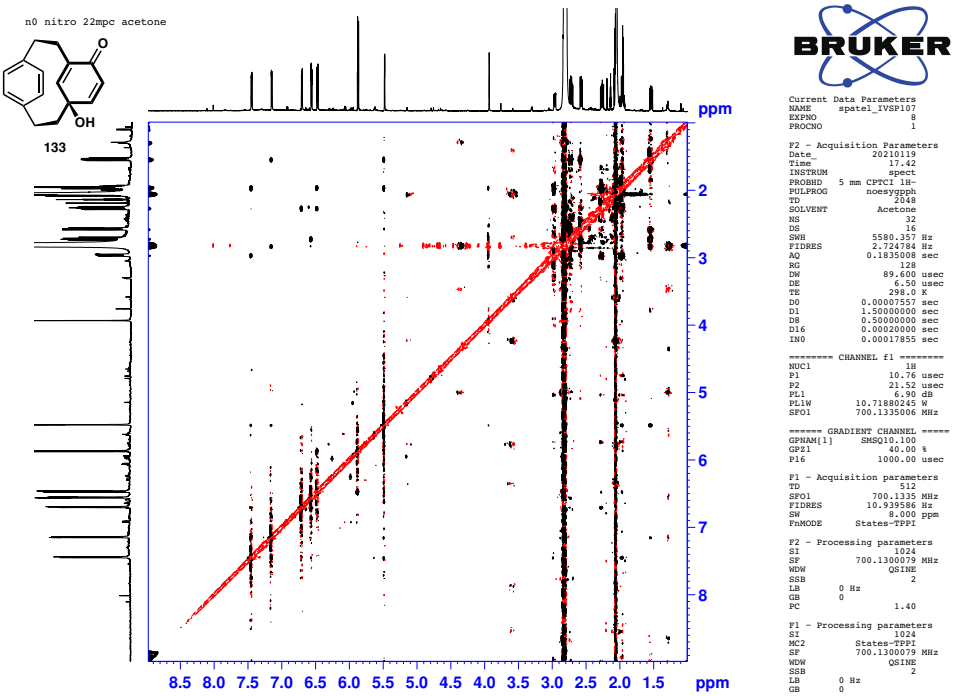

COSY spectrum of **133** in $(CD_3)_2CO$

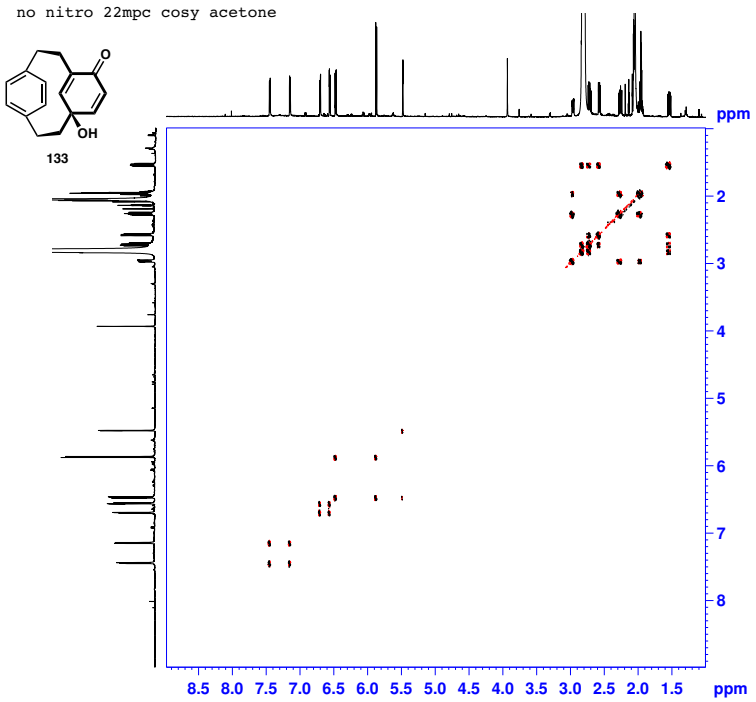


```
Current Data Parameters
NAME      spatel_IVSP107
EXPNO                  4
PROCNO                 1

F2 - Acquisition Parameters
Date_           20210119
Time              11.08
INSTRUM             spect
PROBHD   5 mm CPTCI 1H-
PULPROG       cosygpmfph
TD                  2048
SOLVENT          Acetone
NS                     4
DS                     8
SWH             5580.357 Hz
FIDRES          2.724784 Hz
AQ              0.1835008 sec
RG                    64
DW                89.600 usec
DE                 6.50 usec
TE                298.0 K
D0             0.00007557 sec
D1             1.48689198 sec
D13            0.00000400 sec
D16            0.00020000 sec
IN0            0.00017855 sec

======== CHANNEL f1 ========
NUC1                  1H
P1                 10.76 usec
P2                 21.52 usec
PL1                 6.90 dB
PL1W         10.71880245 W
SFO1         700.1335006 MHz

====== GRADIENT CHANNEL =====
GPNAM[1]      SMSQ10.100
GPNAM[2]      SMSQ10.100
GPZ1               10.00 %
GPZ2               20.00 %
P16              1000.00 usec

F1 - Acquisition parameters
TD                   256
SFO1          700.1335 MHz
FIDRES        21.879171 Hz
SW                8.000 ppm
FnMODE       States-TPPI

F2 - Processing parameters
SI                  1024
SF          700.1300079 MHz
WDW                QSINE
SSB                    2
LB         0 Hz
GB         0
PC                  1.40

F1 - Processing parameters
SI                  1024
MC2          States-TPPI
SF          700.1300079 MHz
WDW                QSINE
SSB                    2
LB         0 Hz
GB         0
```

Long range COSY spectrum of **133** in $(CD_3)_2CO$

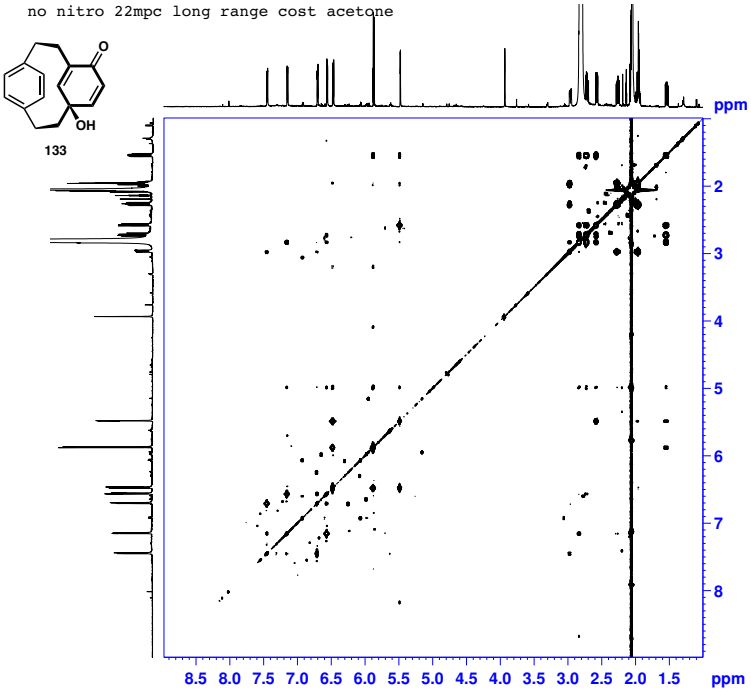


```
Current Data Parameters
NAME      spatel_IVSP107
EXPNO                  5
PROCNO                 1

F2 - Acquisition Parameters
Date_           20210119
Time              11.38
INSTRUM             spect
PROBHD   5 mm CPTCI 1H-
PULPROG        cosylrqf
TD                  2048
SOLVENT          Acetone
NS                     8
DS                    16
SWH             5580.357 Hz
FIDRES          2.724784 Hz
AQ              0.1835008 sec
RG                   512
DW                89.600 usec
DE                 6.50 usec
TE                298.0 K
D0             0.00000300 sec
D1             1.50000000 sec
D6             0.20000000 sec
IN0            0.00017855 sec

======== CHANNEL f1 ========
NUC1                  1H
P1                 10.76 usec
PL1                 6.90 dB
PL1W         10.71880245 W
SFO1         700.1335006 MHz

F1 - Acquisition parameters
TD                   512
SFO1          700.1335 MHz
FIDRES        10.939586 Hz
SW                8.000 ppm
FnMODE               QF

F2 - Processing parameters
SI                  1024
SF          700.1300079 MHz
WDW                SINE
SSB                    0
LB         0 Hz
GB         0
PC                  1.40

F1 - Processing parameters
SI                  1024
MC2                  QF
SF          700.1300079 MHz
WDW                SINE
SSB                    0
LB         0 Hz
GB         0
```

HMQC spectrum of **133** in $(CD_3)_2CO$

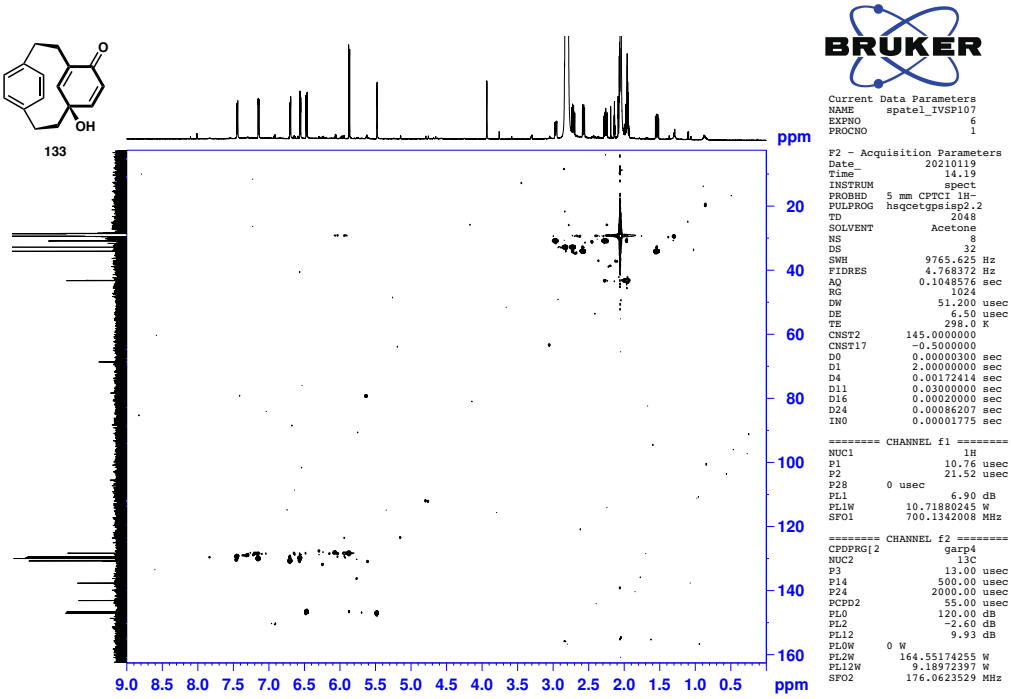


BRUKER

```
Current Data Parameters
NAME      spatel_IVSP107
EXPNO                  6
PROCNO                 1

F2 - Acquisition Parameters
Date_           20210119
Time              14.19
INSTRUM           spect
PROBHD   5 mm CPTCI 1H-
PULPROG  hsqcetgpsisp2.2
TD                2048
SOLVENT        Acetone
NS                   8
DS                  32
SWH           9765.625 Hz
FIDRES        4.768372 Hz
AQ           0.1048576 sec
RG                1024
DW              51.200 usec
DE               6.50 usec
TE              298.0 K
CNST2       145.0000000
CNST17       -0.5000000
D0          0.00000300 sec
D1          2.00000000 sec
D4          0.00172414 sec
D11         0.03000000 sec
D16         0.00020000 sec
D24         0.00086207 sec
IN0         0.00001775 sec

======== CHANNEL f1 ========
NUC1                 1H
P1                10.76 usec
P2                21.52 usec
P28       0 usec
PL1                6.90 dB
PL1W       10.71880245 W
SFO1       700.1342008 MHz

======== CHANNEL f2 ========
CPDPRG[2           garp4
NUC2                13C
P3                13.00 usec
P14              500.00 usec
P24             2000.00 usec
PCPD2             55.00 usec
PL0              120.00 dB
PL2               -2.60 dB
PL12               9.93 dB
PL0W      0 W
PL2W       164.55174255 W
PL12W        9.18972397 W
SFO2       176.0623529 MHz
```

HMBC spectrum of **133** in $(CD_3)_2CO$

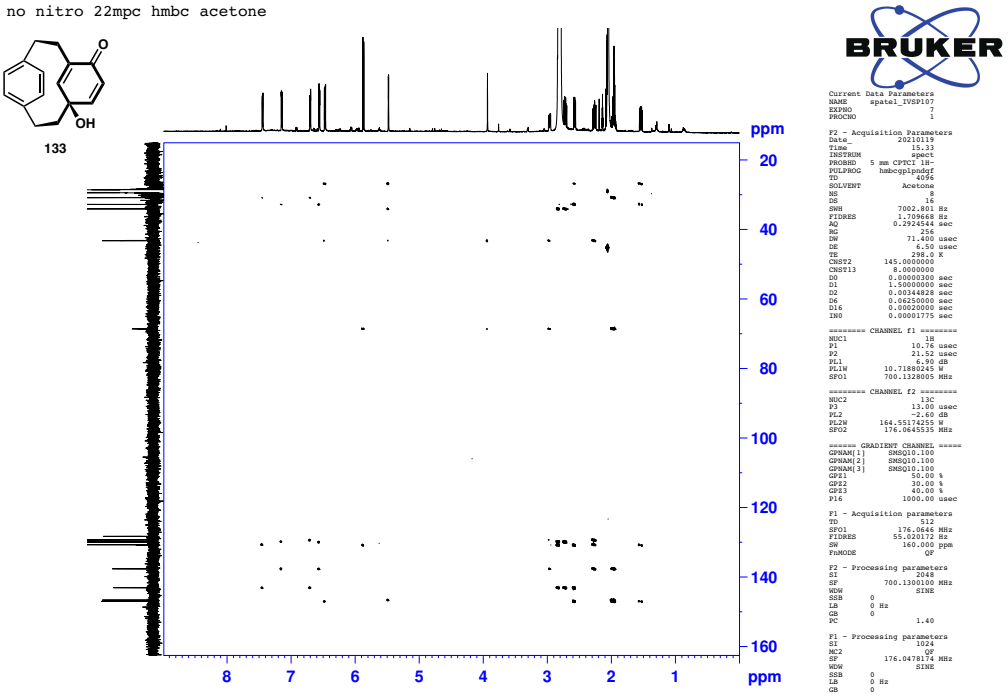


BRUKER

```
Current Data Parameters
NAME     spatel_IVSP107
EXPNO                 7
PROCNO                1

F2 - Acquisition Parameters
Date_           20210119
Time              15.33
INSTRUM           spect
PROBHD   5 mm CPTCI 1H-
PULPROG    hmbcgplpndqf
TD                4096
SOLVENT        Acetone
NS                   8
DS                  16
SWH           7002.801 Hz
FIDRES        1.709668 Hz
AQ           0.2924544 sec
RG                 256
DW              71.400 usec
DE               6.50 usec
TE              298.0 K
CNST2       145.0000000
CNST13        8.0000000
D0          0.00000300 sec
D1          1.50000000 sec
D2          0.00344828 sec
D6          0.06250000 sec
D16         0.00020000 sec
IN0         0.00001775 sec

======== CHANNEL f1 ========
NUC1                 1H
P1                10.76 usec
P2                21.52 usec
PL1                6.90 dB
PL1W       10.71880245 W
SFO1       700.1328005 MHz

======== CHANNEL f2 ========
NUC2                13C
P3                13.00 usec
PL2               -2.60 dB
PL2W       164.55174255 W
SFO2       176.0645535 MHz

====== GRADIENT CHANNEL =====
GPNAM[1]      SMSQ10.100
GPNAM[2]      SMSQ10.100
GPNAM[3]      SMSQ10.100
GPZ1                50.00 %
GPZ2                30.00 %
GPZ3                40.00 %
P16               1000.00 usec

F1 - Acquisition parameters
TD                 512
SFO1          176.0646 MHz
FIDRES        55.020172 Hz
SW               160.000 ppm
FnMODE                QF

F2 - Processing parameters
SI                2048
SF          700.1300100 MHz
WDW                SINE
SSB       0
LB        0 Hz
GB        0
PC                1.40

F1 - Processing parameters
SI                1024
MC2                QF
SF          176.0478174 MHz
WDW                SINE
SSB       0
LB        0 Hz
GB        0
```

$^{1}$H NMR spectrum of **134** in $CDCl_3$

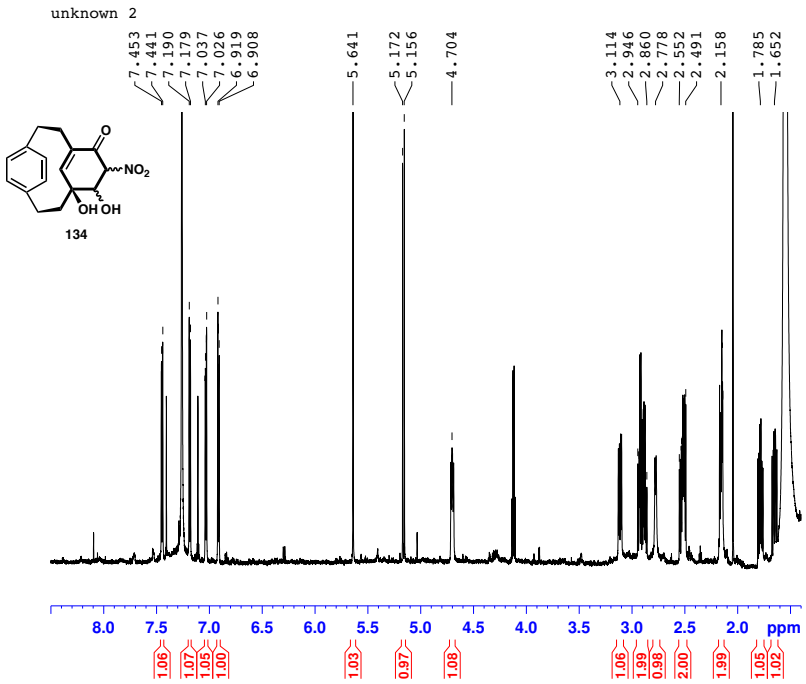


BRUKER

```
Current Data Parameters
NAME      spatel_IVSP71F25
EXPNO                    1
PROCNO                   1

F2 - Acquisition Parameters
Date_              20201125
Time                 10.31
INSTRUM              spect
PROBHD    5 mm CPTCI 1H-
PULPROG              zg30
TD                  65536
SOLVENT             CDCl3
NS                    128
DS                      2
SWH             14492.754 Hz
FIDRES          0.221142 Hz
AQ              2.2609921 sec
RG                     64
DW                34.500 usec
DE                 6.50 usec
TE                298.0 K
D1             1.00000000 sec
TD0                     2

======== CHANNEL f1 ========
NUC1                   1H
P1                  10.00 usec
PL1                  6.90 dB
PL1W          10.71880245 W
SFO1         700.1343236 MHz

F2 - Processing parameters
SI                  65536
SF            700.1300204 MHz
WDW                    EM
SSB        0
LB                  0.10 Hz
GB         0
PC                  1.00
```

$^{13}$C NMR spectrum of **134** in $CDCl_3$

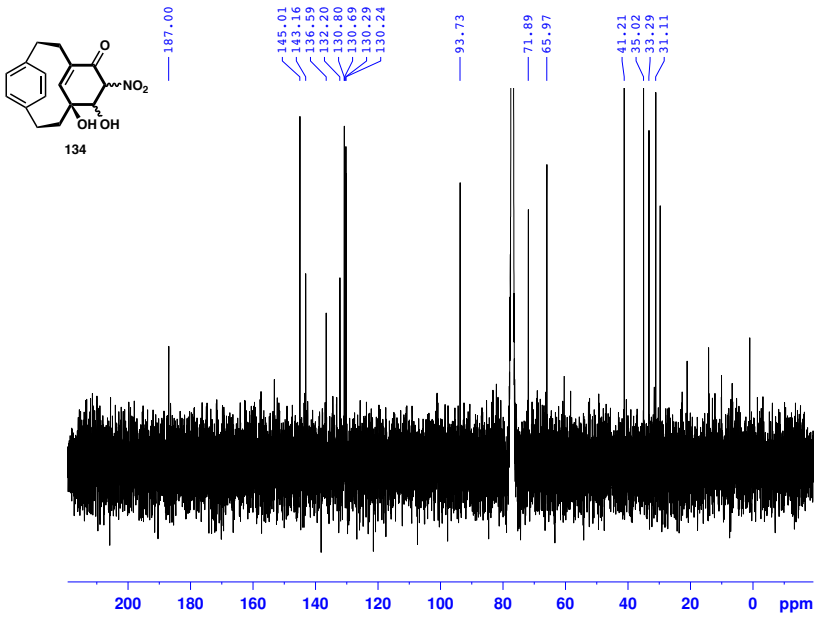


BRUKER

```
Current Data Parameters
NAME      spatel_IVSP71F25
EXPNO                   11
PROCNO                   1

F2 - Acquisition Parameters
Date_              20201206
Time                 18.10
INSTRUM              spect
PROBHD    5 mm CPTCI 1H-
PULPROG            zgpg30
TD                  65536
SOLVENT             CDCl3
NS                  20480
DS                      4
SWH             42016.809 Hz
FIDRES          0.641126 Hz
AQ              0.7798784 sec
RG                  32768
DW                11.900 usec
DE                 6.50 usec
TE                298.0 K
D1             2.00000000 sec
D11            0.03000000 sec
TD0                    22

======== CHANNEL f1 ========
NUC1                  13C
P1                  13.00 usec
PL1                 -2.60 dB
PL1W         164.55174255 W
SFO1          176.0654333 MHz

======== CHANNEL f2 ========
CPDPRG[2          waltz16
NUC2                   1H
PCPD2               80.00 usec
PL2                  6.90 dB
PL12                24.96 dB
PL13                19.50 dB
PL2W          10.71880245 W
PL12W          0.16755076 W
PL13W          0.58904201 W
SFO2         700.1328005 MHz

F2 - Processing parameters
SI                  32768
SF            176.0478290 MHz
WDW                    EM
SSB        0
LB                  2.00 Hz
GB         0
PC                  1.40
```

DEPT spectrum of **134** in $CDCl_3$

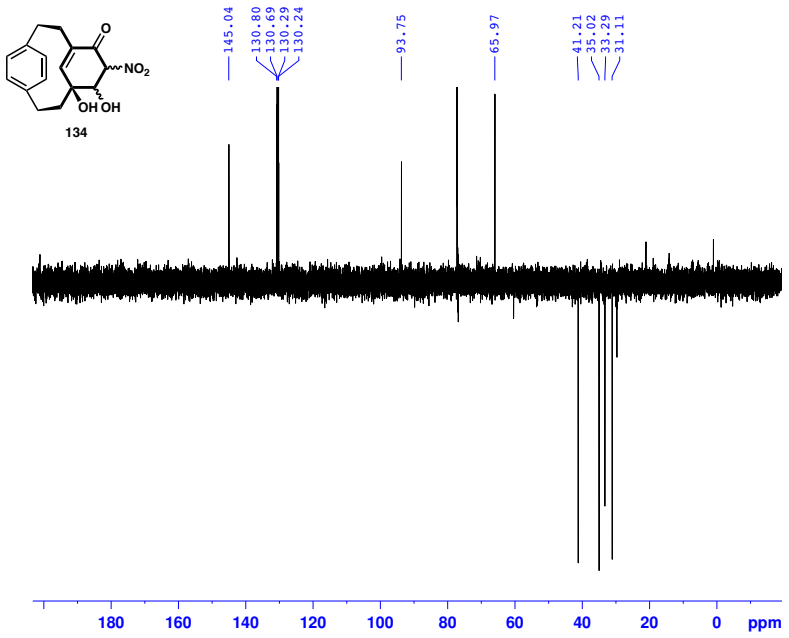



```
Current Data Parameters
NAME      spatel_IVSP71F25
EXPNO                   12
PROCNO                   1

F2 - Acquisition Parameters
Date_           20210121
Time              11.25
INSTRUM             spect
PROBHD   5 mm CPTCI 1H-
PULPROG         deptsp135
TD                  65536
SOLVENT             CDCl3
NS                  24576
DS                      4
SWH           42016.809 Hz
FIDRES        0.641126 Hz
AQ            0.7798784 sec
RG                    256
DW               11.900 usec
DE                6.50 usec
TE                298.0 K
CNST2         145.0000000
D1              2.00000000 sec
D2              0.00344828 sec
D12             0.00002000 sec
TD0                     24

======== CHANNEL f1 ========
NUC1                   13C
P1                   13.00 usec
P12                2000.00 usec
PL0                 120.00 dB
PL1                  -2.30 dB
PL0W       0 W
PL1W       153.56861877 W
SFO1        176.0654333 MHz
SP2                  2.33 dB
SPNAM[2]      Crp80comp.4
SPOAL2             0.500
SPOFFS2   0 Hz

======== CHANNEL f2 ========
CPDPRG[2          waltz16
NUC2                   1H
P3                   12.00 usec
P4                   24.00 usec
PCPD2                80.00 usec
PL2                   8.20 dB
PL12                 24.68 dB
PL2W          7.94595861 W
PL12W         0.17870893 W
SFO2        700.1328005 MHz

F2 - Processing parameters
SI                   32768
SF              176.0478290 MHz
WDW                     EM
SSB       0
LB                    1.00 Hz
GB        0
PC                    1.40
```

NOSEY spectrum of **134** in $CDCl_3$

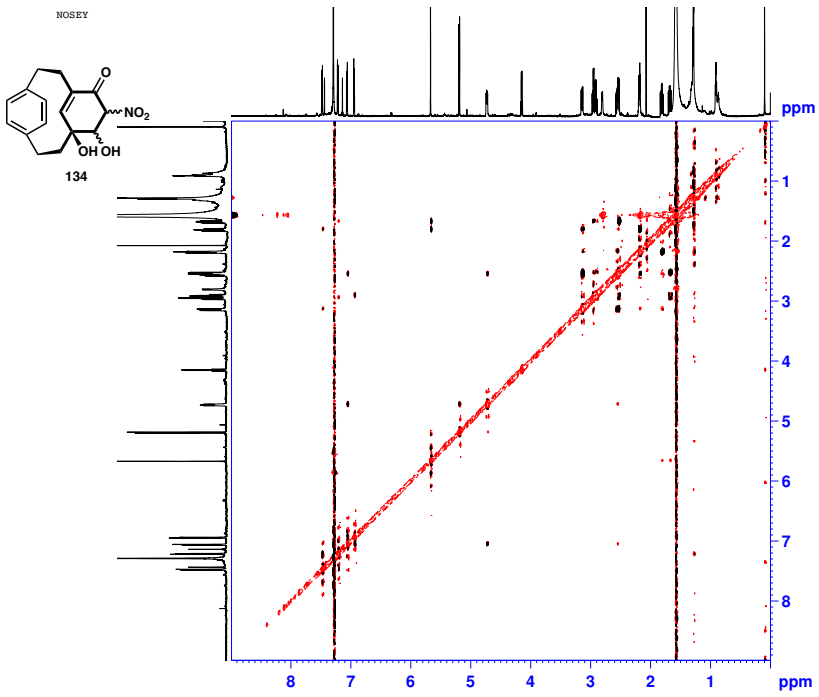



```
Current Data Parameters
NAME      spatel_IVSF71F25
EXPNO                   7
PROCNO                  1

F2 - Acquisition Parameters
Date_           20201126
Time              0.37
INSTRUM             spect
PROBHD   5 mm CPTCI 1H-
PULPROG         noesygpph
TD                  2048
SOLVENT             CDCl3
NS                    40
DS                    16
SWH            7002.801 Hz
FIDRES         3.419337 Hz
AQ             0.1462272 sec
RG                   128
DW               71.400 usec
DE                6.50 usec
TE                298.0 K
D0             0.00005771 sec
D1             1.50000000 sec
D8             0.50000000 sec
D16            0.00020000 sec
IN0            0.00014285 sec

======== CHANNEL f1 ========
NUC1                   1H
P1                   10.76 usec
P2                   21.52 usec
PL1                   6.90 dB
PL1W          10.71880245 W
SFO1        700.1328005 MHz

====== GRADIENT CHANNEL =====
GPNAM[1]       SMSQ10.100
GPZ1                40.00 %
P16               1000.00 usec

F1 - Acquisition parameters
TD                    346
SFO1        700.1328 MHz
FIDRES        20.235052 Hz
SW               10.000 ppm
FnMODE      States-TPPI

F2 - Processing parameters
SI                   1024
SF          700.1300079 MHz
WDW                 QSINE
SSB                     2
LB        0 Hz
GB        0
PC                    1.40

F1 - Processing parameters
SI                   1024
MC2         States-TPPI
SF          700.1300079 MHz
WDW                 QSINE
SSB                     2
LB        0 Hz
GB        0
```

COSY spectrum of **134** in $CDCl_3$

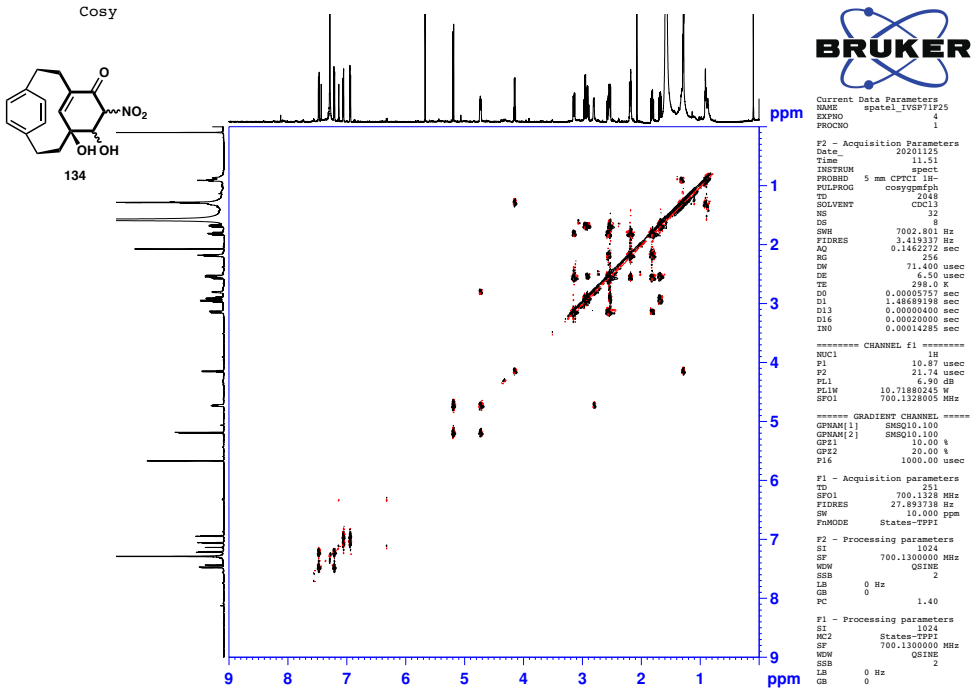


```
Current Data Parameters
NAME      spatel_IVSP71F25
EXPNO                4
PROCNO               1

F2 - Acquisition Parameters
Date_          20201125
Time              11.51
INSTRUM           spect
PROBHD   5 mm CPTCI 1H-
PULPROG      cosygpmfph
TD                2048
SOLVENT           CDCl3
NS                  32
DS                   8
SWH           7002.801 Hz
FIDRES        3.419337 Hz
AQ            0.1462272 sec
RG                 256
DW              71.400 usec
DE               6.50 usec
TE              298.0 K
D0          0.00005757 sec
D1          1.48689198 sec
D13         0.00000400 sec
D16         0.00020000 sec
IN0         0.00014285 sec

======== CHANNEL f1 ========
NUC1               1H
P1              10.87 usec
P2              21.74 usec
PL1              6.90 dB
PL1W       10.71880245 W
SFO1      700.1328005 MHz

====== GRADIENT CHANNEL =====
GPNAM[1]     SMSQ10.100
GPNAM[2]     SMSQ10.100
GPZ1            10.00 %
GPZ2            20.00 %
P16           1000.00 usec

F1 - Acquisition parameters
TD                 251
SFO1          700.1328 MHz
FIDRES       27.893738 Hz
SW               10.000 ppm
FnMODE       States-TPPI

F2 - Processing parameters
SI                1024
SF          700.1300000 MHz
WDW               QSINE
SSB                   2
LB        0 Hz
GB        0
PC                1.40

F1 - Processing parameters
SI                1024
MC2          States-TPPI
SF          700.1300000 MHz
WDW               QSINE
SSB                   2
LB        0 Hz
GB        0
```

Long range COSY spectrum of **134** in $CDCl_3$

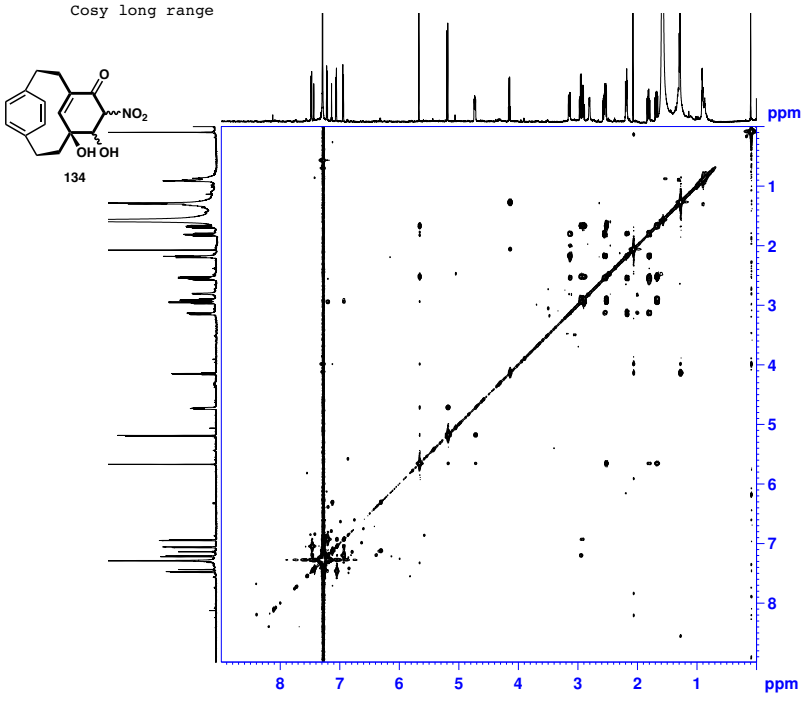


```
Current Data Parameters
NAME      spatel_IVSP71F25
EXPNO                5
PROCNO               1

F2 - Acquisition Parameters
Date_          20201125
Time              15.34
INSTRUM           spect
PROBHD   5 mm CPTCI 1H-
PULPROG         cosylrqf
TD                2048
SOLVENT           CDCl3
NS                  16
DS                  16
SWH           7002.801 Hz
FIDRES        3.419337 Hz
AQ            0.1462272 sec
RG                 512
DW              71.400 usec
DE               6.50 usec
TE              298.0 K
D0          0.00000300 sec
D1          1.50000000 sec
D6          0.20000000 sec
IN0         0.00014285 sec

======== CHANNEL f1 ========
NUC1               1H
P1              10.76 usec
PL1              6.90 dB
PL1W       10.71880245 W
SFO1      700.1328005 MHz

F1 - Acquisition parameters
TD                 512
SFO1          700.1328 MHz
FIDRES       13.674469 Hz
SW               10.000 ppm
FnMODE              QF

F2 - Processing parameters
SI                1024
SF          700.1300079 MHz
WDW               SINE
SSB       0
LB        0 Hz
GB        0
PC                1.40

F1 - Processing parameters
SI                1024
MC2                 QF
SF          700.1300079 MHz
WDW               SINE
SSB       0
LB        0 Hz
GB        0
```

HMQC spectrum of **134** in $CDCl_3$

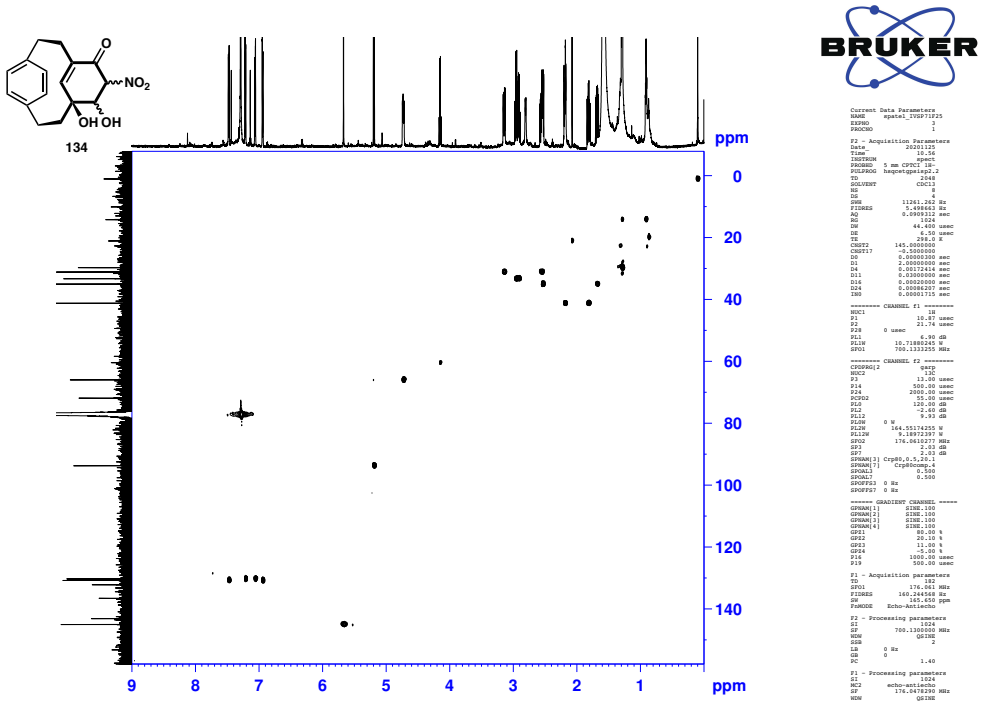


HMBC spectrum of **134** in $CDCl_3$